

“Metallo- β -lactamase-like enzymes from non-pathogenic organisms: an illustration of functional promiscuity”

Joint PhD Thesis
By
Manfredi Miraula



**Maynooth
University**
National University
of Ireland Maynooth

Principal Supervisor

Natasa Mitic (Maynooth University)

Co-Supervisor

Gary Schenk (The University of Queensland)

**Academic Year
2013 – 2016**

Dedication

Dedication

A mia madre Mirella e mio padre Saverio, che hanno sempre creduto in me. Mi hanno fatto diventare l'uomo che sono e saranno sempre accanto a me, a supportare le mie decisioni. Questa tesi è dedicata a loro che sono le mie radici.

Alla mia famiglia che ha stretto la mia mano e mi ha accompagnato lungo la mia strada in un momento della mia vita pieno di dolore e sofferenza. Vi ringrazio perché ho sempre Saputo che dovunque io fossi stato, avrei sempre potuto contare su di voi. E so che questo sarà sempre vero anche in futuro.

To Serena, that shared my path and crossed my life many times. You pull out the best part of me and for this I thank you. You will soon achieve the same accomplishment and I know you will be great! You will be part of me, always.

To my friends. To those that I know since I was a teenager and to those that I met during my travels, thank you for being part of my life, for sharing with me many joyful moments and for making me laugh.

To the researchers that I met and that share their knowledge with me. This thesis took a lot of effort and you all helped me to fulfil this outstanding personal accomplishment. To Marcelo, Chris, Charmaine, J.J., and Emer, thank you because you taught me more than you can imagine. To my exceptional mentors Natasa, Gary, and John. To Gary and Natasa because they are more than mentors, they were friends and family and I will preserve the memories with you as precious gifts. To John, who supported me at the end of my path with kindness.

Table of Content

Table of Content

LIST OF FIGURES	4
LIST OF TABLES	6
LIST OF ENZYME ABBREVIATIONS	8
Declaration by author	9
Thesis outline	11
Abstract	12
Chapter 1: An Introduction to metallo-β-lactamases and their role in the bacterial resistance to antibiotics.	15
1.1. Metallohydrolases and the metallo-β-lactamase fold.	17
1.2. The spread of antibiotic resistance and the role of MBLs	21
1.3 Metallo-β-lactamases: a diverse group of enzymes	24
1.4 MBLs in details: B1 and B3 subgroups	28
1.5 MBLs in details: B2 subgroup	35
1.6 MBLs in details: B4 subgroup	37
1.7 Mono- and binuclear enzymes: two mechanisms, one reaction	38
1.8 Conclusions	43
Chapter 2: Identification and preliminary characterization of novel B3-type metallo-β-lactamases	45
2.1 Introduction	46
2.2 Materials and Methods	48
2.2.1 Selection of the Query Sequence and Protein Database Search Using BLAST	48
2.2.2 Multiple Sequence Alignments	48
2.3. Results and Discussion	48
2.3.1. Protein Database Search, Nomenclature and Classification of Novel MBLs.....	48
Chapter 3: β-Lactam antibiotic-degrading enzymes from non-pathogenic marine organisms: a potential threat to human health	55
3.1 Introduction	56
3.2 Materials and Methods	57
3.2.1 Materials	57
3.2.2 Protein expression and purification	57
3.2.3 Steady-state kinetics and substrate specificity of Zn-containing MIM-1 and MIM-2.....	59
3.2.4 Kinetic data analysis.....	61
3.2.5 pH dependence of catalytic parameters	62
3.2.6 Preparation of the metal ion-free apoproteins	63
3.2.7 Estimation of metal ion binding affinities using reconstitution assays	63
3.3 Results and Discussion	64
3.3.1 Overexpression and purification of MIM-1 and MIM-2	64
3.3.2 Kinetic parameters of MIM-1 and MIM-2	66
3.3.3 Mechanism of action of MIM-1 and MIM-2.....	74
3.3.4 The role of the metal ions in the reactions catalyzed by MIM-1 and MIM-2	77
3.4 Conclusions	83
Chapter 4: Promiscuous metallo-β-lactamases: MIM-1 and MIM-2 may play an essential role in quorum sensing networks	84
4.1 Introduction	85
4.2 Materials and methods	90

Table of Content

4.2.1 Materials	90
4.2.2 Database search, sequence alignments and phylogenetic analysis	90
4.2.3 Structural homology modelling and docking	91
4.2.4 Protein expression and purification	91
4.2.5 Enzymatic assays and data analysis.....	92
4.3 Results and discussion.....	94
4.3.1 Sequence and phylogenetic analysis.....	94
4.3.2 Structural models of MIM-1 and MIM-2	98
4.3.3 N-acyl homoserine lactonase activities of MIM-1 and MIM-2.....	104
4.4 Conclusion.....	113
Chapter 5: Active site geometry and reaction mechanism of MIM-1 and MIM-2.....	115
5.1 Introduction.....	115
5.2 Materials and Methods	116
5.2.1. Materials	116
5.2.2. Protein expression and purification	116
5.2.3. Enzymatic assays and data analysis.....	117
5.2.5. Magnetic circular dichroism.....	119
5.2.6. Electron paramagnetic resonance	119
5.2.7. ¹ H Paramagnetic NMR	120
5.3. Results and Discussion	120
5.3.2 Characterisation of the steady-state catalytic parameters for the hydrolysis of nitrocefin	120
5.3.3 Rapid single-turnover kinetics experiments	123
5.3.3. Spectroscopic characterization of the active site structures of MIM-1 and MIM-2	130
5.4 Conclusion	138
Chapter 6: Concluding Remarks and Future Directions.....	141
Annex: 1 Inteins—A Focus on the Biotechnological Applications of Splicing-Promoting Proteins	145
Annex: 2 Identification and characterization of an unusual metallo-β-lactamase from Serratia proteamaculans	146
Annex: 3 Intrinsic disorder and metal binding in UreG proteins from Archae hyperthermophiles: GTPase enzymes involved in the activation of Ni(II) dependent urease	147
References	154

LIST OF FIGURES

CHAPTER 1:

- **Figure 1.1 Binuclear metal ion centre representatives.....18**
- **Figure 1.2 MBL structure.....21**
- **Figure 1.3 β -lactam antibiotic core structures.....23**
- **Figure 1.4 Active site structure of MBL representatives.....25**
- **Figure 1.5 Comparison of the complexes formed with the substrates and B1-, B2- and B3 type MBLs (previous page).....36**
- **Figure 1.6 Mononuclear mechanism of β -lactam hydrolysis.....39**
- **Figure 1.7 Dinuclear mechanism of β -lactam hydrolysis.....41**

CHAPTER 2:

- **Figure 2.1 Multiple sequence alignment between known (AIM-1, L1 and SMB-1) and putative (MIM-1 and MIM-2) B3-type MBLs.....52**

CHAPTER 3:

- **Figure 3.1 SDS-PAGE of MIM-1 and MIM-2.....59**
- **Figure 3.2 Equilibration curve (top panel) and elution profiles (bottom panel) of MIM-1 (blue) and MIM-2 (red).....65**
- **Figure 3.3 A Catalytic activity of MIM-1 towards the antibiotic penicillins (top), penems (middle) and cephalosporins (bottom).....67**
- **Figure 3.3 B Catalytic activity of MIM-2 towards the antibiotic penicillins (top), penems (middle) and cephalosporins (bottom).....68**
- **Figure 3.4 Inhibition by D-captopril.....73**
- **Figure 3.5 Effect of pH in the hydrolysis of ampicillin (green), biapenem (red) and cefuroxime (blue) for MIM-1 (left panel) and MIM-2 (right panel).....75**
- **Figure 3.6 Analysis of the titration curve of apo-MIM-1 and apo-MIM-2 in the presence of increasing concentrations of zinc.....82**

CHAPTER 4:

- **Figure 4.1 Metallo- β -lactamase fold and active site geometries.....87**
- **Figure 4.2 Substrates (A), (C) and reaction mechanisms (B).....88**
- **Figure 4.3 Multiple Sequence Alignment of B3 MBLs with AHL representatives (previous page).....95**
- **Figure 4.4 Phylogenetic analysis of MIM-1, MIM-2 and AHLs.....98**
- **Figure 4.5 MIM-1 and MIM-2 structural models.....101**

List of Figures

- **Figure 4.6 MIM-1 structural model dockings.....102**
- **Figure 4.7 MIM-2 structural model dockings.....103**
- **Figure 4.8 Methanol Inhibition of MIM-1 (left panel) and MIM-2 (right panel).....104**
- **Figure 4.9 Kinetic parameters analysis of the N-acyl homoserine lactonase activities of MIM-1.....106**
- **Figure 4.10 Kinetic parameters analysis of the N-acyl homoserine lactonase activities of MIM-2.....107**

CHAPTER 5:

- **Figure 5.1 Nitrocefin core structure.....116**
- **Figure 5.2 Schematic representation of the catalytic mechanism for the reaction of MIM-1 and MIM-2 with the β -lactam substrate nitrocefin.....118**
- **Figure 5.3 Rate vs [nitrocefin] profiles of metal ion derivatives of MIM-1 and MIM-2..... 122**
- **Figure 5.4 Stopped-flow spectroscopy of the Zn(II)-, Co(II)- and Ca(II)-derivatives of MIM-1 and MIM-2.....124**
- **Figure 5.5 Time course of concentration changes in single turnover experiments with MIM-1 and MIM-2.....125**
- **Figure 5.6 Schematic representation of a possible catalytic mechanism for the reaction of MIM-1 and MIM-2 with the β -lactam substrate nitrocefin.....126**
- **Figure 5.7 Fluorescence progression curve for MIM-1 (left) and MIM-2 (right) at 280 nm.....128**
- **Figure 5.8 Fluorescence progression curve for MIM-1 (left) and MIM-2 (right) at 280 nm.....131**
- **Figure 5.9 500 MHz ^1H NMR spectra of Co(II) MIM-1 (A) and MIM-2 (B).....133**
- **Figure 5.10 Continuous wave EPR spectra recorded at 20 K in normal perpendicular mode at 9.64 GHz.....134**
- **Figure 5.11 Simulation of the EPR spectra collected for resting MIM-1 (left) and MIM-2 (right).....136**
- **Figure 5.12 Power saturation of EPR signals for MIM-1.137**

CHAPTER 6:

- **Figure 6.1 Crystals grown for MIM-1 (left) and MIM-2 (right) using the hanging drop method.....142**
- **Figure 6.2 Partially refined crystal structure of MIM-2 (left).....143**
- **Figure 6.3 Thiol derivatives and corresponding inhibition constants (K_i values), determined for the B1-type MBL IMP-1.....144**

List of Tables

LIST OF TABLES

CHAPTER 1:

- Table 1.1 Geometries and ligands of the two metal ion binding sites in MBLs from different subclasses.....26
- Table 1.2 List of MBLs divided by class type.....27
- Table 1.3 List of the metal binding constant for the Zn1 and Zn2 sites, obtained using competitive assays.....32
- Table 1.4 List of the metal binding constant for the Zn1 and Zn2 sites, obtained using competitive assays.....33
- Table 1.5 Dissociation constants of Co(II) for the Zn1 and Zn2 sites of wild type and mutant BcII, determined using absorption spectroscopy [48].....34
- Table 1.6 Second-order association rate constants of wild type BcII for the binding of Zn(II), Co(II) and Cd(II), followed by fluorescence spectroscopy [48].....34

CHAPTER 2:

- Table 2.1 Pairwise sequence comparison between MBL-like sequences from *N. pentaromatorans* (MIM-1) and *S. agarivorans* (MIM-2) and selected MBLs from the B1 (NDM-1), B2 (CphA) and B3 (AIM-1, L1, SMB-1) subgroups.....50

CHAPTER 3:

- Table 3.1 Wavelengths and the corresponding extinction coefficients of the substrates used in this study.....60
- Table 3.2 Steady-state catalytic constants obtained for MIM-1 and MIM-2 incorporating (A) or neglecting the effect of substrate inhibition (B). For comparison, kinetics corresponding parameters for the well-studied MBLs L1 [39], AIM-1 [40], BcII [41, 42] and CphA [22] were included (C).....69
- Table 3.3 Inhibition of MBLs by D-captopril.....73
- Table 3.4 pK_a values for the hydrolysis of ampicillin, biapenem and cefuroxime by MIM-1 and MIM-2.....75
- Table 3.5 pK_a values for the β-lactams used to study the pH dependence of MIM-1 and MIM-2 [156, 157].....76
- Table 3.6 Catalytic parameters for the hydrolysis of ampicillin, biapenem and cefuroxime by the Co(II), Mn(II), Cu(II) and Ca(II) derivatives of MIM-1 and MIM-2.....80
- Table 3.7 Binding affinity constants for the metal derivatives of MIM-1 and MIM-2.....82

List of Tables

CHAPTER 4:

- **Table 4.1 Sequence identities and similarities of AIM-1, MIM-1 and MIM-2 with representative AHLases and the GLX-II from *A. thaliana* (GLXII-At).....97**
- **Table 4.2 (A) Comparison of the lactonase activities of metal ion-derivatives of MIM-1.....109**
- **Table 4.2 (B) Comparison of the lactonase activities of metal ion-derivatives of MIM-2.....110**
- **Table 4.3 Comparison of lactonase activities (next page).....111**

CHAPTER 5:

- **Table 5.1 Kinetic parameter obtained for MIM-1 and MIM-2 for the hydrolysis of nitrocefin in the presence of Zn(II), Co(II) and Ca(II).....121**
- **Table 5.2 Estimated first-order rate constants (s^{-1}) obtained for the Zn(II)-, Co(II)- and Ca(II)-derivatives of MIM-1 and MIM-2 for the hydrolysis of nitrocefin.....126**
- **Table 5.3 Estimated first-order rate constants (s^{-1}) obtained for MIM-1 and MIM-2, in the presence of Zn(II), Co(II) and Ca(II), during the hydrolysis of nitrocefin, followed by fluorescence measurements.....128**

List of enzymes

LIST OF ENZYME ABBREVIATIONS

AIM-1	Australian Imipenemase
OPDA	Organophosphate-degrading enzyme from <i>Agrobacterium radiobacter</i> P230
PAP	Purple Acid Phosphatase
GpdQ	Glycerophosphodiesterase enzyme
BcII	<i>Bacillus cereus</i> type II
Pce	Phosphoryl coline esterase
N-HSL	N-acyl Homoserine Lactonase
SdA1	alkylsulfatase
NDM-1	New Dehli Metallo- β -lactamase number 1
CphA	Carbapenem hydrolysing and first ('A') from <i>Aeromonas hydrophila</i>
SPR-1	<i>Serratia Proteamaculans</i> MBL
CcrA	Cefoxitin and carbapenem resistant
EBR-1	Ambler class B β -lactamase from <i>Empedobacter brevis</i>
<i>BlaB</i>	β -Lactamase class B
IMP-1	Imipenemase -1
VIM-1	Verona integron-encoded metallo- β -lactamase
SPM-1	Sao Paulo metallo- β -lactamase
GIM-1	German Imipenemase
DIM-1	Dutch Imipenemase
Sfh-1	subclass B2 metallo-beta-lactamase SFH-1 from <i>Serratia fonticola</i>
L1	Labile enzyme from <i>Stenotrophomonas maltophilia</i>
FEZ-1	<i>Legionella (Fluoribacter) gormanii</i> endogenous zinc β -lactamase
BJP-1	Subclass B3 Metallo- β -lactamase from <i>Bradyrhizobium Japonicum</i>
MIM-1	Maynooth Imipenemase -1 from <i>Novosphingobium entaromativorans</i>
MIM-2	Maynooth Imipenemase -2 from <i>Simiduia agarivorans</i>
<i>SMB-1</i>	<i>Serratia</i> metallo- β -lactamase
CAR-1	B3 metallo-beta-lactamase from <i>Pectobacterium atrosepticum</i>
THIN-1	metallo-beta-lactamase from <i>Janthinobacterium lividum</i>
CSA-1	B3-type metallo- β -lactamase from <i>Cronobacter sakazaki</i>
GOB-1	carbapenemase from <i>Elizabethkingia meningoseptica</i>

Declaration by author

Declaration by author

This thesis is composed of my original work, and contains no material previously published or written by another person except where due reference has been made in the text. I have clearly stated the contribution by others to jointly authored works that I have included in my thesis.

I have clearly stated the contribution of others to my thesis as a whole, including statistical assistance, survey design, data analysis, significant technical procedures, professional editorial advice, and any other original research work used or reported in my thesis. The content of my thesis is the result of work I have carried out since the commencement of my research higher degree candidature and does not include a substantial part of work that has been submitted to qualify for the award of any other degree or diploma in any university or other tertiary institution. I have clearly stated which parts of my thesis, if any, have been submitted to qualify for another award.

I acknowledge that an electronic copy of my thesis must be lodged with the University Library and, subject to the General Award Rules of The University of Queensland, immediately made available for research and study in accordance with the *Copyright Act 1968*.

I acknowledge that copyright of all material contained in my thesis resides with the copyright holder(s) of that material.

Acknowledgment

The author acknowledges Maynooth University (Ireland) and The University of Queensland (Australia) for the great opportunity represented by the joint appointment as a PhD student. Thanks also to SFI Ireland to support financially the project and the research effort that ultimately made possible to accomplish this research project and the author's professional development.

Thesis outline

“Metallo- β -lactamase-like enzymes from non-pathogenic organisms: an illustration of functional promiscuity”

Chapter 1: A general overview about the family of metallohydrolases is followed by an up to date summary about the structure and function of the Zn-dependant metallo- β -lactamases (partially based on a published book chapter and mini-review);

Chapter 2: Identification and preliminary characterization of novel B3-type metallo- β -lactamases (based on a published article);

Chapter 3: β -Lactam antibiotic-degrading enzymes from non-pathogenic marine organisms: a potential threat to human health (based on a published article);

Chapter 4: Promiscuous metallo- β -lactamases: MIM-1 and MIM-2 may play an essential role in quorum sensing networks (based on a published article);

Chapter 5: Probing the role of the metal ions in the mechanism of MIM-1 and MIM-2 using spectroscopic and stopped-flow techniques (Publication in preparation);

Chapter 6: Conclusions and future directions;

Annex 1: Side projects and other published work.

Abstract

Abstract

The spread of antibiotic resistance is one major global problem for healthcare systems. One of the most relevant mechanisms of resistance involves the expression, by bacteria, of enzymes able to degrade the antibiotic molecules. This thesis is focused on the study of a particular class of antibiotic-degrading enzymes, the metallo- β -lactamases (MBLs). MBLs are a family of Zn(II)-dependent enzymes that inactivate most of the commonly used β -lactam antibiotics. In *Chapter 1* a detailed review of the properties of these enzymes is presented.

Novel MBLs are continuously discovered and numerous variants of known MBLs emerge, largely due to the introduction and frequent misuse of novel antibiotics. It has also become apparent that MBLs are present in microorganisms that are not pathogenic and inhabit environments that are not likely to be subjected to significant evolutionary pressures (such as the sharp increase in antibiotics). MBLs from such environmental microorganisms may thus pose a future risk for health care, but they may also provide clues about essential factors that enable such enzymes to inactivate antibiotics. In *Chapter 2* the discovery of two novel putative MBLs from the marine organisms *Novosphingobium pentaromativorans* and *Simiduia agarivorans* is described. In adherence with common practice these two enzymes were named **Maynooth IMipenemase-1** (MIM-1) and **Maynooth IMipenemase-2** (MIM-2), respectively.

In *Chapter 3* the biochemical properties of MIM-1 and MIM-2 are discussed and compared to those of known MBLs. From the pH dependence of their catalytic parameters it is evident that both enzymes differ with respect to their mechanisms, with MIM-1 preferring alkaline and MIM-2 acidic conditions. Both enzymes require Zn(II) but activity can also be reconstituted with other metal ions, including Co(II), Mn(II), Cu(II) and Ca(II). Importantly, the substrate preference of MIM-1 and MIM-2 appears to be influenced by their metal ion composition, which may be a relevant factor in determining their precise biological function.

Abstract

However, with respect to their catalytic efficiency towards degrading β -lactam antibiotics MIM-1 and MIM-2 are comparable to MBLs from known pathogenic bacteria such as *Klebsiella pneumonia* or *Pseudomonas aeruginosa*. They are also inhibited by the non-clinical compound D-captopril in a manner characteristic for MBLs. Thus, even though MIM-1 and MIM-2 are currently not associated with antibiotic resistance these enzymes, should they ever enter the human population, certainly could pose a future threat to health care.

Since neither *N. pentaromativorans* nor *S. agarivorans* are human pathogens, the precise biological role(s) of MIM-1 and MIM-2 remains to be established. In **Chapter 4** the possibility of an alternative function of MIM-1 and MIM-2 will be addressed. Although both protein sequence comparisons and homology modelling indicate that these proteins are related to well-known MBLs such as AIM-1, the sequence analysis also indicates that MIM-1 and MIM-2 share similarities with N-acyl homoserine lactonases (AHLases) and glyoxalase II (GLX-II). Steady-state kinetic assays using a series of lactone substrates confirm that MIM-1 and MIM-2 are indeed efficient lactonases, with catalytic efficiencies resembling those of well-known AHLases. Interestingly, unlike their MBL activity the AHLase activity of MIM-1 and MIM-2 is not dependent on the metal ion composition with Zn(II), Co(II), Cu(II), Mn(II) and Ca(II) all being able to reconstitute catalytic activity (with Co(II) being the most efficient). However, these enzymes do not turn over S-lactoylglutathione, a substrate characteristic for GLX-II activity. Since lactonase activity is linked to the process of quorum sensing the bifunctional activity of “non-pathogenic” MBLs such as MIM-1 and MIM-2 may provide insight into one possible evolutionary pathway for the emergence of antibiotic resistance.

In the preceding chapters MIM-1 and MIM-2 were introduced as novel MBL-like enzymes that may provide essential clues about the functional promiscuity that may be inherent to the family of β -lactam-hydrolysing enzymes. It is thus essential to probe the catalytic mechanism of these enzymes in detail to gain insight into essential factors that control their

Abstract

reactivity. In *Chapter 5* a series of physico-chemical experiments are described (including rapid kinetics and spectroscopic techniques) that provide insight into the active site structure and the mechanism of substrate turnover. In brief, while MIM-1 and MIM-2 employ a strategy that is similar to that of other MBLs by using a metal ion-activated hydroxide moiety to initiate the hydrolysis of β -lactam substrates (such as penicillin, cephalothin or imipenem) no reaction intermediate is observed. Such an intermediate is present in many MBL-characterised reactions and indicates that MIM-1 and MIM-2 may use a different mechanistic strategy, one where the identity of the rate-limiting step is different from that of many (but not all) MBLs.

The characterisation of two novel members of the continuously growing family of MBLs has provided detailed insight into the structure and function of an antibiotic resistance mechanism that is not limited to pathogenic microorganisms. The similarity of the physico-chemical properties between MBLs from pathogenic and non-pathogenic sources may provide clues about evolutionary relationships that may underlie the rapid emergence and spread of antibiotic resistance, but it may also assist in the development of urgently needed potent and clinically useful inhibitors for this group of enzymes. In *Chapter 6* some concluding remarks allude to future directions in this area of research, including a brief description of the crystal structures of both MIM-1 and MIM-2, which have been solved by another member of our team as this thesis was being completed. The hope remains that research like the one presented here will, in time, lead to a powerful strategy to combat the rise of antibiotic resistance and the grave dangers this brings to global human health.

Chapter 1: An Introduction to metallo- β -lactamases and their role in the bacterial resistance to antibiotics.

Metallo- β -Lactamases: A Major Threat to Human Health

American Journal of Molecular Biology, 2014, 4, 89-104

Published Online July 2014 in SciRes. <http://www.scirp.org/journal/ajmb>
<http://dx.doi.org/10.4236/ajmb.2014.43011>

Emer K. Phelan^{1,2*}, Manfredi Miraula^{1,2*}, Christopher Selleck², David L. Ollis³, Gerhard Schenk², Nataša Mitić^{1#}

¹Department of Chemistry, National University of Ireland-Maynooth, Maynooth, Ireland ²School of Chemistry and Molecular Biosciences, The University of Queensland, Brisbane, Australia ³Research School of Chemistry, Australian National University, Canberra, Australia Email: [#]natasa.mitic@nuim.ie

Received 15 April 2014; revised 14 May 2014; accepted 13 June 2014

Copyright © 2014 by authors and Scientific Research Publishing Inc. This work is licensed under the Creative Commons Attribution International License (CC BY).
<http://creativecommons.org/licenses/by/4.0/>

Abstract

Antibiotic resistance is one of the most significant challenges facing global healthcare. Since the 1940s, antibiotics have been used to fight infections, initially with penicillin and subsequently with various derivatives including cephalosporins, carbapenams and monobactams. A common characteristic of these antibiotics is the four-membered β -lactam ring. Alarming, in recent years an increasing number of bacteria have become resistant to these antibiotics. A major strategy employed by these pathogens is to use Zn(II)-dependent enzymes, the metallo- β -lactamases (MBLs), which hydrolyse the β -lactam ring. Clinically useful MBL inhibitors are not yet available. Consequently, MBLs remain a major threat to human health. In this review biochemical properties of MBLs are discussed, focusing in particular on the interactions between the enzymes and the functionally essential metal ions. The precise role(s) of these metal ions is still debated and may differ between different MBLs. However, since they are required for catalysis, their binding site may present an alternative target for inhibitor design.

Keywords

Antibiotic Resistance, β -Lactam Antibiotics, Metallo- β -Lactamases, Reaction Mechanism, Metal Ion Binding

Chapter 1: An Introduction to metallo- β -lactamases and their role in the bacterial resistance to antibiotics

Catalytic Mechanisms of Metallohydrolases Containing Two Metal Ions

Catalytic Mechanisms of Metallohydrolases Containing Two Metal Ions

Nataša Mitić^{*,1}, Manfredi Miraula^{*,†}, Christopher Selleck[†], Kieran S. Hadler[†], Elena Uribe[{],
Marcelo M. Pedroso[†],

Gerhard Schenk^{†,1} ^{*}Department of Chemistry, National University of Ireland, Maynooth, Maynooth, Co. Kildare, Ireland

[†]School of Chemistry and Molecular Biosciences, The University of Queensland, Brisbane, Queensland, Australia [{]Department of Biochemistry and Molecular Biology, University of Concepción, Concepción, Chile ¹Corresponding authors: e-mail address: natasa.mitic@nuim.ie; schenk@uq.edu.au

Abstract

At least one-third of enzymes contain metal ions as cofactors necessary for a diverse range of catalytic activities. In the case of polymetallic enzymes (i.e., two or more metal ions involved in catalysis), the presence of two (or more) closely spaced metal ions gives an additional advantage in terms of (i) charge delocalisation, (ii) smaller activation barriers, (iii) the ability to bind larger substrates, (iv) enhanced electrostatic activation of substrates, and (v) decreased transition-state energies. Among this group of proteins, enzymes that catalyze the hydrolysis of ester and amide bonds form a very prominent family, the metallohydrolases. These enzymes are involved in a multitude of biological functions, and an increasing number of them gain attention for translational research in medicine and biotechnology. Their functional versatility and catalytic proficiency are largely due to the presence of metal ions in their active sites. In this chapter, we thus discuss and compare the reaction mechanisms of several closely related enzymes with a view to highlighting the functional diversity bestowed upon them by their metal ion cofactors.

Chapter 1: An Introduction to metallo- β -lactamases and their role in the bacterial resistance to antibiotics

1.1. Metallohydrolases and the metallo- β -lactamase fold.

The chemistry of life is complex. Many reactions, essential for basic and more advanced physiological functions, would not be possible without the support of enzymes. Enzymes are able to reduce the activation barrier of a reaction, thus accelerating reaction rates by many orders of magnitude. For this fundamental and vital ability, enzymes are both essential and ubiquitous in all the kingdoms of life [1, 2].

Enzymes are able to catalyze diverse reactions, being involved in a wide range of chemical pathways. For example, hydrolases are enzymes that are able to hydrolyze ester or amide bonds in specific substrates. Hydrolytic enzymes are involved in many physiological pathways and are necessary to recycle metabolites needed by the cells [1-3]. Among them, the binuclear metallohydrolases are a family of enzymes that use two metal ions in their catalytically active site in order to catalyze the hydrolysis of ester and amide bonds [1, 2, 4] (**Figure 1.1**). The main ligands involved in metal ion coordination in these enzymes are the imidazole groups of histidine the acidic side chains of aspartate and glutamate, and the alcohol groups of tyrosine and serine [1, 2, 4]. Structurally, the two metal ions are separated by $\sim 3.5 - 4 \text{ \AA}$. It is common to find a bridging molecule between the two metal ions, generally an hydroxide (*i.e.*, μ -hydroxide), the carboxyl side chain of an aspartate or glutamate or a combination of both. Frequently, the μ -hydroxide acts as the nucleophile that initiates the chemical reaction [1, 2, 4]. The environment that is created by a bi-metallic centre presents numerous advantages in terms of its catalytic potential, including (i) charge delocalisation, (ii) smaller activation barriers, (iii) the ability to bind larger substrates, (iv) enhanced electrostatic activation of substrates, and (v) decreased

Chapter 1: An Introduction to metallo- β -lactamases and their role in the bacterial resistance to antibiotics

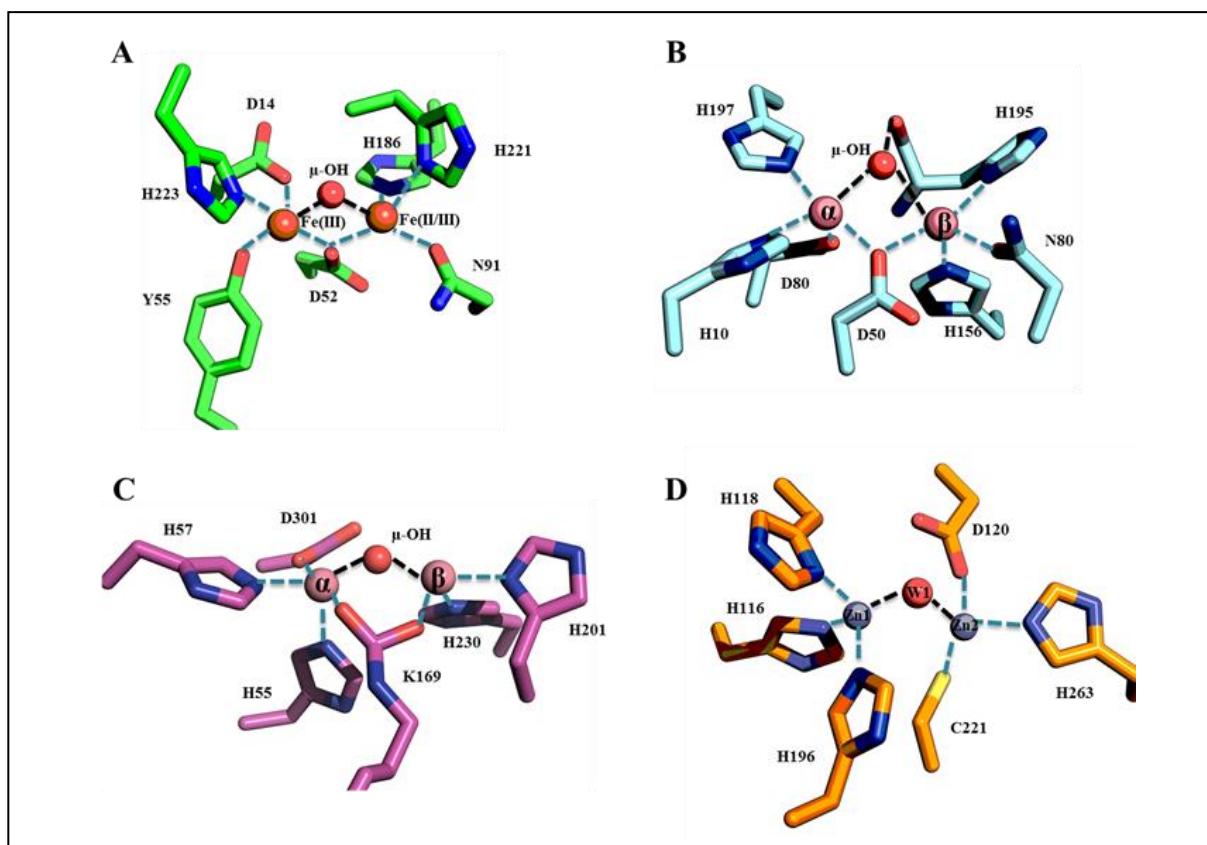


Figure 1.1. Binuclear metal ion centre representatives. A) pig PAP (PDB: 1UTE) [10], B) GpdQ from *Enterobacter aerogenes* (PDB: 3D03) [11], C) OPDA from *Agrobacterium radiobacter* (PDB: 2D2J) [12] and D) BcII from *Bacillus cereus* (PDB: 4C09) [13]. The amino acids involved in the metal binding are showed as sticks. In A) the Fe(II/III) and Fe(III) ions are depicted as orange spheres; in B) and C) the two metal ions are represented as pink spheres and labelled as α and β because of the promiscuity of these enzymes in respect of their metal cofactor requirements; in D) the two zinc ions are shown as grey spheres and the two sites are labelled as Zn1 and Zn2. The water molecules are represented as red spheres. The coordination involving the amino acids and the metal ions is shown with dashed blue lines, the interactions with the terminal water molecule are shown with dashed black lines. The image was generated using PyMOL.

Chapter 1: An Introduction to metallo- β -lactamases and their role in the bacterial resistance to antibiotics

transition-state energies [2, 4, 5].

The binuclear metal centre is associated with a variety of enzymatic structures, serving as the catalytic centre for many and diverse functions. Examples of protein folds possessing such a binuclear centre are the four-helix bundles (*e.g.*, arginase), TIM barrels (*e.g.*, the organophosphate (OP)-degrading enzyme from *Agrobacterium radiobacter*, OPDA), R/ β / β /R folds (*e.g.*, purple acid phosphatase, PAP, and the OP-degrading enzyme from *Enterobacter aerogenes*, GpdQ) and the $\alpha\beta/\beta\alpha$ fold (*e.g.*, metallo- β -lactamases, MBLs) [1, 2, 4]. The scope of this chapter is to introduce the main features characteristic of MBLs, what is known about their structure to function relationship and the role(s) of the metal ion(s) in the catalysis. Over the last twenty years, these enzymes have acquired notoriety for their role in antibiotic resistance, a major challenge to current research endeavours in medicine and biotechnology [4].

The structural fold characteristic for MBLs was first identified in 1997 [6, 7]. Enzymes belonging to the MBL superfamily share a common three-dimensional structure as well as five conserved regions/motifs in their sequences, *i.e.* Asp84, His116-X-His118-X-Asp120-His121, His196, Asp221 and His263 (the standard BBL numbering scheme is used throughout this chapter and thesis [8]) [6, 9].

Despite their conserved fold, represented by the $\alpha\beta/\beta\alpha$ structure (Figure 1.2.), the primary sequences of different MBLs share only low sequence homology. Consequently, the MBLs possessing β -lactamase activity are divided into as many as four subgroups, *i.e.* B1 – B4 [6, 8, 14]. It is also interesting to point out that while all known MBLs can accommodate two metal ions in their active sites, representatives of the B2 subgroup only need one metal ion for catalysis; the presence of the second metal ion leads to an inhibited state [6]. These variations may explain why MBLs are so effective in (i) inactivating most of the commonly used

Chapter 1: An Introduction to metallo- β -lactamases and their role in the bacterial resistance to antibiotics

antibiotics, (ii) adapting rapidly to new imposed challenges, and (iii) displaying functional promiscuity.

Depending on their functions, members of the MBL super family – possessing the characteristic $\alpha\beta/\beta\alpha$ fold - can be divided into as many as 17 different subgroups or classes including the β -lactam antibiotics-hydrolysing MBLs (group 1), the glutathione dependent glyoxalases II (group 2), the rubredoxin oxidoreductases (group 3), the t-RNA³⁰ processing endo-ribonuclease tRNAseZ (group 4), members of the b-CASP family (groups 6 and 7), acid phosphorylcholine esterase Pce (group 9), N-acyl homoserine lactonases (group 12), alkylsulfatase from *Pseudomonas aeruginosa* SdsA1 (group 13) and the methyl parathion hydrolase (group 15). There is currently no structural information for the remaining groups [6]. The proteins belonging to group 1, *i.e.* the MBLs, are the subject of this thesis and will be introduced in detail in the remaining part of this chapter.

Chapter 1: An Introduction to metallo- β -lactamases and their role in the bacterial resistance to antibiotics

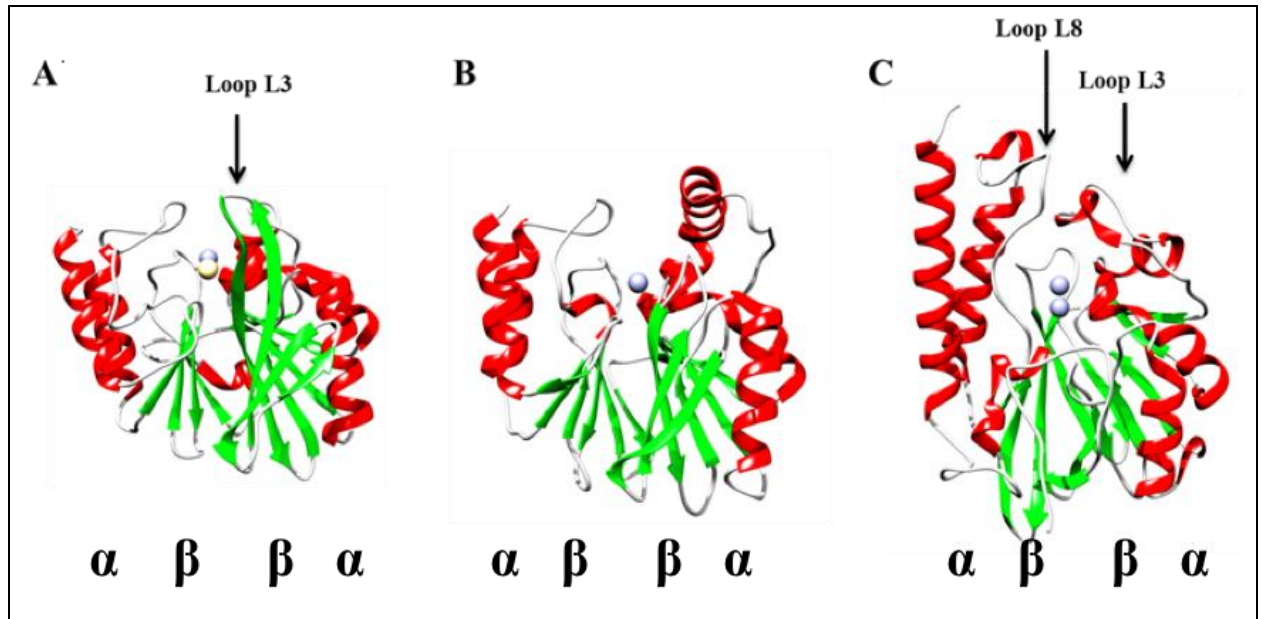


Figure 1.2. MBL structure. The figure shows the $\alpha\beta/\beta\alpha$ fold, characteristic of the MBL protein family. The structures shown are those of three representatives of the three major MBL classes. A) NDM-1 from *Klebsiella pneumoniae* (PDB: 3ZR9) [15]; B) CphA from *A. hydrophylia* (PDB: 1X8G); C) AIM-1 from *P. aeruginosa* (PDB: 4AWY). The representation shows the secondary structure elements as ribbon. The α -helix are coloured in green, the β sheet in red and the loops in grey. The zinc ions are shown as grey sphere; for NDM-1, the second ion occupying the active site is cadmium, shown as a yellow sphere. The black lines indicate the flexible loops, believed to play an important role in the substrate recognition in the B1- and B3-type MBLs. The image was produced using UCF Chimera 10.1.

1.2. The spread of antibiotic resistance and the role of MBLs

The first clinically available β -lactam antibiotic was introduced in 1940, when penicillin was first used to cure bacterial infections [16]. Since then, the chemical structure of β -lactam antibiotics (**Figure 1.3.**) has been extensively modified in order to obtain more powerful drugs, able to kill a wide range of pathogens. Unfortunately, careless use of antibiotics, combined with horizontal gene transfer between different bacterial strains, allowed the genes carrying antibiotic resistances to spread widely. In our modern era, we are facing a considerable risk to regress to a

Chapter 1: An Introduction to metallo- β -lactamases and their role in the bacterial resistance to antibiotics

time when bacterial infections would cause death at high rates.

β -lactam antibiotics have a common core structure, represented by the four-membered β -lactam ring (**Figure 1.3**), and can be divided into four main subgroups: penicillins, cephalosporins, monobactams and carbapenems. The β -lactams possess bactericidal activity. They inhibit cell wall formation and cause the formation of pores. Due to the difference in osmotic pressure between the external medium and the cytosol, they induce cell lysis due to the lack of a perfectly formed cell wall [17, 18].

Even though medicinal chemists have been working on the design of new and more efficient antibiotics, bacteria have continuously evolved ways to escape these antibiotics. Amongst the various possible pathways bacteria possess to fight antibiotics, one of the most efficient is the expression of hydrolytic enzymes able to hydrolyse most of the commonly used antibiotics. The enzymes able to hydrolyse β -lactams are called β -lactamases. These enzymes are able to cleave the cyclic amide bond, characteristic of the shared core structure of these antibiotics (**Figure 1.3**), thus inactivating the drug [18]. β -Lactamases are grouped into four subgroups, *i.e.* A, B, C and D. Subgroup B comprises MBLs [6, 18].

Chapter 1: An Introduction to metallo- β -lactamases and their role in the bacterial resistance to antibiotics

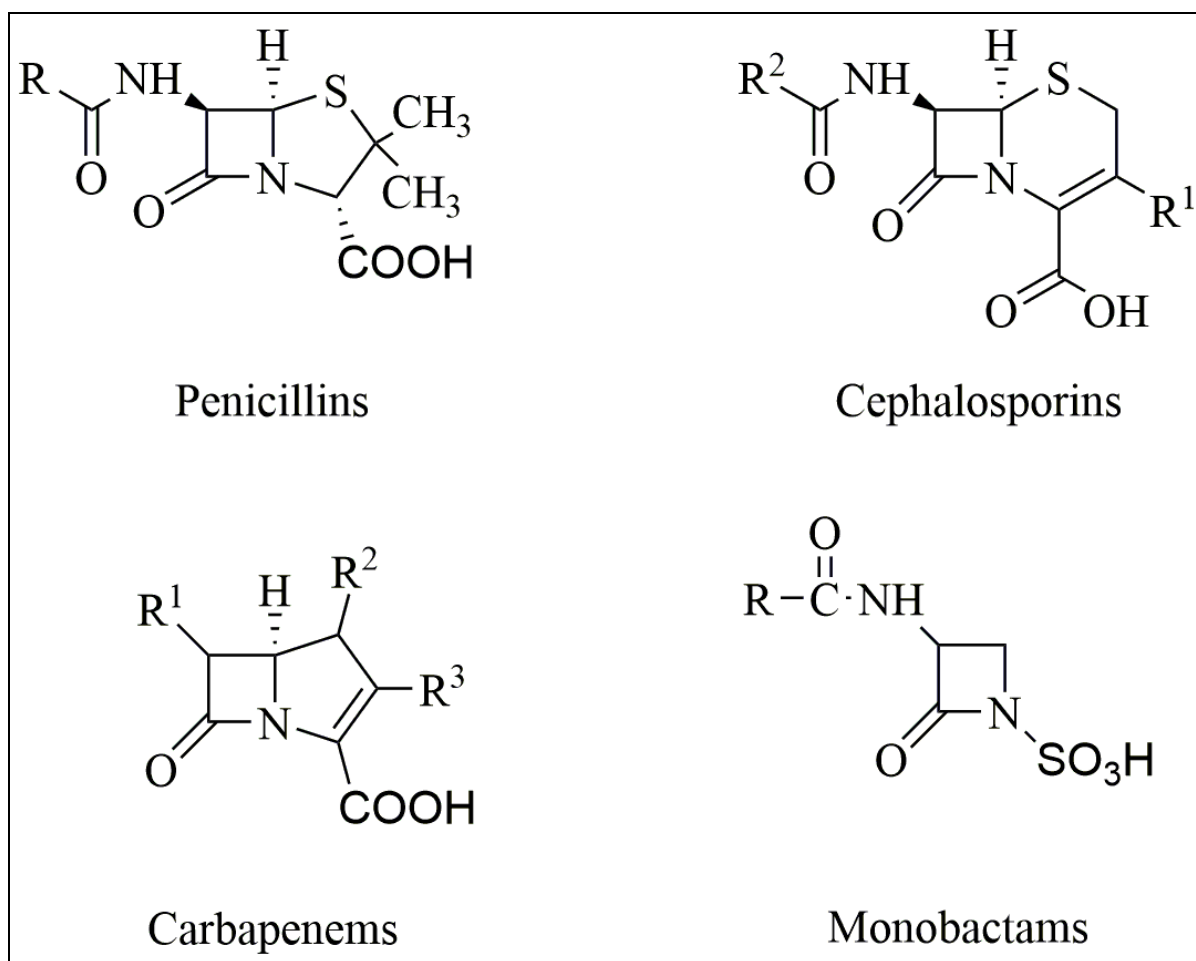


Figure 1.3. β -lactam antibiotic core structures. The figure shows the core structure of the four major β -lactam classes. The image was generated using ChemDraw Professional 15.0.

As discussed above, MBLs recruit up to two Zn(II) ion to hydrolyze β -lactams. In contrast, enzymes belonging to subgroups A, C and D do not require metal ions for their activity. They are called serine- β -lactamases (SBLs) and their mechanism employs an active site serine residue to initiate β -lactam hydrolysis [6]. Clinically useful inhibitors (*e.g.* clavulanic acid [19]) for SBLs are available, lessening their threat to health care [6, 19]. On the other hand, there are currently no clinically useful inhibitors for MBLs, compounding the threat these enzymes pose for global health [19, 20]. The scope of this thesis will focus on these enzymes.

Chapter 1: An Introduction to metallo- β -lactamases and their role in the bacterial resistance to antibiotics

1.3 Metallo- β -lactamases: a diverse group of enzymes

Based on the sequence similarity, substrate specificity and metal ion requirements, the MBL family is further divided into four subgroups. Classes B1, B2 and B3 are well studied [6, 8, 21, 22]. Recently, our group identified a fourth subgroup, termed B4. The first member to be identified in this subgroup is SPR-1 from *Serratia proteomaculans* [14, 23], that appears to be in a catalytically inactive mono-nuclear form in the resting state, but acquires a second metal ion when a substrate is added (substrate-promoted activation) [14, 23]. Insofar, SPR-1 resembles an organophosphate-degrading bimetallic glycerophosphate diesterase from *Enterobacter aerogenes*, GpdQ [11, 24, 25]. Since the discovery of SPR-1 several additional putative B4-type MBLs have been identified by sequence comparisons [14], however no structural information is currently available for any of these enzymes. Despite limited overall sequence homology and mechanistic differences the active site structures of all MBLs investigated to date reveal a common geometry that facilitates the accommodation of two closely spaced metal ions, although B2-type MBLs only require one metal ion for activity and B4-type MBLs may require a second metal ion only upon activation by the substrate (see above). **Figure 1.4.** illustrates active sites of representative MBLs from the B1, B2 and B3 subgroups. **Table 1.1.** summarises relevant amino acid ligands of the metal ions in the different subgroups.

Chapter 1: An Introduction to metallo- β -lactamases and their role in the bacterial resistance to antibiotics

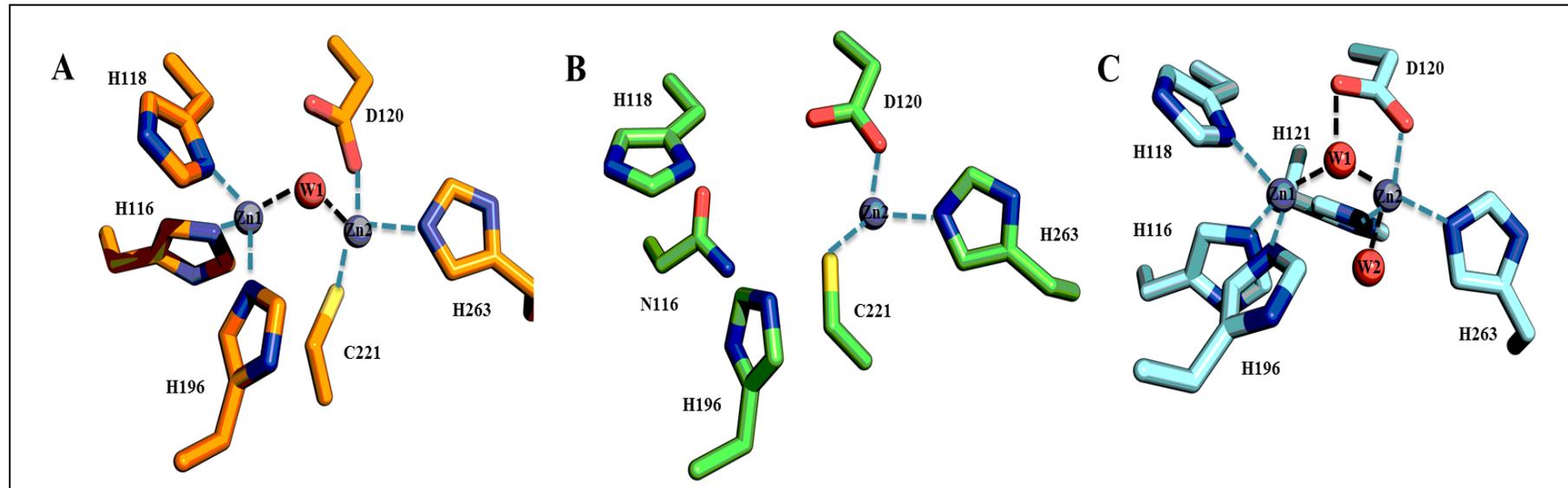


Figure 1.4. Active site structure of MBL representatives. The active site structure of B1, B2 and B3 MBLs is shown. A) B1 BcII from *B. cereus*, B) B2 CphA from *A. hydrophylia*, C) B3 AIM-1 from *P. aeruginosa*. The amino acids involved in the metal binding are shown as sticks. The zinc ions are shown as grey spheres, while the water molecules as red spheres. The blue dashed lines are used to show the amino acid to metal coordinations; the black dashed lines represent the interactions between the metal ions and the amino acids with the water molecules.

Chapter 1: An Introduction to metallo- β -lactamases and their role in the bacterial resistance to antibiotics

Table 1.1. Geometries and ligands of the two metal ion binding sites in MBLs from different subclasses.

Subclass	Zn1 Geometry	Zn1 Ligands	Zn2 Geometry	Zn2 Ligands
B1	Tetrahedral	H116, H118, H196 & W1	Trigonal bipyramidal	D120, C221, H263 & W1
B2	Not occupied		Tetrahedral	D120, C221, H263 & W1
B3	Tetrahedral	H116, H118, H196 & W1	Trigonal bipyramidal	D120, C221, H263, W1 & W2
B4	Tetrahedral	H116, R118, H196	Trigonal bipyramidal	D120, Q121/S221, A262

Chapter 1: An Introduction to metallo- β -lactamases and their role in the bacterial resistance to antibiotics

Table 1.2. List of MBLs divided by class type. The Table presents a list of the B1-, B2- and B3-type MBL identified until now. The microorganisms from which the MBLs were first isolated are reported.

MBL type	Microorganism	MBL type	Microorganism	MBL type	Microorganism
B1		B2		B3	
BcII	<i>Bacillus cereus</i>	CphA	<i>Aeromonas hydrophylia</i>	L1	<i>Streptomonas maltophilia</i>
CcrA	<i>Bacteroides fragilis</i>	CphAII [26]	<i>Aquifex aeolicus</i>	FEZ-1 [27, 28]	<i>Fluoriobacter gormanii</i>
EBR-1 [29]	<i>Empedobacter brevis</i>	ImiS [30]	<i>Aeromonas sobria</i>	GOB-1 [31]	<i>Elizabethkingia meningoseptica</i>
BlaB [32]	<i>Elizabethkingia meningoseptica</i>	Sfh-I [33]	<i>Serratia fonticola</i>	AIM-1	<i>Pseudomonas aeruginosa</i>
NDM-1	<i>Klebsiella pneumoniae</i>			MIM-1	<i>Novosphingobium pentaromativorans</i>
Acquired-B1				MIM-2	<i>Simiduia agarivorans</i>
IMP-1	<i>Serratia marcescens</i>			SMB-1 [34]	<i>Serratia marcescens</i>
IMP-2 [35]	<i>Acinetobacter</i> ssp			SPR-1	<i>Serratia proteamaculans</i>
VIM-1 [36]	<i>Pseudomonas aeruginosa</i>			CSA-1	<i>Cronobacter sakazaki</i>
VIM-2 [37]	<i>Pseudomonas aeruginosa</i>			BJP-1 [38, 39]	<i>Bradyrhizobium japonicum</i>
SPM-1 [40]	<i>Pseudomonas aeruginosa</i>			CAR-1 [41]	<i>Erwinia carotovora</i>
GIM-1 [42, 43]	<i>Pseudomonas aeruginosa</i>			THIN-B [44]	<i>Janthinobacterium lividum</i>
DIM-1 [45]	<i>Pseudomonas stutzeri</i>				

Chapter 1: An Introduction to metallo- β -lactamases and their role in the bacterial resistance to antibiotics

1.4 MBLs in details: B1 and B3 subgroups

The uncertainties regarding the number of zinc ions required *in vivo* by MBLs were further exacerbated by the first crystal structure obtained for the B1-type BcII from *Bacillus cereus* [46]. Although containing space for two zinc ions to be bound, the structure of BcII revealed an active site with only one zinc ion bound to the Zn1 site [46]. Since this structure became available, numerous studies have tried to establish the physiological metal composition of BcII, without success [47-49]. A factor that contributes to this lack in understanding is the absence of reliable data about the metal ion affinities to MBLs. It is apparent that metal binding affinities vary greatly depending on the technique used to analyze the binding phenomenon [16] (**Table 1.3., Table 1.4., Table 1.5. and Table 1.6.**). The B1 subclass is the most prevalent and structurally most extensively studied class of MBLs [6, 29, 46, 50-55] (**Table 1.2.**). Members include IMP [54, 56-63], VIM [64-72] and BcII [14, 18, 48, 73]. More recently, NDM-1 from *Klebsiella pneumoniae* emerged and made global headlines due to its highly pathogenic and dangerous nature because of its ability to degrade most commonly used antibiotics [74-79]. Examples of the B2 and B3 subgroups are CphA from *A. hydrophila* [80-86], ImiS from *A. veronii* bv. Sobria and Sfh-I from *S. fonticola* [33, 82, 86], and L1 from *S. maltophilia* [87-90], FEZ-1 from *F. gormanii* [27], BJP-1 from *B. japonicum* [38], MIM-1 from *N. pentaromativorans* [91, 92], MIM-2 from *S. agarivorans* [91, 92], SMB-1 from *S. marcescens* [93], CAR-1 from *E. carotovora* [41] and THIN-B from *J. lividum* [44]. The recently proposed B4 subgroup is represented by SPR-1 from *S. proteamaculans* [23] and CSA-1 from *C. sakazaki* [14] (**Table 1.2.**).

B1-type MBLs have two peptide loops, L3 and L8, in the vicinity of the metal ion-containing active site (**Fig. 1.2**). These loops are believed to be crucial for the determination

Chapter 1: An Introduction to metallo- β -lactamases and their role in the bacterial resistance to antibiotics

of the substrate specificity of these enzymes [6]. In contrast, MBLs from the B2 subgroup lack the extended L3 loop. Instead these enzymes have a kinked α -helix positioned directly above the active site cleft [6, 94] (**Fig. 1.2**). This feature facilitates the formation of a narrow, well-defined substrate binding pocket. Consequently, these enzymes display a tighter selectivity for antibiotic substrates than other MBLs, hydrolysing only carbapenam substrates with high efficiency [6]. Of the three known representatives from this subgroup (**Fig. 1.2 and Table 1.2**), CphA is the most extensively studied [80-85, 95]. MBLs from the B3 subgroup also lack the extended L3 loop. However, they have an extra loop, located above the active site, which may also influence the substrate specificity of these enzymes. A preference for cephalosporins has been noted for this subgroup [6, 80]. Initially, SPR-1 from *S. proteamaculans* was also assigned to the B3 subgroup [23]. However, an analysis of its active site structure (**Fig. 1.4**), together with a homology sequence analysis has indicated that SPR-1 may represent the prototype of the B4 subgroup of MBLs [14, 23]. Its substrate preference is similar to that of the B3-type MBL L1 from *S. maltophilia* [23]; no crystallographic data for SPR-1 is currently available.

Differences at the sequence level are not the only characteristic features that distinguish the three major subgroups. The metal ion content and the role(s) of the metal ions in catalysis also vary between the subgroups [16, 96, 97]. The B1- and B3-type MBLs generally require two zinc ions to work optimally, while the MBLs of the B2 subgroup only require one zinc (located in the Zn2 site) to be catalytically active (**Fig. 1.4**). The presence of a second zinc ion (in the Zn1 site) diminishes or inhibits enzyme activity [16, 96]. For example, when fluorescence spectroscopy was used to monitor the protein fluorescence, the binding constants for the Zn1 and Zn2 sites are 0.62 nM and 1.5 μ M, respectively [48]. However, when the same binding interaction was studied using equilibrium dialysis,

Chapter 1: An Introduction to metallo- β -lactamases and their role in the bacterial resistance to antibiotics

corresponding values of 0.3 and 3 μM were reported [98] (**Table 1.3.**, **Table 1.4.**, **Table 1.5.** and **Table 1.6.**). Ignoring the variations of the magnitude of reported binding constants (which might be explained, at least in parts, by the use of different experimental conditions and/or different sensitivity of the technique used) the binding studies appear to be in agreement with the initial crystal structure of BcII: the two binding sites are distinct and possess different binding affinities. Moreover, it has been shown that the presence of the substrate can greatly enhance the affinity of the Zn1 binding site into the picomolar range, but have a modest effect on the affinity of the Zn2 site for the metal ion [99]. Since the physiological concentration of zinc in cells ranges from the femto- to the nanomolar range, the available metal ion binding constants suggest that BcII operates as mononuclear enzymes *in vivo* [99, 100]. The characterisation of an active mono-nuclear form of BcII was complicated by the observation that upon the addition of a single equivalent of zinc to apo-BcII a mixture of two monometallic species was formed [48, 49, 98, 101]. Nonetheless, when the activity was measured under saturating $[\text{Zn(II)}]$ condition, it doubled with respect to the mononuclear form of the enzyme, indicating that the catalytically optimal form of BcII is binuclear.

The differences between MBLs are evident even within the same subgroup. In fact, other well-studied B1-type MBLs, *e.g.* CcrA from *Bacteroides fragilis*, tightly binds two zinc ions [102] (**Table 1.3.**, **Table 1.4.**, **Table 1.5.** and **Table 1.6.**). Kinetic studies have shown that only the binuclear form of CcrA is catalytically active. Previously reported activity of a putative mononuclear form was in fact the activity arising from a mixture of the apo- and binuclear forms of the enzyme [103, 104].

Similarly to the B1 class, proteins belonging to the B3-type MBLs display optimal activity in the bimetallic form (**Table 1.3.**, **Table 1.4.**, **Table 1.5.** and **Table 1.6.**). Another

Chapter 1: An Introduction to metallo- β -lactamases and their role in the bacterial resistance to antibiotics

characteristic shared with the B1 class is their broad substrate specificity. Despite these functional similarities, B1- and B3-type MBLs share only minimal overall sequence homology (20% or less) [105, 106]. Well-studied representatives of the B3 class are the proteins L1 from *Stenotrophomonas maltophilia*, FEZ-1 from *Legionella gormanii* and BJP-1 from *Bradyrhizobium japonicum* [28, 39, 107, 108]. The majority of the currently known B3-type MBLs are believed to act as binuclear enzymes *in vivo*. The reported nanomolar affinities of their Zn1 and Zn2 sites support this hypothesis [28, 39, 107]. One notable exception is GOB-18 from *Elizabethkingia meningoseptica* which has maximum activity when only one zinc ion is bound to the Zn2 site [31, 109].

Chapter 1: An Introduction to metallo- β -lactamases and their role in the bacterial resistance to antibiotics

Table 1.3. List of the metal binding constant for the Zn1 and Zn2 sites, obtained using competitive assays. Binding constants for B1-type MBLs.

Enzyme	Substrate	K_{d1} nM Zn(II)	K_{d1} nM Cd(II)	K_{d2} μ M Zn(II)	K_{d2} μ M Cd(II)
BcII WT	No	0.6 (\pm 0.1) ^[48]	8.3 (\pm 0.5) ^[48]	1.50 (\pm 0.71) ^[48]	5.9 (\pm 1.0) ^[48]
	No	0.7 μ M ^[110]		890 μ M ^[110]	
	No	1.8 (\pm 0.3) ^[99]		1.8 (\pm 0.3) μ M ^[99]	
	No			> 80 nM ^[111]	
	Imipenem	13.6 (\pm 5) pM ^[99]		0.8 (\pm 0.2) μ M ^[99]	
H86S	No	5.3 (\pm 2.3) ^[48]	3.8 (\pm 0.3) ^[48]	0.3 (\pm 0.1) ^[48]	1.4 (\pm 0.1) ^[48]
H88S	No	0.4 (\pm 0.1) ^[48]		1.1 (\pm 0.2) ^[48]	
H149S	No	3.1 (\pm 0.1) ^[48]		0.2 ^[48]	
D90N	No	2.0 (\pm 0.4) ^[48]		5.0 (\pm 2.4) ^[48]	
C168S	No	0.6 (\pm 0.2) ^[48]		2.3 (\pm 0.6) ^[48]	
C168A	No	ND		ND	
H210S	No	0.4 (\pm 0.1) ^[48]		2.5 (\pm 0.5) ^[48]	
R121C	No	3.6 μ M ^[110]		570 μ M ^[110]	
BcII-HS	Nitrocefin			18 (\pm 12) μ M ^[112]	
BcII-HD	Nitrocefin			< 0.2 nM ^[112]	
BlaB	No	5.1 (\pm 1.5) nM ^[99]	0.007 (\pm 0.002) μ M ^[99]		
	Nitrocefin	1.8 (\pm 0.2) pM ^[99]	0.025 (\pm 0.004) μ M ^[99]		
NDM-1			2 μ M ^[113]		

Chapter 1: An Introduction to metallo- β -lactamases and their role in the bacterial resistance to antibiotics

Table 1.4. List of the metal binding constant for the Zn1 and Zn2 sites, obtained using competitive assays (continuation). Binding constants for B2- and B3-type MBLs.

Enzyme	Substrate	K _{d1} nM	K _{d1} nM	K _{d1} nM	K _{d1} nM	K _{d2} μ M	K _{d2} μ M	K _{d2} μ M	K _{d2} μ M
		Zn(II)	Cd(II)	Co(II)	Cu(II)	Zn(II)	Cd(II)	Co(II)	Cu(II)
CphA WT	No	7 (\pm 2) ^[95] pM (pH 6.5)	60 (\pm 10) pM ^[95] (pH 6.5)	220 (\pm 25) pM ^[95] (pH 6.5)	620 (\pm 55) pM ^[95] (pH 6.5)	40 (\pm 6) μ M ^[95] (pH 6.5)	82 (\pm 8) μ M ^[95] (pH 6.5)	>5 mM ^[95] (pH 6.5)	<10 μ M ^[95] (pH 6.5)
	No	6 (\pm 2) pM ^[95] (pH 7.5)	80 (\pm 72) pM ^[95] (pH 7.5)	330 (\pm 40) nM ^[95] (pH 7.5)	550 (\pm 58) nM ^[95] (pH 7.5)	10 (\pm 3) μ M ^[95] (pH 7.5)	4 (\pm 2) μ M ^[95] (pH 7.5)	500 (\pm 48) μ M ^[95] (pH 7.5)	<20 μ M ^[95] (pH 7.5)
	Imipenem	1.2 (\pm 0.2) pM ^[99]				1.9 (\pm 0.3) μ M ^[99]			
L1 WT	No	2.6 (\pm 1.0) nM ^[99]				0.006 (\pm 0.002) μ M ^[99]			
	Imipenem	5.7 (\pm 2.0) pM ^[99]				0.12 (\pm 0.03) μ M ^[99]			

Chapter 1: An Introduction to metallo- β -lactamases and their role in the bacterial resistance to antibiotics

Table 1.5. Dissociation constants of Co(II) for the Zn1 and Zn2 sites of wild type and mutant BcII, determined using absorption spectroscopy [48].

Enzyme	K_{d1} μM Co(II)	K_{d2} μM Co(II)
BcII WT	0.093 (\pm 0.015)	66.7 (\pm 10.0)
H86S	10.5 (\pm 1.5)	
H88S	9.1 (\pm 1.1)	
H149S	2.7 (\pm 0.3)	
D90N	20.0 (\pm 3.5)	
C168S	3.1 (\pm 0.4)	
C168A	1.1 (\pm 0.1)	
H210S	0.35 (\pm 0.05)	

Table 1.6. Second-order association rate constants of wild type BcII for the binding of Zn(II), Co(II) and Cd(II), followed by fluorescence spectroscopy [48].

Zn(II)		Co(II)		Cd(II)	
k_{on1} $\mu\text{M}^{-1}\text{s}^{-1}$	k_{on2} $\mu\text{M}^{-1}\text{s}^{-1}$	k_{on1} $\mu\text{M}^{-1}\text{s}^{-1}$	k_{on2} $\mu\text{M}^{-1}\text{s}^{-1}$	k_{on1} $\mu\text{M}^{-1}\text{s}^{-1}$	k_{on2} $\mu\text{M}^{-1}\text{s}^{-1}$
14.1 (\pm 0.3)		0.3 (\pm 0.01)		26.0 (\pm 1.3)	0.5 (\pm 0.01)

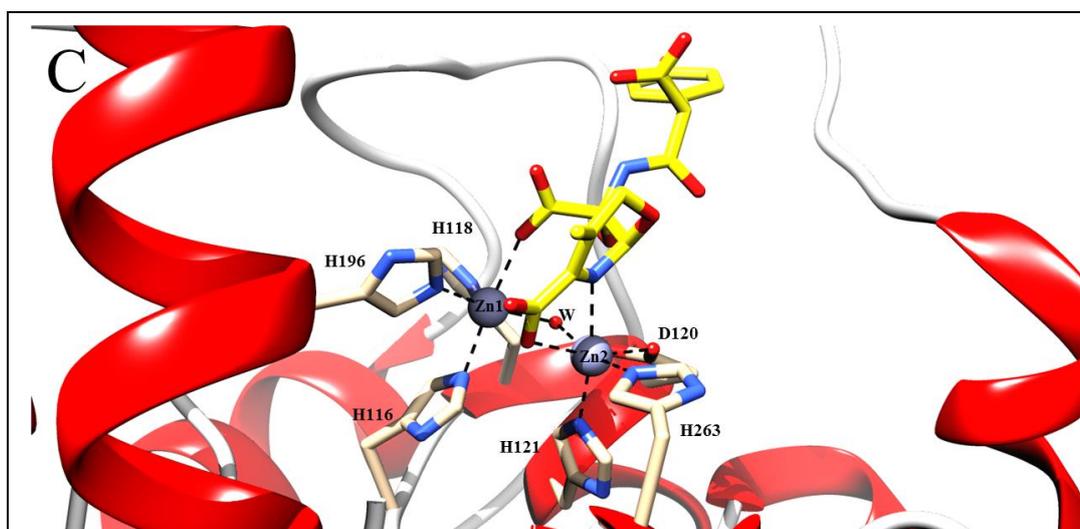
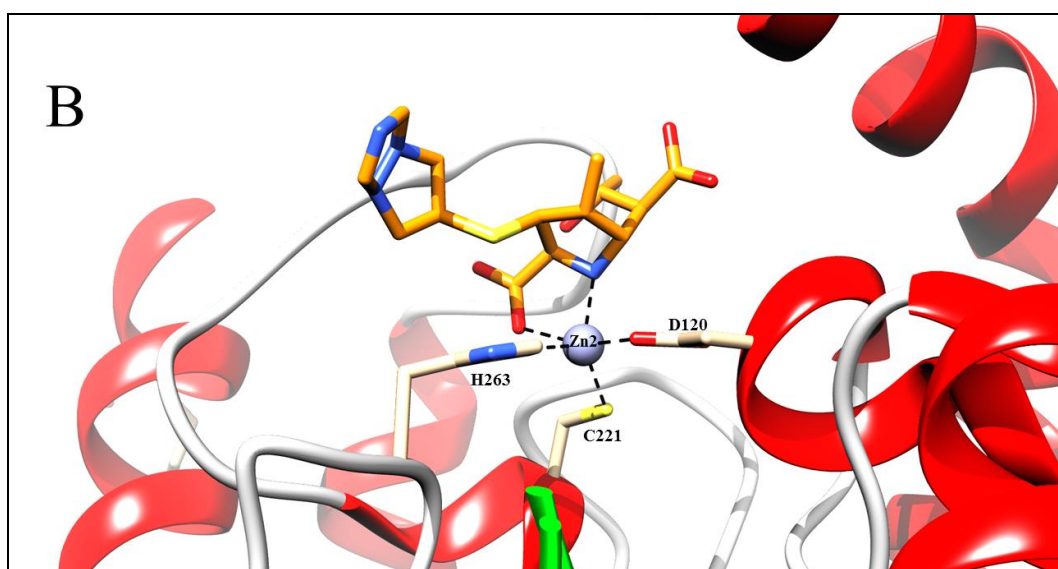
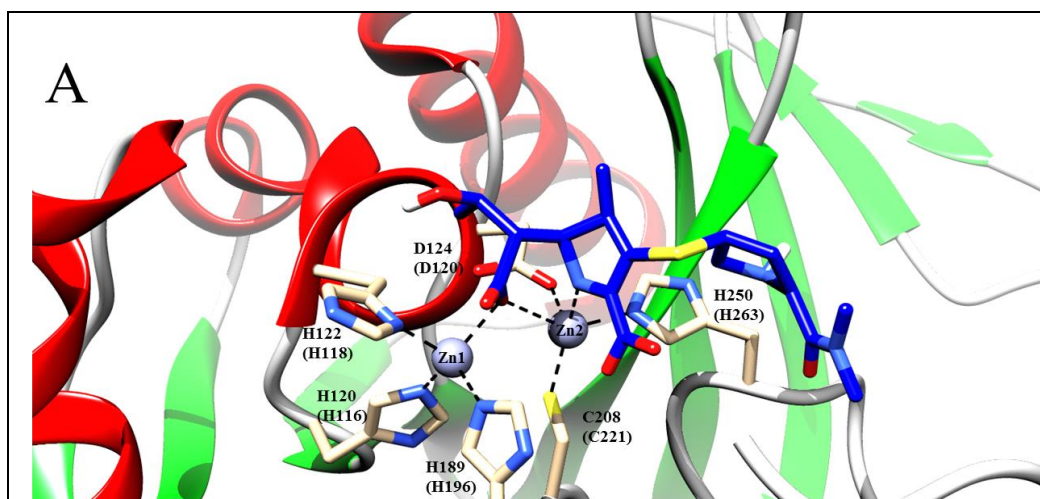
Chapter 1: An Introduction to metallo- β -lactamases and their role in the bacterial resistance to antibiotics

1.5 MBLs in details: B2 subgroup

B2-type MBLs require only one zinc ion coordinated to the Zn2 site for full catalytic activity [114] (**Table 1.3.**, **Table 1.4.**, **Table 1.5.** and **Table 1.6.**). When a second metal ion is bound to the Zn1 site, the activity is inhibited in a noncompetitive manner [115]. In contrast to the broad substrate specificity displayed by the B1 and B3 subclasses, the B2-type MBLs are strictly carbapenemase-specific [115]. Representatives of this group are ImiS from *Aeromonas sobria*, Sfh-1 from *Serratia fonticola*, and CphA from *A. hydrophila* [83, 116, 117].

The requirement for the B2-type MBLs for a mononuclear catalytically competent active site was supported by the crystal structure of CphA in complex with the substrate biapenem (**Figure 1.5.**). The crystal structure shows only one zinc bound to the Zn2 site [83]. Inhibition studies have led to the suggestion that when the Zn1 site is occupied by Zn(II), the catalytically relevant residues His118 and His196 are immobilized and the Gly232-Asn233 loop folds into the active site, thus occluding the entrance to the substrate [6, 86]. The affinities of the Zn1 and Zn2 sites have been investigated by competition experiments, using the chromophoric chelator quin-2; the Zn2 site has a very high affinity for zinc ($K_d < 10$ pM), whereas the inhibitory Zn1 site has a considerably weaker affinity (~ 46 μ M) for this metal ion [99, 115].

Chapter 1: An Introduction to metallo- β -lactamases and their role in the bacterial resistance to antibiotics



Chapter 1: An Introduction to metallo- β -lactamases and their role in the bacterial resistance to antibiotics

Figure 1.5 Comparison of the complexes formed with the substrates and B1-, B2- and B3 type MBLs (previous page). The figure shows the complex of NDM-1 from *K. pneumonia* with the substrate meropenem (blue) (PDB: 4EYL) [118], CphA from *A. hydrophylia* with the substrate biapenem (orange) (PDB: 1X8I) [83] and L1 from *S. maltophilia* with the substrate moxalactam (yellow) (PDB: 2AIO) [119]. The residues involved in the metal binding are shown coordinating the zinc ion present in the Zn² site (represented as a grey sphere). The substrates are bound to the active site and positioned via the metal ion coordination.

1.6 MBLs in details: B4 subgroup

Recently, the discovery of a putative novel MBL from *Serratia proteamaculans*, SPR-1, further highlighted the functional differences within the MBL family. Preliminary spectroscopic and kinetic investigation led to the observation that SPR-1 may be mononuclear in its resting state. Only in the presence of the substrate the catalytically active binuclear center is formed, providing the platform for a substrate-mediated regulatory mechanism [23]. A similar behaviour was observed for the organophosphate-degrading enzyme GpdQ, thus suggesting an evolutionary link between metalloenzymes with largely different biological functions [2].

The above discussion illustrates the diversity of various MBLs with respect to their interactions with their metal ion cofactors. Not surprisingly, the proposed reaction mechanisms employed by MBLs are equally flexible and have been shown to be influenced by a variety of factors including the source of the enzyme, the identity of the metal ion(s) bound to the active site and the substrate being turned over [22, 47, 56, 83, 108, 120]. However, the proposed models can be generally categorized as mono- and binuclear models and their overall features are briefly outlined in the following paragraphs.

Chapter 1: An Introduction to metallo- β -lactamases and their role in the bacterial resistance to antibiotics

1.7 Mono- and binuclear enzymes: two mechanisms, one reaction

The mononuclear reaction model has been proposed using BcII from *B. cereus* as representative of the MBL proteins (**Fig. 1.6.**). The substrate cefotaxim makes contact in the active site exploiting both the hydrogen bond network involving the second ligand sphere residues Asn223 and Lys224, and an hydroxide coordinated by the zinc ion (**Fig. 1.6.**) [46, 121]. This hydroxide is believed to initiate the nucleophilic attack on the β -lactam ring. It is oriented and stabilized by residues Asp120, Cys221 and His263, all Zn²⁺ ligands in the B1- and B3-type MBLs, and Arg121 [48, 73]. The role of these residues is to activate the nucleophile, while the metal ion acts as a Lewis acid, increasing the nucleophilicity of the hydroxide. The combination of these interactions has been shown, by pH-dependent kinetic studies, to reduce the pK_a of the nucleophilic water molecule from 15.7 to 5.6 [122]. Upon the nucleophilic attack a penta-coordinate transition-state may be formed, supported by computational but no experimental data to date [123]. The rate-limiting step is proposed to be the proton donation, from another Zn(II)-bound water molecule to the cyclic amide ring nitrogen [88] (**Fig. 1.6.**).

Chapter 1: An Introduction to metallo- β -lactamases and their role in the bacterial resistance to antibiotics

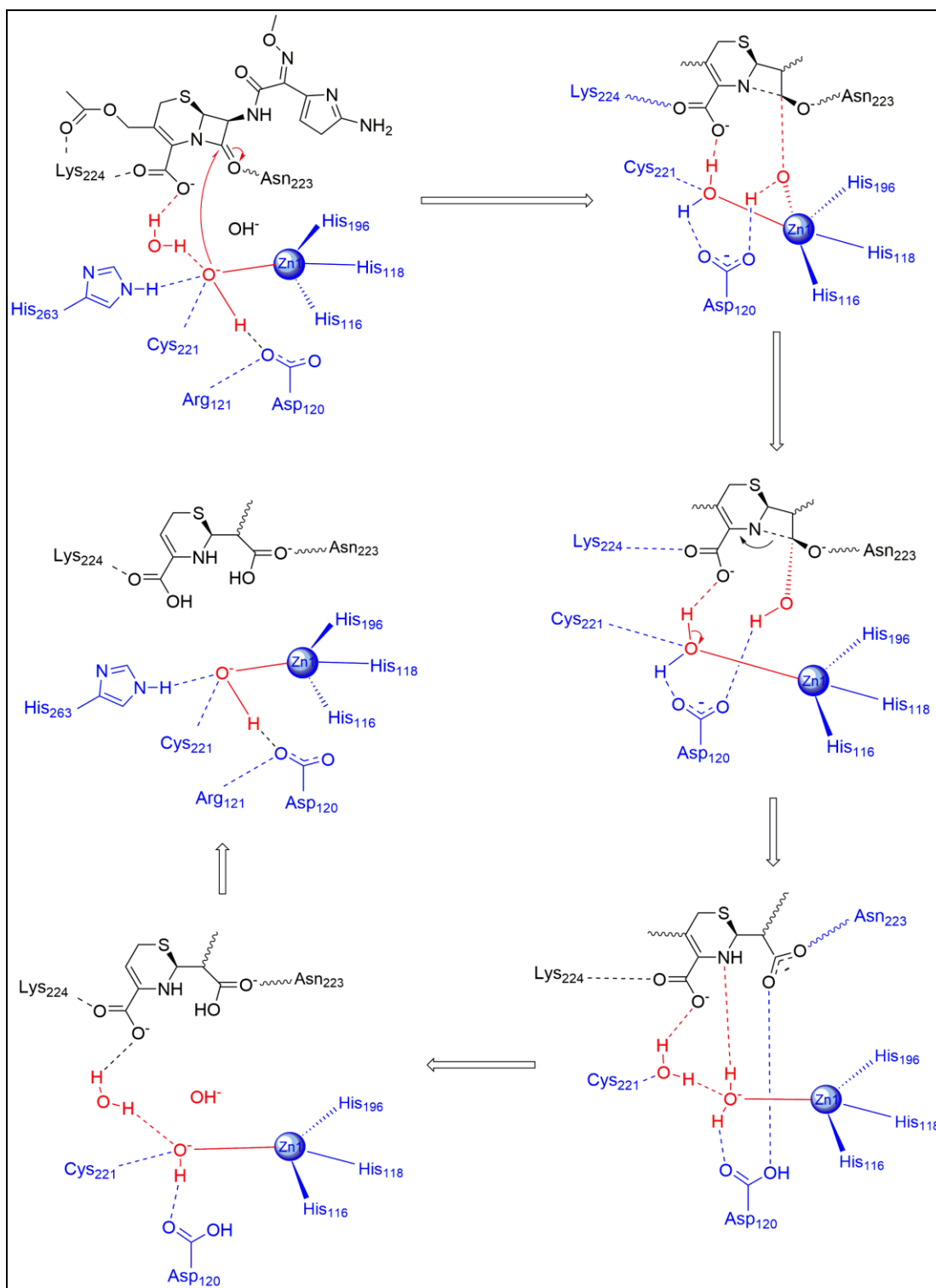


Figure 1.6. Mononuclear mechanism of β -lactam hydrolysis. Proposed reaction mechanism for mononuclear MBLs. The reaction is based on the crystal structure of monozinc BcII from *B. cereus*.

Chapter 1: An Introduction to metallo- β -lactamases and their role in the bacterial resistance to antibiotics

The reaction between cefotaxime and the enzyme CcrA from *B. fragilis* served as a model to probe the binuclear mechanism employed by MBLs. The major difference between the mono- and binuclear mechanisms resides in the lower activation barrier required by the latter to perform the reaction (**Figure 1.7**).

When the second zinc is involved, the catalytic mechanism follows a quicker and more efficient single-step reaction [123-126]. Both Zn(II) ions in the active site coordinate the nucleophilic hydroxide. The presence of the second zinc decreases the electrostatic interaction between the water molecule and the substrate but, on the other hand, is compensated by the double-Lewis acid activation (**Fig. 1.7**). Interestingly, it appears that the binuclear mechanism can occur in two alternative routes, one involving a tetrahedral reaction intermediate (*e.g.* NDM-1, L1, CcrA [127, 128]), and one involving no intermediate (*e.g.* Bla2). Furthermore, the B3-type MBL AIM-1 can utilize either route, although it is not yet understood what factors control the selection of the pathway [129].

Chapter 1: An Introduction to metallo- β -lactamases and their role in the bacterial resistance to antibiotics

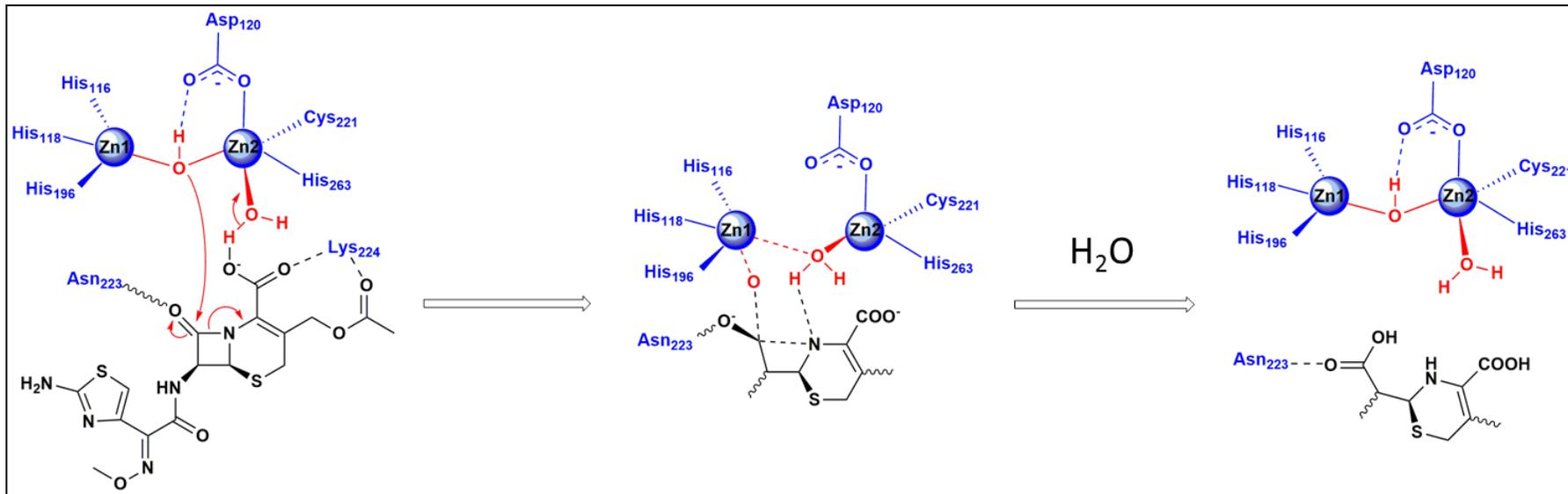


Figure 1.7. Dinuclear mechanism of β -lactam hydrolysis. Proposed reaction mechanism for dinuclear MBLs. The reaction is based on the crystal structure of di-zinc CcrA from *B. fragilis*.

Chapter 1: An Introduction to metallo- β -lactamases and their role in the bacterial resistance to antibiotics.

In conclusion, the higher reaction rates and efficiencies observed for the binuclear systems can be explained by the lower activation barrier for the nucleophilic attack on the amide ring carbonyl group, and the more efficient protonation mechanism for the leaving product (**Fig. 1.7.**) [123]. When looking at the entire MBL family, their rapid evolution can be partially explained by the evolutionary pressure to which these enzymes were subjected. Indeed, the uncontrolled usage of new antibiotics would have greatly accelerated this process, facilitating the appearance of many varieties of MBLs. Novel MBL-like proteins are frequently discovered that already contain an inherent ability to degrade a broad range of antibiotics via different mechanisms, using alterations of the same three-dimensional scaffold, with different metal ion requirements and different substrate-coordinating residues [21, 47, 98, 109, 117, 123, 130]. It is possible that MBLs emerged from a range of progenitor enzymes that may have rather diverse and unrelated functions. This may explain why some MBLs are strictly mono-metallic, others are mono- and bimetallic and yet another group could be activated by converting a monometallic centre into a bimetallic one (see the discussion in the previous sections). The observed mechanistic versatility of the various members of the MBL family may also be a major, if not the major reason why it has been proven so difficult to establish clinically useful universal MBL inhibitors as drug leads to combat antibiotic resistance [20]. Developing an understanding of the factors that contribute to the mechanistic diversity among the MBLs is thus an important task in order to design new drugs to stop the spread of antibiotic resistance.

Chapter 1: An Introduction to metallo- β -lactamases and their role in the bacterial resistance to antibiotics.

1.8 Conclusions

MBLs have emerged as a major threat to global health. They inactivate an increasing number of commonly used antibiotics and spread easily among various pathogens on mobile genetic elements. Crystal structures for several MBLs have been determined and an extensive amount of information about their biochemical properties has been accumulated. Some potent *in vitro* inhibitors of MBLs have also been detected. However, to date none of the available MBL inhibitors are of clinical use. The search for universal and clinically applicable MBL antagonists is still very much at the beginning.

This search is complicated further by the fact that MBLs are able to mutate rapidly and thus evade inhibition. This large mutational space is illustrated by the small degree of sequence and structure conservation in the substrate binding pockets of various MBLs; accordingly, their substrate preference and response to potential inhibitors can vary considerably. Thus, new strategies to comprehensively inhibit MBLs are needed. The main common aspect of their function is their requirement for metal ions, one (in the Zn²⁺ site) for B₂-type MBLs, and mostly two in the remaining ones (see discussion above). It is thus surprising that the precise role(s) of metal ions in the catalytic mechanism of MBLs, and in particular their binding interactions in the active sites are still obscure. It appears unlikely that the metal ion binding site can afford a large mutational degree of freedom - metal ion affinities are expected to be severely affected by most changes in their coordination environment. Hence, it is possible to propose that universal MBL inhibitors that may retain their effect long-term should target the metal ion binding site. It is thus essential to investigate and compare metal binding interactions among different MBLs under experimentally well-defined and conserved conditions. A detailed characterisation of comparative metal ion affinities in various MBLs will provide essential information to design and develop

Chapter 1: An Introduction to metallo- β -lactamases and their role in the bacterial resistance to antibiotics.

compounds that effectively interfere with metal ion binding in these enzymes. Such compounds are not expected to be affected by mutations as significantly as molecules that compete with substrates, and hence they may prove to be highly useful as clinical chemotherapeutics in the fight against antibiotic resistance.

This thesis and the research project behind it started from the belief that understanding the role of the metallic centre for MBL function(s) is crucial to design strategies to effectively inhibit their catalytic action. In order to fully comprehend the role(s) of the metal ions in the mechanisms employed by MBLs two major questions need to be addressed: (i) how many metal ions bind under resting conditions, (ii) how many metal ions are required to achieve maximal activity and can this change depending on the substrate or other experimental or environmental (*i.e.* physiological) conditions, including changes in pH or temperature?

The aim of this thesis is to address these questions, focusing on two recently discovered MBL-like proteins isolated from non-pathogenic, marine bacteria (see Chapter 2). In my studies I deliberately focused on two MBL-like proteins that already have the capability to degrade antibiotics without having experienced evolutionary pressures to do so. These enzymes may thus provide clues about intrinsic factors that constitute the minimal requirements for enzymes to have MBL-like activities. The two proteins were identified by a sequence homology search and are from now on referred to as **Maynooth IMipenemases 1 and 2**, *i.e.* MIM-1 and MIM-2.

Chapter 2: Identification and preliminary characterization of novel B3-type metallo- β -lactamases

American Journal of Molecular Biology, 2013, 3, 198-203 **AJMB**
<http://dx.doi.org/10.4236/ajmb.2013.34026> Published Online October 2013
(<http://www.scirp.org/journal/ajmb/>)

Identification and preliminary characterization of novel B3-type metallo- β -lactamases

Manfredi Miraula^{1,2}, Conor S. Brunton¹, Gerhard Schenk², Nataša Mitić¹

¹Department of Chemistry, National University of Ireland—Maynooth, Maynooth, Co., Kildare, Ireland ²School of Chemistry and Molecular Biosciences, The University of Queensland, Brisbane, Australia Email: schenk@uq.edu.au, natasa.mitic@nuim.ie

Received 30 May 2013; revised 23 June 2013; accepted 9 July 2013

Copyright © 2013 Manfredi Miraula *et al.* This is an open access article distributed under the Creative Commons Attribution License, which permits unrestricted use, distribution, and reproduction in any medium, provided the original work is properly cited.

ABSTRACT

Antibiotic resistance has emerged as a major global threat to human health. Among the strategies employed by pathogens to acquire resistance the use of metallo- β -lactamases (MBLs), a family of dinuclear metalloenzymes, is among the most potent. MBLs are subdivided into three groups (*i.e.* B1, B2 and B3) with most of the virulence factors belonging to the B1 group. The recent discovery of AIM-1, a B3-type MBL, however, has illustrated the potential health threat of this group of MBLs. Here, we employed a bioinformatics approach to identify and characterize novel B3-type MBLs from *Novosphingobium pentaromativorans* and *Simiduia agarivorans*. These enzymes may not yet pose a direct risk to human health, but their structures and function may provide important insight into the design and synthesis of a still elusive universal MBL inhibitor.

Keywords: Antibiotic Resistance; β -Lactam Antibiotics; Metallo- β -Lactamases; Sequence Homology; *Novosphingobium Pentaromativorans*; *Simiduia Agarivorans*

Chapter 2: Identification and preliminary characterization of novel B3-type metallo- β -lactamases.

2.1 Introduction

The introduction of β -lactam antibiotics (**Fig. 1.2. - Chapter 1**) in the 1940s has been considered as a breakthrough, if not the most significant breakthrough in the history of medicine. However, after only a few years penicillin resistance was observed in *Staphylococcus aureus* and meanwhile a large and increasing number of pathogens have acquired resistance to the most commonly used antibiotics [131, 132], triggering some experts to link antibiotic resistance to terrorism in terms of its global impact (<http://www.bbc.co.uk/news/health-21737844>). As outlined in Chapter 1, one of the most frightening forms of antibiotic resistance occurs through the action of MBLs, enzymes which are capable of breaking down most widely used β -lactam antibiotics [18, 132, 133]. The common features of MBLs were described in Chapter 1 [6, 18, 132, 134]. Most of the known MBL virulence factors belong to subgroup B1 and include BcII from *B. cereus* [46], CcrA from *B. fragilis* [102], as well as IMP-1 and SPM-1, both initially identified in *P. aeruginosa* [56, 135] (**Table 1.2.**). The recently identified NDM-1 (“New Delhi Imipenemase-1”) has acquired particular notoriety as it induces resistance to virtually all known β -lactam antibiotics [113]. Subgroup B2 enzymes share only ~11% sequence homology with B1-type MBLs, hydrolyse exclusively carbapenems (*e.g.* meropenem and imipenem) and require only one metal ion for catalysis [18, 95] (see Chapter 1, section 1.5, for more detailed information) [82, 116, 136]. Subgroup B3 is more closely related to B1-type MBLs rather than B2-type MBLs, requiring two bound metal ions for catalysis (**Fig. 1.4.** and **Fig 1.5** in Chapter 1). The most studied representative is the tetrameric L1 from *S. maltophilia* [107]. Other members include FEZ-1 from *L. gormanii* [28], GOB-1 from *E. meningoseptica* (of which to date 18 variants have been reported) [137] and SMB-1 from *S. marcesens* [34], the most recently identified MBL, which has a higher hydrolytic activity against a wide range of β -lactams than

Chapter 2: Identification and preliminary characterization of novel B3-type metallo- β -lactamases.

other B3-type MBLs [34]. Of clinical relevance in particular is the enzyme AIM-1 from *P. aeruginosa*, which has been identified recently in a multi-drug resistant pathogen in a hospital in Adelaide, Australia (hence, the nomenclature of “Adelaide Imipenemase-1”—AIM-1) [138].

Despite rather modest homology across their full length amino acid sequences MBLs share considerable similarities in their active site structures [18]. For more details regarding the metal ion compositions of the different subgroups refer to Chapter 1 (**Fig. 1.4.**, and **Table 1.1.**). As stated in the introductory chapter, the standard MBL numbering will be applied throughout the thesis [6, 139, 140]. In light of the rapid spread of antibiotic resistance and the increasing emergence of novel virulence factors (exemplified by NDM-1 and AIM-1), it is essential to identify novel putative MBLs, ideally before they become a threat to health care. Furthermore, novel MBLs may also provide essential insight into the structure and/or functional aspects relevant to the design and synthesis of universal inhibitors that may be clinically useful to combat antibiotic resistance. This chapter is focused on the discovery of two novel putative MBLs. specifically, a bioinformatics approach was employed to identify novel B3-type MBLs from *Novosphingobium pentaromativorans* and *Simiduia agarivorans*, two marine microorganisms that would have had minimal direct contact with the human population [141, 142]. These enzymes may not yet pose a direct risk to human health, but their structures and function may provide important insight into the design and synthesis of a still elusive universal MBL inhibitor.

2.2 Materials and Methods

2.2.1 Selection of the Query Sequence and Protein Database Search Using BLAST

The B3-type AIM-1 from *P. aeruginosa* was used as a query sequence for the protein database search. The protein sequence of AIM-1 was obtained from the Protein Data Bank (PDB; accession code: 4AWY), and the Basic Local Alignment Search Tool (BLAST; <http://blast.ncbi.nlm.nih.gov/Blast.cgi>) was used to identify homologues. The two most promising candidates, from *Novosphingobium pentaromativorans* and *Simiduia agarivorans*, were selected for multiple sequence comparisons including known B3-type MBLs.

2.2.2 Multiple Sequence Alignments

Multiple sequence alignments including the novel B3-type MBLs and well known members of this group of enzymes (*i.e.* AIM-1 [138], L1 [107] and SMB-1 [34]) were carried out using ClustalW2, a multiple sequence alignment program, available via The European Bioinformatics Institute website (<http://www.ebi.ac.uk/Tools/msa/clustalw2/>).

2.3. Results and Discussion

2.3.1. Protein Database Search, Nomenclature and Classification of Novel MBLs

Using the BLAST search engine with AIM-1 as the query two promising candidate sequences were retrieved, *i.e.* MBL-like sequences from *N. pentaromativorans* (accession code: ZP_09194167.1) and *S. agarivorans* (accession code: YP_006917856.1). These microorganisms are both Gram-negative.

Chapter 2: Identification and preliminary characterization of novel B3-type metallo- β -lactamases.

N. pentaromativorans is a poly-cyclic aromatic hydrocarbon-degrading bacterium [141], while *S. agarivorans* is a heterotrophic marine bacterium [142]. None of these organisms poses a direct current threat to human health, however, the observation that they harbour a potential MBL may not only foreshadow a future problem as they may represent a genetic “pool” for future modifications of MBLs that may enhance both their reactivity and evasiveness towards inhibition. It is thus essential to investigate the properties of these novel MBL-like proteins and compare them with those of well-known MBLs (e.g. AIM-1, L1 or SMB-1).

As a step towards their characterization, the sequences of the *N. pentaromativorans* and *S. agarivorans* MBL-like proteins were compared with those of well-characterized MBLs from the B3 subgroup, *i.e.* AIM-1 [138], L1 [107] and SMB-1 [34]. The results from pairwise sequence comparisons are summarized in **Table 2.1**. Not surprisingly, the two sequences are most closely related to AIM-1. The MBL-like protein from *N. pentaromativorans* shares 53% sequence identity and 65% homology (including conserved amino acid substitutions) with AIM-1. The sequence identity/homology to the other two well characterized B3-type MBLs, L1 and SMB-1, is smaller (38%/54% and 41%/58%, respectively) but still strongly indicative that the *N. pentaromativorans* protein is indeed a B3-type MBL. In comparison, pairwise sequence comparisons with the B1-type NDM-1 and B2-type CphA indicate only 26%/39% and 23%/42%, respectively. A similar conclusion can be drawn for the MBL-like sequence from *S. agarivorans*. Its similarity/homology with AIM-1 (47%/64%) is less than that of the *N. pentaromativorans* MBL, but it appears to be more closely related to SMB-1 instead (**Table 2.1**). The two MBL-like proteins share 47%/63% identity/homology in a direct pairwise sequence comparison. In summary, these pairwise comparisons strongly support the classification of these novel proteins sequences from *N. pentaromativorans* and *S. agarivorans* as MBLs from the B3 subgroup. In accordance with frequently applied

Chapter 2: Identification and preliminary characterization of novel B3-type metallo- β -lactamases.

nomenclature procedures (e.g. “Adelaide IMipenemase-1” or AIM-1) the MBL-like sequences from *N. pentaromativorans* and *S. agarivorans* are labeled here “Maynooth IMipenemase-1” (MIM-1) and “Maynooth IMipenemase- 2” (MIM-2), respectively.

Table 2.1. Pairwise sequence comparison between MBL-like sequences from *N. pentaromativorans* (MIM-1) and *S. agarivorans* (MIM-2) and selected MBLs from the B1 (NDM-1), B2 (CphA) and B3 (AIM-1, L1, SMB-1) subgroups.

	MBL	Identity (%)	Homology (%)
MIM-1	AIM-1	53	65
	L1	38	54
	SMB-1	41	58
	NDM-1	26	39
	CphA	23	42
MIM-2	MIM-1	47	63
	AIM-1	47	64
	L1	33	51
	SMB-1	43	63
	NDM-1	37	59
	CphA	24	44

2.3.2. Important Amino Acid Residues

The above discussion demonstrated that the MBL-like sequences in the genomes of *N. pentaromativorans* and *S. agarivorans* are likely members of the B3 subgroup in the MBL family. However, in order to substantiate this interpretation, it is essential to ascertain whether amino acid residues that are essential for MBL function are conserved in the amino acid sequences of MIM-1 and MIM-2. The most relevant amino acid residues with respect to MBL function are those that form the metal binding site. Other residues in the proximity of the metal ion binding sites may be important for substrate or inhibitor binding or both. In order to

Chapter 2: Identification and preliminary characterization of novel B3-type metallo- β -lactamases.

evaluate the functionality of MIM-1 and MIM-2 a multiple sequence alignment between these sequences and the structurally well-characterized AIM-1 [138], L1 [107] and SMB-1 [34] was carried out (**Figure 2.1**).

Importantly, the six amino acids that form the metal ion binding site are also invariant in both MIMs (*i.e.* His116, His118 and His196 in the Zn1 site and Asp120, His121 and His263 in the Zn2 site; see also **Fig. 2.1**). Other amino acid side chains that were identified as important in MBL function are well conserved, including those in positions 221 (Ser) and 223 (Ser/Thr) that line the pocket where the β -lactam substrate may bind [18]. Tyr228, a residue that aids the polarization of the β -lactam carbonyl oxygen as a means to increase the susceptibility of the carbonyl bond for a nucleophilic attack by the “bridging” hydroxide is conserved in all MBLs compared here except AIM-1 (**Fig. 2.1**). Conserved is also Trp39, another residue that has been shown to play an important role in substrate binding [143]. Furthermore, in AIM-1 and to a large extent SMB-1 (but not L1) the structure of the enzyme is stabilized by the presence of three disulphide bridges (*i.e.* the pairs Cys32-Cys66, Cys208-Cys213 and Cys256-Cys290 [34, 138]). These six cysteine residues are conserved in both MIM-1 and MIM-2, suggesting that these enzymes possess a similar overall fold as AIM-1 and SMB-1.

Some observed sequence variations may, however, deserve mentioning here as they may be significant for differences in substrate preference, inhibitor binding and/or catalysis (see also Chapters 3 and 4). The region between residues 152 and 164 forms a flexible loop that may clamp down on the bound substrate and thus assist catalysis [18]. In this loop, the degree of sequence conservation is low (**Fig. 2.1**) which may indicate variations in substrate selection, catalytic efficiency and possibly also interactions with potential enzyme inhibitors.

Chapter 2: Identification and preliminary characterization of novel B3-type metallo-β-lactamases.

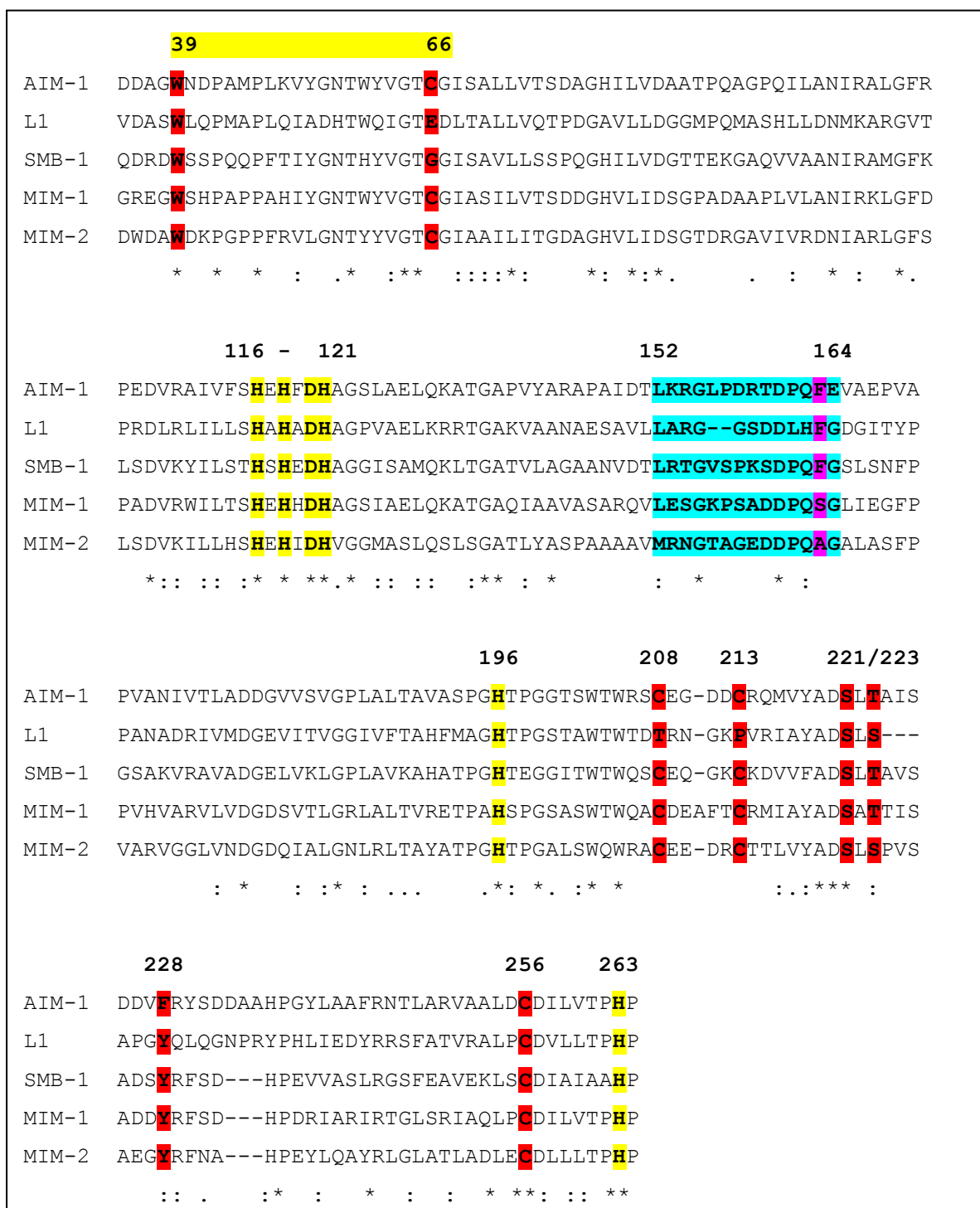


Figure 2.1. Multiple sequence alignment between known (AIM-1, L1 and SMB-1) and putative (MIM-1 and MIM-2) B3-type MBLs. Amino acid side chains involved in Zn²⁺ binding are shown in yellow. Other relevant residues are also indicated in colour and described in the text.

Chapter 2: Identification and preliminary characterization of novel B3-type metallo- β -lactamases.

While there is currently no clinically useful MBL inhibitor available, mercaptoacetates (MCRs) are known to be potent *in vitro* inhibitors of some MBLs [144]. A recent crystallographic study with SMB-1 has shown that MCR interacts with active site residues Ser221 and Thr223 and has a $K_i = 9.4 \pm 0.4 \mu\text{M}$ (**Fig. 2.1.**) [34]. MIM-1 and AIM-1 have a sequence identical to that of SMB-1 in this so-called “MCR binding” region, whereas L1 and MIM- 2 have a Ser instead of Thr. Although this represents a conserved substitution, it may nonetheless be of significance as the different sizes of these side chains may affect the modes of substrate/inhibitor binding. Of particular interest may also be the residue in position 162, occupied by the bulky and nonpolar Phe residue in AIM-1, L1 and SMB-1, but by the small and polar Ser in MIM-1 and the small and nonpolar Ala in MIM-2. This residue lies within the flexible loop mentioned in the previous paragraph and may thus play an essential role in substrate and inhibitor binding.

It is essential to characterize the properties of these novel B3-type MBLs to determine which of these variations are functionally relevant and in particular which of those may affect the mode and magnitude of inhibition by known inhibitors (such as MCR). Ultimately, it is anticipated that the functional and structural comparison of a multitude of related MBLs will identify residues that are suitable targets to develop universally applicable inhibitors that may be resistant to frequent mutational changes characteristic of this family of enzymes. Consequently, the following chapters focus on the enzymatic characterization of MIM-1 and MIM-2.

Chapter 2: Identification and preliminary characterization of novel B3-type metallo- β -lactamases.

2.4. Conclusion

The main finding of this study is the identification of two novel MBLs from *N. pentaromativorans* (MIM-1) and *S. agarivorans* (MIM-2) that belong to the B3 sub-group of this family of enzymes. Both proteins containing the amino acid ligands necessary to bind two zinc ions in their active sites and various residues in the vicinity of the catalytic centre are invariant or highly conserved, indicating that MIM-1 and MIM-2 should be efficient catalysts for the hydrolysis of β -lactam antibiotics. While MIM-1 and MIM-2 are not expected to represent an immediate threat to human health, they may harbour information that is crucial for 1) our understanding of the reaction mechanism(s) that MBLs may employ; and 2) the development of universal MBL inhibitors that are resistant to frequent mutational variations observed among members of this family of enzymes. This study is an initial step towards the characterization of these novel MBLs. Their recombinant expression and purification, as well as their catalytic and structural characterization are described in the chapters that follow.

Chapter 3: β -Lactam antibiotic-degrading enzymes from non-pathogenic marine organisms: a potential threat to human health

J Biol Inorg Chem (2015) 20:639–651 DOI 10.1007/s00775-015-1250-x

ORIGINAL PAPER

β -Lactam antibiotic-degrading enzymes from non-pathogenic marine organisms: a potential threat to human health

Manfredi Miraula^{1,2} · Jacob J. Whitaker² · Gerhard Schenk² · Nataša Mitic¹

Received: 15 January 2015 / Accepted: 2 March 2015 / Published online: 14 March 2015 © SBIC 2015

Abstract Metallo- β -lactamases (MBLs) are a family of Zn(II)-dependent enzymes that inactivate most of the commonly used β -lactam antibiotics. They have emerged as a major threat to global healthcare. Recently, we identified two novel MBL-like proteins, Maynooth IMipenemase-1 (MIM-1) and Maynooth IMipenemase-2 (MIM-2), in the marine organisms *Novosphingobium pentaromativorans* and *Simiduia agarivorans*, respectively. Here, we demonstrate that MIM-1 and MIM-2 have catalytic activities comparable to those of known MBLs, but from the pH dependence of their catalytic parameters it is evident that both enzymes differ with respect to their mechanisms, with MIM-1 preferring alkaline and MIM-2 acidic conditions. Both enzymes require Zn(II) but activity can also be reconstituted with other metal ions including Co(II), Mn(II), Cu(II) and Ca(II). Importantly, the substrate preference of MIM-1 and MIM-2 appears to be influenced by their metal ion composition. Since neither *N. pentaromativorans* nor *S. agarivorans* are human pathogens, the precise biological role(s) of MIM-1 and MIM-2 remains to be established. However, due to the similarity of at least some of their *in vitro* functional properties to those of known MBLs, MIM-1 and MIM-2 may provide essential structural insight that may guide the design of as of yet elusive clinically useful MBL inhibitors.

Electronic supplementary material The online version of this article (doi:[10.1007/s00775-015-1250-x](https://doi.org/10.1007/s00775-015-1250-x)) contains supplementary material, which is available to authorized users.

Keywords Antibiotic resistance · β -Lactam antibiotics · Metallo- β -lactamase · Metallohydrolase · Catalysis

Chapter 3: β -Lactam antibiotic-degrading enzymes from non-pathogenic marine organisms: a potential threat to human health

3.1 Introduction

As discussed in Chapter 1, one of, if not the most poignant problem for current global healthcare, is the rise of antibiotic-resistant microorganisms. In brief, since the 1940s antibiotics have been used to fight infections, initially with the β -lactam-based penicillin, and subsequently with various of its derivatives, including cephalosporins, cephamycins, carbapenems and monobactams (**Figure 1.2 – Chapter 1**). These compounds share a common core structure represented by the four-membered β -lactam ring. A major defence strategy employed by pathogens is to enzymatically hydrolyse this β -lactam ring, thus inactivating the antibiotics [19, 132, 145]. Two main enzyme groups have evolved for this purpose, the serine β -lactamases (SBLs) and the metallo- β -lactamases (MBLs). Clinically useful inhibitors are currently only available for SBLs [19, 20]; MBLs consequently remain a major threat to human health. In addition, the ability of MBLs to spread easily between species, mainly through horizontal gene transfer, further exacerbates the risk of generating multi-drug resistant pathogens [146-148].

The task to develop universally and clinically useful MBL inhibitors is exacerbated by the continuous emergence of novel MBLs, exemplified by the broad-spectrum enzyme NDM-1 [75, 113], and the frequent tolerance of a particular MBL to mutations as illustrated by the multiple variants of enzymes such as the NDM, IMP or VIM groups [58, 68]. Furthermore, the discovery of genes encoding MBL-like proteins in microorganisms that are not pathogenic and/or have not been exposed to the human population (*e.g.*, the MBL-like proteins identified in microorganisms in the frozen Alaskan tundra [149]) may harbour clues about functionally essential elements that contribute to MBL activity. Identifying such elements may thus provide an alternative avenue to developing potent MBL inhibitors. In a recent study (see Chapter 2), we thus attempted to identify novel putative MBLs from non-pathogenic hosts

Chapter 3: β -Lactam antibiotic-degrading enzymes from non-pathogenic marine organisms: a potential threat to human health

and identified MIM-1 from *N. pentaromativorans* and MIM-2 from *S. agarivorans* [91]. Little is known about these microorganisms, but both are Gram-negative bacteria found in marine environments [141, 142]. *N. pentaromativorans* is a poly-cyclic aromatic hydrocarbon-degrading bacterium, while *S. agarivorans* is a heterotrophic bacterium; neither of these organisms is pathogenic [141, 142]. This Chapter will demonstrate the propensity of these enzymes to act as efficient MBLs and also how different metal ion compositions may affect the substrate preference of these enzymes, and thus potentially also their biological function(s).

3.2 Materials and Methods

3.2.1 Materials

The sequences encoding MIM-1 and MIM-2 were cloned into the commercial vector pJ411 – the gene encoding MIM-1 and MIM-2 genes were commercially synthesized and bought as an expression vector from the company DNA 2.0. All chemicals were of analytical or equivalent grade. *Escherichia coli* BL21 (DE3) pLysS cells (Agilent) were used for recombinant expression of the proteins. All chemicals were purchased from Sigma-Aldrich unless stated otherwise.

3.2.2 Protein expression and purification

Recombinant MIM-1 and MIM-2 were expressed using Luria–Bertani (LB) medium supplemented with 0.2 mM Zn(II) and 1 % glucose. The cultures were grown at 37 °C until an optical density (OD₆₀₀) of 0.4–0.5 was reached, and then cooled to 18 °C (MIM-1) or 25

Chapter 3: β -Lactam antibiotic-degrading enzymes from non-pathogenic marine organisms: a potential threat to human health

$^{\circ}\text{C}$ (MIM-2) prior to induction with 0.2 mM isopropyl β -d-1-thiogalactopyranoside (IPTG). The cultures were further incubated for 48 h (MIM-1) and 18 h (MIM-2), respectively. The purification protocols for MIM-1 and MIM-2 are similar. The cells were harvested by centrifugation at 5000g for 20 min at 4 $^{\circ}\text{C}$. The resulting pellet was resuspended in 15–20 mL of buffer containing 20 mM Tris (HCl; pH 7.0) and 0.15 mM ZnCl_2 . To improve the lysis step, lysozyme (1 mg/mL) was added to the resuspended cells, followed by incubation at room temperature for 30 min. Subsequently, DNase (20 $\mu\text{g}/\text{mL}$) and MgCl_2 (5 mM) were added and the mixture was kept on ice for 20 min. The cells were then disrupted using five rounds of sonication (60% of the maximal output power for 30 s in each round). The procedure was carried out on ice to avoid overheating of the cells. The lysate was centrifuged at 20,000g for 30 min and 4 $^{\circ}\text{C}$, and then filtered through a 0.22 μm membrane (Millipore) to remove remaining debris. The supernatant was loaded onto a HiTrap Q FF 5 mL column (GE Healthcare), pre-equilibrated with 20 mM Tris (HCl; pH 7.0) and 0.15 mM ZnCl_2 . Proteins were eluted using a linear gradient from 0 to 0.5 M NaCl. MIM-1 eluted between 55 and 175 mM of NaCl, while MIM-2 eluted between 35 and 135 mM of NaCl. The fractions possessing ampicillinase activity were pooled and loaded onto a HiPrep 16/60 Sephacryl S-200 HR column (GE Health-care), pre-equilibrated with 50 mM Hepes (pH 7.5) containing 0.2 M NaCl and 0.15 mM ZnCl_2 . Both proteins eluted as single peaks. SDS-PAGE analysis indicated that the purity of the enzymes is >95 % (**Figure 3.1. SDS-PAGE**). The protein concentrations were estimated using theoretical (calculated) extinction coefficients ($\epsilon_{280} = 36,815 \text{ M}^{-1}\text{cm}^{-1}$ for MIM-1 and $41,285 \text{ M}^{-1}\text{cm}^{-1}$ for MIM-2), calculated from the sequence using the ProtParam webtool (<http://web.expasy.org/protparam/>).

Chapter 3: β -Lactam antibiotic-degrading enzymes from non-pathogenic marine organisms: a potential threat to human health

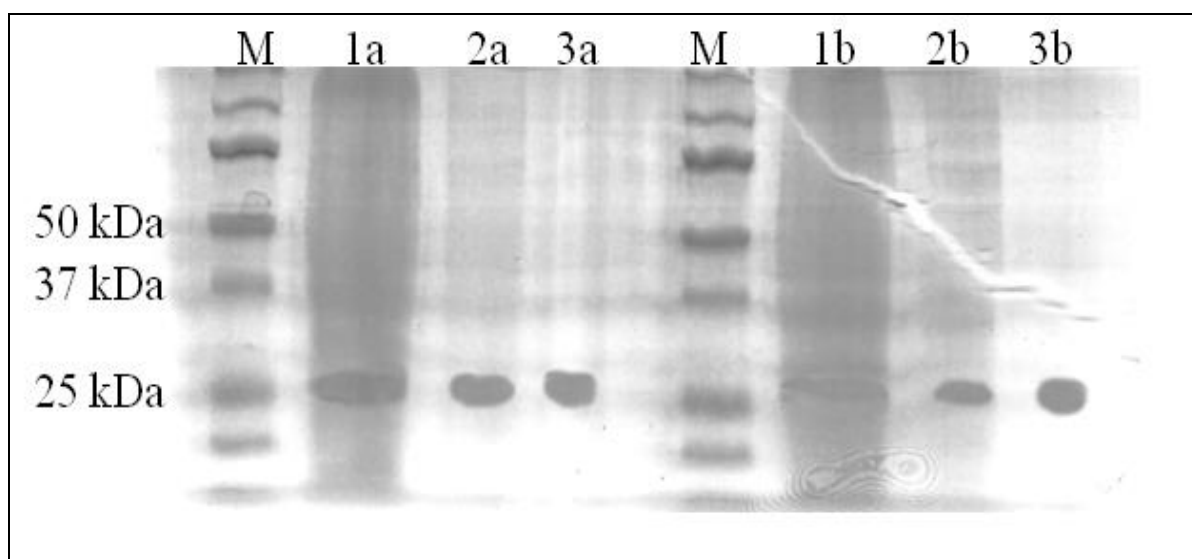


Figure 3.1. SDS-PAGE of MIM-1 and MIM-2. Lane 1a was loaded with the total protein fraction, 2a and 3a were loaded with the sample eluted after the anion exchange and after the size exclusion, respectively after MIM-1 purification. Lane 1b contains the total protein fraction, 2b and 3b contain the sample collected during MIM-2 purification after the anion exchange and the size exclusion, respectively. M denotes the molecular weight markers.

Both proteins are stable at 4 °C for at least two months (stored at a concentration of 10–20 mg/mL). To assess the molecular weight and the oligomeric state of the proteins in solution, MIM-1 and MIM-2 (2 mg/mL) were loaded onto a gel filtration column, HiPrep 16/60 Sephacryl S-200 HR (GE Healthcare), pre-equilibrated with 50 mM HEPES (pH 7.5), 0.2 M NaCl, 0.15 mM ZnCl₂. The calibration curve (**Figure 3.2.**) was obtained using the Low Molecular Weight standards kit (GE Healthcare).

3.2.3 Steady-state kinetics and substrate specificity of Zn-containing MIM-1 and MIM-2

The β -lactamase activity of the proteins towards different substrates was measured spectrophotometrically by monitoring the depletion of these substrates (ampicillin, penicillin

Chapter 3: β -Lactam antibiotic-degrading enzymes from non-pathogenic marine organisms: a potential threat to human health

G, biapenem, meropenem, imipenem, cefuroxime and cefoxitin) for 60 s at 25 °C and at the appropriate wavelengths. Relevant extinction coefficients and wavelengths are listed in **Table 3.1**. Reactions were performed as a continuous assay in 50 mM HEPES (pH 7.5), 50 mM NaCl; rates were determined from the initial linear portion of the reaction progress curves. All the measurements were carried out using a Varian Cary 50-BIO spectrophotometer connected to a Peltier Thermostat system. The reactions were carried out without the addition of extra zinc to the buffer.

Table 3.1. Wavelengths and the corresponding extinction coefficients of the substrates used in this study.

Antibiotic	ϵ ($M^{-1}cm^{-1}$)	λ (nm)
Biapenem	7600	293
Meropenem	6500	300
Imipenem	9000	300
Ampicillin	820	235
PenicillinG	936	235
Cephalothin	6500	260
Cefoxitin	7700	260
Cefuroxime	-7600	260

Chapter 3: β -Lactam antibiotic-degrading enzymes from non-pathogenic marine organisms: a potential threat to human health

3.2.4 Kinetic data analysis

Kinetic rate data (velocities) were analysed by non-linear regression using GraphPad (Prism) and t to either the Michaelis–Menten equation (**Eq. 1**) or an equation accounting for the observed substrate inhibition (**Eq. 2**). In these equations V_{\max} and K_m are the maximum velocity and Michaelis constant, respectively, and K_i is the dissociation constant describing substrate binding to an inhibitory site [150]. The inhibitory effect of D-captopril on the MIM-1- or MIM-2-catalyzed hydrolysis of ampicillin was assessed with inhibitor concentrations ranging from 0 to 20 μM . The inhibition constant (K_{ic} , describing a competitive mode of binding) was obtained by analyzing the data with **Eq. 3** [150]. The same experimental conditions were used to evaluate the catalytic parameters of metal ion derivatives of both MIM-1 and MIM-2, using Chelex-treated 50 mM Hepes buffer (pH 7.5), 50 mM NaCl, in the presence of CoCl_2 , MnCl_2 , CuCl_2 or CaCl_2 at concentrations of 50 μM .

$$\mathbf{v} = \frac{V_{\max}[S]}{K_m + [S]} \quad (1)$$

$$\mathbf{v} = \frac{V_{\max}[S]}{K_m + [S] \left(1 + \frac{[S]}{K_i}\right)} \quad (2)$$

$$\mathbf{v} = \frac{V_{\max}[S]}{[S] + K_m \left(1 + \frac{[I]}{K_{ic}}\right)} \quad (3)$$

Chapter 3: β -Lactam antibiotic-degrading enzymes from non-pathogenic marine organisms: a potential threat to human health

3.2.5 pH dependence of catalytic parameters

pH-rate profiles were determined using substrates representing three of the major β -lactam groups. The assays were conducted using a multi-component buffer system containing 50 mM sodium acetate, 50 mM MES, 50 mM TES, 50 mM CHES and 50 mM CAPS, in addition to 50 mM NaCl and 50 μ M ZnCl₂. The pH dependence of the catalytic parameters was evaluated from rate measurements that were conducted at various pH values between 4.0 and 10.0. The enzymes were stable over the entire pH range studied; auto-hydrolysis of the substrates was taken into account at each pH. The data were fitted using Graph Pad (Prism) and the appropriate equations derived for mono- or diprotic systems (*i.e.*, **Eqs. 4, 5**), respectively) [150].

$$\log(\mathbf{v}_0) = \frac{a}{\left(1 + \frac{[H^+]}{K_a}\right)} + c \quad (4)$$

$$\log(\mathbf{v}_0) = \frac{a}{1 + \frac{[H^+]}{K_{a1}} + \frac{K_{a2}}{[H^+]}} + c \quad (5)$$

In these equations, “*a*” represents the pH-independent maximum value of the catalytic parameter (*i.e.*, k_{cat} or k_{cat}/K_m), while K_a represents relevant acid dissociation constants; *c* is a fitting parameter.

Chapter 3: β -Lactam antibiotic-degrading enzymes from non-pathogenic marine organisms: a potential threat to human health

3.2.6 Preparation of the metal ion-free apoproteins

A protein sample (MIM-1 or MIM-2) was diluted in Chelex-treated metal ion-free buffer containing 50 mM Hepes (pH 7.5) and 50 mM NaCl, to a final concentration of 0.5–1 mg/mL, and then incubated in the presence of 150 mM EDTA at 4 °C for 48 h. The solution was then loaded onto an Econo-Pac 10DG (Bio-Rad) gel filtration column that was pre-treated with a chelating solution containing 5 mM EDTA, 5 mM 1,10-phenanthroline, 5 mM 2,6-pyridine dicarboxylic acid, 5 mM 8-hydroxyquinoline-5-sulfonic acid, and 5 mM 2-mercaptoethanol, and then equilibrated with the Chelex-treated buffer prior to use. The residual enzyme activity of the collected apoenzyme was measured using ampicillin as the substrate and was found to be less than 1% of the maximum activity of the holo-enzyme, and atomic absorption measurements indicated that the metal ion content was below the detection limits of the apparatus. The addition of an excess of zinc restored at least 90% of the maximum activity.

3.2.7 Estimation of metal ion binding affinities using reconstitution assays

An estimate for the binding affinities of various metal ions ($M = \text{CoCl}_2$, MnCl_2 , CuCl_2 , CaCl_2 or ZnCl_2) to MIM-1 and MIM-2 was obtained by recording catalytic activities as a function of added metal ion concentrations. The assay buffer containing 50 mM Hepes (pH 7.5) and 50 mM NaCl was again treated with Chelex-100 to avoid any metal ion contaminations. Assays were carried out both in the absence and presence of 1 mM β -mercaptoethanol in order to evaluate if a possible oxidation of Co(II) or Mn(II) may affect the activity of MIM-1 and MIM-2. Over several days the activities for each sample remained stable and β -mercaptoethanol did not lead to any measurable difference in catalytic rates. The concentration of the apoenzyme was kept constant at 10 nM while the substrate concentration

Chapter 3: β -Lactam antibiotic-degrading enzymes from non-pathogenic marine organisms: a potential threat to human health

(*i.e.*, ampicillin, biapenem and cefuroxime) was kept constant at two-fold the K_m to avoid the effect of substrate inhibition. The metal ion concentration was gradually increased from 0 to 100 μ M. The addition of M(II) to the apo forms of MIM-1 and MIM-2 demonstrated saturation- type behaviour similar to that described by the Michaelis-Menten equation (Eq. 1). The data were analysed as previously reported [11].

3.3 Results and Discussion

3.3.1 Overexpression and purification of MIM-1 and MIM-2

The genes harbouring the coding sequence of MIM-1 and MIM-2 were used to transform *E. coli* BL21 (DE3) pLysS cells. The expression vector (pJ411) uses a T7 promoter, and contains the kanamycin gene for the selection of transformants. To optimize the yield of pure protein, the expressions were carried out at low temperatures, 18 or 25 °C for MIM-1 and MIM-2, respectively. The established purification protocol employs two chromatographic steps, anion exchange followed by size exclusion. Routinely, purifications yielded approximately 15 mg of MIM-1 and 6.5 mg of MIM-2 per liter of cell culture with high purity (>95 %) as visualized by SDS-PAGE analysis (**Fig. 3.1.** - note that the calculated molecular weights for MIM-1 and MIM-2 based on their sequence are 30 and 29 kDa, respectively). To assess the oligomeric state of MIM-1 and MIM-2, size-exclusion chromatography with appropriate molecular weight markers was used. For MIM-1, a dimeric species is prevalent (~54 kDa), while MIM-2 appears to be monomeric (~27 kDa); (**Fig. 3.2.**). While the majority of known MBLs are also monomeric, the L1 enzyme from *S. maltophilia* is tetrameric [88].

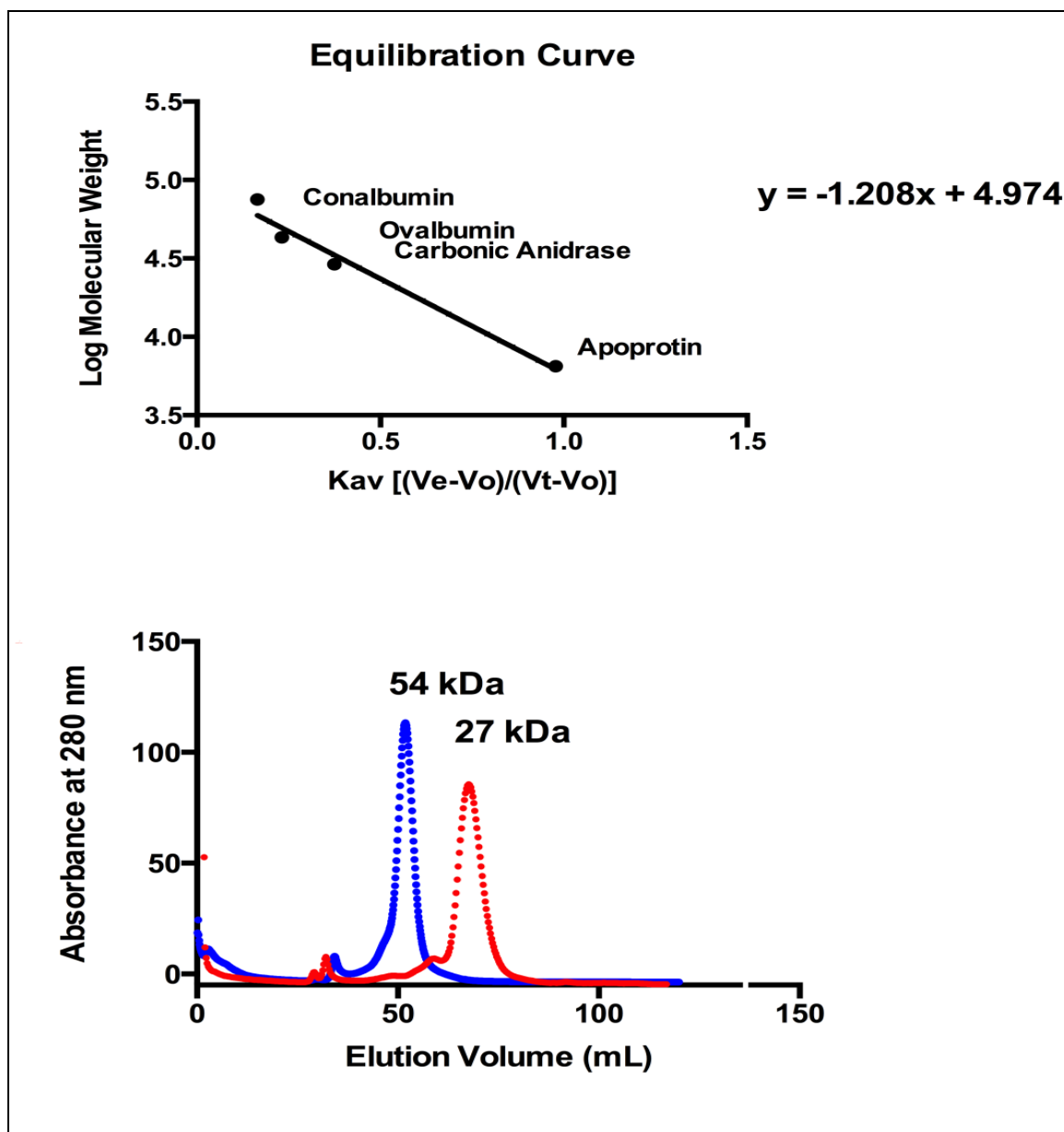


Figure 3.2. Equilibration curve (top panel) and elution profiles (bottom panel) of MIM-1 (blue) and MIM-2 (red). The equilibration curve was determined using the commercially available Low Molecular Weight kit (Sigma-Aldrich) on a size exclusion column HiPrep 16/60 Sephacryl S-200 HR column (GE Healthcare). MIM-1 elutes as a major peak with a corresponding weight consistent with the dimeric form of the protein (54 kDa). MIM-2 elutes as a major peak corresponding to a molecular weight of 27 kDa, consistent with the monomeric form of the enzyme.

Chapter 3: β -Lactam antibiotic-degrading enzymes from non-pathogenic marine organisms: a potential threat to human health

3.3.2 Kinetic parameters of MIM-1 and MIM-2

The aim of this work was to determine whether MIM-1 and MIM-2 are effectively able to hydrolyse β -lactam antibiotics. Thus, the catalytic efficiency of the two enzymes were studied towards different substrates representing three major groups of β -lactam antibiotics (*i.e.*, penicillins, cephalosporins and carbapenems). For all the substrates used, both MIM-1 and MIM-2 showed considerable reactivity but at sufficiently high concentrations substrate inhibition was also observed (**Figure 3.3. A**). To obtain relevant kinetic parameters (k_{cat} , K_{m} , $k_{\text{cat}}/K_{\text{m}}$ and K_{i} , the substrate inhibition constant), the catalytic rates were fitted using an equation that also incorporates an uncompetitive, inhibitory binding mode for the substrate (Eq. 2) [150]. For comparison, the rates measured at low substrate concentrations were analysed separately using the Michaelis–Menten equation (Eq. 1). The experimental data and corresponding fits are shown in **Figure 3.3.A** and **Figure 3.3.B** for MIM-1 and MIM-2, respectively. The relevant kinetic parameters are summarized in **Tables 3.2. A and B**. Corresponding parameters of well-known B3-type MBLs (*i.e.*, L1 [107] and AIM-1 [138]), as well as those of the B1- and B2-type-type MBLs BcII [112, 151] and CphA [81], respectively, are also listed for comparative purposes (**Table 3.2.C**). Both MIM-1 and MIM-2 are potent MBLs with catalytic parameters comparable to those of well-known virulent MBLs; both are in particular efficient penicillinases. Furthermore, similar to MBLs such as CcrA from *B. fragilis*, high concentrations of substrate lead to a reduction of the catalytic rate (deviation from Michaelis–Menten-type behaviour) [152].

Chapter 3: β -Lactam antibiotic-degrading enzymes from non-pathogenic marine organisms: a potential threat to human health

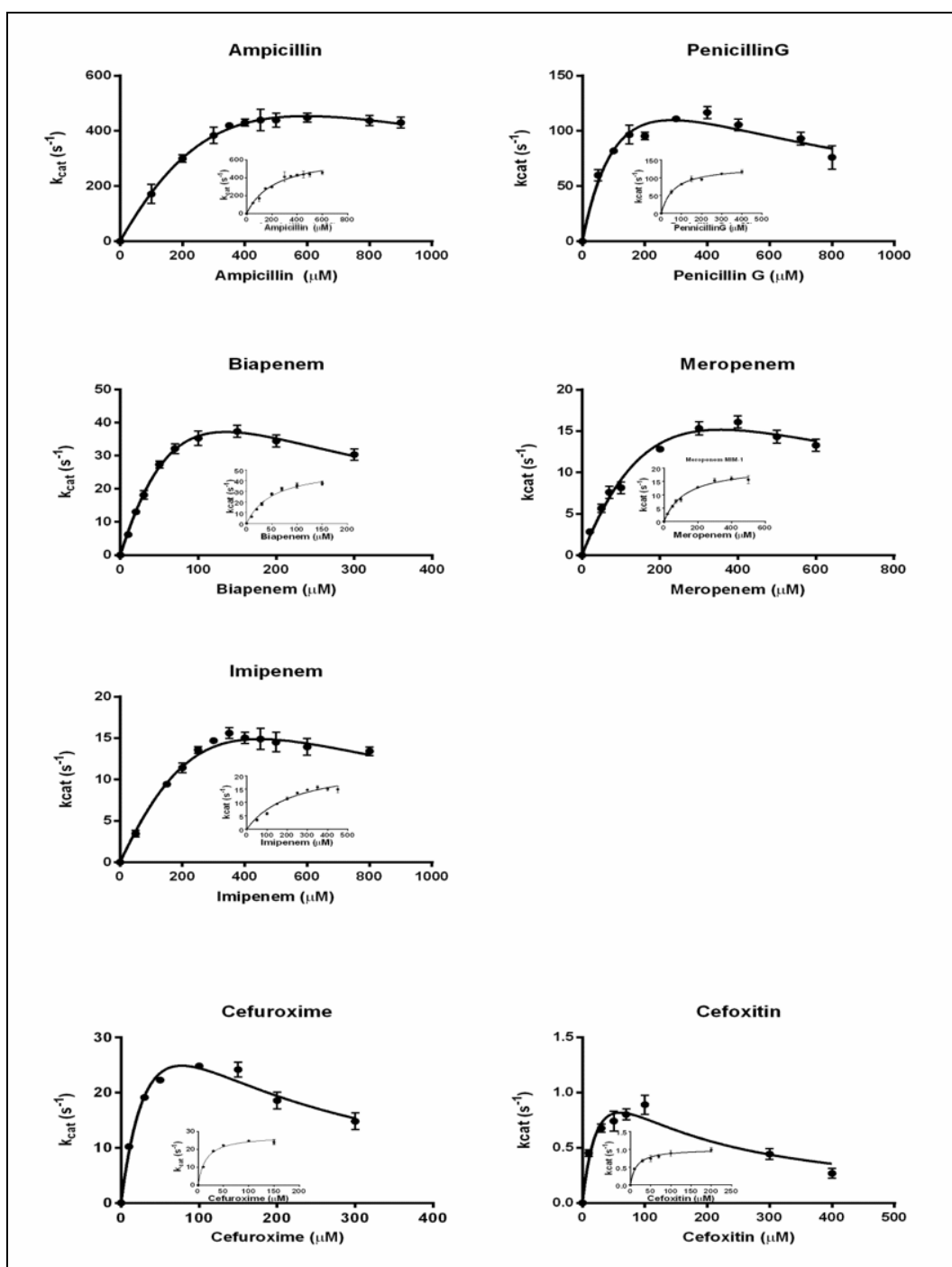


Figure 3.3. (A). Catalytic activity of MIM-1 towards the antibiotic penicillins (top), penems (middle) and cephalosporins (bottom). For each antibiotic, the data were analysed using the Michaelis–Menten model (for low substrate concentrations only; inset) and an equation that also incorporates an uncompetitive, inhibitory binding site for the substrate (main figure).

Chapter 3: β -Lactam antibiotic-degrading enzymes from non-pathogenic marine organisms: a potential threat to human health

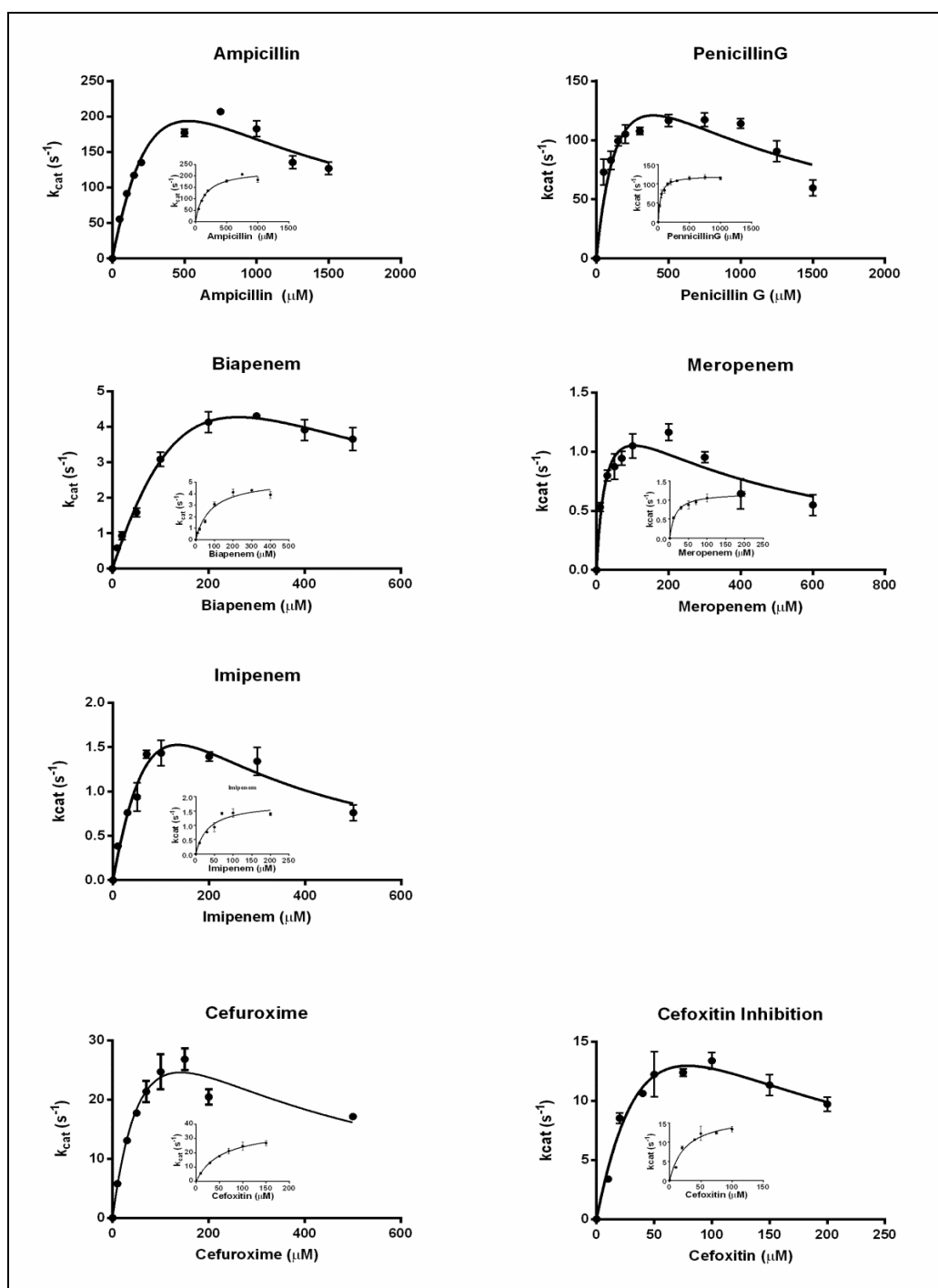


Figure 3.3. (B). Catalytic activity of MIM-2 towards the antibiotic penicillins (top), penems (middle) and cephalosporins (bottom). For each antibiotic, the data were analyzed using the Michaelis–Menten model (for low substrate concentrations only; inset) and an equation that also incorporates an uncompetitive, inhibitory binding site for the substrate (main figure).

Chapter 3: β -Lactam antibiotic-degrading enzymes from non-pathogenic marine organisms: a potential threat to human health

Table 3.2. Steady-state catalytic constants obtained for MIM-1 and MIM-2 incorporating (A) or neglecting the effect of substrate inhibition (B). For comparison, kinetics corresponding parameters for the well-studied MBLs L1 [39], AIM-1 [40], BcII [41, 42] and CphA [22] were included (C).

Substrate	MIM-1				MIM-2			
	k_{cat} (s^{-1})	K_M (μM)	k_{cat} (s^{-1}) / K_M ($s^{-1}M^{-1}$)	K_I (μM)	k_{cat} (s^{-1})	K_M (μM)	k_{cat} (s^{-1}) / K_M ($s^{-1}M^{-1}$)	K_I (μM)
Ampicillin	1995 \pm 80.5	1011 \pm 495	1.9 * 10 ⁶	350.4 \pm 190.5	701.3 \pm 25.4	691.8 \pm 31.1	1.06 * 10 ⁶	402.8 \pm 196.5
Penicillin G	237.4 \pm 55.6	167.2 \pm 65.0	4.4 * 10 ⁶	494.5 \pm 201.6	244.9 \pm 72.8	200.9 \pm 10.4	1.2 * 10 ⁶	766.7 \pm 390.1
Biapenem	143.1 \pm 57.2	193.2 \pm 57.2	7.4 * 10 ⁵	95.3 \pm 31.7	5.3 \pm 0.3	84.1 \pm 16.2	6.3 * 10 ⁴	122.8 \pm 87.6
Imipenem	97.2 \pm 74.3	123.6 \pm 10.6	7.8 * 10 ⁵	161.6 \pm 14.8	6.9 \pm 3.9	236.6 \pm 16.4	2.9 * 10 ⁴	73.6 \pm 43.5
Meropenem	53.9 \pm 18.8	455.8 \pm 19.4	1.1 * 10 ⁵	248.6 \pm 17.6	1.6 \pm 0.2	28.2 \pm 9.2	6.7 * 10 ⁴	385.0 \pm 118
Cefuroxime	60.4 \pm 13.1	55.6 \pm 3.6	1.0 * 10 ⁶	108.7 \pm 35.7	98.1 \pm 4.4	186.1 \pm 10.5	5.2 * 10 ⁵	71.7 \pm 47.6
Cefoxitin	1.8 \pm 0.4	36.1 \pm 1.4	4.9 * 10 ⁴	100.3 \pm 36.4	39.6 \pm 11.9	81.3 \pm 33.3	4.5 * 10 ⁵	77 \pm 33.9

Chapter 3: β -Lactam antibiotic-degrading enzymes from non-pathogenic marine organisms: a potential threat to human health

Table 3.2. (B).

Substrate	MIM-1			MIM-2		
	k_{cat} (s^{-1})	K_M (μM)	k_{cat} (s^{-1}) / K_M ($s^{-1}M^{-1}$)	k_{cat} (s^{-1})	K_M (μM)	k_{cat} (s^{-1}) / K_M ($s^{-1}M^{-1}$)
Ampicillin	663.6 ± 42.7	226 ± 35.6	$2.9 * 10^6$	226.8 ± 6.5	141.6 ± 13.2	$1.6 * 10^6$
Penicillin G	124.3 ± 3.9	50.7 ± 7.5	$2.4 * 10^6$	121.4 ± 2.1	36.4 ± 3.3	$3.3 * 10^6$
Biapenem	52.6 ± 2.9	53.0 ± 7.1	$9.9 * 10^5$	5.3 ± 0.3	84.1 ± 16.2	$6.3 * 10^4$
Imipenem	21.8 ± 1.7	186.7 ± 37.7	$1.1 * 10^5$	1.8 ± 0.1	34.2 ± 7.4	$5.2 * 10^4$
Meropenem	20.7 ± 1.0	121.6 ± 17.4	$1.7 * 10^5$	1.2 ± 0.1	14.6 ± 2.2	$8.2 * 10^4$
Cefuroxime	27.9 ± 0.8	15.0 ± 1.8	$1.8 * 10^6$	37.1 ± 2.3	53.4 ± 8.1	$6.9 * 10^5$
Cefoxitin	1.0 ± 0.1	14.6 ± 2.2	$6.8 * 10^4$	17.2 ± 1.1	25.3 ± 4.7	$6.8 * 10^5$

Chapter 3: β -Lactam antibiotic-degrading enzymes from non-pathogenic marine organisms: a potential threat to human health

Table 3.2. (C).

Substrate	AIM-1			L1			BcII			CphA		
	k_{cat} (s^{-1})	K_M (μM)	k_{cat}/K_M ($s^{-1}M^{-1}$)	k_{cat} (s^{-1})	K_M (μM)	k_{cat}/K_M ($s^{-1}M^{-1}$)	k_{cat} (s^{-1})	K_M (μM)	k_{cat}/K_M ($s^{-1}M^{-1}$)	k_{cat} (s^{-1})	K_M (μM)	k_{cat}/K_M ($s^{-1}M^{-1}$)
Ampicillin	150 \pm 5	24 \pm 3	6.2 * 10 ⁶	580 \pm 20	300 \pm 15	1.9*10 ⁶	NA	NA	8.2 * 10 ⁴	>0.01	2500	>4
Penicillin G	590 \pm 31	110 \pm 21	5.3 * 10 ⁶	410 \pm 20	300 \pm 15	5.5*10 ⁶	NA	NA	NA	NA	700	100
Biapenem	NA	NA	NA	64 \pm 4	75 \pm 11	8.5 * 10 ⁵	NA	NA	NA	300	166	1.8 * 10 ⁶
Imipenem	2200 \pm 50	410 \pm 16	5.3 \pm 10 ⁶	NA	NA	NA	279	687	1.4 * 10 ⁵	1200	340	3.5 * 10 ⁶
Meropenem	760 \pm 16	41 \pm 4	1.8 * 10 ⁷	NA	NA	NA	NA	NA	NA	NA	NA	NA
Cefuroxime	170 \pm 5	35 \pm 4	4.8 * 10 ⁶	53 \pm 9	130 \pm 40	4.0 * 10 ⁵	NA	NA	NA	NA	NA	NA
Cefoxitin	52 \pm 1	22 \pm 2	2.4 * 10 ⁵	2.2 \pm 0.1	3.3 \pm 0.4	6,6 * 10 ⁵	122 \pm 22	175 \pm 43	6.9 * 10 ⁵	NA	NA	NA

Chapter 3: β -Lactam antibiotic-degrading enzymes from non-pathogenic marine organisms: a potential threat to human health

Due to the structural similarities between MBLs and some binuclear phosphatases such as the enzyme methyl parathion hydrolase [153] I tested if MIM-1 and MIM-2 may be able to hydrolyze generic phosphate ester substrates such as *p*-nitrophenyl phosphate (pNPP), bis(4-nitrophenyl) phosphate (bpNPP) or paraoxon, but no quantifiable amount of product was formed in these reactions.

To further validate the association of MIM-1 and MIM-2 with the MBL family, I analyzed the inhibitory effect of D-captopril, a well-known in vitro MBL inhibitor, but also an angiotensin-converting enzyme (ACE) inhibitor used to treat hypertension and some heart-related diseases [20, 62, 154, 155]. The experimental data were consistent with a competitive mode of inhibition and fitted to Eq. 3 (**Figure 3.4.**). The inhibition constants (K_{iC}) for both enzymes are approximately 6.0 μ M, comparable to those reported for other MBLs (**Table 3.3.**) [20].

Chapter 3: β -Lactam antibiotic-degrading enzymes from non-pathogenic marine organisms: a potential threat to human health

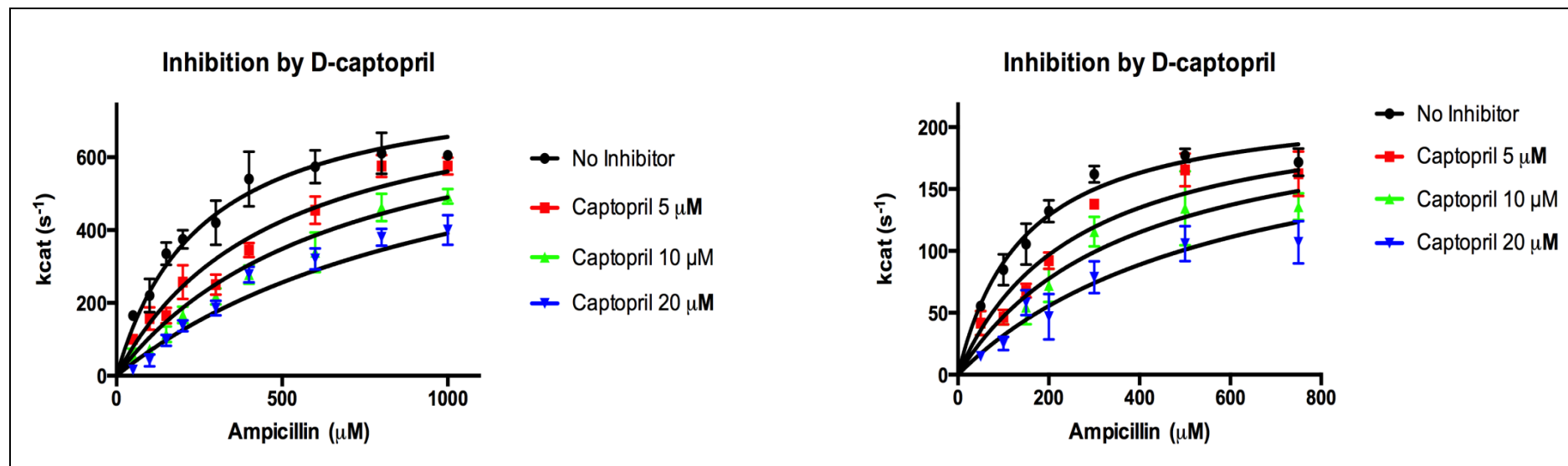


Figure 3.4. Inhibition by D-captopril. Steady-state assays with the inhibitor were measured with the substrate ampicillin for MIM-1 (left) and MIM-2 (right).

Table 3.3. Inhibition of MBLs by D-captopril. Competitive inhibition constants (K_{ic} in μM) for MIM-1 and MIM-2 are compared to corresponding values for BcII, CphA and L1

MIM-1	Inhibition by D-captopril			
	MIM-2	BcII	CphA	L1
8.8±0.9	7.4±0.8	45±5	72±6	20

Chapter 3: β -Lactam antibiotic-degrading enzymes from non-pathogenic marine organisms: a potential threat to human health

3.3.3 Mechanism of action of MIM-1 and MIM-2

The study of the effect(s) of pH on the catalytic properties of an enzyme-mediated reaction can provide essential clues about the molecular details of this reaction, but it can also highlight functional variations between different enzymes. Thus, steady-state assays as described above were carried out with MIM-1 and MIM-2 at a number of pH values, using representative substrates from three major groups of β -lactam antibiotics (**Figure 3.5**). It is evident that the effect of the pH varies considerably when the two proteins are compared. As an example, the turnover numbers (*i.e.*, k_{cat} values) for each substrate tested are enhanced at high pH values in MIM-1-catalyzed reactions, but MIM-2 prefers a lower pH (*i.e.*, an increase of pH leads to a reduction of the catalytic rate). In terms of the catalytic efficiency ($k_{\text{cat}}/K_{\text{M}}$), however, a higher pH appears to be preferred for both enzymes. Differences are also observed when the catalytic parameters measured with different substrates are compared. For instance, for MIM-1, the slope of the pH profile for the reaction with ampicillin is considerably smaller than 1, whereas for the other substrates it is approximating unity, suggesting that the rate-limiting steps in the reactions with different substrates may vary (*i.e.*, in the reaction with ampicillin the relevant protonation equilibria are not fully rate limiting [156]). Nonetheless, the data presented in **Fig. 3.5**. can be fitted to equations derived for mono- or diprotic systems (*i.e.*, **Eqs. 4, 5**, respectively) and relevant $\text{p}K_{\text{a}}$ values are summarized in **Table 3.4**.

The pH dependence of k_{cat} provides information about catalytically relevant protonation equilibria for the enzyme–substrate (ES or Michaelis) complex [150]. The assignment of particular residues to experimentally determined protonation equilibria is generally a difficult task and fraught with ambiguities. However, from a direct comparison between substrates and enzymes, some essential insights may be gained (note that only biapenem has a $\text{p}K_{\text{a}}$ value that lies within the pH range relevant to MIM-1 and MIM-2 [157, 158]; see also **Table 3.5**).

Chapter 3: β -Lactam antibiotic-degrading enzymes from non-pathogenic marine organisms: a potential threat to human health

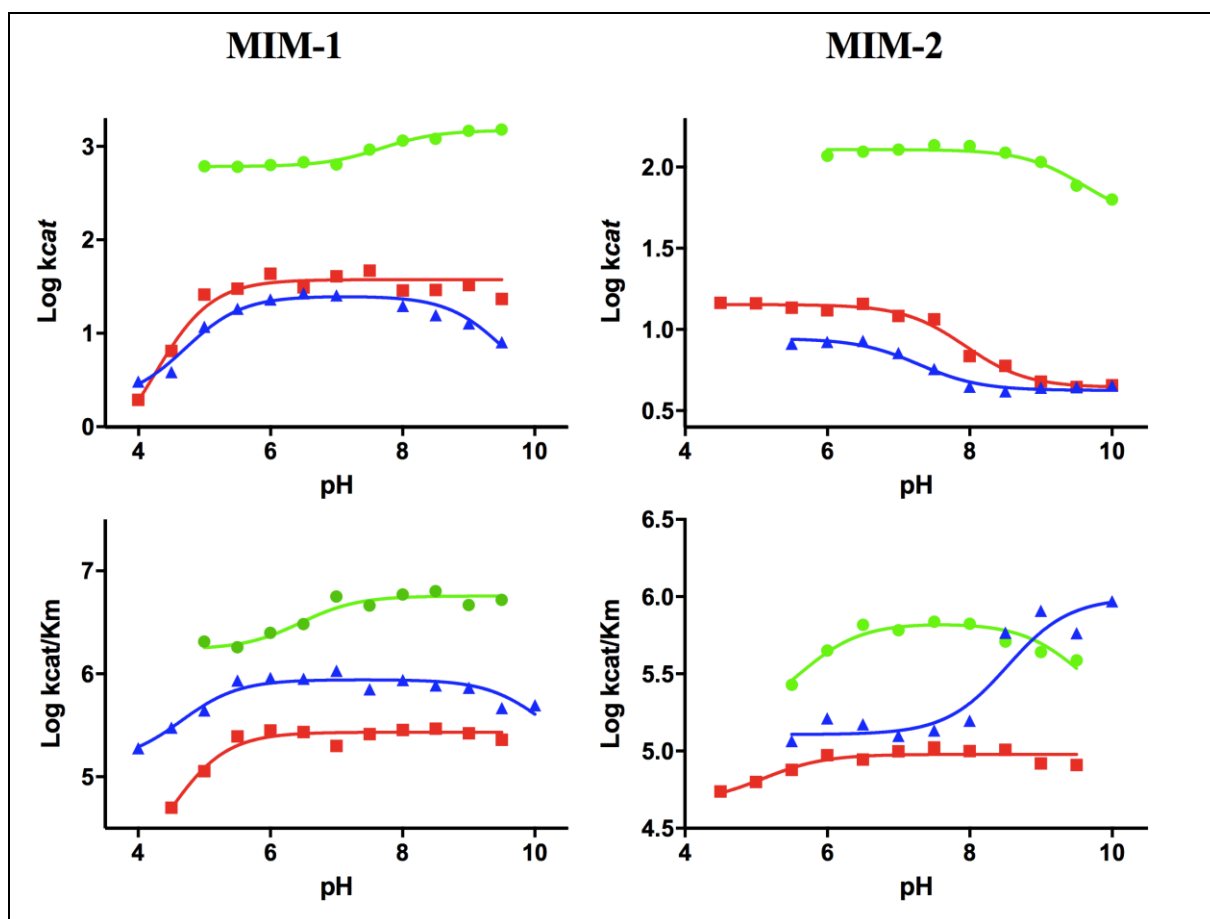


Figure 3.5. Effect of pH in the hydrolysis of ampicillin (green), biapenem (red) and cefuroxime (blue) for MIM-1 (left panel) and MIM-2 (right panel). For each substrate, the top panel shows the pH dependence of k_{cat} and the bottom panel shows the pH dependence of k_{cat}/K_m .

Table 3.4. pK_a values for the hydrolysis of ampicillin, biapenem and cefuroxime by MIM-1 and MIM-2.

	MIM-1			MIM-2		
	Ampicillin	Biapenem	Cefuroxime	Ampicillin	Biapenem	Cefuroxime
pK_{es1}	7.7 ± 0.7	4.2 ± 0.5	4.7 ± 0.8	-	-	-
pK_{es2}			9.5 ± 0.7	9.6 ± 0.3	7.9 ± 0.6	7.3 ± 0.2
pK_{e1}	6.4 ± 0.5	4.5 ± 0.2	4.6 ± 0.5	5.6 ± 0.2	5.1 ± 0.1	8.5 ± 0.4
pK_{e2}			10.1 ± 0.5	9.6 ± 0.1	-	-

Chapter 3: β -Lactam antibiotic-degrading enzymes from non-pathogenic marine organisms: a potential threat to human health

Table 3.5. pK_a values for the β -lactams used to study the pH dependence of MIM-1 and MIM-2 [156, 157]

Antibiotic	pK_a
Ampicillin	2.5-3.0
Biapenem	~4.3
Cefuroxime	2.0-2.5

For MIM-1 pK_{es1} values determined for the reaction with biapenem and cefuroxime (~4.5) are similar, indicating that the relevant protonation equilibria are likely to be associated with the enzyme in both reactions, not the substrate. While a pK_a of ~4.5 is consistent with the deprotonation of a metal ion-bridging water molecule, leading to the formation of a μ -hydroxide (the proposed nucleophile in MBL-catalysed reactions [16, 18, 22, 96]), currently it cannot be excluded that a water molecule terminally coordinated to only one of the metal ions may be associated with pK_{es1} , provided it is activated by the presence of negatively charged residues (e.g, carboxylate groups). In contrast, pK_{es1} recorded for the reaction with ampicillin is three orders of magnitude more alkaline, lying in the region anticipated for the pK_a of a water molecule bound to only one of the metal ions in the active site, independent of the presence of “activating” negative charges or hydrogen bonds [159]. Thus, while an assignment of pK_a values may ultimately need to be substantiated through site-directed mutagenesis studies it is evident that within the same active site different substrates are turned over in distinctly different ways. This is further corroborated by the observation that pK_{es2} is only observed for the reaction with cefuroxime.

Chapter 3: β -Lactam antibiotic-degrading enzymes from non-pathogenic marine organisms: a potential threat to human health

For MIM-2, we will focus our attention solely on the pH dependence of the k_{cat} values as they demonstrate the most significant variation in comparison to MIM-1 (**Fig. 3.5.**); the pH dependence of $k_{\text{cat}}/K_{\text{m}}$ ratios is different for the three substrates but upon formation of the catalytically relevant Michaelis (ES) complex a similar behaviour is observed for each substrate. Only $\text{p}K_{\text{es}2}$ is observed in MIM-2, contrasting sharply the corresponding data of MIM-1. As discussed above, $\text{p}K_{\text{a}}$ values in the range between 7.5 and 9.5 are consistent with terminally coordinated water molecules [159]. Thus, the pH profiles for MIM-2 do not provide any information about the potential reactive nucleophile (i.e., a bridging or terminally bound hydroxide), but they do indicate that the three substrates may bind in a similar mode in the catalytically relevant complex. The fact that in MIM-2 the nucleophile is not apparent in the pH profile (in contrast to MIM-1) indicates that the two enzymes have different rate-limiting steps.

The data in the preceding paragraph demonstrate a functional plasticity that appears to be very common among MBLs and MBL-like enzymes [16, 18, 22, 96], and which may be a major contributor to these enzymes' ability to adapt rapidly to new environmental challenges (*e.g.*, the use of novel antibiotics, or the introduction of inhibitors). MIM-1 and MIM-2, despite originating from non-pathogenic microorganisms, thus share the same functional diversity and/or flexibility as known MBLs.

3.3.4 The role of the metal ions in the reactions catalyzed by MIM-1 and MIM-2

The catalytically relevant *in vivo* metal ion for all known MBLs is Zn(II) [16, 18, 22, 96], but their contribution to the mechanism varies from one MBL subgroup to another (see Chapter 1, section 1.7, for detailed information regarding the MBL mechanism). Metal ion replacement

Chapter 3: β -Lactam antibiotic-degrading enzymes from non-pathogenic marine organisms: a potential threat to human health

studies [including Mn(II), Co(II), Cd(II) and Cu(II)] were employed for several MBLs to probe the catalytic roles of the metal ions [16]. For MIM-1 and MIM-2, the native metal ion composition is not known. The enzymes were expressed and purified in medium and buffers that were supplemented with Zn(II), and metal ion analyses of these enzymes indicate the presence of two Zn(II) ions per active site in their fully active state. In an attempt (1) to probe the catalytic role(s) of the metal ions, but also (2) to address the likely *in vivo* metal ion composition of MIM-1 and MIM-2, the metal ion-free apo forms of the two enzymes were generated by incubation with the metal ion chelator EDTA. The removal of the metal ions did not result in structural damage of the enzymes as could be demonstrated by reconstitution of the catalytic activity upon addition of an excess of Zn(II). On average, between 90 and 95 % of the activity of the holoenzyme could be recovered; maximum activity was reached within 2 min after the addition of the metal ion to the apoenzyme.

Using the same batch of apoenzyme, derivatives were generated by adding Co(II), Mn(II), Cu(II) and Ca(II) and their catalytic parameters (**Table 3.6.**) were determined at pH 7.5 for representative substrates from three major β -lactam groups (*i.e.*, ampicillin, biapenem and cefuroxime). Although not shown here it should be noted that substrate inhibition similar to that observed for the Zn(II) derivatives of MIM-1 and MIM-2 was observed (**Fig. 3.3 A and B**). The metal ion derivatives are far more selective with respect to substrates they can hydrolyse when compared to the Zn(II) form of the enzymes. For instance, with respect to ampicillin, only Zn(II) can reconstitute activity in MIM-2, while for MIM-1 Ca(II) is also reasonably effective. For cefuroxime, only marginal activities were measurable for the Co(II) and Ca(II) derivatives. In contrast, all metal ion derivatives are active towards biapenem although, by and large, Zn(II) appears to be the most effective metal ion. The exception is Cu(II), which renders MIM-2 significantly more reactive than its Zn(II) counterpart (with k_{cat}

Chapter 3: β -Lactam antibiotic-degrading enzymes from non-pathogenic marine organisms: a potential threat to human health

values of 75 vs. 5 s⁻¹, respectively). Furthermore, although Zn(II) is overall the most efficient metal ion in reconstituting activity, in the other derivatives, substrate affinities are mostly enhanced (*i.e.*, reduced K_m values).

While the data in **Table 3.6.** indicate that with respect to the β -lactamase activity of MIM-1 and MIM-2, Zn(II) is the preferred metal ion, they also demonstrate that substrate preference is affected by the metal ion composition, and thus alternative *in vivo* functions may be possible for these enzymes. A similar behaviour was observed previously for the B3-type MBL L1 from *S. maltophilia*, where the substrate specificity for the Ni(II) and Cu(II) derivatives of that enzyme varies distinctly from that of the Zn(II) derivative [160].

Here, a particularly intriguing observation was that Ca(II) was rather proficient in reconstituting ampicillinase activity in MIM-1 (**Table 3.6.**). While Ca(II) is known to bind tightly to regulatory proteins such as calmodulin (K_d for Ca(II) as low as 0.1 μ M) [161] or α -lactoalbumin (K_d 3–6 nM) [162], it is rarely associated with hydrolytic metalloenzymes. A notable exception is the cyclic nucleotide diesterase Rv0805 from *Mycobacterium tuberculosis*; in this enzyme Ca(II) does not only regulate catalytic activity but it is also the most optimal metal ion [163]. The significance of Ca(II) in a variety of metabolic functions (*e.g.*, signal transduction, muscle contraction, fertilization, as well as maintaining the potential difference of the cellular membrane [164, 165]), together with its abundance in most cells, raises the possibility that at least MIM-1 may play a role in *N. pentaromativorans* that is not related to its *in vitro* MBL activity.

Chapter 3: β -Lactam antibiotic-degrading enzymes from non-pathogenic marine organisms: a potential threat to human health

Table 3.6. Catalytic parameters for the hydrolysis of ampicillin, biapenem and cefuroxime by the Co(II), Mn(II), Cu(II) and Ca(II) derivatives of MIM-1 and MIM-2.

MIM-1

	Ampicillin			Biapenem			Cefuroxime		
	k_{cat} (s ⁻¹)	K_M (μ M)	k_{cat}/K_M (s ⁻¹ M ⁻¹)	k_{cat} (s ⁻¹)	K_M (μ M)	k_{cat}/K_M (s ⁻¹ M ⁻¹)	k_{cat} (s ⁻¹)	K_M (μ M)	k_{cat}/K_M (s ⁻¹ M ⁻¹)
Co(II)	NA	NA	NA	28.33 \pm 2.2	103.2 \pm 16.21	2.6 * 10 ⁶	4.0 \pm 0.4	9.43 \pm 3.6	4.2 * 10 ⁵
Mn(II)	NA	NA	NA	4.6 \pm 0.9	268.2 \pm 85.9	1.7 * 10 ⁴	NA	NA	NA
Cu(II)	NA	NA	NA	103.1 \pm 18.3	211.7 \pm 73.2	4.6 * 10 ⁵	NA	NA	NA
Ca(II)	53.0 \pm 7.8	261.2 \pm 91.9	2.0 * 10 ⁵	8.6 \pm 0.3	20.9 \pm 3.8	4.1 * 10 ⁵	3.3 \pm 0.1	7.8 \pm 1.4	4.6 * 10 ⁵

MIM-2

	k_{cat} (s ⁻¹)	K_M (μ M)	k_{cat}/K_M (s ⁻¹ M ⁻¹)	k_{cat} (s ⁻¹)	K_M (μ M)	k_{cat}/K_M (s ⁻¹ M ⁻¹)	k_{cat} (s ⁻¹)	K_M (μ M)	k_{cat}/K_M (s ⁻¹ M ⁻¹)
Co(II)	NA	NA	NA	1.2 \pm 0.1	25.8 \pm 7.9	4.6 * 10 ⁴	1.1 \pm 0.3	36.3 \pm 2.39	3.0 * 10 ⁴
Mn(II)	NA	NA	NA	1.7 \pm 0.2	43.4 \pm 15.9	3.7 * 10 ⁴	NA	NA	NA
Cu(II)	NA	NA	NA	75.4 \pm 7.2	164.2 \pm 34.2	4.5 * 10 ⁵	NA	NA	NA
Ca(II)	NA	NA	NA	0.8 \pm 0.1	11.4 \pm 8.6	7.2 * 10 ⁴	1.6 \pm 0.4	62.7 \pm 23.2	2.5 * 10 ⁴

Chapter 3: β -Lactam antibiotic-degrading enzymes from non-pathogenic marine organisms: a potential threat to human health

To be physiologically relevant, the binding affinity of a metal ion for a particular protein ought to be within a range that is similar to the concentration of that metal ion within a cell. The concentrations of metal ions vary greatly from one metal ion to another, and they can change throughout the life cycle of a cell. Reported concentrations for Zn(II), Mn(II), Cu(II) and Ca(II) are covering a range from pico- to micro- molar, while Co(II) is a trace element [166]. We obtained an estimate of the binding affinities of MIM-1 and MIM-2 for the biologically potentially relevant metal ions [*i.e.*, Zn(II), Mn(II), Cu(II) and Ca(II)] by measuring their catalytic activities towards biapenem degradation as a function of added metal ion concentrations. Although unlikely to be physiologically relevant, Co(II) was included in the comparison as it may provide a useful spectroscopic probe for future mechanistic studies. As exemplified in **Figure 3.6.**, the reactivation of the apo forms of MIM-1 and MIM-2 upon titrating increasing amounts of the metal ions resulted in a saturation-type behaviour for the catalytic activity, reminiscent of Michaelis–Menten-type kinetics (to avoid substrate inhibition the substrate concentration was two-fold the respective K_M).

Since the reconstitution experiments were conducted under pseudo-first-order kinetics and the metal ion concentrations far exceeded those of the enzymes, no accurate estimate of the stoichiometry of metal ion binding can be obtained—instead atomic absorption measurements of fully reconstituted enzyme samples, following a gel filtration step to remove excess metal ions, indicated a stoichiometry of ~ 2 in each case. An approximation of the affinities of the catalytically required metal ions (**Table 3.7**) can be estimated from a fit to the data in **Fig. 3.6.** using a hyperbolic function related to the Michaelis–Menten equation.

Chapter 3: β -Lactam antibiotic-degrading enzymes from non-pathogenic marine organisms: a potential threat to human health

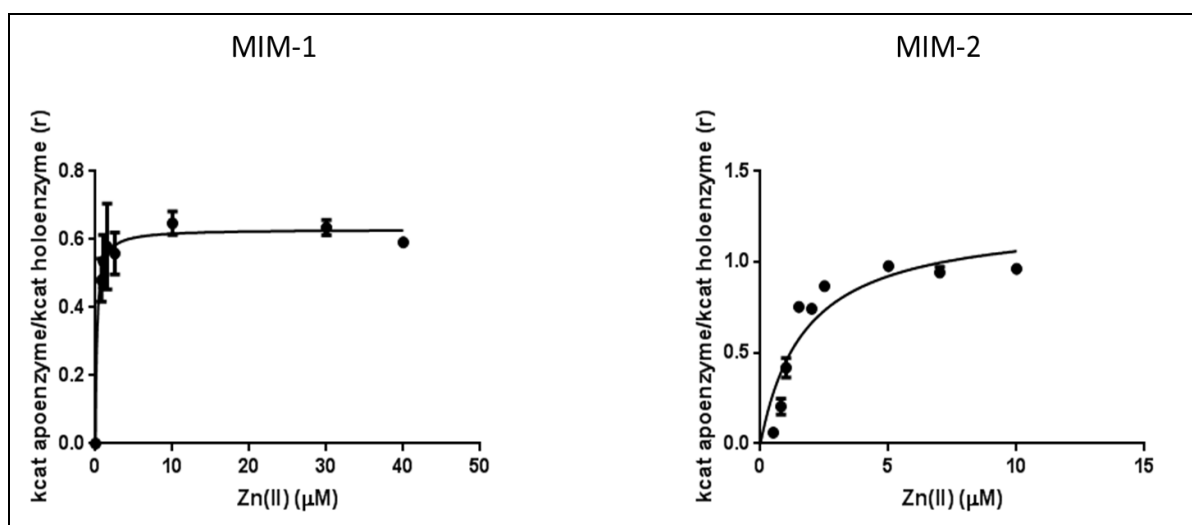


Figure 3.6. Analysis of the titration curve of apo-MIM-1 and apo-MIM-2 in the presence of increasing concentrations of zinc. The reactivation of the enzyme is followed by the hydrolysis of ampicillin. In the case of Zn(II) K_d values are 0.2 and 1.7 μM for MIM-1 and MIM-2, respectively.

Table 3.7. Binding affinity constants for the metal derivatives of MIM-1 and MIM-2.

MIM-1				MIM-2			
k_{obs} (μM)				k_{obs} (μM)			
Zn(II)	Co(II)	Mn(II)	Cu(II)	Zn(II)	Co(II)	Mn(II)	Cu(II)
204 ± 72 (nM)	4.3 ± 0.8	662 ± 251 (nM)	10.3 ± 2.8	1.7 ± 0.4	12.14 ± 4.1	NA	108 ± 93.8

Overall, MIM-1 has a higher affinity for all the metal ions under investigation, and Zn(II) is the most tightly bound metal ion in both enzymes. Based on these affinity data and the catalytic parameters summarized in **Table 3.6.**, it is thus likely that MIM-2 is solely a Zn(II)-dependent enzyme. However, the binding affinities of Mn(II) and Ca(II), and potentially Cu(II) are within a reasonable range to be biologically relevant, thus supporting the above speculation that at least MIM-1 may adopt biological roles independent of its MBL activity.

Chapter 3: β -Lactam antibiotic-degrading enzymes from non-pathogenic marine organisms: a potential threat to human health

3.4 Conclusions.

In this chapter I presented data that confirm that the putative proteins MIM-1 and MIM-2, associated with non-pathogenic microorganisms, are indeed efficient *in vitro* MBLs. The catalytic parameters of MIM-1 and MIM-2 are comparable with those reported for clinically relevant MBLs, thus confirming the potential of these proteins as novel enzymatic agents, able to confer efficient resistance toward β -lactam antibiotics. The observed mechanistic plasticity of MIM-1 and MIM-2 is characteristic for MBLs, but the efficient use of Ca(II) as catalytically competent metal ion by MIM-1 has not been observed before. This leads to the hypothesis that at least MIM-1 may have biological functions unrelated to its MBL activity. The search for alternative substrates (*i.e.*, substrates other than β -lactam antibiotics) is thus of importance and will be described in the next chapter. Especially the observation that different metal ion compositions may affect the selection of substrates (and thus the function of the enzymes), together with a possible association between some MBLs [167] with proteins involved in biofilm production may provide insight into a previously unexplored link between two major factors that contribute to antibiotic resistance. Although the establishment of the precise biological function(s) of MIM-1 and MIM-2 awaits further investigations, it is anticipated that a characterization of factors that lead to functional variations between closely related enzymes may guide future strategies for the development of leads (*i.e.*, clinically useful MBL inhibitors) to combat the spread of antibiotic resistance.

Chapter 4: Promiscuous metallo- β -lactamases: MIM-1 and MIM-2 may play an essential role in quorum sensing networks

Manfredi Miraula^{a,b}, Gerhard Schenk^b, Nataša Mitić^a,

^a Department of Chemistry, Maynooth University, Maynooth, Co. Kildare, Ireland ^b School of Chemistry and Molecular Biosciences, The University of Queensland, St. Lucia, QLD 4072, Australia

article info Article history: Received 21 October 2015 Received in revised form 4 December 2015 Accepted 16 December 2015 Available online xxxx Keywords: Antibiotic resistance Metallo-beta-lactamases Binuclear metallohydrolases Quorum sensing

Functional promiscuity

Abstract MIM-1 and MIM-2 are two recently identified metallo- β -lactamases (MBLs) from *Novosphingobium pentaromativorans* and *Simiduia agarivorans*, respectively. Since these organisms are non-pathogenic we speculated that the biological role(s) of MIM-1 and MIM-2 may not be related to their MBL activity. Although both sequence comparison and homology modeling indicate that these proteins are homologous to well-known MBLs such as AIM-1, the sequence analysis also indicated that MIM-1 and MIM-2 share similarities with N-acyl homoserine lactonases (AHLases) and glyoxalase II (GLX-II). Steady-state kinetic assays using a series of lactone substrates confirm that MIM-1 and MIM-2 are efficient lactonases, with catalytic efficiencies resembling those of well-known AHLases. Interestingly, unlike their MBL activity the AHLase activity of MIM-1 and MIM-2 is not dependent on the metal ion composition with Zn(II), Co(II), Cu(II), Mn(II) and Ca(II) all being able to reconstitute catalytic activity (with Co(II) being the most efficient). However, these enzymes do not turn over S-lactoylglutathione, a substrate characteristic for GLX-II activity. Since lactonase activity is linked to the process of quorum sensing the bifunctional activity of “non-pathogenic” MBLs such as MIM-1 and MIM-2 may provide insight into one possible evolutionary pathway for the emergence of antibiotic resistance.

Chapter 4: Promiscuous metallo- β -lactamases: MIM-1 and MIM-2 may play an essential role in quorum sensing networks

4.1 Introduction

Antibiotic resistance is a major problem for modern health care systems across the globe. A major strategy employed by pathogens to acquire resistance to commonly used antibiotics involves the use of enzymes that inactivate these compounds. Of particular concern are the metallo- β -lactamases (MBLs), a large group of enzymes that are highly efficient in inactivating the majority of the available β -lactam-based antibiotics (e.g. penicillins, cephalosporins, carbapenems; refer to **Fig. 1.3.** in Chapter 1 for β -lactam core structures). Not only are these enzymes highly efficient catalysts, but there is also currently no clinically useful inhibitor available [16, 18, 20, 96, 132]. Novel MBLs are frequently discovered (e.g. NDM-1 or AIM-1 [113, 138]) and horizontal gene transfer further exacerbates the problem of a rapid spread of MBLs among pathogenic bacteria [146-148]. MBLs belong to a large group of metal ion-dependent hydrolytic enzymes (i.e. metallohydrolases) that include, among others, amino-peptidases, pesticide-degrading enzymes and numerous phosphatases [2, 4, 96]. The identity of the metal ions used by metallohydrolases varies considerably. For instance, urease has a specific requirement for two Ni(II) ions [168], while purple acid phosphatases (PAPs) contain a heterovalent Fe(III)-M(II) centre, where M = Fe, Zn or Mn [4, 96, 169]. Interestingly, in animal PAPs the divalent metal ion is exclusively Fe, which can easily and reversibly be oxidized, leading to the speculation that this enzyme may also act as a Fenton catalyst *in vivo* [170]. Other metallohydrolases such as a glycerophosphate diesterase (GpdQ) from *Enterobacter aerogenes* or an organophosphate (OP)-degrading enzyme from *Agrobacterium radiobacter* (OPDA) are highly promiscuous with respect to metal ions they can utilize for their catalytic functions [11, 24, 25, 171-174] (refer to Chapter 1 for more details regarding metallohydrolases). In contrast, the *in vivo* metal ion associated with MBLs is exclusively Zn(II), but *in vitro* assays have demonstrated that other divalent metal ions such

Chapter 4: Promiscuous metallo- β -lactamases: MIM-1 and MIM-2 may play an essential role in quorum sensing networks

as Co(II), Mn(II) or Ca(II) can reconstitute full or partial catalytic activity [89, 92, 175]. The crystal structures of several MBLs have been reported [16, 54, 77, 86, 138] (**Fig. 4.1.**); interestingly, the fold characteristic for MBLs is also used by metalloenzymes with rather different functions, including the organophosphate-pesticide degrading enzyme methyl parathion hydrolase [153, 176] and enzymes involved in quorum quenching (QQ) [9, 177].

QQ is used by bacteria to regulate quorum sensing (QS) networks [177-181]. QS is defined as an effect on a population of unicellular organisms that triggers them to act as a multicellular organism when their cellular density reaches a characteristic threshold [177-180, 182]. Bacteria use QS to promote processes such as bioluminescence, the formation of biofilms and the expression of virulence-related genes [177-180, 182]. There are various signalling molecules used by bacteria to communicate among each other, but N-acyl homoserine lactones (AHLs) are the most studied and prevalent QS mediators [177-181, 183, 184]. Common AHLs contain a characteristic five-membered lactone ring in their core and are distinguished based on the identity of their alkyl chains (**Fig. 4.2.**). The length of the aliphatic chain is a determining factor for the substrate preference of enzymes that are capable of inactivating AHLs [177-181, 183, 184].

Chapter 4: Promiscuous metallo- β -lactamases: MIM-1 and MIM-2 may play an essential role in quorum sensing networks

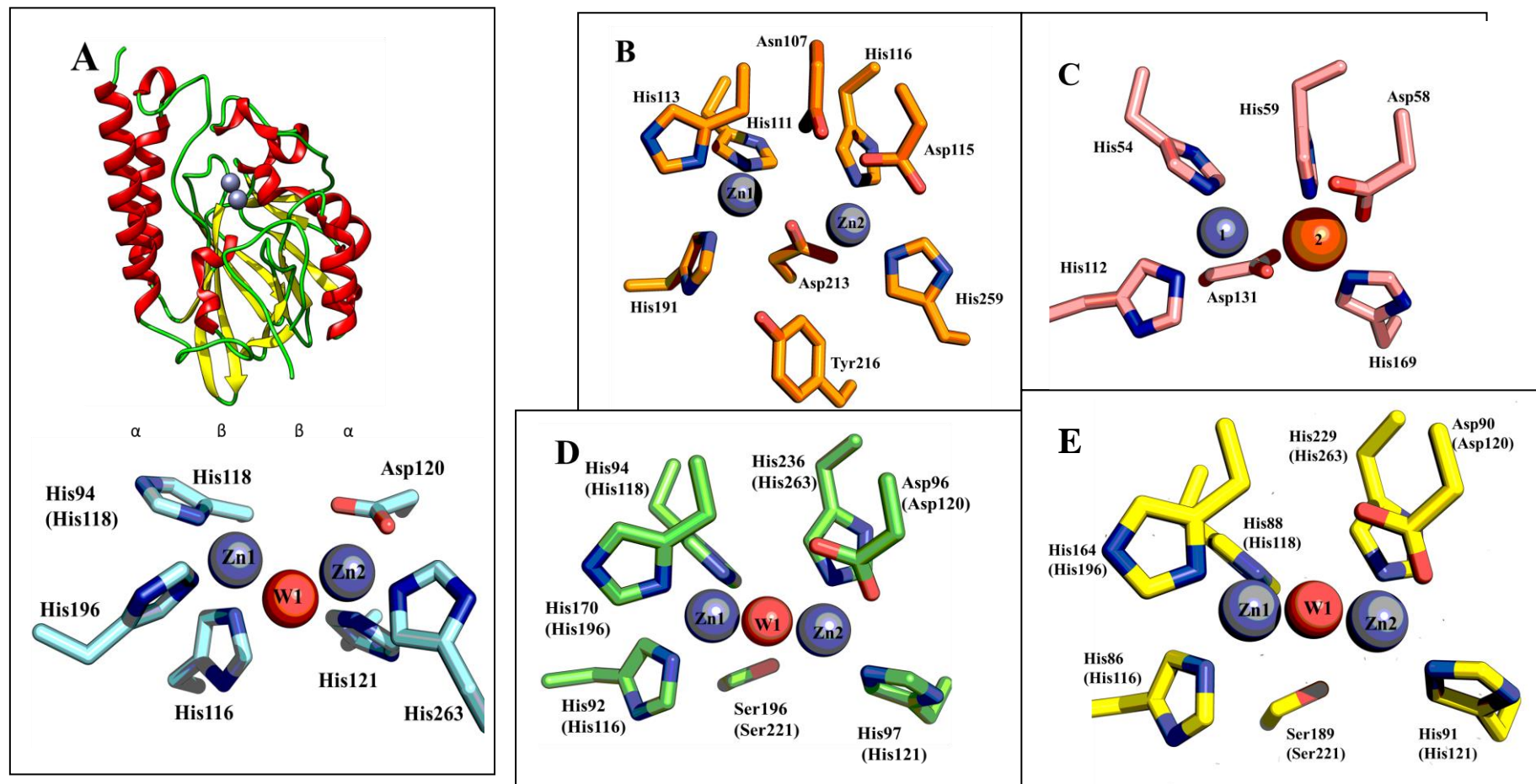


Figure 4.1. Metallo- β -lactamase fold and active site geometries. In (A) the overall structure of the *D3 MBL* *MIM-1* from *P. aeruginosa* (top; PDB: 4AWY) displaying the $\alpha\beta/\beta\alpha$ fold characteristic to the MBL protein family, and the corresponding active site structure (bottom) are shown. The zinc ions are represented as grey spheres, (B)-(E): The active sites of AiiB (2R2D), GLXII from *A. thaliana* (2Q4D), MIM-1 and MIM-2, respectively, are shown for comparison. The residues are depicted as sticks, the water molecules as red spheres, the zinc and iron ions as grey and orange spheres. The residues are numbered according to individual protein amino acid sequences as well as the MBL numbering scheme (in bracket).

Chapter 4: Promiscuous metallo- β -lactamases: MIM-1 and MIM-2 may play an essential role in quorum sensing networks

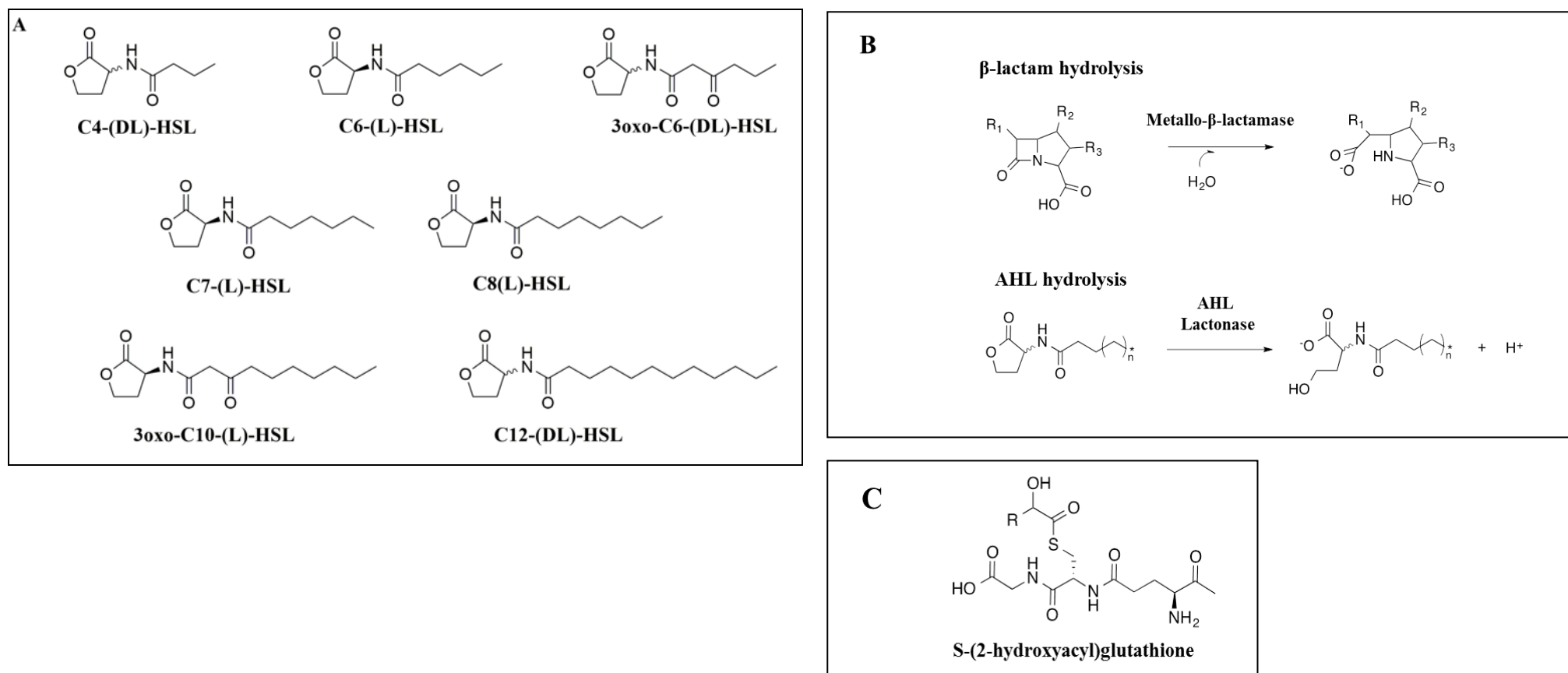


Figure 4.2. Substrates (A), (C) and reaction mechanisms (B). Core structures of the substrates used and the mechanism of action of metallo- β -lactamases and N-acyl homoserine lactonases.

Chapter 4: Promiscuous metallo- β -lactamases: MIM-1 and MIM-2 may play an essential role in quorum sensing networks

Two distinct enzymatic mechanisms are known to inactivate AHLs, one involving the hydrolysis of the lactone ring, catalysed by AHLases, and the other one using AHL acylases to hydrolyse the amide bond of the substrate [178, 180, 181, 184]. Only AHLases have the characteristic MBL fold and contain a di-metallic center in their active site; the reaction catalysed by these enzymes resembles that of MBLs and involves ring opening (**Fig. 4.2 B**) [177, 180].

In **Chapter 3** I focused on the “MBL-like” properties of MIM-1 from *Novosphingobium pentaromativorans* and MIM-2 from *Simiduia agarivorans* [91, 92]. Both enzymes are Zn(II)-dependent and have a preference for β -lactam substrates from the penam group (*e.g.* penicillin G, ampicillin). Interestingly, while catalytic activity could be reconstituted with other divalent metal ions the substrate preference was affected by the identity of the metal ion. For example, while penams are the preferred substrate for the Zn(II) derivative of both MIM-1 and MIM-2 their Cu(II) derivatives displayed no measurable activity towards these reactants. In contrast, the reactivity towards biapenem, a β -lactam substrate from the carbapenem group, is only mildly reduced for MIM-1 and significantly enhanced for MIM-2 upon the replacement of Zn(II) by Cu(II) [92]. Furthermore, modest activity could also be reconstituted for most substrates tested in the presence of Ca(II), not a metal ion commonly found in the active sites of metallohydrolases. Neither *N. pentaromativorans* nor *S. agarivorans* are known pathogens. While it cannot be ruled out that these organisms may have evolved MBL-like enzymes due to antibiotic pollution in their habitats, it is possible that the biologically relevant substrate(s) and thus the corresponding *in vivo* functions of MIM-1 and MIM-2 are unrelated to their *in vitro* MBL activity. In this Chapter the plasticity of the MBL fold will be investigated. Bioinformatics tools as well as kinetic assays were used to highlight the functional promiscuity of MIM-1 and MIM-2 and their ability to operate as bi-functional enzymes. The outcomes discussed in this Chapter may be of relevance for medicinal chemistry as they

Chapter 4: Promiscuous metallo- β -lactamases: MIM-1 and MIM-2 may play an essential role in quorum sensing networks

demonstrate that some promiscuous enzymes may have the capability to link the inactivation of chemotherapeutics (*i.e.* antibiotics) to processes such as QS (and in particular its association with biofilm formation), thus compounding the challenge associated with antibiotic resistance.

4.2 Materials and methods

4.2.1 Materials

The sequences encoding MIM-1 and MIM-2 were cloned into the commercial vector pJ411 (DNA 2.0). All chemicals were of analytical grade. *Escherichia coli* BL21 (DE3) pLysS cells (Agilent) were used for recombinant expression of the proteins. All chemicals were purchased from Sigma-Aldrich unless stated otherwise.

4.2.2 Database search, sequence alignments and phylogenetic analysis

A BLAST search (<http://blast.ncbi.nlm.nih.gov/Blast.cgi>), using the amino acid sequences of MIM-1 and MIM-2 as templates, was used to identify homologs of these enzymes. The search was conducted within the non-redundant protein database. Proteins of interest were compared in a multiple sequence alignment using the free software Jalview2 on the Muscle server [185-188]; the alignment was edited using ESPript 3.0 (<http://esprict.ibcp.fr/ESPript/ESPript/index.php>) [189]. The phylogenetic analysis was carried out using the MEGA 6 software package [190]. The phylogenetic tree was built using the Maximum Likelihood model (1000 iterations were used to test the goodness of the analysis). The tree was then edited using the software FigTree, available online (<http://tree.bio.ed.ac.uk/software/figtree/>).

Chapter 4: Promiscuous metallo- β -lactamases: MIM-1 and MIM-2 may play an essential role in quorum sensing networks

4.2.3 Structural homology modelling and docking

The protein sequences of both MIM-1 and MIM-2 were used to build homology structural models using the comparative structural building tool MODELER in the EasyModeller v4.0 graphical environment [191].

The models were built using the structure of the MBL AIM-1 from *Pseudomonas aeruginosa* as template (PDB: 4AWY; [138]). The structural alignments were conducted using the Swiss PDB Viewer software (<http://spdbv.vital-it.ch>), using the annotated MBL structures of AIM-1 and L1 from *Stenotrophomonas maltophilia* (PDB: 2FM6 for the native form; 2FU8 for the inhibitor (D-captopril)-bound form [192]), the AHLase AiiA from *Bacillus thuringiensis* (PDB: 2A7M for the native form [193]; 3DHA and 3DHB for the complex with the substrate C6-HSL [194, 195]), and GLX-II from both *Homo sapiens* (PDB: 1QH3; [196]) and *Arabidopsis thaliana* (PDB: 2Q42; [197]). The root mean square (rms) deviations for structural superimpositions were obtained using the free software SuperPose [198]. The images were edited using the software PyMOL and USCF Chimera 1.9 (<http://www.cgl.ucsf.edu/chimera>) [199]. The structure of the inhibitor D-captopril was generated using the software Avogadro. This inhibitor was then docked into the active sites of the MIM-1 and MIM-2 models using AUTODOCK 4.0 [200].

4.2.4 Protein expression and purification

The protocols for the expression and purification of recombinant MIM-1 and MIM-2 were previously optimized [92]. In brief, following expression the soluble fraction of the cell lysate was loaded onto a HiTrap Q FF 5 mL column (GE Healthcare). The enzymes were eluted with a NaCl gradient and loaded onto a HiPrep 16/60 Sephacryl S-200 HR column (GE Healthcare). Fractions containing MBL activity were pooled and stored at 4 °C in 50 mM

Chapter 4: Promiscuous metallo- β -lactamases: MIM-1 and MIM-2 may play an essential role in quorum sensing networks

Hepes (pH 7.5) containing 0.2 M NaCl and 0.15 mM ZnCl₂. The protein concentrations were estimated using theoretical extinction coefficients ($\epsilon_{280} = 36,815 \text{ M}^{-1} \text{ cm}^{-1}$ for MIM-1 and $41,285 \text{ M}^{-1} \text{ cm}^{-1}$ for MIM-2), calculated using the ProtParam tool (<http://web.expasy.org/protparam/>). Metal ion derivatives of MIM-1 and MIM-2 were prepared as described elsewhere [92].

4.2.5 Enzymatic assays and data analysis

The MBL activity of MIM-1 and MIM-2 was reported previously [92]. Here, the activity of these enzymes towards various AHLs and S-lactoylglutathione, a GLX-II substrate, was assessed. In order to increase the solubility of the AHL substrates solvents such as methanol need to be added into the assay mixture. Thus, in initial assays the sensitivity of MIM-1 and MIM-2 towards methanol was tested by following the MBL activity of the enzymes as a function of the solvent concentration. Meropenem was used as the substrate. The assays were carried out in 50 mM HEPES buffer, pH 7.5, 10 mM NaCl, with an enzyme concentration of 15 nM.

The AHLase activity assay employed a protocol previously described for enzymes such as carbonic anhydrase or haloalkane dehalogenase [201-206], and follows AHL hydrolysis by measuring the protons released during the reaction. The increase in the proton concentration is evaluated spectrophotometrically using an appropriate pH indicator. Here, we used Phenol Red in HEPES buffer to investigate the reaction between pH 7.4 and 7.6. The assay was recorded at 25 °C and 557 nm using 100–150 nM of enzyme in 1 mM HEPES, pH 7.5, 0.1 M NaCl₂ and 0.2 mM Phenol Red. After incubation of this mixture for 2 min the reaction was initiated by adding substrate. For each substrate concentration the rate of the non-enzymatic AHL hydrolysis (i.e. autohydrolysis) was subtracted from that of the enzyme-catalysed

Chapter 4: Promiscuous metallo- β -lactamases: MIM-1 and MIM-2 may play an essential role in quorum sensing networks

reaction. The net rate (i.e. the absorbance change (ΔAbs) per second) was then plotted against the substrate concentration fitted to the Michaelis–Menten equation to obtain relevant catalytic parameters (V_{max} and K_M). The V_{max} value was used to calculate the corresponding k_{cat} value using **Eq. 6**:

$$k_{cat} = V_{max} \left(\Delta Abs \frac{units}{s} \right) \div \left[\left(\theta \left(\Delta Abs \frac{units}{s} \right) \times [Enz]_T \right) \right] \quad (6)$$

In **Eq. 6** $[Enz]_T$ is the total enzyme concentration in the assay and the value of θ is obtained experimentally by titrating a Phenol Red solution in HEPES buffer with a standard solution of HCl 0.1 M. The assay was typically conducted using the same Phenol Red concentration used in the enzymatic assay. The HCl dependency was studied using a 10 mM stock solution of HCl. In our measurements the value of θ was 0.003 Abs units/ μ M.

Glyoxylase activity was measured using S-lactoylglutathione (SLG; 10 mM stock solution) in a 1 mL cuvette containing 20 mM 3-(N-morpholino)propanesulfonic acid (MOPS), pH 7.4. Both a continuous assay (at 240 nm) and a coupled one were employed to detect activity. In the coupled assay the hydrolysis of SLG was monitored by adding 20 μ M 5,5'-dithiobis-2-nitrobenzoate (DTNB), and following the increase in absorbance at 412 nm. When SLG is hydrolysed by GLX-II activity it releases D-lactic acid and reduced glutathione, which reduces DTNB to the yellow product 5-thio-2-nitrobenzoic acid (TNB) [206].

Metal ion derivatives of MIM-1 and MIM-2 were also assayed as described above. The assay mixtures were supplemented with 50 μ M of the respective divalent metal ion (i.e. Co(II), Mn(II), Cu(II) or Ca(II)). Negative controls containing only 50 μ M metals ions in the reaction mixture were carried out to confirm that the substrates are not hydrolysed in the absence of enzymes.

Chapter 4: Promiscuous metallo- β -lactamases: MIM-1 and MIM-2 may play an essential role in quorum sensing networks

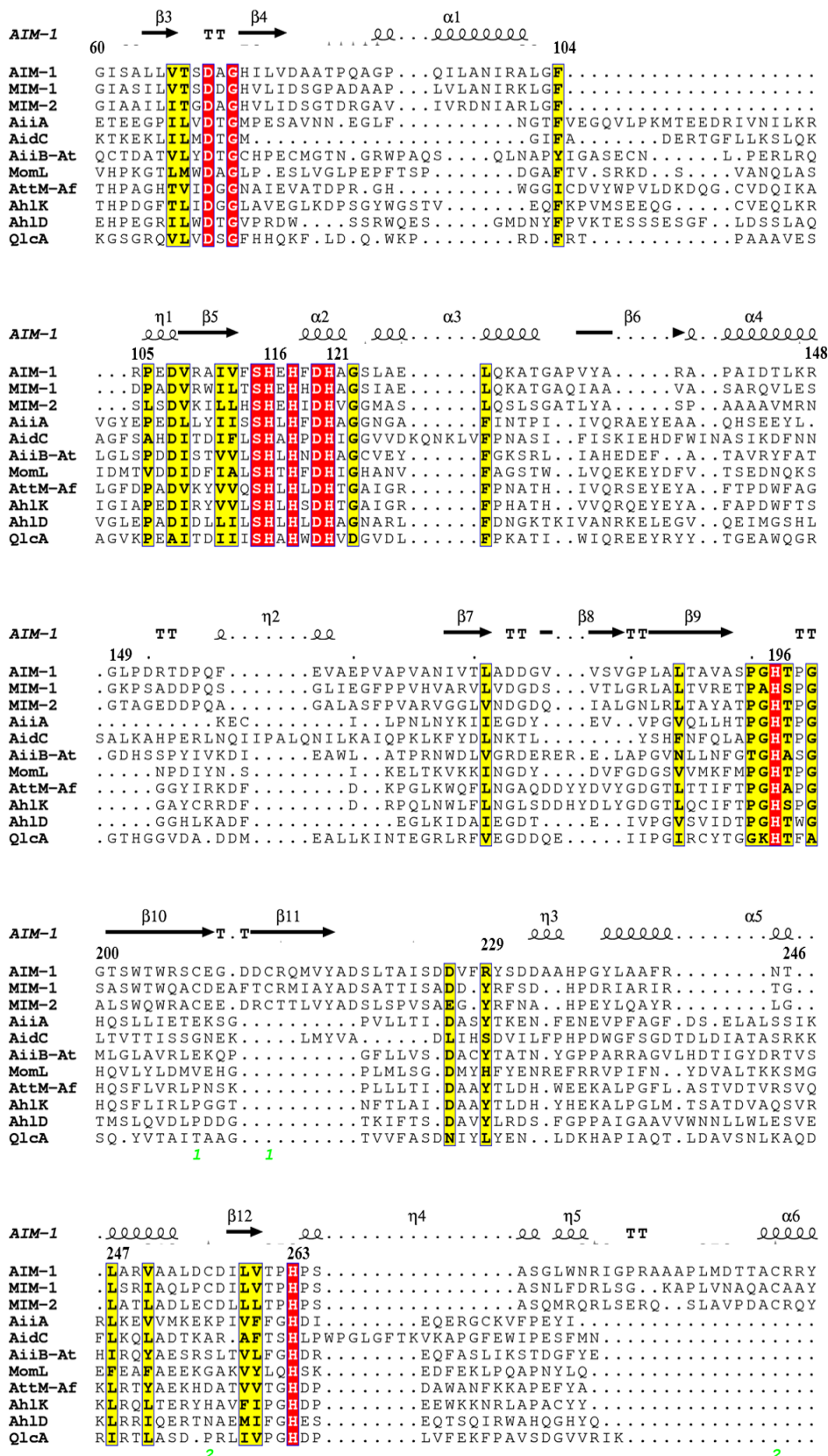
4.3 Results and discussion

4.3.1 Sequence and phylogenetic analysis

MIM-1 and MIM-2 were initially identified in a homology database search using the MBL AIM-1 as probe [91] (see Chapter 2 for more details). This MBL shares approximately 50% sequence identity with MIM-1 and MIM-2 and all the amino acid residues that are involved in binding the two essential Zn(II) ions in the active site are invariant in each of the three proteins (**Fig. 4.3.**). It was thus plausible to assume that MIM-1 and MIM-2 may act as MBLs. Indeed, catalytic assays with a range of β -lactam substrates (**Fig. 1.3.**) demonstrated that both enzymes are potent MBLs *in vitro* [92] (see Chapter 3 for further details). In an attempt to address possible alternative biological roles the sequence database was searched using both MIM-1 and MIM-2 as probes.

Not surprisingly, the closest homologs retrieved were MBLs (data not shown). These were followed by glyoxalase II (GLX-II; [206]) from *A. thaliana* (~45% similarity) and several AHLases including AttM [214-216] from *Azhorizobium caulinodans* and AhlK [212] from *Klebsiella pneumoniae*, with up to ~40% sequence similarity to both MIM-1 and MIM-2 (**Table 4.1.**). As mentioned above AHLases play an intricate role in the QS network while GLX-II is involved in detoxification pathways. Known structures of GLX-II and AHLase indicate that they possess the $\alpha\beta/\beta\alpha$ fold characteristic of MBLs and can also accommodate two metal ions in their active sites (**Fig. 4.1.**). Although the overall sequence identity between MIM-1 and MIM-2 and GLX-II and various AHLases is, by and large, below 30%, essential amino acids are well conserved as illustrated in the multiple sequence alignment in **Fig.4.3.**

Chapter 4: Promiscuous metallo- β -lactamases: MIM-1 and MIM-2 may play an essential role in quorum sensing networks



Chapter 4: Promiscuous metallo- β -lactamases: MIM-1 and MIM-2 may play an essential role in quorum sensing networks

Figure 4.3. Multiple Sequence Alignment of B3 MBLs with AHL representatives (previous page). The sequences of AIM-1, MIM-1 and MIM-2 are aligned with N-acyl homoserine lactone representatives, AiiA from *Bacillus sp. (240B1 [207])*, AidC from *Chryseobacterium sp. StRB126 [208]*, AiiB from *A. tumefaciens [205]*, MomL from *Muricauda olearia [209]*, AttM-Af from *Agrobacterium fabrum* str. C58 [210] , AhlK from *Klebsiella pneumonia [211]*, AhlD from *Arthrobacter sp. IBN110 [212] , QlcA from uncultured bacterium [213] .* Above the alignment, secondary structure elements are drawn using AIM-1 as template. Highly conserved residues are highlighted in red; conserved regions are coloured in yellow. The residues involved in the metal binding are indicated by a black diamond; the residues known to be critical for lactonase activity and which are conserved in MIM-1 and MIM-2 are indicated by a grey star. Residue D115 is involved in metal binding and plays a critical role in lactone hydrolysis. The numbering scheme follows the canonical MBL numbering of AIM-1 (PDB: 4AWY) [138, 139].

The six residues involved in coordination of the two metal ions in the active site of AIM-1 (*i.e.* His116, His118 and His196 for metal site 1 and Asp120, His121 and His263 for metal site 2, **Fig. 4.1.**) are invariant in MIM-1, MIM-2 and AHLases. In contrast to MBLs, but similar to the majority of binuclear metallohydrolases [2, 96, 138], AHLases and GLX-II have an aspartate ligand that bridges the two metal ions (Asp213 and Asp131 in **Fig. 4.1. B and C**, respectively). In GLX-II this bridging aspartate (*i.e.* Asp131) replaces one of the three histidine ligands but Site 2 is identical to that of AIM-1 and AHLases. Both MIM-1 and MIM-2, like the majority of known MBLs [217], possess a putative signal peptide that may facilitate their transfer into the periplasmic space. The presence of such a signal peptide is not common among the currently known AHLases, with MomL from *Muricauda olearia* being the only exception [208]. In summary, the sequence comparison revealed that MIM-1 and MIM-2 are closer related to MBLs than AHLases or GLX-II as illustrated in a phylogenetic analysis (**Fig. 4.4.**).

Chapter 4: Promiscuous metallo- β -lactamases: MIM-1 and MIM-2 may play an essential role in quorum sensing networks

Table 4.1. Sequence identities and similarities of AIM-1, MIM-1 and MIM-2 with representative AHLases and the GLX-II from *A. thaliana* (GLXII-At). The sequence similarity percentage was obtained using the PAM250 matrix available in the free web tool SIAS. The following AHLases were used in the comparison: AiiA from *Bacillus* sp 240B1 [218], AidC from *Chryseobacterium* sp. StRB126 [208], AttM from *Agrobacterium tumefaciens* [219], AiiB from *Agrobacterium tumefaciens* [205], MomL from *Muricauda olearia* [209], AttM from *Agrobacterium fabrum* [219], AhlK from *Klebsiella pneumoniae* [211], Attb from *Agrobacterium fabrum* [210], AhlD from *Arthrobacter* sp. IBN110 [212], QlcA from uncultured bacteria [213] and GLX-II from *Arabidopsis thaliana* [220].

	Identity (%)			Similarity (%)		
	AIM-1	MIM-1	MIM-2	AIM-1	MIM-1	MIM-2
AiiA	29%	29%	31%	39%	41%	39%
AidC	30%	29%	31%	35%	37%	39%
AttM-At	29%	30%	30%	40%	41%	40%
AiiB-At	15%	16%	17%	38%	41%	40%
MomL	25%	24%	29%	36%	36%	39%
AttM	23%	23%	27%	32%	33%	34%
AhlK	15%	16%	17%	39%	41%	41%
AttB-Af	29%	30%	32%	37%	38%	38%
AhlD	26%	29%	31%	35%	39%	40%
QlcA	16%	18%	19%	25%	27%	28%
GLXII-At	29%	28%	31%	39%	37%	39%

Chapter 4: Promiscuous metallo- β -lactamases: MIM-1 and MIM-2 may play an essential role in quorum sensing networks

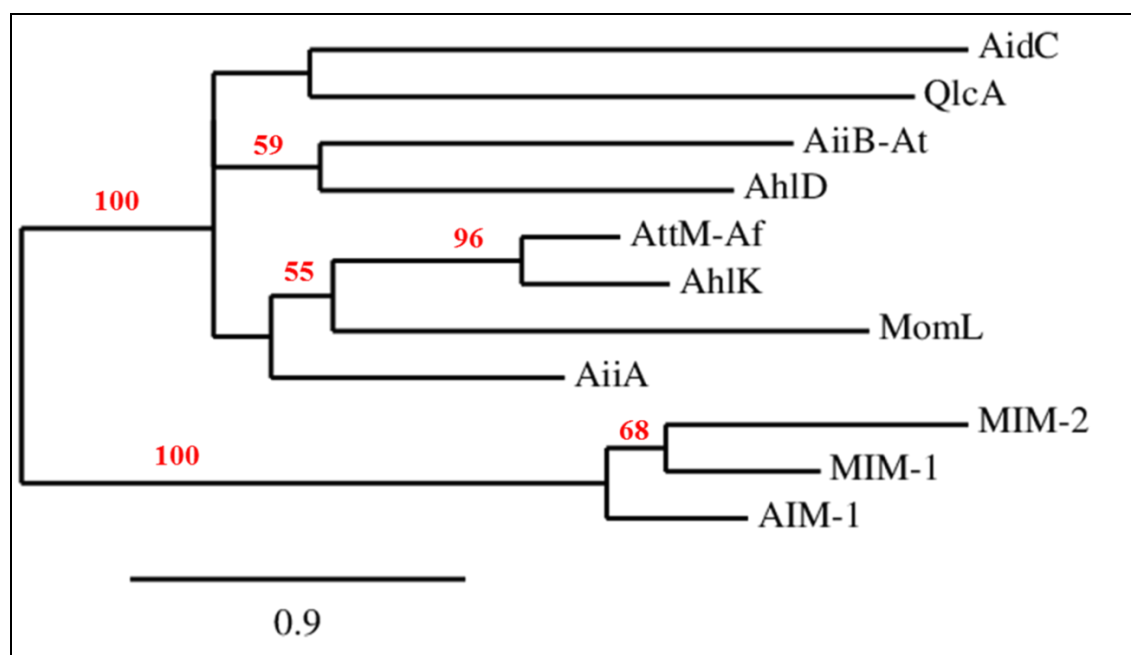


Figure 4.4. Phylogenetic analysis of MIM-1, MIM-2 and AHLs. The phylogenetic tree relates the B3 AIM-1, MIM-1 and MIM-2 with well-known AHLs. The analysis was conducted using the Neighbor-joining tree model, based on the amino acid sequences, using the software MUSCLE (2000 bootstrap replicates). Bootstrap coefficient below 50% are not shown. Scale bar, 0.9 amino acid substitution per amino acid position.

4.3.2 Structural models of MIM-1 and MIM-2

Crystals suitable for X-ray diffraction studies of MIM-1 and MIM-2 are currently not yet available. Hence, in the absence of experimental structural information homology models of the two proteins were generated using the crystal structure of their closest homolog, AIM-1 (PDB: 4AWY), as template (**Fig. 4.1.**). The entire α carbon backbones of the MIM-1 and MIM-2 models superimposed with rms values of 0.43 Å and 0.36 Å with the AIM-1 structure, respectively. The models are shown in **Fig. 4.5.** A similar approach using either a AHLase or GLX-II structure did not result in plausible models (data not shown). The most significant

Chapter 4: Promiscuous metallo- β -lactamases: MIM-1 and MIM-2 may play an essential role in quorum sensing networks

deviations occur at the N-terminus, where only MIM-1 possesses an elongated tail which may be a reflection of its homo-dimeric nature, in contrast to MIM-2 and AIM-1, which are monomeric proteins [92]. In **Fig. 4.1.** the active sites of MIM-1 and MIM-2 are shown, each with two Zn(II) ions. The modelled water molecule (W) bridges the two metal ions and is believed to be the hydrolysis- initiating nucleophile in most MBLs [16, 18, 96].

The main reason for generating homology models of MIM-1 and MIM-2 was to probe the possibility if their active sites are able to accommodate diverse substrates that may account for different biological functions. For calibration D-captopril was docked into the active sites of the two enzymes since a crystal structure of this molecule bound to the active site of the MBL L1 from *S. maltophilia* is known [192]. D-Captopril is a potent non-clinical, competitive inhibitor of MBLs with inhibition constants in the low micromolar range [16, 23, 92, 96, 221].

We have shown previously that this compound binds to MIM-1 and MIM-2 in a mode and with an affinity similar to that observed for MBLs; the recorded competitive inhibition constants (K_{ic} values) are $\sim 6 \mu\text{M}$ for both enzymes [92] (refer to Chapter 3 for details regarding the inhibition studies). In the models of MIM-1 and MIM-2 the best docking scores were obtained when D-captopril bound to the metal centers in a bidentate mode as shown in **Fig. 4.6. A** and **Fig. 4.7. A**. Although this best fit disagrees with the mode of binding observed in the crystal structure of the MBL L1 (where the thiol group of D-captopril bridges the two metal ions [192]) it is in good agreement with the computational data reported for the MBL BcII from *Bacillus subtilis*. In the next phase of modeling, since kinetic measurements indicated that penicillin G is the most efficient substrate for both MIM-1 and MIM-2 [92], this substrate was also docked into the active sites of these enzymes (**Fig. 4.6. B** and **Fig. 4.7. B**). While no comparison to experimental structures can be made for these substrate-bound complexes the positioning of the scissile β -lactam bond in the vicinity of the metal ion-

Chapter 4: Promiscuous metallo- β -lactamases: MIM-1 and MIM-2 may play an essential role in quorum sensing networks

bridging water molecule (see arrow in **Fig. 4.6. B** and **Fig. 4.7. B**) is in good agreement with currently accepted models for the reaction mechanism whereby the bridging water/hydroxide attacks the carbonyl carbon atom of the β -lactam ring to initiate ring opening [16, 18]. The docked mode of binding also resembles that observed for the complex of the MBL NDM-1 with hydrolyzed ampicillin [77].

The docking studies provide some confidence that reasonable insight may be gained for enzyme–substrate interactions relevant to MIM-1 and MIM-2. Thus, the AHL substrate C6-L-HSL (**Fig. 4.2. A**) and S-(2-hydroxyacyl)lglutathione (**Fig. 4.2. C**) were also docked into the active sites of MIM-1 and MIM-2. Both enzymes bind the lactone in a similar fashion, with the two oxygen atoms of the lactone ring coordinating each to one of the metal ions in the active site (**Figs 4.6. C** and **4.7. C**). This mode of binding is consistent with the structural complex of AiiA from *B. thuringensis* with hydrolyzed N-hexanoyl-L-homoserine lactone [194, 195]. No consistent binding modes were obtained when S-lactoylglutathione was docked into the active sites of these enzymes, irrespective of the protonation state of the substrates carboxyl group. Docking thus suggests that MIM-1 and MIM-2 may act as AHLases but not as glyoxylases.

Chapter 4: Promiscuous metallo- β -lactamases: MIM-1 and MIM-2 may play an essential role in quorum sensing networks

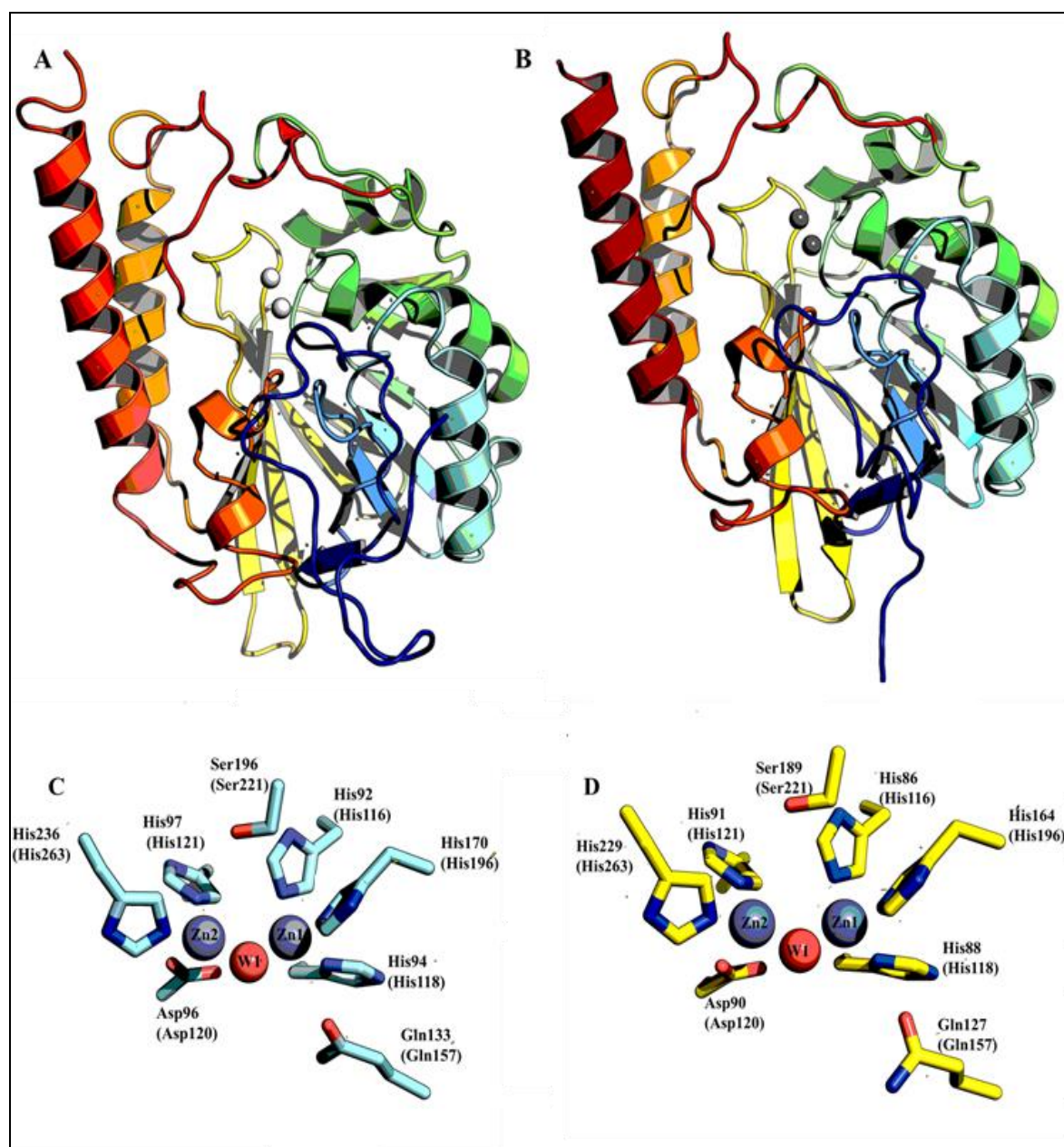


Figure 4.5. MIM-1 and MIM-2 structural models. The homology model was built using AIM-1 (PDB: 4AWY) as template. Both MIM-1 (A) and MIM-2 (B) show the characteristic $\alpha/\beta/\alpha$ fold, common to the MBL superfamily. The loops believed to play a major role in the contact with the substrates are coloured in red; the zinc in the active sites are coloured in light grey (A) and grey (B). In C and D are shown the amino acids involved in the metal binding and the active site cleft formation. The amino acids are drawn as ball and sticks, the zinc ions are depicted as grey spheres and the putative bridging water molecule present in the active site is shown as a red sphere.

Chapter 4: Promiscuous metallo- β -lactamases: MIM-1 and MIM-2 may play an essential role in quorum sensing networks

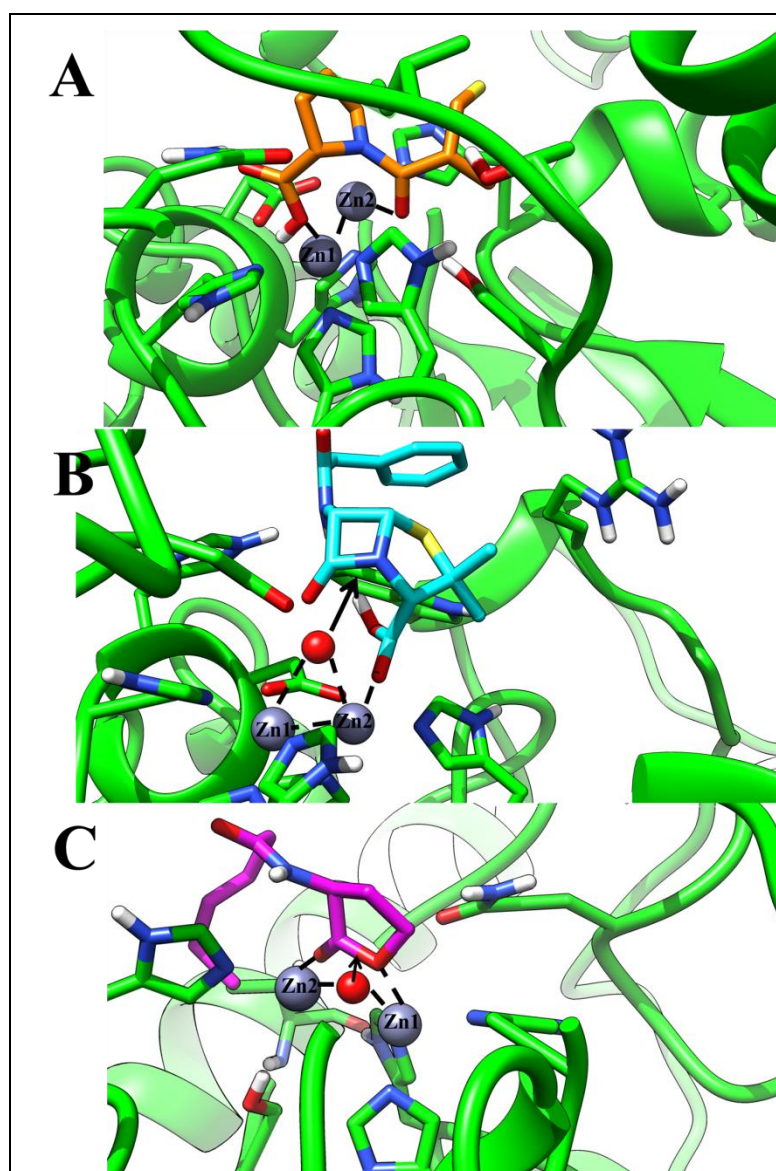


Figure 4.6. MIM-1 structural model dockings. The figure shows the model of MIM-1 docked with the D-captopril (A), with the penicillin G (B) and with N-hexanoyl homoserine lactone (C6-L-HSL) (C), using the software AUTODOCK 4.2. It is showing the detail of the active site, with the two zinc ions (grey spheres), the amino acids involved in the metal binding (represented as green ball and sticks) and the D-captopril (orange), penicillinG (cyan) and C6-L-HSL (magenta) interacting with the active site. The image was made using USCF Chimera 1.9.

Chapter 4: Promiscuous metallo- β -lactamases: MIM-1 and MIM-2 may play an essential role in quorum sensing networks

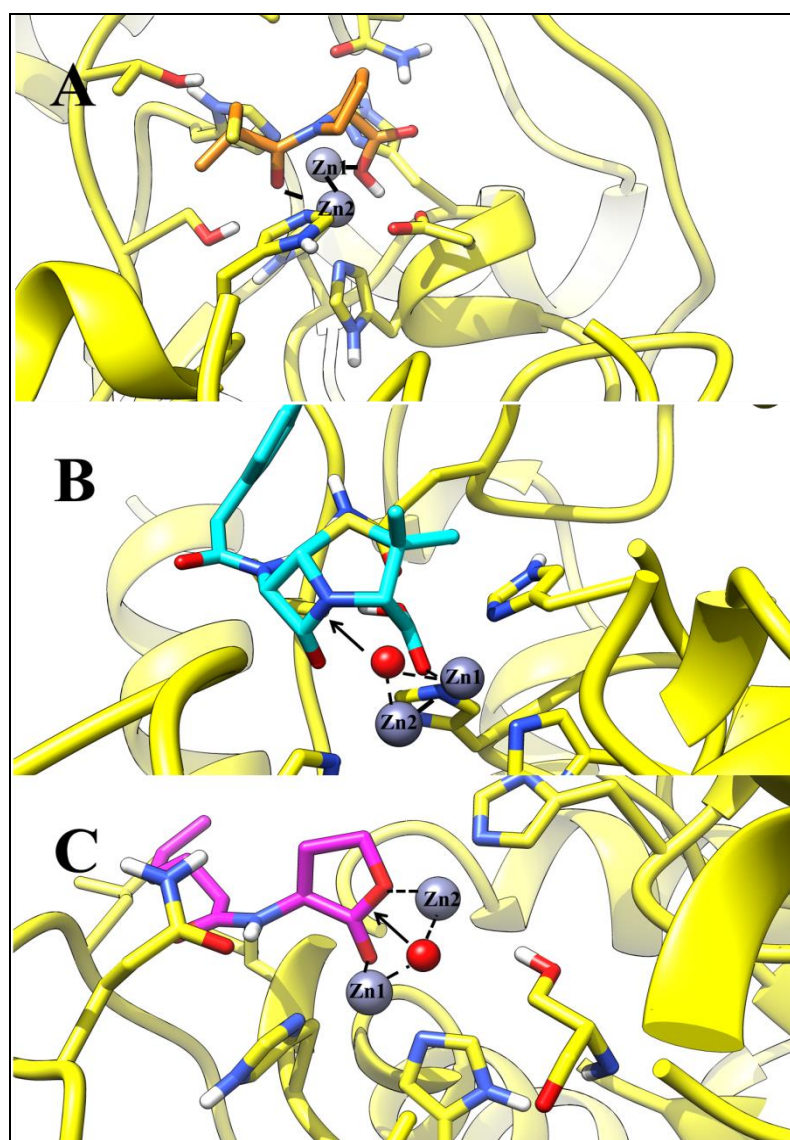


Figure 4.7. MIM-2 structural model dockings. The figure shows the model of MIM-2 docked with the D-captopril (A), with the penicillin G (B) and with N-hexanoyl homoserine lactone (C6-L-HSL) (C), using the software AUTODOCK 4.2. It is showing the detail of the active site, with the two zinc ions (grey spheres), the amino acids involved in the metal binding (represented as green ball and sticks) and the D-captopril (orange), penicillinG (cyan) and C6-L-HSL (magenta) interacting with the active site. The image was made using USCF Chimera 1.9.

Chapter 4: Promiscuous metallo- β -lactamases: MIM-1 and MIM-2 may play an essential role in quorum sensing networks

4.3.3 N-acyl homoserine lactonase activities of MIM-1 and MIM-2.

Both the sequence and homology model analysis have indicated that MIM-1 and MIM-2 may act primarily as MBLs, but the possibility of alternative functions, especially as AHLases, could not be ruled out conclusively. Thus, both GLX-II and AHLase activity were tested by using either S-D-lactoylglutathione or a range of acyl-homoserine lactones, respectively, as substrates. Consistent with the docking studies no GLX-II activity was measurable for either enzyme but both are efficient AHLases. Since the alkyl chains of the lactone substrates lower their solubility in an aqueous environment the effect of methanol on enzyme stability was initially tested by recording the MBL activity of MIM-1 and MIM-2 as a function of added methanol. MIM-1 activity was not significantly altered using methanol concentrations up to 20% in the assay mixtures (**Fig. 4.8.**). In contrast, MIM-2 is less stable in the presence of this solvent, losing almost half its activity at a methanol concentration of 10% (**Fig. 4.8.**). Thus, the AHLase assays were conducted in the presence of 20% or 5% methanol in the reaction mixture for MIM-1 and MIM-2, respectively.

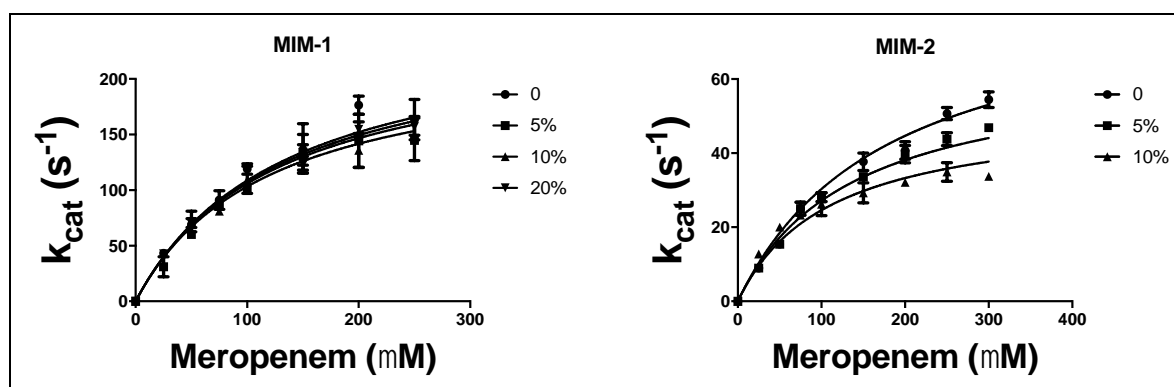


Figure 4.8. Methanol Inhibition of MIM-1 (left panel) and MIM-2 (right panel). The inhibition by methanol was tested following the hydrolysis of meropenem.

The alkyl chain lengths for the various N-acyl homoserine lactone substrates tested ranged

Chapter 4: Promiscuous metallo- β -lactamases: MIM-1 and MIM-2 may play an essential role in quorum sensing networks

from C4 to C12 (**Fig. 4.2 A**). Data were measured using the native Zn(II)-bound forms of MIM-1 and MIM-2, as well as several metal ion derivatives including Co(II), Cu(II), Mn(II) and Ca(II). In **Fig. 4.9.** and **Fig. 4.10** experimental data for the various derivatives of MIM-1 and MIM-2 are shown for the reaction with the HSL substrate.

Relevant kinetic parameters (*i.e.* k_{cat} , K_{M} and $k_{\text{cat}}/K_{\text{M}}$) are listed in **Tables 4.2 and 4.3**. For the Zn(II)-derivatives of MIM-1 and MIM-2 k_{cat} values range between $\sim 0.5 \text{ s}^{-1}$ to $\sim 3.5 \text{ s}^{-1}$, and $\sim 0.5 \text{ s}^{-1}$ to $\sim 8 \text{ s}^{-1}$, respectively, without an apparent trend connected to the length of the alkyl chain (**Table 4.2.**). Similarly, the corresponding K_{M} values do not appear to be directly linked to the alkyl side chain, and values range from $\sim 1 \text{ }\mu\text{M}$ to $\sim 200 \text{ }\mu\text{M}$. For both MIM-1 and MIM-2 the most efficiently hydrolysed AHL substrate is C10-3oxo-DL-HSL, with $k_{\text{cat}}/K_{\text{M}}$ values of $2.5 \times 10^6 \text{ s}^{-1}/\text{M}$ and $8.0 \times 10^5 \text{ s}^{-1}/\text{M}$, respectively. By and large, the catalytic efficiency of MIM-1 and MIM-2 towards the various AHL substrates is favourable to that of well-established AHLases such as AiiA from *Bacillus* sp. 240B1, AiiB from *A. tumefaciens* or AidC from *Chryseobacterium* sp. StRB126 (**Table 4.3.**). The more recently discovered AHLase MomL from *M. olearia* [219] has higher k_{cat} values than the remaining enzymes, but its affinity for the tested substrates is generally weaker than in MIM-1 or MIM-2.

Chapter 4: Promiscuous metallo- β -lactamases: MIM-1 and MIM-2 may play an essential role in quorum sensing networks

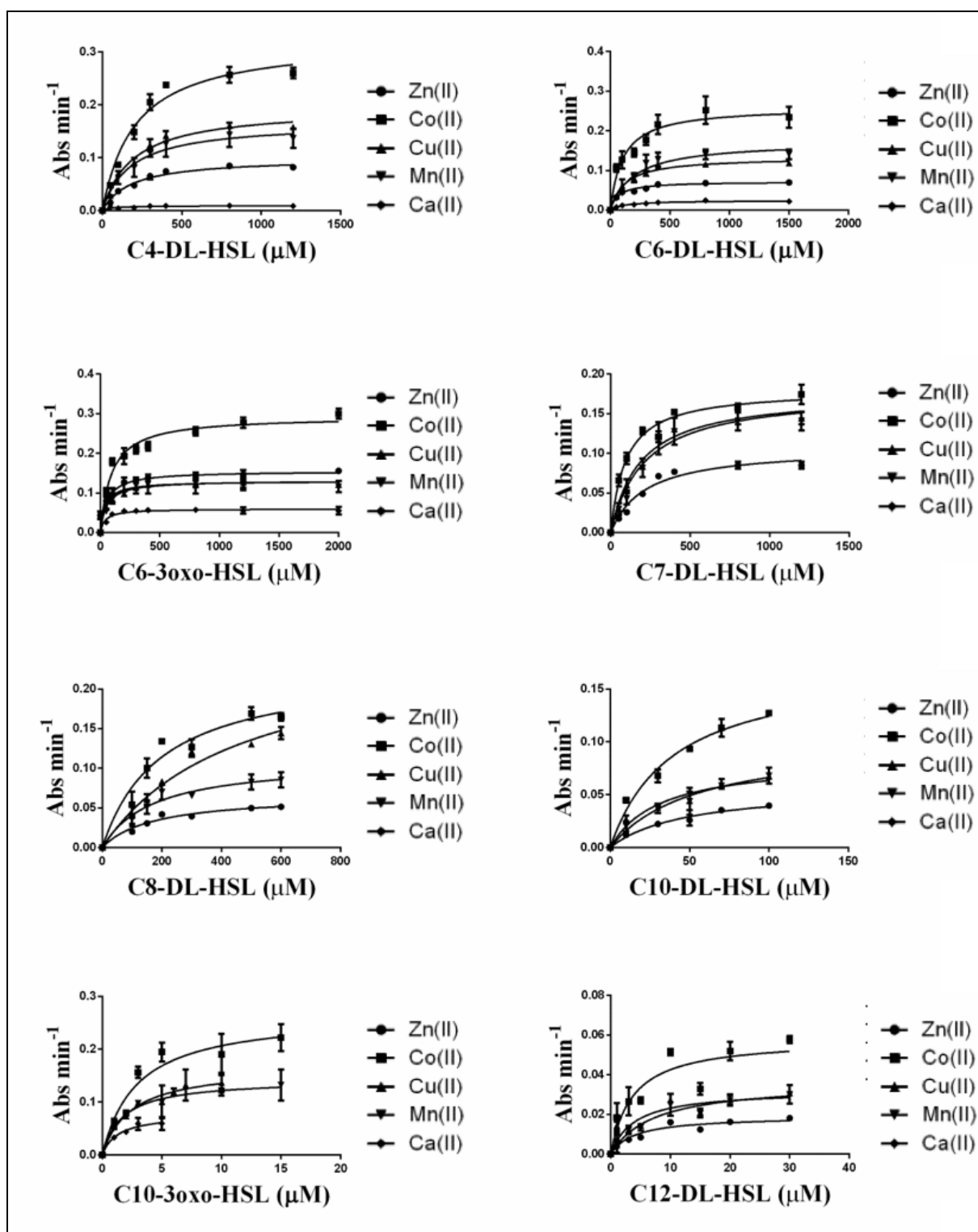


Figure 4.9. Kinetic parameters analysis of the N-acyl homoserine lactonase activities of MIM-1. Michaelis-Menten kinetic data for the Zn(II)- (circle), Co(II)- (square), Cu(II)- (triangle), Mn(II)- (inverted triangle) and Ca(II)- (diamond) substituted MIM-1 for the hydrolysis of various HSL substrates are shown.

Chapter 4: Promiscuous metallo- β -lactamases: MIM-1 and MIM-2 may play an essential role in quorum sensing networks

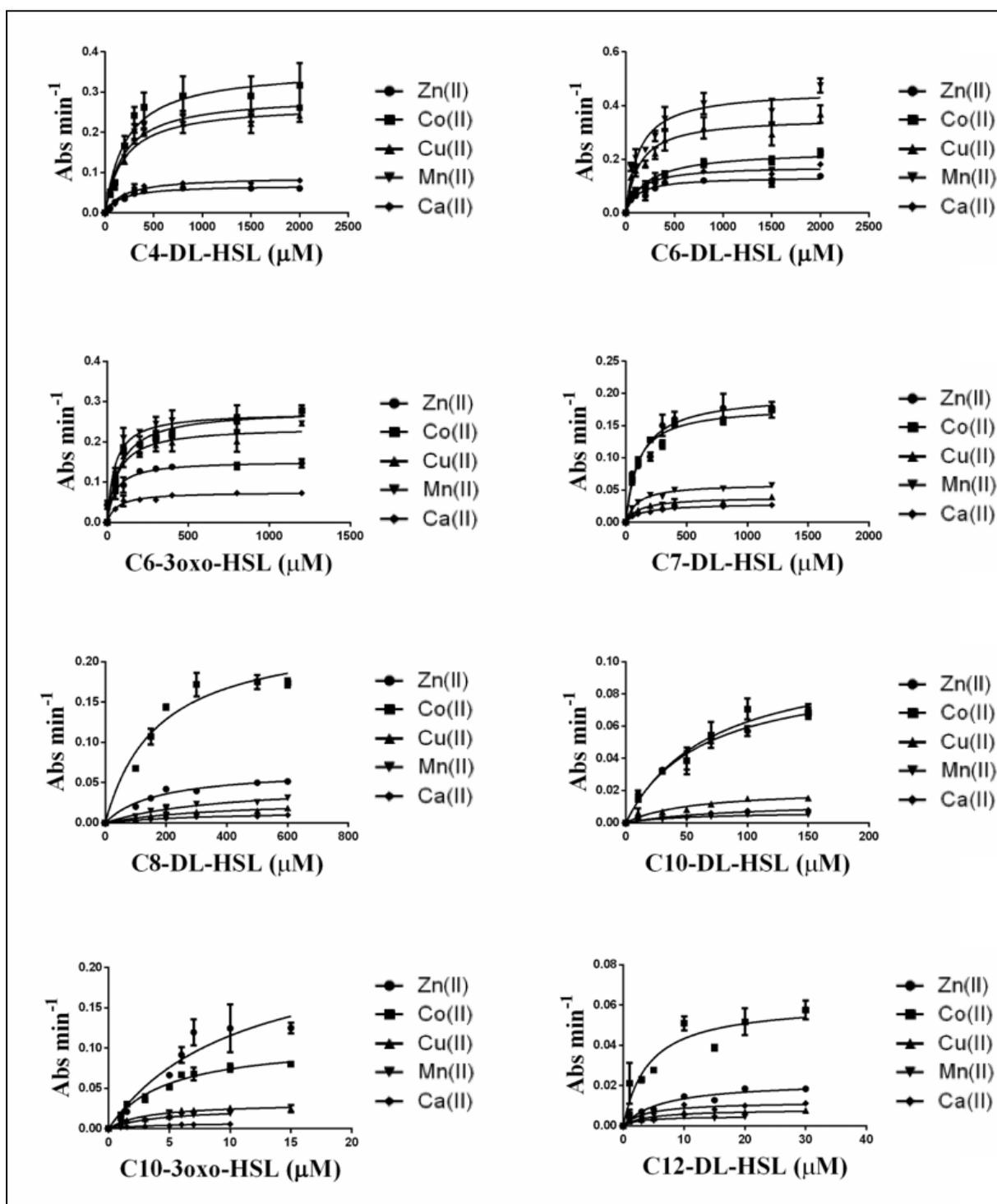


Figure 4.10. Kinetic parameters analysis of the N-acyl homoserine lactonase activities of MIM-2. Michaelis-Menten data for the Zn(II)- (circle), Co(II)- (square), Cu(II)- (triangle), Mn(II)- (inverted triangle) and Ca(II)- (diamond) substituted MIM-2 for the hydrolysis of various HSL substrates are shown.

Chapter 4: Promiscuous metallo- β -lactamases: MIM-1 and MIM-2 may play an essential role in quorum sensing networks

The catalytic data strongly suggest that MIM-1 and MIM-2 are bifunctional enzymes, with both being very efficient AHLases and MBLs. However, they are not the first AHLases that may display functional promiscuity. The enzymes SsoPox from *Sulfolobus solfataricus* [222] and OPH from *Rhodococcus erythropolis* and *R. ruber* [223] were initially identified as organophosphate (OP)-degrading hydrolases, but both possess AHLase activity as well (**Table 4.3**).

Chapter 4: Promiscuous metallo- β -lactamases: MIM-1 and MIM-2 may play an essential role in quorum sensing networks

Table 4.2 A. Comparison of the lactonase activities of metal ion-derivatives of MIM-1. The kinetic parameters of Zn(II)-, Co(II)-, Cu(II)-, Mn(II)- or Ca(II)-substituted MIM-1 are compared. The activity assays were conducted in the presence of excess of M(II) and in the presence of different N-acyl homoserine lactones (Fig. 1B).

Substrate	MIM-1														
	Zn(II)			Co(II)			Cu(II)			Mn(II)			Ca(II)		
	k_{cat} (s^{-1})	K_m (μM)	$k_{cat}/K_m(s^{-1}/M)$	k_{cat} (s^{-1})	K_m (μM)	$k_{cat}/K_m(s^{-1}/M)$	k_{cat} (s^{-1})	K_m (μM)	$k_{cat}/K_m(s^{-1}/M)$	k_{cat} (s^{-1})	K_m (μM)	$k_{cat}/K_m(s^{-1}/M)$	k_{cat} (s^{-1})	K_m (μM)	$k_{cat}/K_m(s^{-1}/M)$
C12-DL-HSL	0.6 ± 0.1	4.0 ± 1.1	$1.5 \cdot 10^5$	1.9 ± 0.9	3.6 ± 1.2	$5.2 \cdot 10^6$	1.0 ± 0.1	3.9 ± 1.2	$2.5 \cdot 10^5$	1.2 ± 0.4	7.2 ± 1.8	$1.6 \cdot 10^5$	1.7 ± 0.6	1.4 ± 0.4	$1.2 \cdot 10^6$
C10-3oxo-DL-HSL	2.5 ± 0.9	1.1 ± 0.4	$2.5 \cdot 10^6$	8.8 ± 1	2.9 ± 0.7	$3.0 \cdot 10^6$	5.3 ± 1	1.8 ± 0.7	$2.9 \cdot 10^6$	4.6 ± 0.3	1.4 ± 0.4	$3.2 \cdot 10^6$	0.7 ± 0.1	1.2 ± 0.4	$5.8 \cdot 10^5$
C10-DL-HSL	1.9 ± 0.7	48.4 ± 12.2	$3.9 \cdot 10^4$	5.8 ± 0.8	39.5 ± 6.9	$1.4 \cdot 10^5$	2.7 ± 0.3	31.4 ± 9.2	$8.7 \cdot 10^4$	3.4 ± 1.1	54.2 ± 17.2	$6.2 \cdot 10^4$	0.5 ± 0.1	36.8 ± 1.4	$1.4 \cdot 10^4$
C8-DL-HSL	2.2 ± 1.0	170.8 ± 28.9	$1.2 \cdot 10^4$	7.4 ± 0.5	188.3 ± 34.2	$3.9 \cdot 10^4$	3.5 ± 0.8	136.4 ± 2.6	$2.5 \cdot 10^4$	3.7 ± 0.6	170.1 ± 37.4	$2.1 \cdot 10^5$	0.7 ± 0.3	187.4 ± 5.8	$3.7 \cdot 10^3$
C7-DL-HSL	3.6 ± 0.2	214.7 ± 30.8	$1.6 \cdot 10^4$	11.5 ± 1.0	214.5 ± 3.3	$5.3 \cdot 10^4$	5.88 ± 0.2	183.4 ± 2.1	$3.2 \cdot 10^4$	5.9 ± 1.2	211.8 ± 39	$2.7 \cdot 10^4$	0.9 ± 0.2	120.0 ± 5.3	$8.2 \cdot 10^3$
C6-3oxo-DL-HSL	2.7 ± 0.7	50.2 ± 9.7	$5.4 \cdot 10^4$	8.5 ± 0.1	46.2 ± 7.8	$1.8 \cdot 10^5$	4.3 ± 0.4	26.3 ± 3.4	$1.6 \cdot 10^5$	4.3 ± 0.4	40.2 ± 3.4	$1.0 \cdot 10^5$	2.3 ± 0.5	491.0 ± 81.6	$4.7 \cdot 10^3$
C6-DL-HSL	2.4 ± 0.9	67.9 ± 8.9	$3.5 \cdot 10^4$	8.7 ± 0.5	105.7 ± 20.2	$8.2 \cdot 10^4$	4.4 ± 0.1	122.7 ± 1.3	$3.6 \cdot 10^4$	4.0 ± 0.9	69.1 ± 13.4	$5.7 \cdot 10^4$	0.5 ± 0.1	53.0 ± 10.0	$9.4 \cdot 10^3$
C4-DL-HSL	3.2 ± 0.5	170.8 ± 23.4	$1.8 \cdot 10^4$	10.5 ± 0.4	194.1 ± 26.5	$5.4 \cdot 10^4$	6.3 ± 0.2	181.8 ± 2.9	$3.4 \cdot 10^4$	5.4 ± 0.2	165.6 ± 36.7	$3.2 \cdot 10^4$	0.4 ± 0.1	44.6 ± 7.6	$9.2 \cdot 10^3$

Chapter 4: Promiscuous metallo- β -lactamases: MIM-1 and MIM-2 may play an essential role in quorum sensing networks

Table 4.2. Comparison of the lactonase activities of metal ion-derivatives of MIM-2. The kinetic parameters of Zn(II)-, Co(II)-, Cu(II)-, Mn(II)- or Ca(II)-substituted MIM-2 are compared. The activity assays were conducted in the presence of excess of M(II) and in the presence of different N-acyl homoserine lactones (Fig. 1B).

Substrate	MIM-2														
	Zn(II)			Co(II)			Cu(II)			Mn(II)			Ca(II)		
	k_{cat} (s^{-1})	K_m (μM)	$k_{cat}/K_m(s^{-1}/M)$	k_{cat} (s^{-1})	K_m (μM)	$k_{cat}/K_m(s^{-1}/M)$	k_{cat} (s^{-1})	K_m (μM)	$k_{cat}/K_m(s^{-1}/M)$	k_{cat} (s^{-1})	K_m (μM)	$k_{cat}/K_m(s^{-1}/M)$	k_{cat} (s^{-1})	K_m (μM)	$k_{cat}/K_m(s^{-1}/M)$
C12-DL-HSL	0.7 ± 0.4	6.4 ± 1.4	$1.1 \cdot 10^5$	2.0 ± 0.2	4.2 ± 1.1	$4.8 \cdot 10^5$	0.3 ± 0.1	4.1 ± 0.9	$7.3 \cdot 10^4$	0.1 ± 0.1	2.5 ± 0.9	$6.3 \cdot 10^5$	0.4 ± 0.1	3.7 ± 1.0	$1.0 \cdot 10^5$
C10-3oxo-DL-HSL	8.0 ± 0.9	10.8 ± 3.6	$8.0 \cdot 10^5$	3.8 ± 0.5	5.4 ± 0.6	$7.0 \cdot 10^5$	1.0 ± 0.3	2.6 ± 0.6	$3.7 \cdot 10^5$	0.7 ± 0.1	2.9 ± 0.4	$2.3 \cdot 10^5$	0.2 ± 0.1	2.7 ± 0.8	$7.4 \cdot 10^5$
C10-DL-HSL	3.2 ± 0.2	60.9 ± 10.5	$5.2 \cdot 10^4$	3.0 ± 0.1	50.3 ± 7.8	$6.0 \cdot 10^4$	0.6 ± 0.1	46.7 ± 8.8	$1.4 \cdot 10^4$	0.2 ± 0.3	35.5 ± 8.5	$5.7 \cdot 10^3$	0.4 ± 0.1	77.8 ± 18.9	$5.1 \cdot 10^3$
C8-DL-HSL	2.6 ± 0.7	186.9 ± 39.8	$1.4 \cdot 10^4$	7.9 ± 1.1	172.3 ± 33.5	$4.6 \cdot 10^4$	0.8 ± 0.2	193.9 ± 27.2	$4.2 \cdot 10^3$	1.4 ± 0.5	284.5 ± 49.9	$4.8 \cdot 10^3$	0.4 ± 0.1	292.3 ± 56.3	$1.5 \cdot 10^3$
C7-DL-HSL	6.6 ± 0.2	118.2 ± 18.6	$5.5 \cdot 10^4$	6.0 ± 0.8	94.0 ± 10.4	$6.4 \cdot 10^5$	1.3 ± 0.2	123.5 ± 23.2	$1.0 \cdot 10^4$	1.9 ± 0.7	93.8 ± 10.1	$2.1 \cdot 10^5$	0.8 ± 0.2	103.3 ± 12.2	$2.9 \cdot 10^4$
C6-3oxo-DL-HSL	5.1 ± 0.9	50.9 ± 14.1	$1.0 \cdot 10^5$	9.7 ± 1.1	92.9 ± 10.8	$1.0 \cdot 10^5$	8.1 ± 0.3	37.1 ± 5.7	$2.2 \cdot 10^5$	8.9 ± 0.5	42.9 ± 7.2	$2.1 \cdot 10^5$	2.5 ± 0.2	58.5 ± 9.0	$4.3 \cdot 10^3$
C6-DL-HSL	3.9 ± 0.7	93.0 ± 3.0	$4.1 \cdot 10^4$	7.7 ± 0.5	223.4 ± 34.8	$3.4 \cdot 10^4$	11.8 ± 0.8	136.8 ± 24.6	$8.6 \cdot 10^4$	15.2 ± 1.0	136.0 ± 22.6	$1.1 \cdot 10^5$	5.8 ± 0.8	135.9 ± 23.5	$4.2 \cdot 10^4$
C4-DL-HSL	2.4 ± 0.9	175.8 ± 27.1	$1.3 \cdot 10^4$	11.9 ± 2.4	215.4 ± 42.0	$5.5 \cdot 10^4$	9.0 ± 1.0	196.1 ± 26.5	$4.5 \cdot 10^4$	9.6 ± 1.1	190.9 ± 21.0	$5.0 \cdot 10^4$	3.0 ± 0.3	194.0 ± 28.5	$1.5 \cdot 10^4$

Table 4.3. Comparison of lactonase activities (next page). The kinetic parameters for the N-acyl homoserine lactonase activities found for MIM-1 and MIM-2, in the presence of different substrates, are compared with those reported for AiiB from *Agrobacterium tumefaciens* [205], AiiA from *Bacillus* sp 240B1 [218], MomL from *Muricauda olearia* [209], AidC from *Chryseobacterium* sp. StRB126 [208], SsoPox from *Sulfolobus solfataricus* [222] and OPH from *Brevundimonas diminuta* [223].

Chapter 4: Promiscuous metallo-β-lactamases: MIM-1 and MIM-2 may play an essential role in quorum sensing networks

Substrate	AiiA ^[218]			AiiB ^[205]			AidC ^[208]		
	k _{cat} (s ⁻¹)	K _m (μM)	k _{cat} /K _m (s ⁻¹ /M)	k _{cat} (s ⁻¹)	K _m (μM)	k _{cat} /K _m (s ⁻¹ /M)	k _{cat} (s ⁻¹)	K _m (μM)	k _{cat} /K _m (s ⁻¹ /M)
C12-3oxo-DL-HSL	NA	NA	NA	NA	NA	NA	NA	NA	NA
C12-DL-HSL	NA	NA	NA	NA	NA	NA	NA	NA	NA
C10-3oxo-DL-HSL	NA	NA	NA	NA	NA	NA	1.97 ± 0.11	72 ± 5.3	2.7*10 ⁴
C10-DL-HSL	NA	NA	NA	0.28 ± 0.08	110 ± 50	1.5*10 ³	NA	NA	NA
C8-3oxo-DL-HSL	NA	NA	NA	3.7 ± 0.1	2.5 ± 0.3 (mM)	1.5*10 ³	2.12 ± 0.24	64 ± 3.7	3,3*10 ⁴
C8-DL-HSL	NA	NA	NA	10.3 ± 0.2	1.0 ± 0.1 (mM)	1.0*10 ⁴	2.01 ± 0.31	64 ± 4.9	3,1*10 ⁴
C7-DL-HSL	NA	NA	NA	NA	NA	NA	NA	NA	NA
C6-3oxo-DL-HSL	NA	NA	NA	11.0 ± 0.4	4.6 ± 0.5 (mM)	2.4*10 ³	2.35 ± 0.29	46 ± 2.1	5.1*10 ⁴
C6-DL-HSL	91 ± 3	5.6 ± 0.6 (mM)	1.6*10 ⁴	24.8 ± 0.9	1.6 ± 0.2 (mM)	1.6*10 ⁴	2.31 ± 0.16	55.0 ± 4.3	4.2*10 ⁴
C4-DL-HSL	NA	NA	NA	5.8 ± 0.3	15 ± 1 (mM)	3.9*10 ²	NA	NA	NA

Substrate	MomL ^[209]			SsoPox ^[222]			OPH ^[223]		
	k _{cat} (s ⁻¹)	K _m (μM)	k _{cat} /K _m (s ⁻¹ /M)	k _{cat} (s ⁻¹)	K _m (μM)	k _{cat} /K _m (s ⁻¹ /M)	k _{cat} (s ⁻¹)	K _m (μM)	k _{cat} /K _m (s ⁻¹ /M)
C12-3oxo-DL-HSL	NA	NA	NA	0.95 ± 0.03	170 ± 2	5.5*10 ³	1.83 ± 0.05	101 ± 7	1.8*10 ⁴
C12-DL-HSL	NA	NA	NA	NA	NA	NA	NA	NA	NA
C10-3oxo-DL-HSL	224 ± 12	440 ± 100	5.1*10 ⁵	1.5 ± 0.2	50 ± 0.1	3.0*10 ⁵	2.67 ± 0.03	184 ± 4	1.4*10 ⁴
C10-DL-HSL	NA	NA	NA	NA	NA	NA	NA	NA	NA
C8-3oxo-DL-HSL	218 ± 14	490 ± 110	4.5*10 ⁵				4.66 ± 0.03	608 ± 8	7.6*10 ³
C8-DL-HSL	158 ± 17	440 ± 160	3.6*10 ⁵	2.0 ± 0.3	93 ± 27	2.1*10 ⁴	NA	NA	NA
C7-DL-HSL	NA	NA	NA	NA	NA	NA	NA	NA	NA
C6-3oxo-DL-HSL	293 ± 17	950 ± 160	3.1*10 ⁵	0.52 ± 0.05	5.6 ± 0.9 (mM)	18 ± 7	NA	NA	NA
C6-DL-HSL	226 ± 8	790 ± 80	2.9*10 ⁵	NA	NA	NA	3.17 ± 0.02	526 ± 9	6.3*10 ³
C4-DL-HSL	135 ± 5	850 ± 90	1.6*10 ⁵	NA	NA	5.5*10 ³	2.62 ± 0.02	412 ± 6	6.3*10 ³

Chapter 4: Promiscuous metallo- β -lactamases: MIM-1 and MIM-2 may play an essential role in quorum sensing networks

Furthermore, OP-degrading activity has previously also been associated with the MBL structural fold; the enzyme methyl parathion hydrolase (MPH) from *Pseudomonas* sp. WBC-3 has the overall fold characteristic of MBLs but it is a highly efficient OP hydrolase without any measurable MBL activity [153, 176]. Functional promiscuity is thus not unprecedented among metallohydrolases, further exemplified by the enzyme purple acid phosphatase, which may act as a phosphatase in some tissue types or organisms, but as a peroxidase elsewhere [169]. Changes in the metal ion composition in the active site may contribute to observed functional changes in that enzyme [224, 225]. Since we previously demonstrated that metal ion replacements lead to changes in the substrate preference of both MIM-1 and MIM-2 [92] we probed the effect of such replacements on the catalytic parameters of the AHLase activity of these two enzymes (**Table 4.2.**). The effects of these substitutions are more subtle than observed for the MBL activity of these enzymes. Each of the metal ions tested is capable of reconstituting AHLase activity, with Co(II) being the most effective metal ion for most substrates and Ca(II) the worst. Co(II) was also found to be the most effective metal ion for other AHLases, including AiiB from *A. tumefaciens*, AiiA from *B. thuringensis* and MomL from *M. olearia* [204, 208, 209, 218].

Chapter 4: Promiscuous metallo- β -lactamases: MIM-1 and MIM-2 may play an essential role in quorum sensing networks

4.4 Conclusion.

MIM-1 and MIM-2 are two enzymes that demonstrate the plasticity of the MBL fold, a fold that promotes a range of seemingly unrelated functions. For instance, the organophosphate pesticide-degrading MPH uses this fold but has no MBL activity [176]. Our study into possible biological functions of MIM-1 and MIM-2 was triggered by the observation that both enzymes are very efficient lactamases *in vitro* despite residing in organisms that are not likely to have been subjected to evolutionary pressures associated with the increasing use of β -lactam-based antibiotics since World War II [92]. Indeed, at the primary sequence level the closest homologs of MIM-1 and MIM-2 are known MBLs associated with the pathogenic effect of antibiotic resistance (**Fig. 4.1., 4.3., 4.4.**), but considerable similarity was also apparent to other enzymes of the family of dinuclear metallohydrolases, in particular glyoxalases and AHLases (**Table 4.1.**). Structural models of MIM-1 and MIM-2 indicated that their active sites can accommodate two metal ions using ligands identical to those used by some MBLs such as AIM- 1, FEZ-1 or L1 [27, 138, 192], but these models did not provide conclusive information about preferred substrates, an outcome that was not surprising considering the structural plasticity of the MBL fold. However, kinetic measurements ruled out that MIM-1 and MIM-2 may act as glyoxalases. In contrast, both enzymes are very efficient AHLases with catalytic parameters rivalling or even exceeding those of well-characterized lactonases (**Table 4.3.**). This bifunctional behaviour of MIM- 1 and MIM-2 is thus another illustration of the versatility of the MBL fold, but it also poses an interesting conundrum with respect to the biological function(s) of these enzymes – based on their *in vitro* catalytic efficiencies it is not evident if they act preferably as MBLs or AHLases. Insofar, MIM-1 and MIM-2 are different from known MBLs, for which generally only one preferred function is reported. Similarly, we are not aware of any studies linking AHLases to

Chapter 4: Promiscuous metallo- β -lactamases: MIM-1 and MIM-2 may play an essential role in quorum sensing networks

MBL activity, nor their inhibition by established MBL inhibitors such as D-captopril [177, 180]. Of interest was also the observation that the metal ion composition of MIM-1 and MIM-2 affects only their substrate preference for their MBL but not their AHLase activity (**Table 4.2.**). While the *in vivo* metal ion composition of these enzymes remains uncertain it is possible that they may alter their function as a consequence of the identity of the metal ions bound in their active sites. In this context, it is interesting that MIM-1 and MIM-2 are active in presence of Ca(II), the concentration of which may potentially be regulated by their host organisms. This question may only be addressed when more information about the cellular metabolism of *N. pentaromativorans* or *S. agarivorans* becomes available. However, irrespective of the role(s) of MIM-1 or MIM-2 in their host organisms these enzymes are attractive targets to investigate structural factors that dictate substrate preference and concomitant functions of enzymes that possess the versatile MBL fold. As an essential step towards gaining functional insight our group is currently optimizing protocols to obtain crystals of a quality sufficient for X-ray diffraction studies. Ultimately, MIM-1 and MIM-2 may hold important clues about structural factors that may be exploited to develop potent inhibitors as leads for novel chemotherapeutics to combat antibiotic resistance. The link between antibiotic resistance and QS may also be of relevance in future drug development strategies – enzymes such as MIM-1 and MIM-2 may, in principle, be a threat to health care due to their strong potential to degrade commonly used antibiotics, but they are also capable of preventing biofilm formation due to their ability to cleave AHLs. Since biofilms are frequently associated with antibiotic resistance [132, 180] MIM-1 and MIM-2 are bifunctional enzymes that possess activities with opposing effects with respect to antibiotic resistance. The question to address in future studies is if these two activities may be controlled and/or modulated separately.

Chapter 5: Active site geometry and reaction mechanism of MIM-1 and MIM-2

5.1 Introduction

In the previous chapters the enzymatic properties of two novel MBL-like enzymes from environmental microorganisms, *i.e.* MIM-1 from *N. pentaromativorans* and MIM-2 from *S. agarivorans*, were discussed in detail. Specifically, the two enzymes were identified due to their sequence homology to MBLs from subgroup B3 (see Chapter 2) and their proficiency in hydrolysing a range of relevant β -lactam antibiotics (see Chapter 3). The reaction mechanism employed by MBLs has been studied extensively using a range of techniques from chemical kinetics and spectroscopy. Variations are observed when different substrates were employed, as illustrated by the effects of pH on enzyme catalysis (*e.g.* **Fig. 3.5** in Chapter 3). Furthermore, it has emerged that in some MBLs (*e.g.* the B1 representative NDM-1 and the B3-representative L1) the rate-limiting step in the reaction with the model substrate nitrocefin (**Fig. 5.1**) is the decay of an anionic tetrahedral reaction intermediate formed upon the nucleophilic attack, while in other MBLs (*e.g.* the B1 representative Bla2) no reaction intermediate is observed [120, 226, 227].

Interestingly, the B3-representative AIM-1 appears to be capable of adopting two alternative mechanistic strategies, one where a reaction intermediate is observed and one where no intermediate is apparent [129]. In this chapter the reaction mechanism of MIM-1 and MIM-2 is probed using an approach similar to that described in the studies of NDM-1, L1, Bla2 and AIM-1. Specifically, the substrate nitrocefin was used to facilitate a direct comparison of catalytic parameters.

Chapter 5: Active site geometry and reaction mechanism of MIM-1 and MIM-2

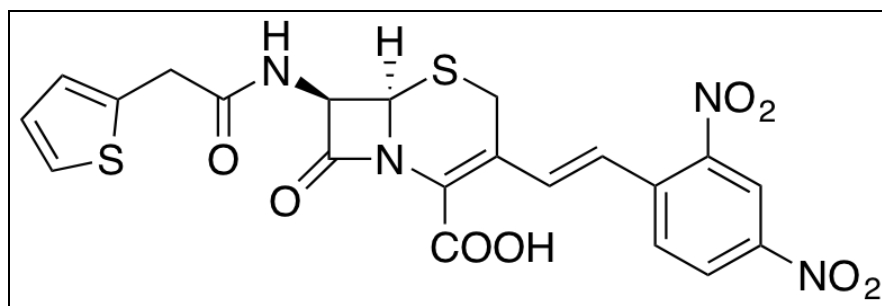


Figure 5.1. Nitrocefirin core structure. Due to the presence of the dinitro phenol functional group this cephalosporin derivative has a characteristic yellow colour, facilitating a simple colourimetric assay to monitor catalysis.

5.2 Materials and Methods

5.2.1. Materials

All chemicals were of analytical grade. *E. coli* BL21 (DE3) pLysS cells (Agilent) were used for recombinant expression of the proteins. All chemicals were purchased from Sigma-Aldrich unless stated otherwise.

5.2.2. Protein expression and purification

The protocols for the expression and purification of recombinant MIM-1 and MIM-2 were previously described (see Chapter 3). In brief, the expression of the recombinant enzymes was induced with 0.2 mM isopropyl β -D-1-thiogalactopyranoside (IPTG). The cells were harvested by centrifugation and pellets were resuspended in ~20 mL of buffer containing 20 mM Tris (HCl; pH 7.0) and 0.15 mM ZnCl₂. The cells were then disrupted using five rounds of sonication (60% of the maximal output power for 30 seconds in each round). The supernatant was loaded onto a HiTrap Q FF 5 mL column (GE Healthcare), pre-equilibrated with 20 mM Tris (HCl; pH 7.0) and

Chapter 5: Active site geometry and reaction mechanism of MIM-1 and MIM-2

0.15 mM ZnCl₂. Proteins were eluted using a linear gradient from 0 to 0.5 M NaCl. MIM-1 eluted between 55 mM and 175 mM of NaCl, while MIM-2 eluted between 35 mM and 135 mM of NaCl. Relevant fractions with MBL activity were pooled and loaded onto a HiPrep 16/60 Sephacryl S-200 HR column (GE Healthcare), pre-equilibrated with 50 mM Hepes (pH 7.5), containing 0.2 M NaCl and 0.15 mM ZnCl₂. The purity of the protein samples was confirmed by SDS-PAGE analysis. The protein concentrations were estimated using theoretical extinction coefficients ($\epsilon_{280} = 36,815 \text{ M}^{-1}\text{cm}^{-1}$ for MIM-1 and $41,285 \text{ M}^{-1}\text{cm}^{-1}$ for MIM-2), calculated using the ProtParam tool (<http://web.expasy.org/protparam/>).

Metal ion derivatives of MIM-1 and MIM-2 were prepared as described in Chapters 3 and 4.

5.2.3. Enzymatic assays and data analysis

Steady-state kinetic assays were conducted with the Zn(II)-, Co(II)- and Ca(II)-derivatives of MIM-1 and MIM-2, following the hydrolysis of the cephalosporin derivative nitrocefim (**Fig. 5.1**) at 390 nm. The substrate conversion rate was calculated using an extinction coefficient $\epsilon_{390} = 11\,500 \text{ M}^{-1}\text{cm}^{-1}$. All the measurements were conducted in 20 mM TRIS, pH 7.0, in the presence of $[\text{M(II)}] = 200 \text{ }\mu\text{M}$ (where M = Zn, Co or Ca), at 25° C with a Shimadzu UV-2550 spectrophotometer, using a 1 cm path length quartz cuvette. The final protein concentration in the assays was 20 nM.

Stopped-flow measurements were carried out using an Applied Photophysics SXPRO-20 spectrophotometer equipped with a photodiode array and fluorometer detector. Absorbance and fluorescence measurements were performed with a final concentration of enzyme and substrate (*i.e.* nitrocefim) 30 μM and 20 μM , respectively. The excitation and emission wavelengths used in the fluorescence experiments were 295 nm and 330 nm, respectively. The wavelength range for the

Chapter 5: Active site geometry and reaction mechanism of MIM-1 and MIM-2

absorbance measurements was from 300 nm to 700 nm. The path lengths used were 1 cm or 0.2 cm for absorbance or fluorescence experiments, respectively, while the respective slit widths were 4 mm and 2 mm. Reaction progress curves at 390 nm (*i.e.* substrate decay) and 485 nm (*i.e.* product formation) were generated from the diode array absorption measurements by converting the experimental data to concentration values using the following respective extinction coefficients: 11 500 M⁻¹cm⁻¹ and 17 400 M⁻¹cm⁻¹ [228, 229]. Rate constants k_{obs} for substrate decay and product formation were obtained by fitting the data to first-order exponentials of the following form (**Equation 5.1**):

$$[M]_t = ([M]_0 - b) \exp(-k_{\text{obs}} \cdot t) + b \quad \text{Eq. 5.1}$$

where $[M]_t$ and $[M]_0$ represent the concentration of the substrate or the product at time t or at the beginning of the reaction, respectively; b is a fitting parameter and t is the time in seconds.

The data were also modelled using FITSIM software in order to obtain an estimate of individual microscopic rate constants [120, 230, 231]. The model used to fit the experimental data is shown in **Fig. 5.2** and assumes reversibility (characterised by forward and reverse rate constants) at every step of the reaction. A similar model was previously employed to characterise the catalytic turnover of Bla2 and AIM-1 [120, 129].

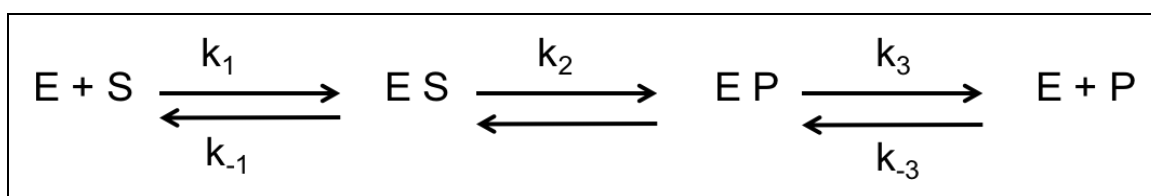


Figure 5.2. Schematic representation of the catalytic mechanism for the reaction of MIM-1 and MIM-2 with the β -lactam substrate nitrocefin. The model assumes three fully reversible steps for the mechanism.

Chapter 5: Active site geometry and reaction mechanism of MIM-1 and MIM-2

5.2.5. Magnetic circular dichroism

The Co(II)-derivatives of MIM-1 and MIM-2 were dissolved in a 60%/40% (v/v) mixture of glycerol/buffer (20 mM TRIS, pH 7.0) and filled in a 0.62 cm path length nickel-plated copper sample cell with quartz windows. The MCD system used a JASCO J815 spectropolarimeter and an Oxford Instruments SM4000 cryostat/magnet. Data were collected at increments of 0.5 Tesla (T) from 0 to 7.0 T and at a temperature of 1.4 K. Each spectrum was corrected for any natural CD by subtracting the zero-field spectrum of the sample. Even when there is no sample present the instrument baseline exhibits a small deviation from zero that is both field- and wavelength-dependent [232]. Therefore, each spectrum was also corrected by subtraction of a spectrum recorded at the same magnetic field but with no sample present. The resultant spectra were fitted to the minimum number of Gaussian peaks to achieve a satisfactory composite spectrum using the GRAMS AI software and analysed as described elsewhere [232].

5.2.6. Electron paramagnetic resonance

Low-temperature EPR spectra were obtained on a Bruker Elexsys EMX EPR spectrometer equipped with an Oxford Instruments ESR900 liquid helium flow cryostat. The spectra were recorded at 9.64 GHz ($B_0 \perp B_1$) or 9.38 GHz ($B_0 \parallel B_1$) using a Bruker DM4116 dual-mode cavity, with 10 G (1 mT) magnetic field modulation (100 kHz), with a constant/conversion time of 42 ms and a receiver gain at 1×10^4 . Spin Hamiltonian parameters were estimated from computer simulations carried out using XSophe (Bruker Biospin), assuming $H_0 = \beta B_0 g \hat{S} / \hbar + \hat{S} D \hat{S}$, where $S = 3/2$, $|D| \gg |\beta g B S / \hbar|$, and where $D > 0$ implies the $M_S = \pm 1/2$ Kramers doublet lies lowest and all observed EPR transitions are from this doublet, and $D < 0$ implies the $M_S = \pm 3/2$ Kramers doublet lie lowest and all observed EPR transitions are from this doublet.

Chapter 5: Active site geometry and reaction mechanism of MIM-1 and MIM-2

5.2.7. ¹H Paramagnetic NMR

¹H NMR spectra were collected on a Bruker Avance 500 spectrometer operating at 500.13 MHz, 298 K, magnetic field of 11.7 T, recycle delay (AQ) of 41 ms, and sweep width of 400 ppm. Proton chemical shifts were calibrated by assigning the H₂O signal the value of 4.70 ppm. A modified pre-saturation pulse sequence was used to suppress the proton signals originating from solvent. The presaturation pulse was as short as possible (500 ms) to avoid saturation of solvent-exchangeable proton signals. The concentration of NMR samples was generally in the range of 1.0-1.2 mM. Samples in D₂O were prepared by performing three or more dilution/concentration cycles in a Centricon-10 column.

5.3. Results and Discussion

5.3.2 Characterisation of the steady-state catalytic parameters for the hydrolysis of nitrocefin

In order to compare catalytic parameters of MIM-1 and MIM-2 with corresponding parameters from well-known MBLs (*e.g.* AIM-1, NDM-1 [128] and Bla2 [120]) the steady-state parameters for the turnover of the substrate nitrocefin needed to be established. Relevant experimental data and catalytic parameters for the Zn(II)-, Co(II)- and Ca(II)-derivatives of both enzymes are shown in **Fig. 5.3** and **Table 5.1**.

For both enzymes and every metal ion derivative tested the data reveal Michaelis-Menten-type saturation behaviour; no substrate inhibition as observed with other substrates (see Chapter 3) was evident. This indicates that nitrocefin only has one binding site in the vicinity of the active centre, possibly preventing binding of a second substrate molecule to an inhibitory site due to its large size (compare **Figs 5.1** and **Fig. 1.3**). Interestingly, nitrocefin appears to bind with similar affinity to

Chapter 5: Active site geometry and reaction mechanism of MIM-1 and MIM-2

both enzymes, irrespective of the metal ion composition, based on the relatively conserved K_m values (ranging from ~ 40 to $\sim 70 \mu\text{M}$).

Table 5.2. Kinetic parameter obtained for MIM-1 and MIM-2 for the hydrolysis of nitrocefin in the presence of Zn(II), Co(II) and Ca(II).

	MIM-1			MIM-2		
	k_{cat} (s^{-1})	K_m (μM)	k_{cat}/K_m (s^{-1}/M)	k_{cat} (s^{-1})	K_m (μM)	k_{cat}/K_m (s^{-1}/M)
Zn(II)	899 ± 53	73 ± 10	$1.2 \cdot 10^7$	1073 ± 48	49 ± 6	$2.1 \cdot 10^7$
Co(II)	57 ± 2	64 ± 6	$8.9 \cdot 10^5$	12 ± 0.5	47 ± 5	$2.5 \cdot 10^5$
Ca(II)	3 ± 0.1	44 ± 6	$6.8 \cdot 10^4$	17 ± 0.7	48 ± 6	$3.4 \cdot 10^5$

However, great variations are observed with respect to the k_{cat} when different metal ion derivatives are compared (**Table 5.1**). With a k_{cat} in the range of $\sim 1000 \text{ s}^{-1}$ for both native, Zn(II)-containing enzymes nitrocefin is turned over considerably faster than other cephalosporin substrates (*i.e.* cefuroxime and cefoxitin; see **Table 3.2** in Chapter 3). However, the Co(II)- and Ca(II)-derivatives are far less reactive than their Zn(II)-counterparts; indeed, nitrocefin is turned over at a rate similar to that recorded for other cephalosporin substrates. Thus, while metal ion replacements do not appear to affect substrate binding significantly, they have a profound influence on the catalytic steps that follow initial substrate binding. In order to shed light into those steps the reactions were probed under single turnover conditions using stopped-flow techniques.

Chapter 5: Active site geometry and reaction mechanism of MIM-1 and MIM-2

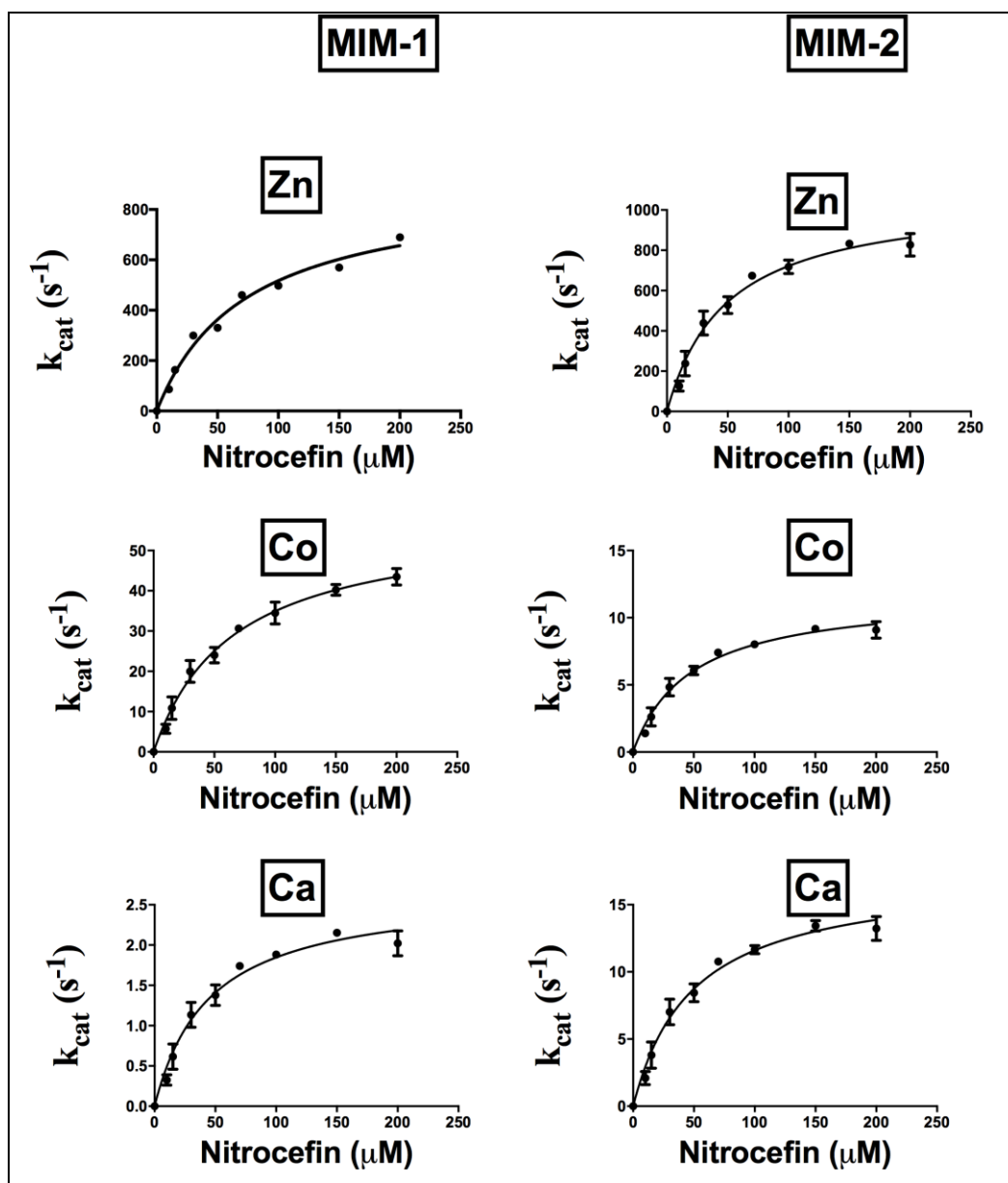


Figure 5.3. Rate vs [nitrocefin] profiles of metal ion derivatives of MIM-1 and MIM-2. The data were analysed by fits to the Michaelis-Menten equation as described in Chapter 3.

Chapter 5: Active site geometry and reaction mechanism of MIM-1 and MIM-2

5.3.3 Rapid single-turnover kinetics experiments

The hydrolysis of nitrocefin by metal ion derivatives of MIM-1 and MIM-2 was recorded with a photodiode array detector in the range between 300 and 700 nm (**Figure 5.4**) and shows the disappearance of the substrate at 390 nm and the emergence of the ring-opened product at 485 nm. For each derivative the reaction is completed after ~0.6 ms. In **Figure 5.5** the time courses of the concentration change for the substrate and product are shown. It should be pointed out that only in the case of the Co(II)- and Ca(II)-derivatives of MIM-1 and MIM-2 an intermediate was observable, however at insignificant concentrations and with a half-life not consistent with the substrate depletion. This could indicate that, in the presence of different metal ions the proteins hydrolyse the substrate through a different mechanism, exploiting the acyl-enzyme intermediate observed in the case of other well-known MBLs [120]. However, further investigation is needed to support this hypothesis. This observation indicates that MIM-1 and MIM-2 are likely to operate like the MBLs Bla2 and AIM-1, but different to NDM-1 or L1 (where a reaction intermediate was observable; see Section 5.1).

Chapter 5: Active site geometry and reaction mechanism of MIM-1 and MIM-2

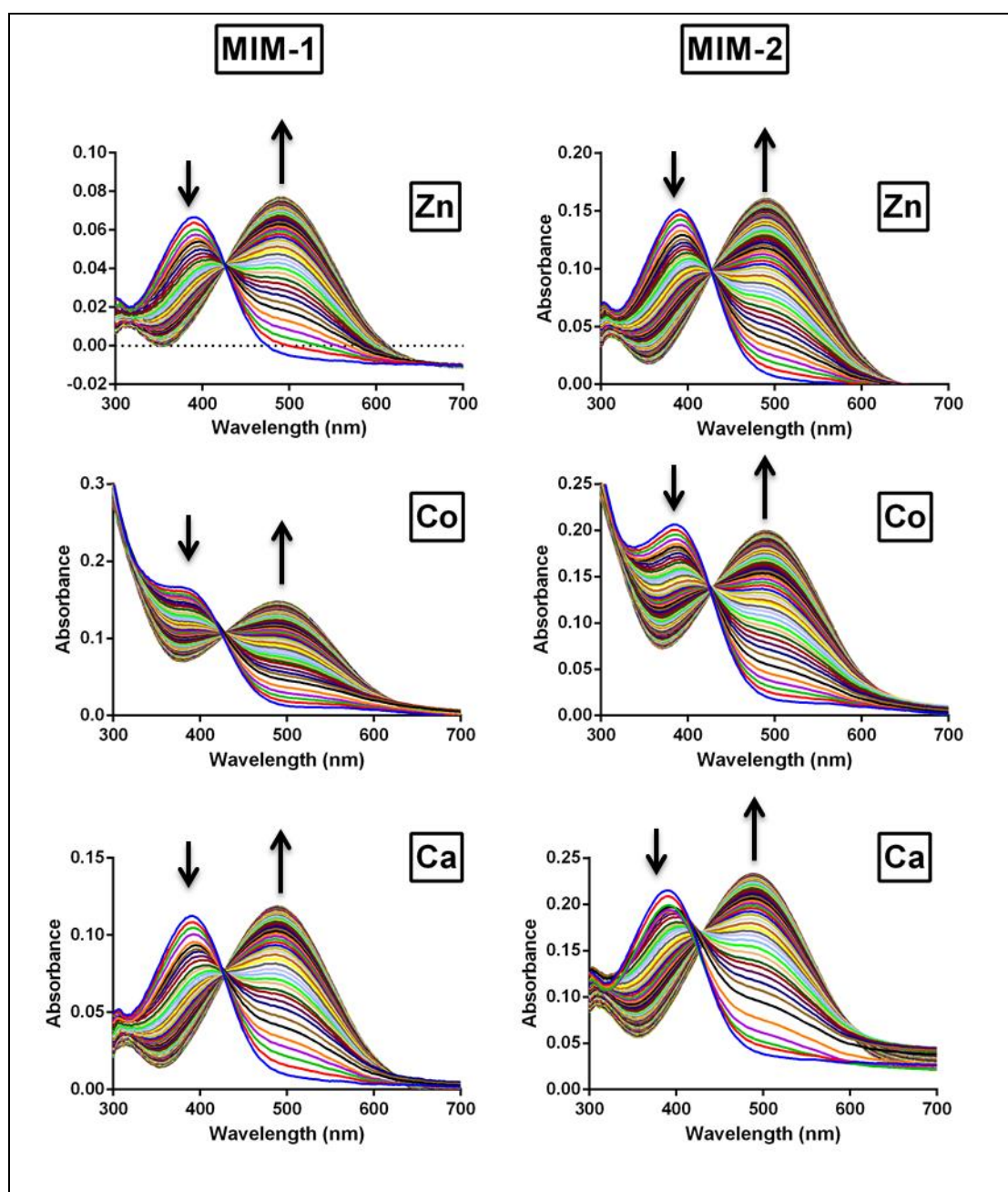


Figure 5.4. Stopped-flow spectroscopy of the Zn(II)-, Co(II)- and Ca(II)-derivatives of MIM-1 and MIM-2. The hydrolysis of 30 μM nitrocefin by 20 μM MIM-1 and MIM-2 was followed in 20 mM TRIS, pH 7.0, at 25 $^{\circ}\text{C}$. Absorbance spectra from 300 to 775 nm were recorded ~ 1.28 ms after mixing (deadtime of the instrument). The reaction was complete after ~ 0.6 s. The absorbance decreased at 390 nm (substrate), and increased at 485 nm (product).

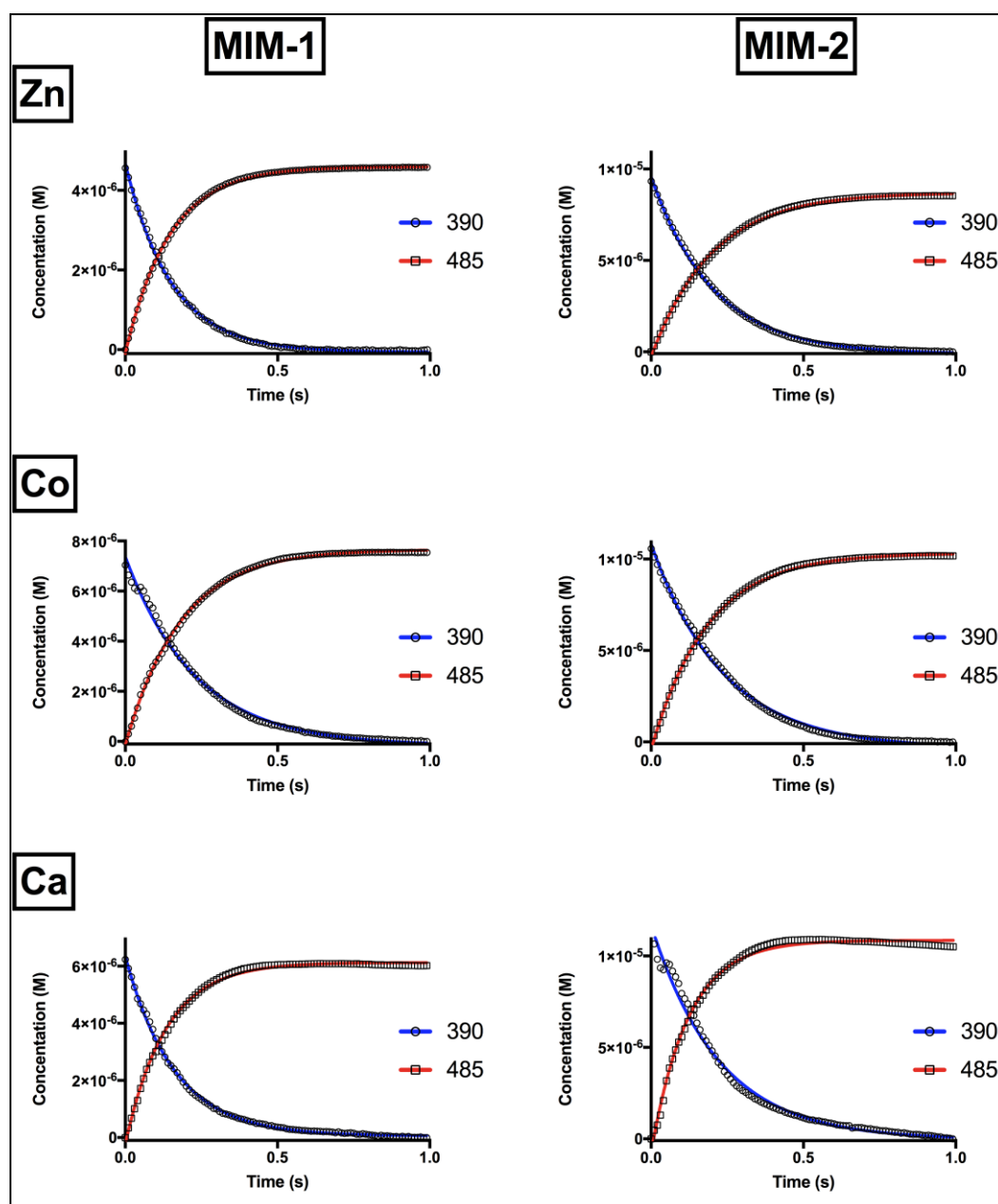


Figure 5.5. Time course of concentration changes in single turnover experiments with MIM-1 and MIM-2. Concentrations for substrate (circle void dots) and product (square void dots). The absorbances were converted to concentration units as described in Materials and Methods. The experimental data were fitted to a first-order exponential. The fitted lines are shown as blue (substrate) and red (product) lines.

Chapter 5: Active site geometry and reaction mechanism of MIM-1 and MIM-2

The data in **Fig. 5.5** were analysed by fitting the time course of substrate decay and product formation to an exponential (Eq. 5.1), resulting in first-order rate constants k_{obs} (**Table 5.2**). For both enzymes, independent of their metal ion composition, similar k_{obs} values in the order of $\sim 5 - 8 \text{ s}^{-1}$ were recorded.

Table 5.2. Estimated first-order rate constants (s^{-1}) obtained for the Zn(II)-, Co(II)- and Ca(II)-derivatives of MIM-1 and MIM-2 for the hydrolysis of nitrocefin.

	MIM-1 $k_{\text{obs}} (\text{s}^{-1})$		MIM-2 $k_{\text{obs}} (\text{s}^{-1})$	
	Substrate (390 nm)	Product (485 nm)	Substrate (390 nm)	Product (485 nm)
Zn(II)	6.6 ± 0.1	6.9 ± 0.1	4.9 ± 0.1	5.0 ± 0.1
Co(II)	4.3 ± 0.1	5.5 ± 0.1	4.2 ± 0.1	5.4 ± 0.1
Ca(II)	6.2 ± 0.1	7.5 ± 0.1	4.5 ± 0.1	8.3 ± 0.1

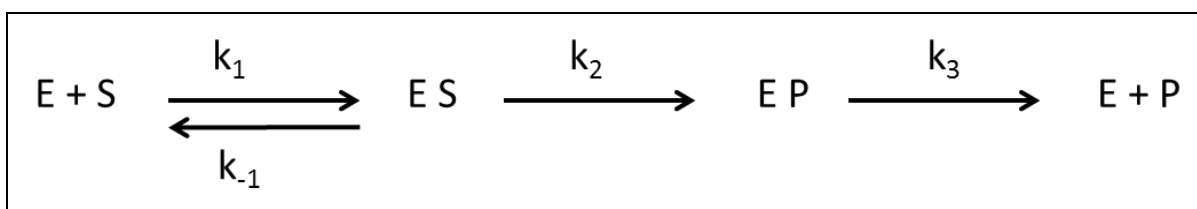


Figure 5.6. Schematic representation of a possible catalytic mechanism for the reaction of MIM-1 and MIM-2 with the β -lactam substrate nitrocefin.

The data pose a significant conundrum in the interpretation of the mechanism. In the single turnover experiments product is formed at a rate of $\sim 5 \text{ s}^{-1}$ while the k_{cat} measured under steady-state conditions (see **Fig. 5.3** and **Table 5.1**), in particular for the native Zn(II)-derivatives of MIM-1 and MIM-2, are in the order of $\sim 1000 \text{ s}^{-1}$. It needs to be pointed out that while both the steady-state and single turnover experiments measure the same process

Chapter 5: Active site geometry and reaction mechanism of MIM-1 and MIM-2

(*i.e.* the emergence of hydrolysed nitrocefin) differences might be expected if the regeneration of the active site for the next catalytic cycle requires the presence of substrate. In other words, in a single turnover experiment the release of product from the EP complex (**Fig. 5.6**) might be slow but in the presence of excess substrate the product gets easily displaced by this reactant due to its higher affinity. This would imply that substrate binding is rather rapid but that the regeneration of the active site to its resting state might be considerably slower as, ultimately, in the final catalytic cycle no substrate remains available to promote product expulsion.

In an attempt to probe this hypothesis the stopped-flow single turnover experiments were carried out in fluorescence mode (**Fig. 5.7**). The underlying idea behind this approach is that MBLs have a conserved tryptophan residue (*i.e.* Trp93 in NDM-1, Trp38 in L1 and Trp38 in AIM-1) [129] in the vicinity of the active site. Its perturbation, promoted by the binding of the substrate, is anticipated to result in changes in the intrinsic fluorescence properties of the enzymes. Indeed, stopped-flow fluorescence measurements with NDM-1, L1 and AIM-1 have demonstrated that their interaction with the substrate nitrocefin leads to an initial rapid quench in fluorescence, followed by a slower regain [129, 143, 227]. In MIM-1 and MIM-2 the corresponding tryptophan residue is also conserved (Trp86 and Trp33, respectively). For each metal ion derivative of both enzymes a very rapid quench in fluorescence is observed, followed by a slower regain, thus matching the behaviour reported for other MBLs (**Fig. 5.7**). The rate of the fluorescence decay could not be accurately estimated as the process was complete close to the dead time of the instrument (thus, a rate exceeding 500 s^{-1} is a reasonable estimate). In contrast, reliable estimates for the rate constants for the fluorescence regain could be obtained from fitting the experimental data to single exponential functions. Relevant parameters are listed in **Table 5.3**. Interestingly, these rates are in reasonable agreement with the rates of product formation recorded in single

Chapter 5: Active site geometry and reaction mechanism of MIM-1 and MIM-2

turnover experiments (see above). The rates, for all the metal derivatives both for MIM-1 and MIM-2, are in the order of $\sim 5 \text{ s}^{-1}$, in agreement with the observed rates for NDM-1 and L-1 but in contrast to what has been recently observed for AIM-1, in which the regain in fluorescence is greater by one order of magnitude [129].

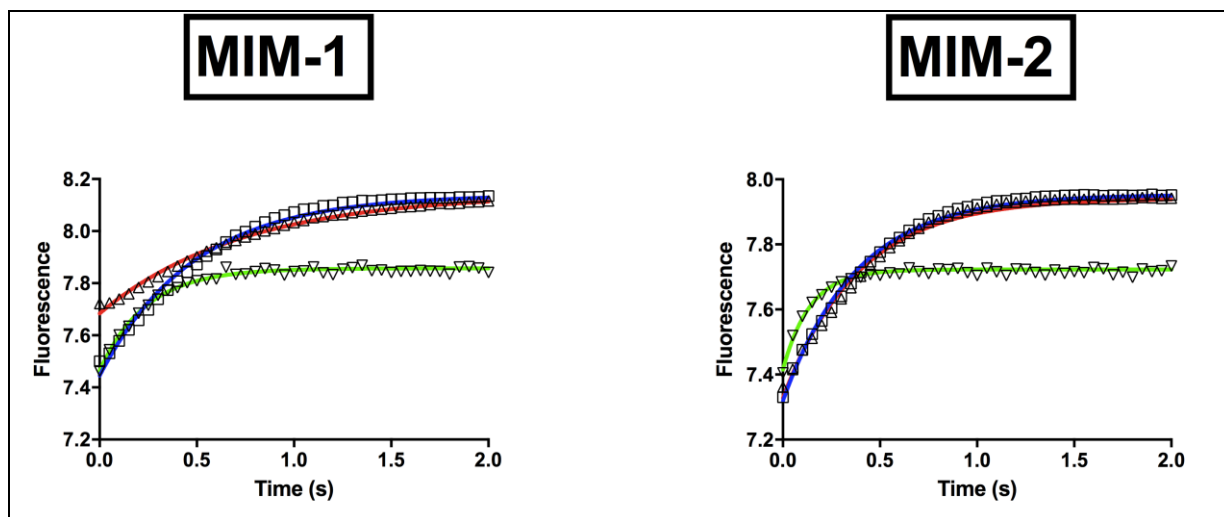


Figure 5.7. Fluorescence progression curve for MIM-1 (left) and MIM-2 (right) at 280 nm. The Figure shows the experimental data points for the Zn(II) (void squares), Co(II) (void triangles) and Ca(II) (void inverted triangles) derivatives. The experimental data points were fitted to a first-order exponential and the resulting fits are shown as blue (for the Zn(II)), red (for the Co(II)) and green (for the Ca(II)).

Table 5.3. Estimated first-order rate constants (s^{-1}) obtained for MIM-1 and MIM-2, in the presence of Zn(II), Co(II) and Ca(II), during the hydrolysis of nitrocefin, followed by fluorescence measurements.

MIM-1 k _{obs} (s^{-1})			MIM-2 k _{obs} (s^{-1})		
Zn(II)	Co(II)	Ca(II)	Zn(II)	Co(II)	Ca(II)
2.1 ± 0.1	1.4 ± 0.3	4.2 ± 0.5	2.6 ± 0.1	2.6 ± 0.2	7.1 ± 0.3

Chapter 5: Active site geometry and reaction mechanism of MIM-1 and MIM-2

In summary, the combined kinetic data provide insight into how metal ions may influence the catalytic turnover. It was already demonstrated in Chapter 3 that a change in the metal ion composition may affect the substrate specificity of both MIM-1 and MIM-2 (see **Table 3.6**), an observation that suggested that different metal ions may lead to subtle conformational (*i.e.* structural) variations that affect substrate binding. Here, it was demonstrated that the mechanism of a single catalytic turnover may be conserved, independent of the metal ion composition (**Figs 5.3 – 5.7**). However, with respect to the steady-state rate constant measured under pseudo-first order conditions there is a great difference between the three metal ion derivatives tested (**Fig. 5.2** and **Table 5.1**). Zn(II), the native metal ion, is by far the most efficient promoter of catalysis, likely due to the increased lability of the enzyme-product complex in the presence of this metal ion. This interpretation opens a novel, not previously recognised possibility for the design of a strategy to combat antibiotic resistance. If it was possible to develop antibiotics that, albeit hydrolysed, remain tightly bound to the metal centre, they may inactivate the enzymes sufficiently to have a significant detrimental effect on pathogenic virulence.

Extensive kinetic data for different metal ion derivatives as described in this Chapter are currently not available for other MBLs. Hence, it is not yet possible to generalise the above hypothesis. But based on the similarities of available catalytic parameters (as described in Chapters 3 and 5) it appears likely that the active sites of MIM-1 and MIM-2 share extensive homology with those of other MBLs. In order to substantiate this assumption spectroscopic studies were carried out, using the Co(II)-derivatives of both MIM-1 and MIM-2. Co(II) was used as it is a suitable spectroscopic probe for methods such as electron paramagnetic resonance (EPR) and magnetic circular dichroism (MCD). Furthermore, comparable data are available for a range of MBLs, including NDM-1, L1, Bla2 and AIM-1 [120, 129, 227, 229].

Chapter 5: Active site geometry and reaction mechanism of MIM-1 and MIM-2

5.3.3. Spectroscopic characterization of the active site structures of MIM-1 and MIM-2

MCD has been demonstrated to be a useful probe for the active site geometry and the reaction mechanism of a range of binuclear metallohydrolases, including aminopeptidases, organophosphate-degrading enzymes and corresponding biomimetic complexes [11, 24, 25, 97, 172, 174, 232, 233]. Recently, this method was also applied to study the active site of the MBL AIM-1 [129]. Corresponding data were collected for the Co(II)-derivatives of MIM-1 and MIM-2 (**Fig. 5.8**). For MIM-1, in the resting state, the MCD spectrum could be fit to no fewer than five transitions between ~460 and ~560 nm. These d-d transitions are very similar to those observed for AIM-1 and were thus assigned to two six-coordinate Co(II) species [129]. Similarly, the spectrum of resting MIM-2 could be resolved into a minimum of five transitions, although they were shifted to higher energy (spanning ~420 to 520 nm). While it is currently unknown why there is a stronger ligand effect on the d orbital splitting in MIM-2 when compared to MIM-1 and AIM-1, this observation is indicative of structural variations between these enzymes (*e.g.* differences in bond lengths and angles, etc). However, common to all three enzymes is that there are two six-coordinate Co(II) ions in the active site. Importantly, the addition of the inhibitor D-captopril did not affect the position of the transitions in either sample, again in agreement with a similar observation recently reported for AIM-1 [129]. Considering the relatively tight binding of this inhibitor to both MIM-1 and MIM-2 (see Chapter 3) and also available crystal structures that show D-captopril bound to the metal centres of the MBLs L1 and AIM-1 the lack of any spectral changes was surprising [129, 192].

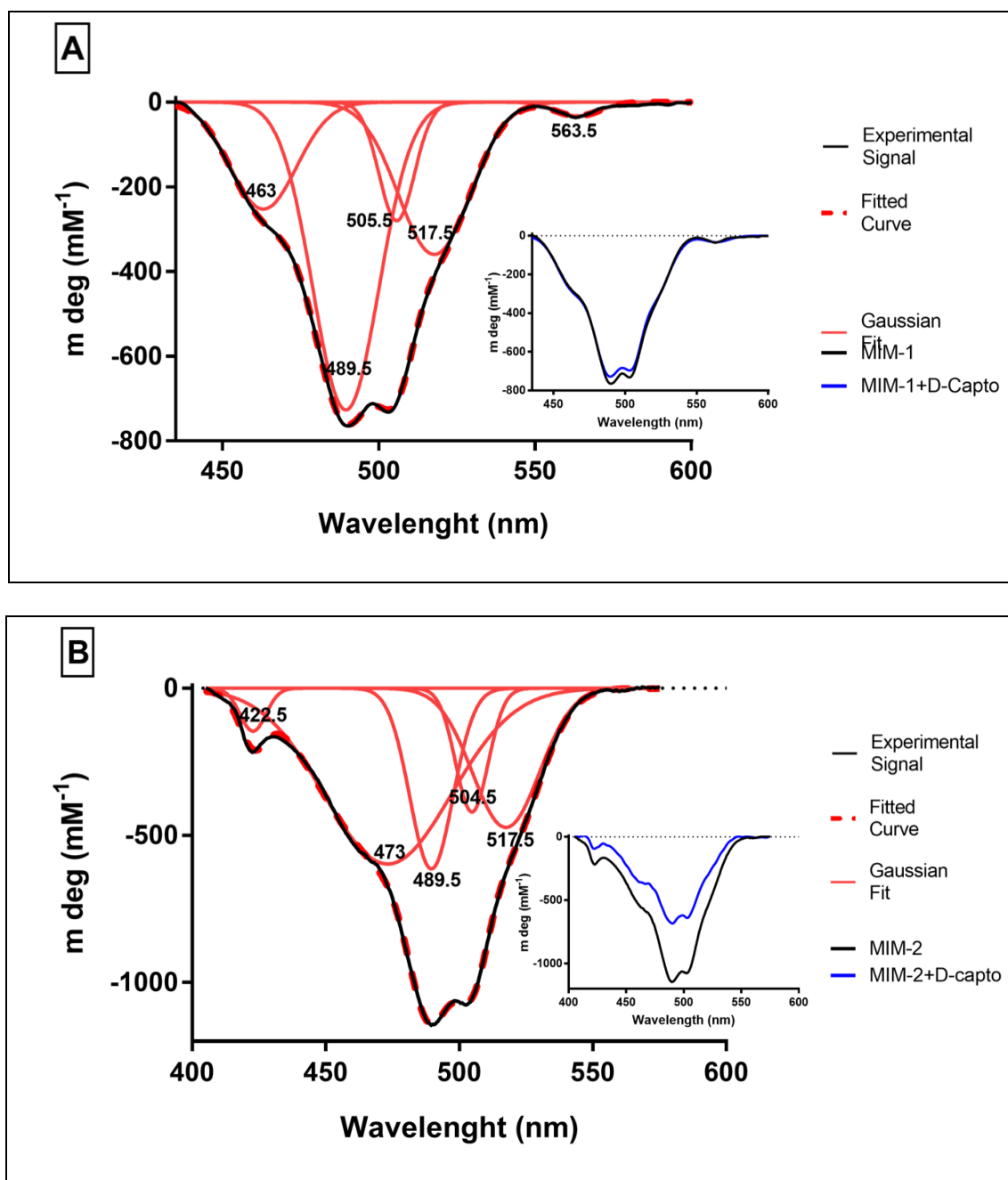


Figure 5.8. MCD spectra of MIM-1 (A) and MIM-2 (B). Data were measured at 7 T and 1.4 K in the absence and presence of the inhibitor D-captopril. The raw spectral data were resolved into individual transitions by fitting the minimum number of Gaussians.

Chapter 5: Active site geometry and reaction mechanism of MIM-1 and MIM-2

However, in AIM-1 the crystal structure of the AIM-1-D-captopril complex indicates that the thiol group of the inhibitor displaces the bridging water molecule, thus coordinating to both metal ions. Nonetheless, corresponding MCD data did not reveal significant spectral changes. This was interpreted in terms of D-captopril (i) either not binding to the metal ions at all in solution (in contrast to the solid state arrangement), or (ii) coordinating via its carboxyl group to one or both metal ions, a coordination ligand and mode that would be expected to have a considerably weaker effect on the ligand field than a thiol group. The same interpretation thus appears plausible for MIM-1 and MIM-2.

The electronic structure and in particular the effect of D-captopril binding was also investigated by paramagnetic ^1H NMR spectroscopy. The spectra acquired for MIM-1 and MIM-2 do not show any of the complexity reported for other well-characterized MBLs that show numerous hyperfine-shifted resonances between 170 to -80 ppm [227, 234, 235]. For instance, the spectra of MIM-1 and MIM-2 are missing the downfield signals at \sim -40 ppm, previously assigned to secondary metal interactions with proton ligands [227, 234, 235]. However, both MIM-1 and MIM-2 display a distinct feature at 45 ppm that has also been observed in other MBLs and which was assigned to Co(II)-coordinated NH groups (**Figure 5.9**) [120] [236-238]. It was previously proposed, for MBLs from the B1 subgroup, that the peak at \sim 45 ppm may be assigned to the NH protons of the His ligands in the Zn1 site (*i.e.* His116, His118 and His196) [120], residues that are conserved in MIM-1 and MIM-2 (**Figure 1.4** and **Figure 4.5**). In addition MIM-1 also has a resonance at 120 ppm, which, based on metal ion replacement studies, was previously assigned to the NH proton of the only histidine ligand in the Zn2 site of the B1 MBL NDM-1 [227].

Chapter 5: Active site geometry and reaction mechanism of MIM-1 and MIM-2

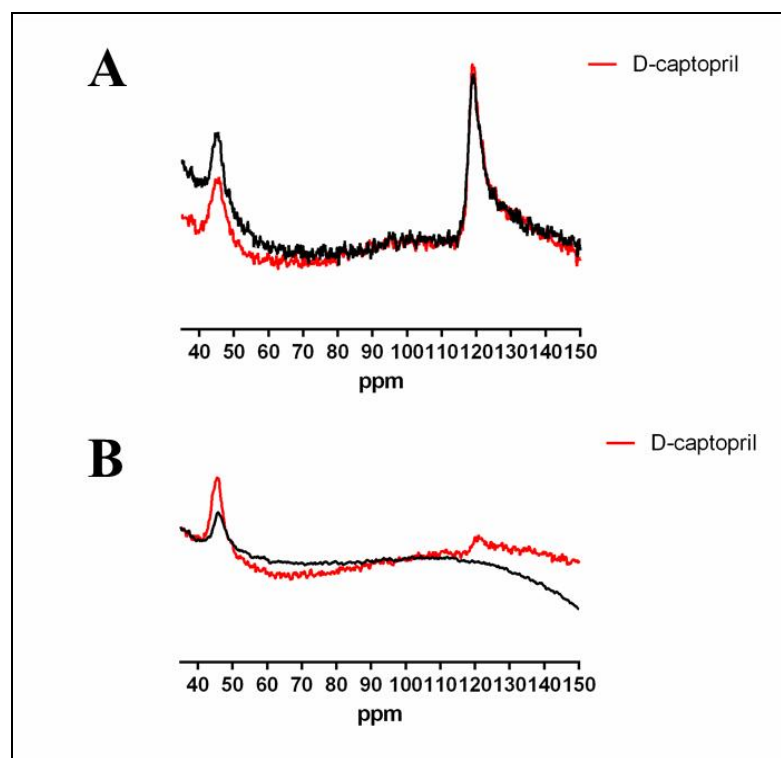


Figure 5.9. 500 MHz ^1H NMR spectra of Co(II) MIM-1 (A) and MIM-2 (B). The spectra were acquired in 90% D_2O .

MIM-1 has two histidine ligands in that site (*i.e.* His121 and His263) and hence either or both may contribute to the observed resonance. MIM-2 has ligands identical to those of MIM-1 in that site and a similar NMR signal would thus be expected. It is currently not known why the resonance is absent but it is yet another demonstration that the family of MBLs may display extensive structural flexibility even within the constraints of highly conserved active site residues. This interpretation is further supported when the effect of captopril binding is investigated by paramagnetic ^1H NMR spectroscopy (**Figure 5.9**). For MIM-1, in agreement with the MCD data, the presence of D-captopril does not affect the spectrum significantly. In contrast, the presence of the inhibitor has a more significant effect on the NMR spectrum of MIM-2. The feature at 45 ppm is still present but a faint resonance at ~ 120 ppm is now also visible, suggesting that the Zn^{2+} site has been perturbed by its interaction with D-captopril. Thus, it appears likely that this inhibitor, despite binding with similar affinity to MIM-1 and

Chapter 5: Active site geometry and reaction mechanism of MIM-1 and MIM-2

MIM-2 (based on the similarity of the respective K_i values; Chapter 3) and the fact that all of the metal ion-coordinating ligands are conserved in the two enzymes, may bind in a different orientation.

In order to gain a better understanding of inhibitor binding the interaction between the metal centres of MIM-1 and MIM-2 and D-captopril was further analysed by electron paramagnetic resonance (**Figure 5.10**).

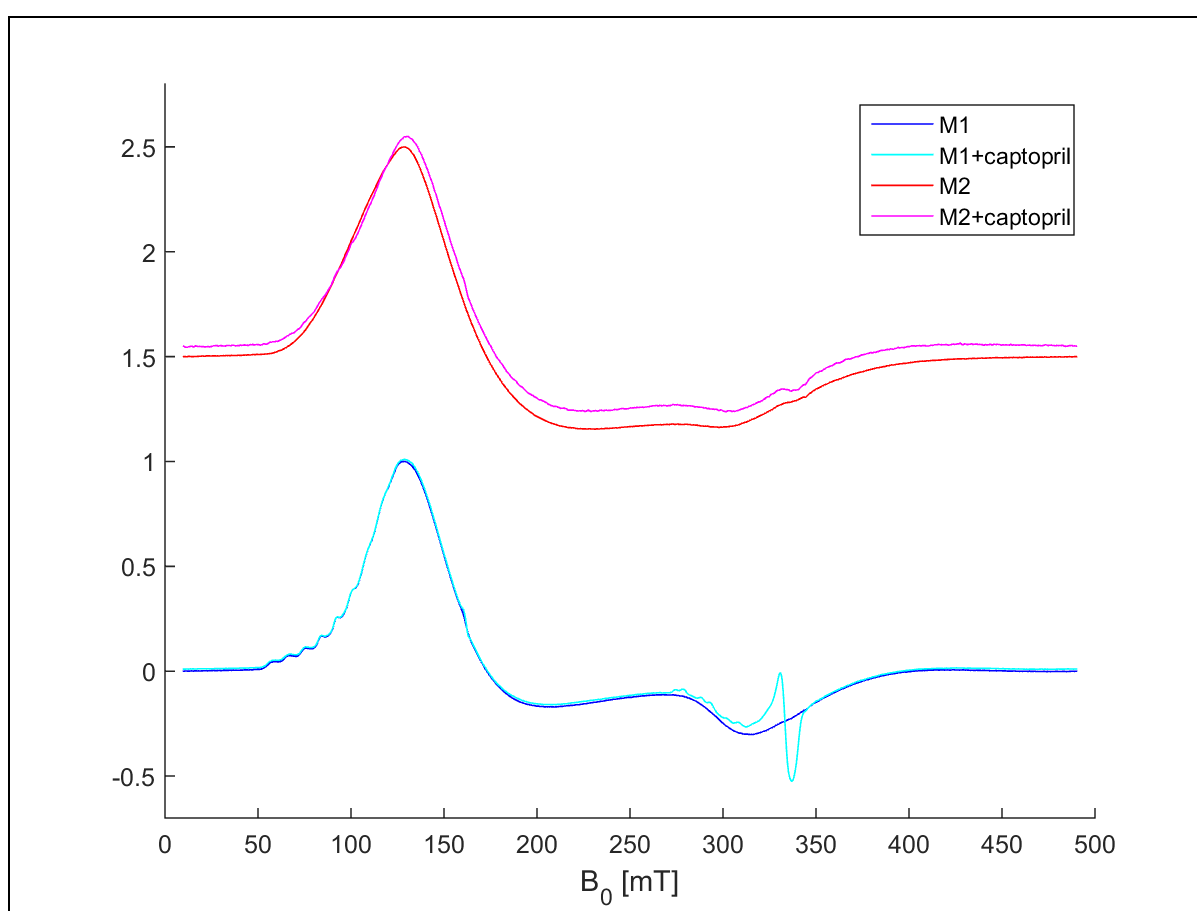


Figure 5.10. Continuous wave EPR spectra recorded at 20 K in normal perpendicular mode at 9.64 GHz. Data were recorded in absence and presence of D- captopril for MIM-1 and MIM-2.

For both MIM-1 and MIM-2 the general features of the spectra are characteristic of a bimetallic Co(II) system with five or six ligands (the spectral data for Co(II) systems are not

Chapter 5: Active site geometry and reaction mechanism of MIM-1 and MIM-2

sensitive enough to distinguish between five or six ligands in the coordination environment of the metal centres) [120, 226]. The spectra were simulated using the software XSophe (Bruker Biospin) by Assoc. Prof. Jeffrey Harmer (Centre of Advanced Imaging; University of Queensland), using the parameters listed in **Figure 5.11**.

For MIM2 the addition of D-captopril leads to a small shift in the peak positions (**Figure 5.10**), which are indicative of some minor perturbation of the metal ion centre(s). However, the shifts are too small to be interpreted accurately by data simulations but do suggest that D-captopril interacts weakly with the active site.

For MIM1 the low field signals (*i.e.* below 250 mT; **Figure 5.10**) are essentially identical in the absence or presence of the inhibitor. However, in the region between 260 - 350 mT there is a significant change. The sharp signal at 332 mT, $g = 2.0715$, and the hyperfine coupling down to about 260 mT, is probably from a metal-centred radical. **Figure 5.12** shows the power dependence of this signal at 20 K. The lack of signal saturation is indicative of a metal-centred radical, not an organic radical molecule. Furthermore, the hyperfine resonances in the 260 – 350 mT region could be due to two low spin Co(II) species as there would be eight resonances from the metal centre along the g_z direction. However, the spectrum is not resolved well enough to make an unambiguous assignment, but its formation presumably only after addition of D-captopril suggests that D-captopril binds closely (directly) to the paramagnetic centre and this interaction perturbs the electronic structure.

Chapter 5: Active site geometry and reaction mechanism of MIM-1 and MIM-2

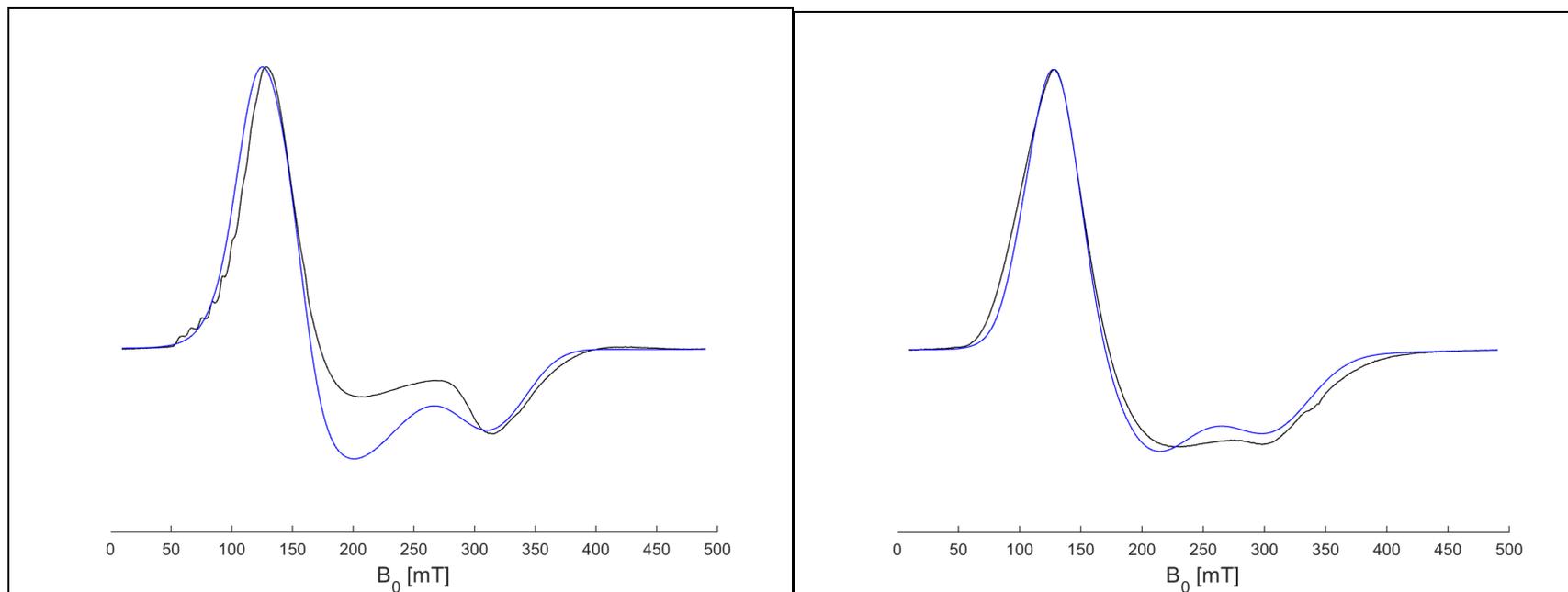


Figure 5.11. Simulation of the EPR spectra collected for resting MIM-1 (left) and MIM-2 (right). The spectra were simulated using XSophe (Bruker Biospin), assuming $H_0 = \beta B_0 g \hat{S} / \hbar + \hat{S} D \hat{S}$, where $S = 3/2$, $|D| \gg |\beta g B S / \hbar|$, and where $D > 0$ implies the $M_S = \pm 1/2$ Kramers doublet lies lowest and all observed EPR transitions are from this doublet, and $D < 0$ implies the $M_S = \pm 3/2$ Kramers doublet lie lowest and all observed EPR transitions are from this doublet. For MIM-1 g_x , g_y and $g_z = 2.30$, 2.30 and 2.20 , respectively, with corresponding linewidths of 1.2 , 0.5 and 0.35 . For MIM-2 the corresponding values are g_x , g_y and $g_z = 2.30$, 2.30 and 2.29 , respectively, with corresponding linewidths of 1.14 , 0.8 and 0.55 .

Chapter 5: Active site geometry and reaction mechanism of MIM-1 and MIM-2

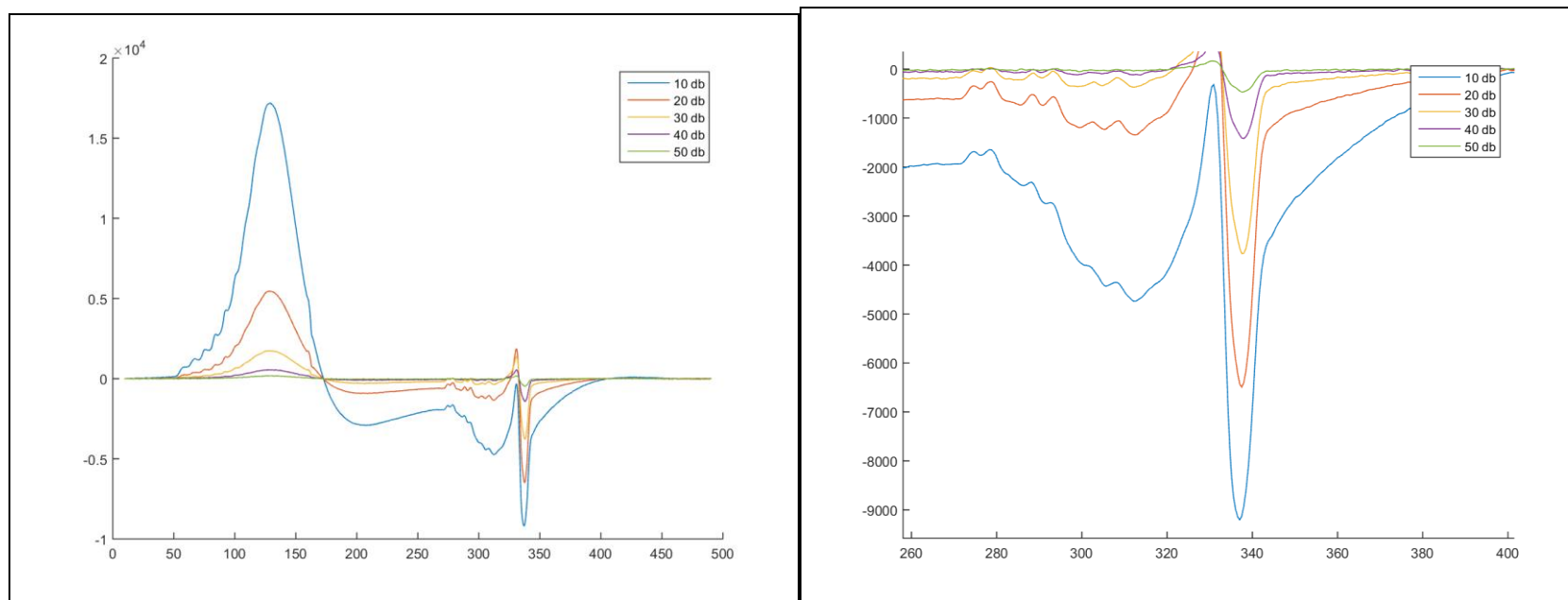


Figure 5.12. Power saturation of EPR signals for MIM-1. Data were measured at microwave powers ranging from 10 db to 50 db for MIM-1 in the presence of D-captopril at 20 K. The spectra on the right are showing a close-up focusing on the region between 260 – 350 mT.

Chapter 5: Active site geometry and reaction mechanism of MIM-1 and MIM-2

In summary, EPR data agree, by and large, with MCD and NMR data and suggest that D-captopril binding may not affect the immediate first coordination sphere significantly. It is possible that this inhibitor binds either only to one of the metal ions or none directly, or it coordinates via its carboxyl group, not its thiol sulfur, as observed in crystal structures of several MBLs. It is important to point out that the spectroscopic studies, especially the EPR-related ones, are still preliminary, but as far as comparisons with other MBLs are possible MIM-1 and MIM-2 behave similar to those enzymes. Further high-resolution pulse EPR experiments (e.g. ENDOR and HYSCORE) aimed at measuring small hyperfine interactions between the paramagnetic metal centre and the magnetic nuclei of the D-captopril (i.e. ^2H and ^1H nuclei) not resolved in the CW EPR spectra may reveal the position and binding of D-captopril, but are presently beyond the scope of this work.

5.4 Conclusion

Previous studies probing the effect of pH on the catalytic reaction of MIM-1 and MIM-2 with a range of substrates indicated that while there are some variations in terms of preferred pH the overall mechanism involving a metal ion-bound nucleophile to initiate the hydrolysis of the β -lactam bond appears to remain conserved (see Chapter 3).

Nitrocefin, a cephalosporin, is a substrate frequently used to probe the mechanism of catalysis of MBLs. Interestingly, while nitrocefin is an excellent substrate for both MIM-1 and MIM-2 no substrate inhibition is observed. This is in contrast to the behaviour of all other substrates tested previously, including cephalosporins (see **Fig. 3.2** in Chapter 3). While substrate inhibition was interpreted in terms of the presence of an alternative binding site for these reactants, nitrocefin may only be able to bind to one site. Indeed, the K_m values of MIM-1 and MIM-2 for nitrocefin are of similar magnitude as those of other cephalosporins (compare **Tables 5.1** and **3.2**), indicating that within the active site nitrocefin binds in a

Chapter 5: Active site geometry and reaction mechanism of MIM-1 and MIM-2

manner similar to that of other substrates. This interpretation is also consistent with a recently reported similar observation for the B3-type MBL AIM-1, where substrate inhibition is common except for nitrocefin [129].

Monitoring the progress of a single catalytic turnover by stopped-flow absorbance measurements leads to an apparent discrepancy with the catalytic rate obtained from steady-state measurements under pseudo first-order conditions. In fact, the rate of product formation appears to be approximately 200-fold slower in a single turnover experiment ($\sim 5 \text{ s}^{-1}$ vs $\sim 1000 \text{ s}^{-1}$; **Tables 5.1** and **5.2**). In fact, under single turnover conditions the reactions monitored with various metal ion derivatives of both MIM-1 and MIM-2 are very similar, suggesting a conserved mechanism. A plausible explanation for the discrepancy observed for the reaction rates monitored under the two different conditions is that in the absence of excess substrate the product remains bound to the active site. However, in the presence of excess substrate, due to its higher affinity when compared to that of the product, the substrate displaces the product and maintains a rapid catalytic rate.

This interpretation may also apply to MBLs such as AIM-1 and Bla2 [120, 129] but not to enzymes such as NDM-1 or L1 where single turnover and steady state assays result in similar catalytic rates [226, 227], and demonstrates the mechanistic flexibility of MBLs, despite largely conserved active site geometries. Indeed, although no crystal structures of MIM-1 and MIM-2 were available before finalising this thesis, spectroscopic data indicated that these enzymes have active sites similar to those of other MBLs (**Figs 1.4** and **1.5**).

In summary, while MIM-1 and MIM-2, two MBLs from non-pathogenic environmental microorganisms, clearly possess all the features characteristic for this class of enzymes they also demonstrate the flexibility of MBLs to perform their reactions. Of particular relevance for the design of potent inhibitors is that product release may be exploited to slow down the catalytic rate sufficiently to be of clinical relevance. In particular, an

Chapter 5: Active site geometry and reaction mechanism of MIM-1 and MIM-2

inhibitor designed to mimic the features of the enzyme-product complex rather than the enzyme-substrate complex may prove to be a potent agent in combating antibiotic resistance. In order to strengthen this hypothesis, crystal structures of MIM-1 and MIM-2 in complex with products may be essential. Efforts towards this goal are currently in progress in our group and will be briefly outlined in the final chapter of this thesis.

Chapter 6: Concluding Remarks and Future Directions

The successful treatment of common bacterial infections has been alarmingly undermined by the emergence of antibiotic resistance in an ever-increasing number of pathogens. Sustained periods of the haphazard application of antibiotics and global mobility have contributed significantly to this global health concern. The prophylactic use of antibiotics in the agricultural industry (supplemented in feed stocks and water sources) is another major contributor to the evolution of antibiotic resistance [239, 240]. Since antibiotic resistance determinants are frequently located on transposable genetic elements, the chance of a horizontal gene transfer connected to urban and environmental microorganisms is a clear and real danger [241-243]. In particular, soil environments have been identified as an important reservoir of a diversity of antibiotic resistant determinants found in uncultured bacteria [244]. Moreover, some soil microorganisms have been shown to contain a wealth of antibiotic resistance genes independent of anthropogenic influence [149]. These instances of antibiotic resistance in the absence of human intervention offer invaluable and rare insights into the origin and evolution of antibiotic resistance prior to the medicinal use of antibiotics, insights which may assist future efforts to counteract or prevent antibiotic resistance [244, 245]. As discussed in Chapter 1, β -lactamases are a family of enzymes that have acquired considerable notoriety due to their ability to hydrolyse most commonly used β -lactam-based antibiotics such as penicillins, cephalosporins and carbapenems. In particular, class B, the so-called MBLs, are of concern since no clinically useful inhibitors are available. In this context MIM-1 and MIM-2, both identified in some environmental marine-based microorganisms, harbor tremendous potential to lead research in both the understanding of a powerful

Chapter 6: Concluding Remarks and Future Directions

antibiotic resistance mechanism and the development of potent drug leads to combat its spread.

An important step towards realizing the potential that MIM-1 and MIM-2 may provide for research in the antibiotic resistance area is the elucidation of their three dimensional structures by X-ray crystallography. I initiated crystallization trials during my candidature, establishing experimental conditions that led to crystal formations. None of these crystals were, however, of a quality sufficient for diffraction, but they formed a reasonable starting point for further optimisations. Another doctoral student in our group, Mr. Christopher Selleck, recently obtained crystals for both enzymes that diffract to resolution of ~ 2.0 Å (Figure 6.1; C. Selleck, unpublished data).

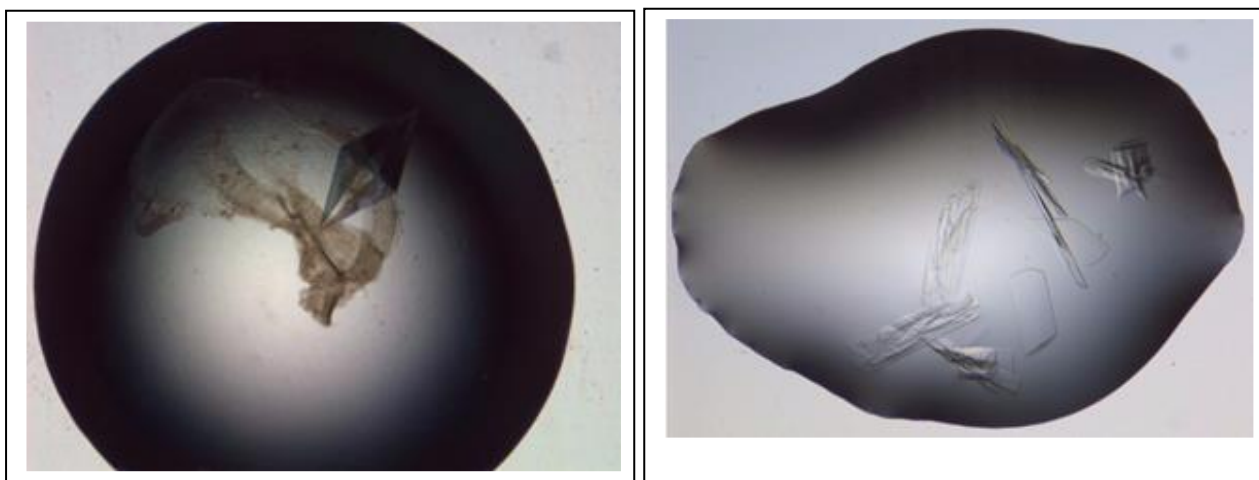


Figure 6.1. Crystals grown for MIM-1 (left) and MIM-2 (right) using the hanging drop method. X-ray diffraction data were collected at the Australian Synchrotron in Melbourne at resolutions of 2.3 and 1.8 Å, respectively, for MIM-1 and MIM-2. The structures were solved by molecular replacement and model refinement is currently in progress.

The structures of MIM-1 and MIM-2 were readily solved by molecular replacement using the coordinates of the B3-type MBL AIM-1 as a template. Refinements of these structures are currently still in progress, but with respect to their overall structure and metal ion binding

Chapter 6: Concluding Remarks and Future Directions

sites in their catalytic centre they are very similar to other MBLs, as anticipated. **Figure 6.2** shows the relevant illustration for MIM-2. It will be interesting to analyse the outer coordination spheres of the enzymes as this is the location where the degree of homology observed between different MBLs is lower than in the direct coordination sphere. It is thus anticipated that variations in terms of substrate specificity (see Chapters 3 and 4) and mechanism (see Chapter 5) are reflected in structural changes in this outer sphere.

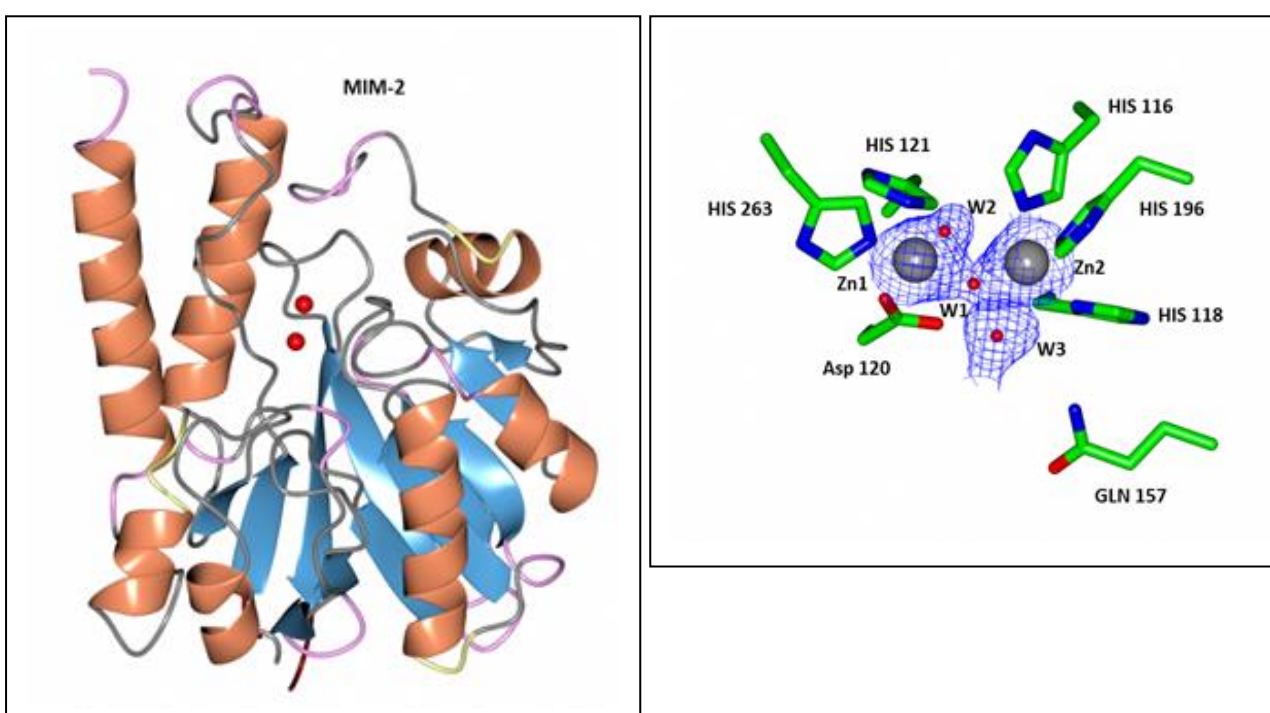


Figure 6.2. Partially refined crystal structure of MIM-2 (left). The red spheres indicate the two Zn(II) binding sites in the active centre. This active site is illustrated on the right, also showing the electron density map around the two metal ions (shown as grey spheres). A total of three water molecules (red spheres) complete the first coordination sphere, two terminally bound to either of the metal ions (W2 and W3), and one bridging the Zn(II) ions (W1). W1 is the likely hydrolysis-initiating nucleophile in the catalytic cycle of MBLs.

Chapter 6: Concluding Remarks and Future Directions

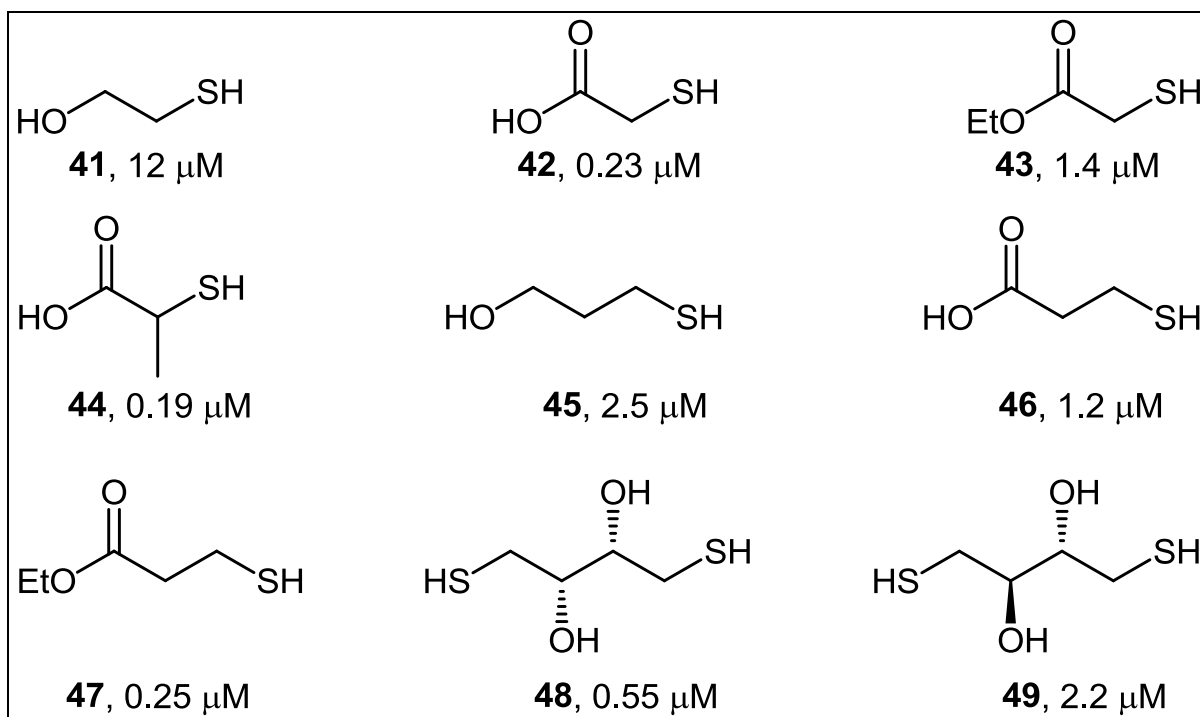


Figure 6.3. Thiol derivatives and corresponding inhibition constants (K_i values), determined for the B1-type MBL IMP-1.

Our group and others have developed an arsenal of *in vitro* MBL inhibitors, including a range of thiols (**Figure 6.3**), ketones, alcohols, dicarboxylic acids, sulfates, hydroxamates, tetrazoles and sulfonamides [20]. While some of those compounds are potent inhibitors for members of one subgroup of MBLs, to my knowledge no “universal” inhibitor that affects representatives of ? in a similar manner has yet been developed. Insofar, the observed plasticity in the active site of MIM-1 and MIM-2 may render these enzymes as ideal targets to improve existing inhibitor leads, especially with a view to developing the first universally useful MBL inhibitor. Time will tell.

Annex: 1 Inteins—A Focus on the Biotechnological Applications of Splicing-Promoting Proteins

American Journal of Molecular Biology, 2015, 5, 42-56

Published Online April 2015 in SciRes. <http://www.scirp.org/journal/ajmb>
<http://dx.doi.org/10.4236/ajmb.2015.52005>

Inteins—A Focus on the Biotechnological Applications of Splicing-Promoting Proteins

Manfredi Miraula^{1,2*}, Charmaine Enculescu², Gerhard Schenk², Nataša Mitić¹

¹Department of Chemistry, Maynooth University, Maynooth, Ireland ²School of Molecular and Microbial Biosciences, The University of Queensland, St. Lucia, Queensland, Australia

Email: * manfredi.miraula@nuim.ie

Received 10 March 2015; accepted 23 March 2015; published 26 March 2015

Copyright © 2015 by authors and Scientific Research Publishing Inc. This work is licensed under the Creative Commons Attribution International License (CC BY).
<http://creativecommons.org/licenses/by/4.0/>

Abstract

The main aim of this mini-review is to illustrate strategies and industrial applications based on inteins (INTERNAL proteINS), which belong to a class of autocatalytic enzymes that are able to perform a catalytic reaction on a single substrate. However, since practical applications of inteins are strongly guided by a detailed understanding of their biological mechanisms and functions, the first part of this review will thus briefly discuss the physiological roles of inteins, describing what is currently known about their mechanisms of action. In the second part, specific biotechnological applications of inteins will be outlined (*i.e.* their use for (i) the purification of recombinant proteins, (ii) the cyclization of proteins and (iii) the production of seleno-proteins), paying attention to both potential strengths and weaknesses of this technology.

Keywords

Intein, Protein Purification, Tagged Protein, Cyclization, Selenoprotein

Annex: 2 Identification and characterization of an unusual metallo- β -lactamase from *Serratia proteamaculans*

J Biol Inorg Chem (2013) 18:855–863 DOI 10.1007/s00775-013-1035-z

ORIGINAL PAPER

Identification and characterization of an unusual metallo- β -lactamase from *Serratia proteamaculans*

Peter Vella • Manfredi Miraula • Emer Phelan • Eleanor W. W. Leung • Fernanda Ely • David L. Ollis • Ross P. McGeary • Gerhard Schenk • Natas̃a Mitic´

Received: 20 May 2013 / Accepted: 14 August 2013 / Published online: 28 August 2013 Ó SBIC 2013

Abstract Metallo- β -lactamases (MBLs) are a family of metalloenzymes that are capable of hydrolyzing β -lactam antibiotics and are an important means by which bacterial pathogens use to inactivate antibiotics. A database search of the available amino acid sequences from *Serratia proteamaculans* indicates the presence of an unusual MBL. A full length amino acid sequence alignment indicates overall homology to B3-type MBLs, but also suggests considerable variations in the active site, notably among residues that are relevant to metal ion binding. Steady-state kinetic measurements further indicate functional differences and identify two relevant pK_a values for catalysis (3.8 for the enzyme–substrate complex and 7.8 for the free enzyme) and a preference for penams with modest reactivity towards some cephalosporins. An analysis of the metal ion content indicates the presence of only one zinc ion per active site in the resting enzyme. In contrast, kinetic data suggest that the enzyme may operate as a binuclear enzyme, and it is thus proposed that a catalytically active di- Zn^{2+} center is formed only once the substrate is present.

Electronic supplementary material The online version of this article (doi:10.1007/s00775-013-1035-z) contains supplementary material, which is available to authorized users.

P. Vella E. W. W. Leung F. Ely R. P. McGeary G. Schenk (&) School of Chemistry and Molecular Biosciences, The University of Queensland,

St. Lucia, QLD 4072, Australia e-mail: schenk@uq.edu.au

M. Miraula E. Phelan N. Mitic´ (&) Department of Chemistry, National University of Ireland, Maynooth, Maynooth, Co. Kildare, Ireland e-mail: natasa.mitic@nuim.ie

D. L. Ollis Research School of Chemistry, The Australian National University, Canberra, ACT 0200, Australia

R. P. McGeary School of Pharmacy, The University of Queensland, St. Lucia, QLD 4072, Australia

Keywords Antibiotics resistance Metallo- β -lactamases Binuclear metallohydrolases Sequence homology Infectious disease

Annex: 3 Intrinsic disorder and metal binding in UreG proteins from Archae hyperthermophiles: GTPase enzymes involved in the activation of Ni(II) dependent urease

J Biol Inorg Chem (2015) 20:739–755 DOI 10.1007/s00775-015-1261-7

ORIGINAL PAPER

Intrinsic disorder and metal binding in UreG proteins from Archae hyperthermophiles: GTPase enzymes involved in the activation of Ni(II) dependent urease

Manfredi Miraula^{1,2} · Stefano Ciurli¹ · Barbara Zambelli¹

Received: 24 December 2014 / Accepted: 20 March 2015 / Published online: 7 April 2015 © SBIC 2015

Abstract Urease is a Ni(II) enzyme present in every domain of life, in charge for nitrogen recycling through urea hydrolysis. Its activity requires the presence of two Ni(II) ions in the active site. These are delivered by the concerted action of four accessory proteins, named UreD, UreF, UreG and UreE. This process requires protein flexibility at different levels and some disorder-to-order transition events that coordinate the mechanism of protein–protein interaction. In particular, UreG, the GTPase in charge of nucleotide hydrolysis required for urease activation, presents a significant degree of intrinsic disorder, existing as a conformational ensemble featuring characteristics that recall a molten globule. Here, the folding properties of UreG were explored in Archaea hyperthermophiles, known to generally feature significantly low level of structural disorder in their proteome. UreG proteins from *Methanocaldococcus jannaschii* (*Mj*) and *Metallosphaera sedula* (*Ms*) were structurally and functionally analyzed by integrating circular dichroism, NMR, light scattering and enzymatic assays. Metal-binding properties were studied using isothermal titration calorimetry. The results indicate that, as the mesophilic counterparts, both proteins contain a significant amount of secondary structure but maintain a flexible fold and a low GTPase activity. As opposed to other UreGs, secondary structure is lost at high temperatures (68 and 75 °C, respectively) with an apparent two-state mechanism. Both proteins bind Zn(II) and Ni(II), with affinities two orders of magnitude higher for Zn(II) than for Ni(II). No major modifications of the average conformational ensemble are observed, but binding of Zn(II) yields a more compact dimeric form in *MsUreG*.

Keywords Intrinsically disordered enzyme · UreG · Urease · Metal binding · Archaea thermophiles

J Biol Inorg Chem (2015) 20:739–755 DOI 10.1007/s00775-015-1261-7

ORIGINAL PAPER

Annex: 4 Identification and preliminary characterization of novel B3-type metallo- β -lactamases

American Journal of Molecular Biology, 2013, 3, 198-203 **AJMB**
<http://dx.doi.org/10.4236/ajmb.2013.34026> Published Online October 2013
(<http://www.scirp.org/journal/ajmb/>)

Identification and preliminary characterization of novel B3-type metallo- β -lactamases

Manfredi Miraula^{1,2}, Conor S. Brunton¹, Gerhard Schenk², Nataša Mitić¹

¹Department of Chemistry, National University of Ireland—Maynooth, Maynooth, Co., Kildare, Ireland ²School of Chemistry and Molecular Biosciences, The University of Queensland, Brisbane, Australia Email: schenk@uq.edu.au, natasa.mitic@nuim.ie

Received 30 May 2013; revised 23 June 2013; accepted 9 July 2013

Copyright © 2013 Manfredi Miraula *et al.* This is an open access article distributed under the Creative Commons Attribution License, which permits unrestricted use, distribution, and reproduction in any medium, provided the original work is properly cited.

ABSTRACT

Antibiotic resistance has emerged as a major global threat to human health. Among the strategies employed by pathogens to acquire resistance the use of metallo- β -lactamases (MBLs), a family of dinuclear metalloenzymes, is among the most potent. MBLs are subdivided into three groups (*i.e.* B1, B2 and B3) with most of the virulence factors belonging to the B1 group. The recent discovery of AIM-1, a B3-type MBL, however, has illustrated the potential health threat of this group of MBLs. Here, we employed a bioinformatics approach to identify and characterize novel B3-type MBLs from *Novosphingobium pentaromativorans* and *Simiduia agarivorans*. These enzymes may not yet pose a direct risk to human health, but their structures and function may provide important insight into the design and synthesis of a still elusive universal MBL inhibitor.

Keywords: Antibiotic Resistance; β -Lactam Antibiotics; Metallo- β -Lactamases; Sequence Homology; *Novosphingobium Pentaromativorans*; *Simiduia Agarivorans*

Annex: 5 Metallo- β -Lactamases: A Major Threat to Human Health

American Journal of Molecular Biology, 2014, 4, 89-104

Published Online July 2014 in SciRes. <http://www.scirp.org/journal/ajmb>
<http://dx.doi.org/10.4236/ajmb.2014.43011>

Metallo- β -Lactamases: A Major Threat to Human Health

Emer K. Phelan^{1,2*}, Manfredi Miraula^{1,2*}, Christopher Selleck², David L. Ollis³, Gerhard Schenk², Nataša Mitić^{1#}

¹Department of Chemistry, National University of Ireland-Maynooth, Maynooth, Ireland ²School of Chemistry and Molecular Biosciences, The University of Queensland, Brisbane, Australia ³Research School of Chemistry, Australian National University, Canberra, Australia Email: #natasa.mitic@nuim.ie

Received 15 April 2014; revised 14 May 2014; accepted 13 June 2014

Copyright © 2014 by authors and Scientific Research Publishing Inc. This work is licensed under the Creative Commons Attribution International License (CC BY).
<http://creativecommons.org/licenses/by/4.0/>

Abstract

Antibiotic resistance is one of the most significant challenges facing global healthcare. Since the 1940s, antibiotics have been used to fight infections, initially with penicillin and subsequently with various derivatives including cephalosporins, carbapenams and monobactams. A common characteristic of these antibiotics is the four-membered β -lactam ring. Alarmingly, in recent years an increasing number of bacteria have become resistant to these antibiotics. A major strategy employed by these pathogens is to use Zn(II)-dependent enzymes, the metallo- β -lactamases (MBLs), which hydrolyse the β -lactam ring. Clinically useful MBL inhibitors are not yet available. Consequently, MBLs remain a major threat to human health. In this review biochemical properties of MBLs are discussed, focusing in particular on the interactions between the enzymes and the functionally essential metal ions. The precise role(s) of these metal ions is still debated and may differ between different MBLs. However, since they are required for catalysis, their binding site may present an alternative target for inhibitor design.

Keywords

Antibiotic Resistance, β -Lactam Antibiotics, Metallo- β -Lactamases, Reaction Mechanism, Metal Ion Binding

Annex: 6 Catalytic Mechanisms of Metallohydrolases Containing Two Metal Ions

Catalytic Mechanisms of Metallohydrolases Containing Two Metal Ions

Nataša Mitić^{*,1}, Manfredi Miraula^{*,†}, Christopher Selleck[†], Kieran S. Hadler[†], Elena Uribe[‡], Marcelo M. Pedroso[†],

Gerhard Schenk^{†,1} ^{*}Department of Chemistry, National University of Ireland, Maynooth, Maynooth, Co. Kildare, Ireland

[†]School of Chemistry and Molecular Biosciences, The University of Queensland, Brisbane, Queensland, Australia [‡]Department of Biochemistry and Molecular Biology, University of Concepción, Concepción, Chile ¹Corresponding authors: e-mail address: natasa.mitic@nuim.ie; schenk@uq.edu.au

Abstract

At least one-third of enzymes contain metal ions as cofactors necessary for a diverse range of catalytic activities. In the case of polymetallic enzymes (i.e., two or more metal ions involved in catalysis), the presence of two (or more) closely spaced metal ions gives an additional advantage in terms of (i) charge delocalisation, (ii) smaller activation barriers, (iii) the ability to bind larger substrates, (iv) enhanced electrostatic activation of substrates, and (v) decreased transition-state energies. Among this group of proteins, enzymes that catalyze the hydrolysis of ester and amide bonds form a very prominent family, the metallohydrolases. These enzymes are involved in a multitude of biological functions, and an increasing number of them gain attention for translational research in medicine and biotechnology. Their functional versatility and catalytic proficiency are largely due to the presence of metal ions in their active sites. In this chapter, we thus discuss and compare the reaction mechanisms of several closely related enzymes with a view to highlighting the functional diversity bestowed upon them by their metal ion cofactors.

Annex: 7 β -Lactam antibiotic-degrading enzymes from non-pathogenic marine organisms: a potential threat to human health

J Biol Inorg Chem (2015) 20:639–651 DOI 10.1007/s00775-015-1250-x

ORIGINAL PAPER

β -Lactam antibiotic-degrading enzymes from non-pathogenic marine organisms: a potential threat to human health

Manfredi Miraula^{1,2} · Jacob J. Whitaker² · Gerhard Schenk² · Nataša Mitic¹

Received: 15 January 2015 / Accepted: 2 March 2015 / Published online: 14 March 2015 © SBIC 2015

Abstract Metallo- β -lactamases (MBLs) are a family of Zn(II)-dependent enzymes that inactivate most of the commonly used β -lactam antibiotics. They have emerged as a major threat to global healthcare. Recently, we identified two novel MBL-like proteins, Maynooth IMipenemase-1 (MIM-1) and Maynooth IMipenemase-2 (MIM-2), in the marine organisms *Novosphingobium pentaromativorans* and *Simiduia agarivorans*, respectively. Here, we demonstrate that MIM-1 and MIM-2 have catalytic activities comparable to those of known MBLs, but from the pH dependence of their catalytic parameters it is evident that both enzymes differ with respect to their mechanisms, with MIM-1 preferring alkaline and MIM-2 acidic conditions. Both enzymes require Zn(II) but activity can also be reconstituted with other metal ions including Co(II), Mn(II), Cu(II) and Ca(II). Importantly, the substrate preference of MIM-1 and MIM-2 appears to be influenced by their metal ion composition. Since neither *N. pentaromativorans* nor *S. agarivorans* are human pathogens, the precise biological role(s) of MIM-1 and MIM-2 remains to be established. However, due to the similarity of at least some of their in vitro functional properties to those of known MBLs, MIM-1 and MIM-2 may provide essential structural insight that may guide the design of as of yet elusive clinically useful MBL inhibitors.

Electronic supplementary material The online version of this article (doi:[10.1007/s00775-015-1250-x](https://doi.org/10.1007/s00775-015-1250-x)) contains supplementary material, which is available to authorized users.

Keywords Antibiotic resistance · β -Lactam antibiotics · Metallo- β -lactamase · Metallohydrolase · Catalysis

Annex: 8 Promiscuous metallo- β -lactamases: MIM-1 and MIM-2 may play an essential role in quorum sensing networks

Promiscuous metallo- β -lactamases: MIM-1 and MIM-2 may play an essential role in quorum sensing networks

Manfredi Miraula ^{a,b}, Gerhard Schenk ^b, Nataša Mitić ^a,

^a Department of Chemistry, Maynooth University, Maynooth, Co. Kildare, Ireland ^b School of Chemistry and Molecular Biosciences, The University of Queensland, St. Lucia, QLD 4072, Australia

article info Article history: Received 21 October 2015 Received in revised form 4 December 2015 Accepted 16 December 2015 Available online xxxx Keywords: Antibiotic resistance Metallo-beta-lactamases Binuclear metallohydrolases Quorum sensing

Functional promiscuity

Abstract MIM-1 and MIM-2 are two recently identified metallo- β -lactamases (MBLs) from *Novosphingobium pentaromativorans* and *Simiduia agarivorans*, respectively. Since these organisms are non-pathogenic we speculated that the biological role(s) of MIM-1 and MIM-2 may not be related to their MBL activity. Although both sequence comparison and homology modeling indicate that these proteins are homologous to well-known MBLs such as AIM-1, the sequence analysis also indicated that MIM-1 and MIM-2 share similarities with N-acyl homoserine lactonases (AHLases) and glyoxalase II (GLX-II). Steady-state kinetic assays using a series of lactone substrates confirm that MIM-1 and MIM-2 are efficient lactonases, with catalytic efficiencies resembling those of well-known AHLases. Interestingly, unlike their MBL activity the AHLase activity of MIM-1 and MIM-2 is not dependent on the metal ion composition with Zn(II), Co(II), Cu(II), Mn(II) and Ca(II) all being able to reconstitute catalytic activity (with Co(II) being the most efficient). However, these enzymes do not turn over S-lactoylglutathione, a substrate characteristic for GLX-II activity. Since lactonase activity is linked to the process of quorum sensing the bifunctional activity of “non-pathogenic” MBLs such as MIM-1 and MIM-2 may provide insight into one possible evolutionary pathway for the emergence of antibiotic resistance.

Annex: 9 Unusual metallo- β -lactamases may constitute a new subgroup in this family of enzymes

American Journal of Molecular Biology, 2014, 4, 11-15 **AJMB**

<http://dx.doi.org/10.4236/ajmb.2014.41002> Published Online January 2014

(<http://www.scirp.org/journal/ajmb/>)

Unusual metallo- β -lactamases may constitute a new subgroup in this family of enzymes

Chun-Feng D. Hou¹, Emer K. Phelan^{2,3}, Manfredi Miraula^{2,3}, David L. Ollis¹, Gerhard Schenk³, Nataša Mitić²

¹Research School of Chemistry, Australian National University, Canberra, Australia ²Department of Chemistry, National University of Ireland-Maynooth, Maynooth, Ireland ³School of Chemistry and Molecular Biosciences, The University of Queensland, Brisbane, Australia Email: schenk@uq.edu.au, natasa.mitic@nuim.ie

Received 1 October 2013; revised 1 November 2013; accepted 18 November 2013

ABSTRACT

Metallo- β -lactamases (MBLs) are a family of Zn^{2+} - dependent enzymes that have contributed strongly to the emergence and spread of antibiotic resistance. Novel members as well as variants of existing members of this family are discovered continuously, compounding their threat to global health care. MBLs are divided into three subgroups, *i.e.* B1, B2 and B3. The recent discovery of an unusual MBL from *Serratia proteamaculans* (SPR-1) suggests the presence of an additional subgroup, *i.e.* B4. A database search reveals that SPR-1 has only one homologue from *Cronobacter sakazakii*, CSA-1. These two MBLs have a unique active site and may employ a mechanism distinct from other MBLs, but reminiscent of some organophosphate-degrading hydrolases.

KEYWORDS

Antibiotic Resistance; β -Lactam Antibiotics; Metallo- β -Lactamases; Sequence Homology; *Serratia proteamaculans*; *Cronobacter sakazakii*

References

1. Wilcox, D. E., Binuclear Metallohydrolases. *Chem Rev* **1996**, 96 (7), 2435-2458.
2. Schenk, G.; Mitic, N.; Gahan, L. R.; Ollis, D. L.; McGeary, R. P.; Guddat, L. W., Binuclear metallohydrolases: complex mechanistic strategies for a simple chemical reaction. *Acc Chem Res* **2012**, 45 (9), 1593-603.
3. Meyers, R. A., *Encyclopedia of molecular biology and molecular medicine*. Weinheim: VCH: 1996.
4. Mitic, N.; Smith, S. J.; Neves, A.; Guddat, L. W.; Gahan, L. R.; Schenk, G., The catalytic mechanisms of binuclear metallohydrolases. *Chem Rev* **2006**, 106 (8), 3338-63.
5. Dismukes, G. C., Manganese Enzymes with Binuclear Active Sites. *Chem Rev* **1996**, 96 (7), 2909-2926.
6. Bebrone, C., Metallo-beta-lactamases (classification, activity, genetic organization, structure, zinc coordination) and their superfamily. *Biochem Pharmacol* **2007**, 74 (12), 1686-701.
7. Neuwald, A. F.; Liu, J. S.; Lipman, D. J.; Lawrence, C. E., Extracting protein alignment models from the sequence database. *Nucleic Acids Res* **1997**, 25 (9), 1665-77.
8. Garau, G.; Garcia-Saez, I.; Bebrone, C.; Anne, C.; Mercuri, P.; Galleni, M.; Frere, J. M.; Dideberg, O., Update of the standard numbering scheme for class B beta-lactamases. *Antimicrob Agents Chemother* **2004**, 48 (7), 2347-9.
9. Daiyasu, H.; Osaka, K.; Ishino, Y.; Toh, H., Expansion of the zinc metallo-hydrolase family of the beta-lactamase fold. *FEBS Lett* **2001**, 503 (1), 1-6.
10. Guddat, L. W.; McAlpine, A. S.; Hume, D.; Hamilton, S.; de Jersey, J.; Martin, J. L., Crystal structure of mammalian purple acid phosphatase. *Structure* **1999**, 7 (7), 757-67.
11. Hadler, K. S.; Tanifum, E. A.; Yip, S. H.; Mitic, N.; Guddat, L. W.; Jackson, C. J.; Gahan, L. R.; Nguyen, K.; Carr, P. D.; Ollis, D. L.; Hengge, A. C.; Larrabee, J. A.; Schenk, G., Substrate-promoted formation of a catalytically competent binuclear center and regulation of reactivity in a glycerophosphodiesterase from *Enterobacter aerogenes*. *J Am Chem Soc* **2008**, 130 (43), 14129-38.
12. Jackson, C.; Kim, H. K.; Carr, P. D.; Liu, J. W.; Ollis, D. L., The structure of an enzyme-product complex reveals the critical role of a terminal hydroxide nucleophile in the bacterial phosphotriesterase mechanism. *Biochim Biophys Acta* **2005**, 1752 (1), 56-64.
13. Brem, J.; van Berkel, S. S.; Zollman, D.; Lee, S. Y.; Gileadi, O.; McHugh, P. J.; Walsh, T. R.; McDonough, M. A.; Schofield, C. J., Structural Basis of Metallo-beta-Lactamase Inhibition by Captopril Stereoisomers. *Antimicrob Agents Chemother* **2015**, 60 (1), 142-50.
14. Hou, Chun-Feng D.; Phelan, E. K.; Miraula, M.; Ollis, D. L.; Schenk, G.; Mitić, N.; Unusual metallo-β-lactamases may constitute a new subgroup in this family of enzymes. *American Journal of Molecular Biology* **2014**, 4 (1), 11-15.
15. Green, V. L.; Verma, A.; Owens, R. J.; Phillips, S. E.; Carr, S. B., Structure of New Delhi metallo-beta-lactamase 1 (NDM-1). *Acta Crystallogr Sect F Struct Biol Cryst Commun* **2011**, 67 (Pt 10), 1160-4.
16. Phelan, E. K.; Miraula, M.; Selleck, C.; Ollis, D. L.; Schenk, G.; Mitić, N.; Metallo-β-Lactamases: A Major Threat to Human Health. *American Journal of Molecular Biology* **2014**, 4 (3), 89-104.

References

17. Pankey, G. A.; Sabath, L. D., Clinical relevance of bacteriostatic versus bactericidal mechanisms of action in the treatment of Gram-positive bacterial infections. *Clin Infect Dis* **2004**, *38* (6), 864-70.
18. Crowder, M. W.; Spencer, J.; Vila, A. J., Metallo-beta-lactamases: novel weaponry for antibiotic resistance in bacteria. *Acc Chem Res* **2006**, *39* (10), 721-8.
19. Bebrone, C.; Lassaux, P.; Vercheval, L.; Sohier, J. S.; Jehaes, A.; Sauvage, E.; Galleni, M., Current challenges in antimicrobial chemotherapy: focus on ss-lactamase inhibition. *Drugs* **2010**, *70* (6), 651-79.
20. McGeary, R. P.; Schenk, G.; Guddat, L. W., The applications of binuclear metallohydrolases in medicine: recent advances in the design and development of novel drug leads for purple acid phosphatases, metallo-beta-lactamases and arginases. *Eur J Med Chem* **2014**, *76*, 132-44.
21. Heinz, U.; Adolph, H. W., Metallo-beta-lactamases: two binding sites for one catalytic metal ion? *Cell Mol Life Sci* **2004**, *61* (22), 2827-39.
22. Page, M. I.; Badarau, A., The mechanisms of catalysis by metallo beta-lactamases. *Bioinorg Chem Appl* **2008**, 576297.
23. Vella, P.; Miraula, M.; Phelan, E.; Leung, E. W.; Ely, F.; Ollis, D. L.; McGeary, R. P.; Schenk, G.; Mitic, N., Identification and characterization of an unusual metallo-beta-lactamase from *Serratia proteamaculans*. *J Biol Inorg Chem* **2013**, *18* (7), 855-63.
24. Hadler, K. S.; Mitic, N.; Ely, F.; Hanson, G. R.; Gahan, L. R.; Larrabee, J. A.; Ollis, D. L.; Schenk, G., Structural flexibility enhances the reactivity of the bioremediator glycerophosphodiesterase by fine-tuning its mechanism of hydrolysis. *J Am Chem Soc* **2009**, *131* (33), 11900-8.
25. Hadler, K. S.; Mitic, N.; Yip, S. H.; Gahan, L. R.; Ollis, D. L.; Schenk, G.; Larrabee, J. A., Electronic structure analysis of the dinuclear metal center in the bioremediator glycerophosphodiesterase (GpdQ) from *Enterobacter aerogenes*. *Inorg Chem* **2010**, *49* (6), 2727-34.
26. Kupper, M.; Bauvois, C.; Frere, J. M.; Hoffmann, K.; Galleni, M.; Bebrone, C., The CphAII protein from *Aquifex aeolicus* exhibits a metal-dependent phosphodiesterase activity. *Extremophiles* **2012**, *16* (1), 45-55.
27. Garcia-Saez, I.; Mercuri, P. S.; Papamicael, C.; Kahn, R.; Frere, J. M.; Galleni, M.; Rossolini, G. M.; Dideberg, O., Three-dimensional structure of FEZ-1, a monomeric subclass B3 metallo-beta-lactamase from *Fluoribacter gormanii*, in native form and in complex with D-captopril. *J Mol Biol* **2003**, *325* (4), 651-60.
28. Mercuri, P. S.; Bouillenne, F.; Boschi, L.; Lamotte-Brasseur, J.; Amicosante, G.; Devreese, B.; van Beeumen, J.; Frere, J. M.; Rossolini, G. M.; Galleni, M., Biochemical characterization of the FEZ-1 metallo-beta-lactamase of *Legionella gormanii* ATCC 33297T produced in *Escherichia coli*. *Antimicrob Agents Chemother* **2001**, *45* (4), 1254-62.
29. Bellais, S.; Girlich, D.; Karim, A.; Nordmann, P., EBR-1, a novel Ambler subclass B1 beta-lactamase from *Empedobacter brevis*. *Antimicrob Agents Chemother* **2002**, *46* (10), 3223-7.
30. Walsh, T. R.; Gamblin, S.; Emery, D. C.; MacGowan, A. P.; Bennett, P. M., Enzyme kinetics and biochemical analysis of ImiS, the metallo-beta-lactamase from *Aeromonas sobria* 163a. *J Antimicrob Chemother* **1996**, *37* (3), 423-31.
31. Horsfall, L. E.; Izougarhane, Y.; Lassaux, P.; Selevsek, N.; Lienard, B. M.; Poirel, L.; Kupper, M. B.; Hoffmann, K. M.; Frere, J. M.; Galleni, M.; Bebrone, C., Broad antibiotic resistance profile of the subclass B3 metallo-beta-lactamase GOB-1, a di-zinc enzyme. *FEBS J* **2011**, *278* (8), 1252-63.

References

32. Gonzalez, L. J.; Vila, A. J., Carbapenem resistance in *Elizabethkingia meningoseptica* is mediated by metallo-beta-lactamase BlaB. *Antimicrob Agents Chemother* **2012**, *56* (4), 1686-92.
33. Fonseca, F.; Bromley, E. H.; Saavedra, M. J.; Correia, A.; Spencer, J., Crystal structure of *Serratia fonticola* Sfh-I: activation of the nucleophile in mono-zinc metallo-beta-lactamases. *J Mol Biol* **2011**, *411* (5), 951-9.
34. Wachino, J.; Yamaguchi, Y.; Mori, S.; Kurosaki, H.; Arakawa, Y.; Shibayama, K., Structural insights into the subclass B3 metallo-beta-lactamase SMB-1 and the mode of inhibition by the common metallo-beta-lactamase inhibitor mercaptoacetate. *Antimicrob Agents Chemother* **2013**, *57* (1), 101-9.
35. Yamaguchi, Y.; Matsueda, S.; Matsunaga, K.; Takashio, N.; Toma-Fukai, S.; Yamagata, Y.; Shibata, N.; Wachino, J.; Shibayama, K.; Arakawa, Y.; Kurosaki, H., Crystal structure of IMP-2 metallo-beta-lactamase from *Acinetobacter* spp.: comparison of active-site loop structures between IMP-1 and IMP-2. *Biol Pharm Bull* **2015**, *38* (1), 96-101.
36. Franceschini, N.; Caravelli, B.; Docquier, J. D.; Galleni, M.; Frere, J. M.; Amicosante, G.; Rossolini, G. M., Purification and biochemical characterization of the VIM-1 metallo-beta-lactamase. *Antimicrob Agents Chemother* **2000**, *44* (11), 3003-7.
37. Poirel, L.; Naas, T.; Nicolas, D.; Collet, L.; Bellais, S.; Cavallo, J. D.; Nordmann, P., Characterization of VIM-2, a carbapenem-hydrolyzing metallo-beta-lactamase and its plasmid- and integron-borne gene from a *Pseudomonas aeruginosa* clinical isolate in France. *Antimicrob Agents Chemother* **2000**, *44* (4), 891-7.
38. Docquier, J. D.; Benvenuti, M.; Calderone, V.; Stoczko, M.; Menciassi, N.; Rossolini, G. M.; Mangani, S., High-resolution crystal structure of the subclass B3 metallo-beta-lactamase BJP-1: rational basis for substrate specificity and interaction with sulfonamides. *Antimicrob Agents Chemother* **2010**, *54* (10), 4343-51.
39. Stoczko, M.; Frere, J. M.; Rossolini, G. M.; Docquier, J. D., Postgenomic scan of metallo-beta-lactamase homologues in rhizobacteria: identification and characterization of BJP-1, a subclass B3 ortholog from *Bradyrhizobium japonicum*. *Antimicrob Agents Chemother* **2006**, *50* (6), 1973-81.
40. Murphy, T. A.; Simm, A. M.; Toleman, M. A.; Jones, R. N.; Walsh, T. R., Biochemical characterization of the acquired metallo-beta-lactamase SPM-1 from *Pseudomonas aeruginosa*. *Antimicrob Agents Chemother* **2003**, *47* (2), 582-7.
41. Stoczko, M.; Frere, J. M.; Rossolini, G. M.; Docquier, J. D., Functional diversity among metallo-beta-lactamases: characterization of the CAR-1 enzyme of *Erwinia carotovora*. *Antimicrob Agents Chemother* **2008**, *52* (7), 2473-9.
42. Castanheira, M.; Toleman, M. A.; Jones, R. N.; Schmidt, F. J.; Walsh, T. R., Molecular characterization of a beta-lactamase gene, blaGIM-1, encoding a new subclass of metallo-beta-lactamase. *Antimicrob Agents Chemother* **2004**, *48* (12), 4654-61.
43. Skagseth, S.; Carlsen, T. J.; Bjerga, G. E.; Spencer, J.; Samuelsen, O.; Leiros, H. S., Investigating the role of residues W228 and Y233 in the structure and activity of the GIM-1 metallo-beta-lactamase. *Antimicrob Agents Chemother* **2015**.
44. Docquier, J. D.; Lopizzo, T.; Liberatori, S.; Prenna, M.; Thaller, M. C.; Frere, J. M.; Rossolini, G. M., Biochemical characterization of the THIN-B metallo-beta-lactamase of *Janthinobacterium lividum*. *Antimicrob Agents Chemother* **2004**, *48* (12), 4778-83.
45. Booth, M. P.; Kosmopoulou, M.; Poirel, L.; Nordmann, P.; Spencer, J., Crystal Structure of DIM-1, an Acquired Subclass B1 Metallo-beta-Lactamase from *Pseudomonas stutzeri*. *PLoS One* **2015**, *10* (10), e0140059.
46. Carfi, A.; Pares, S.; Duee, E.; Galleni, M.; Duez, C.; Frere, J. M.; Dideberg, O., The 3-D structure of a zinc metallo-beta-lactamase from *Bacillus cereus* reveals a new type of protein fold. *EMBO J* **1995**, *14* (20), 4914-21.

References

47. Badarau, A.; Page, M. I., The variation of catalytic efficiency of *Bacillus cereus* metallo-beta-lactamase with different active site metal ions. *Biochemistry* **2006**, *45* (35), 10654-66.
48. de Seny, D.; Heinz, U.; Wommer, S.; Kiefer, M.; Meyer-Klaucke, W.; Galleni, M.; Frere, J. M.; Bauer, R.; Adolph, H. W., Metal ion binding and coordination geometry for wild type and mutants of metallo-beta -lactamase from *Bacillus cereus* 569/H/9 (BcII): a combined thermodynamic, kinetic, and spectroscopic approach. *J Biol Chem* **2001**, *276* (48), 45065-78.
49. Llarrull, L. I.; Tioni, M. F.; Kowalski, J.; Bennett, B.; Vila, A. J., Evidence for a dinuclear active site in the metallo-beta-lactamase BcII with substoichiometric Co(II). A new model for metal uptake. *J Biol Chem* **2007**, *282* (42), 30586-95.
50. Pollini, S.; Maradei, S.; Pecile, P.; Olivo, G.; Luzzaro, F.; Docquier, J. D.; Rossolini, G. M., FIM-1, a new acquired metallo-beta-lactamase from a *Pseudomonas aeruginosa* clinical isolate from Italy. *Antimicrob Agents Chemother* **2013**, *57* (1), 410-6.
51. Borra, P. S.; Samuelsen, O.; Spencer, J.; Walsh, T. R.; Lorentzen, M. S.; Leiros, H. K., Crystal structures of *Pseudomonas aeruginosa* GIM-1: active-site plasticity in metallo-beta-lactamases. *Antimicrob Agents Chemother* **2013**, *57* (2), 848-54.
52. Yamaguchi, Y.; Takashio, N.; Wachino, J.; Yamagata, Y.; Arakawa, Y.; Matsuda, K.; Kurosaki, H., Structure of metallo-beta-lactamase IND-7 from a *Chryseobacterium indologenes* clinical isolate at 1.65-Å resolution. *J Biochem* **2010**, *147* (6), 905-15.
53. Poirel, L.; Heritier, C.; Nordmann, P., Genetic and biochemical characterization of the chromosome-encoded class B beta-lactamases from *Shewanella livingstonensis* (SLB-1) and *Shewanella frigidimarina* (SFB-1). *J Antimicrob Chemother* **2005**, *55* (5), 680-5.
54. Concha, N. O.; Janson, C. A.; Rowling, P.; Pearson, S.; Cheever, C. A.; Clarke, B. P.; Lewis, C.; Galleni, M.; Frere, J. M.; Payne, D. J.; Bateson, J. H.; Abdel-Meguid, S. S., Crystal structure of the IMP-1 metallo beta-lactamase from *Pseudomonas aeruginosa* and its complex with a mercaptocarboxylate inhibitor: binding determinants of a potent, broad-spectrum inhibitor. *Biochemistry* **2000**, *39* (15), 4288-98.
55. Llarrull, L. I.; Tioni, M. F.; Vila, A. J., Metal content and localization during turnover in *B. cereus* metallo-beta-lactamase. *J Am Chem Soc* **2008**, *130* (47), 15842-51.
56. Laraki, N.; Franceschini, N.; Rossolini, G. M.; Santucci, P.; Meunier, C.; de Pauw, E.; Amicosante, G.; Frere, J. M.; Galleni, M., Biochemical characterization of the *Pseudomonas aeruginosa* 101/1477 metallo-beta-lactamase IMP-1 produced by *Escherichia coli*. *Antimicrob Agents Chemother* **1999**, *43* (4), 902-6.
57. Iyobe, S.; Kusadokoro, H.; Ozaki, J.; Matsumura, N.; Minami, S.; Haruta, S.; Sawai, T.; O'Hara, K., Amino acid substitutions in a variant of IMP-1 metallo-beta-lactamase. *Antimicrob Agents Chemother* **2000**, *44* (8), 2023-7.
58. Riccio, M. L.; Franceschini, N.; Boschi, L.; Caravelli, B.; Cornaglia, G.; Fontana, R.; Amicosante, G.; Rossolini, G. M., Characterization of the metallo-beta-lactamase determinant of *Acinetobacter baumannii* AC-54/97 reveals the existence of bla(IMP) allelic variants carried by gene cassettes of different phylogeny. *Antimicrob Agents Chemother* **2000**, *44* (5), 1229-35.
59. Oelschlaeger, P.; Mayo, S. L., Hydroxyl groups in the (beta)beta sandwich of metallo-beta-lactamases favor enzyme activity: a computational protein design study. *J Mol Biol* **2005**, *350* (3), 395-401.
60. Yamaguchi, Y.; Ding, S.; Murakami, E.; Imamura, K.; Fuchigami, S.; Hashiguchi, R.; Yutani, K.; Mori, H.; Suzuki, S.; Arakawa, Y.; Kurosaki, H., A demetallation method for IMP-1 metallo-beta-lactamase with restored enzymatic activity upon addition of metal ion(s). *ChemBiochem* **2011**, *12* (13), 1979-83.

References

61. Griffin, D. H.; Richmond, T. K.; Sanchez, C.; Moller, A. J.; Breece, R. M.; Tierney, D. L.; Bennett, B.; Crowder, M. W., Structural and kinetic studies on metallo-beta-lactamase IMP-1. *Biochemistry* **2011**, *50* (42), 9125-34.
62. Vella, P.; Hussein, W. M.; Leung, E. W.; Clayton, D.; Ollis, D. L.; Mitic, N.; Schenk, G.; McGeary, R. P., The identification of new metallo-beta-lactamase inhibitor leads from fragment-based screening. *Bioorg Med Chem Lett* **2011**, *21* (11), 3282-5.
63. Horton, L. B.; Shanker, S.; Mikulski, R.; Brown, N. G.; Phillips, K. J.; Lykissa, E.; Venkataram Prasad, B. V.; Palzkill, T., Mutagenesis of zinc ligand residue Cys221 reveals plasticity in the IMP-1 metallo-beta-lactamase active site. *Antimicrob Agents Chemother* **2012**, *56* (11), 5667-77.
64. Lauretti, L.; Riccio, M. L.; Mazzariol, A.; Cornaglia, G.; Amicosante, G.; Fontana, R.; Rossolini, G. M., Cloning and characterization of blaVIM, a new integron-borne metallo-beta-lactamase gene from a Pseudomonas aeruginosa clinical isolate. *Antimicrob Agents Chemother* **1999**, *43* (7), 1584-90.
65. Cornaglia, G.; Mazzariol, A.; Lauretti, L.; Rossolini, G. M.; Fontana, R., Hospital outbreak of carbapenem-resistant Pseudomonas aeruginosa producing VIM-1, a novel transferable metallo-beta-lactamase. *Clin Infect Dis* **2000**, *31* (5), 1119-25.
66. Tsakris, A.; Pournaras, S.; Woodford, N.; Palepou, M. F.; Babini, G. S.; Douboyas, J.; Livermore, D. M., Outbreak of infections caused by Pseudomonas aeruginosa producing VIM-1 carbapenemase in Greece. *J Clin Microbiol* **2000**, *38* (3), 1290-2.
67. Giakkoupi, P.; Xanthaki, A.; Kanelopoulou, M.; Vlahaki, A.; Miriagou, V.; Kontou, S.; Papafraggas, E.; Malamou-Lada, H.; Tzouvelekis, L. S.; Legakis, N. J.; Vatopoulos, A. C., VIM-1 Metallo-beta-lactamase-producing Klebsiella pneumoniae strains in Greek hospitals. *J Clin Microbiol* **2003**, *41* (8), 3893-6.
68. Pournaras, S.; Maniati, M.; Petinaki, E.; Tzouvelekis, L. S.; Tsakris, A.; Legakis, N. J.; Maniatis, A. N., Hospital outbreak of multiple clones of Pseudomonas aeruginosa carrying the unrelated metallo-beta-lactamase gene variants blaVIM-2 and blaVIM-4. *J Antimicrob Chemother* **2003**, *51* (6), 1409-14.
69. Miriagou, V.; Tzelepi, E.; Gianneli, D.; Tzouvelekis, L. S., Escherichia coli with a self-transferable, multiresistant plasmid coding for metallo-beta-lactamase VIM-1. *Antimicrob Agents Chemother* **2003**, *47* (1), 395-7.
70. Giske, C. G.; Rylander, M.; Kronvall, G., VIM-4 in a carbapenem-resistant strain of Pseudomonas aeruginosa isolated in Sweden. *Antimicrob Agents Chemother* **2003**, *47* (9), 3034-5.
71. Ktari, S.; Arlet, G.; Mnif, B.; Gautier, V.; Mahjoubi, F.; Ben Jmeaa, M.; Bouaziz, M.; Hammami, A., Emergence of multidrug-resistant Klebsiella pneumoniae isolates producing VIM-4 metallo-beta-lactamase, CTX-M-15 extended-spectrum beta-lactamase, and CMY-4 AmpC beta-lactamase in a Tunisian university hospital. *Antimicrob Agents Chemother* **2006**, *50* (12), 4198-201.
72. Garcia-Saez, I.; Docquier, J. D.; Rossolini, G. M.; Dideberg, O., The three-dimensional structure of VIM-2, a Zn-beta-lactamase from Pseudomonas aeruginosa in its reduced and oxidised form. *J Mol Biol* **2008**, *375* (3), 604-11.
73. Abriata, L. A.; Gonzalez, L. J.; Llarrull, L. I.; Tomatis, P. E.; Myers, W. K.; Costello, A. L.; Tierney, D. L.; Vila, A. J., Engineered mononuclear variants in Bacillus cereus metallo-beta-lactamase BcII are inactive. *Biochemistry* **2008**, *47* (33), 8590-9.
74. Yong, D.; Toleman, M. A.; Giske, C. G.; Cho, H. S.; Sundman, K.; Lee, K.; Walsh, T. R., Characterization of a new metallo-beta-lactamase gene, bla(NDM-1), and a novel erythromycin esterase gene carried on a unique genetic structure in Klebsiella pneumoniae sequence type 14 from India. *Antimicrob Agents Chemother* **2009**, *53* (12), 5046-54.

References

75. Poirel, L.; Hombrouck-Alet, C.; Freneaux, C.; Bernabeu, S.; Nordmann, P., Global spread of New Delhi metallo-beta-lactamase 1. *Lancet Infect Dis* **2010**, *10* (12), 832.
76. Rolain, J. M.; Parola, P.; Cornaglia, G., New Delhi metallo-beta-lactamase (NDM-1): towards a new pandemic? *Clin Microbiol Infect* **2010**, *16* (12), 1699-701.
77. Zhang, H.; Hao, Q., Crystal structure of NDM-1 reveals a common beta-lactam hydrolysis mechanism. *FASEB J* **2011**, *25* (8), 2574-82.
78. Walsh, T. R.; Weeks, J.; Livermore, D. M.; Toleman, M. A., Dissemination of NDM-1 positive bacteria in the New Delhi environment and its implications for human health: an environmental point prevalence study. *Lancet Infect Dis* **2011**, *11* (5), 355-62.
79. Li, N.; Xu, Y.; Xia, Q.; Bai, C.; Wang, T.; Wang, L.; He, D.; Xie, N.; Li, L.; Wang, J.; Zhou, H. G.; Xu, F.; Yang, C.; Zhang, Q.; Yin, Z.; Guo, Y.; Chen, Y., Simplified captopril analogues as NDM-1 inhibitors. *Bioorg Med Chem Lett* **2014**, *24* (1), 386-9.
80. Segatore, B.; Massidda, O.; Satta, G.; Setacci, D.; Amicosante, G., High specificity of cphA-encoded metallo-beta-lactamase from *Aeromonas hydrophila* AE036 for carbapenems and its contribution to beta-lactam resistance. *Antimicrob Agents Chemother* **1993**, *37* (6), 1324-8.
81. Bebrone, C.; Anne, C.; De Vriendt, K.; Devreese, B.; Rossolini, G. M.; Van Beeumen, J.; Frere, J. M.; Galleni, M., Dramatic broadening of the substrate profile of the *Aeromonas hydrophila* CphA metallo-beta-lactamase by site-directed mutagenesis. *J Biol Chem* **2005**, *280* (31), 28195-202.
82. Crawford, P. A.; Sharma, N.; Chandrasekar, S.; Sigdel, T.; Walsh, T. R.; Spencer, J.; Crowder, M. W., Over-expression, purification, and characterization of metallo-beta-lactamase ImiS from *Aeromonas veronii* bv. *sobria*. *Protein Expr Purif* **2004**, *36* (2), 272-9.
83. Garau, G.; Bebrone, C.; Anne, C.; Galleni, M.; Frere, J. M.; Dideberg, O., A metallo-beta-lactamase enzyme in action: crystal structures of the monozinc carbapenemase CphA and its complex with biapenem. *J Mol Biol* **2005**, *345* (4), 785-95.
84. Xu, D.; Zhou, Y.; Xie, D.; Guo, H., Antibiotic binding to monozinc CphA beta-lactamase from *Aeromonas hydrophila*: quantum mechanical/molecular mechanical and density functional theory studies. *J Med Chem* **2005**, *48* (21), 6679-89.
85. Simona, F.; Magistrato, A.; Dal Peraro, M.; Cavalli, A.; Vila, A. J.; Carloni, P., Common mechanistic features among metallo-beta-lactamases: a computational study of *Aeromonas hydrophila* CphA enzyme. *J Biol Chem* **2009**, *284* (41), 28164-71.
86. Bebrone, C.; Delbruck, H.; Kupper, M. B.; Schlomer, P.; Willmann, C.; Frere, J. M.; Fischer, R.; Galleni, M.; Hoffmann, K. M., The structure of the dizinc subclass B2 metallo-beta-lactamase CphA reveals that the second inhibitory zinc ion binds in the histidine site. *Antimicrob Agents Chemother* **2009**, *53* (10), 4464-71.
87. Costello, A.; Periyannan, G.; Yang, K. W.; Crowder, M. W.; Tierney, D. L., Site-selective binding of Zn(II) to metallo-beta-lactamase L1 from *Stenotrophomonas maltophilia*. *J Biol Inorg Chem* **2006**, *11* (3), 351-8.
88. Ullah, J. H.; Walsh, T. R.; Taylor, I. A.; Emery, D. C.; Verma, C. S.; Gamblin, S. J.; Spencer, J., The crystal structure of the L1 metallo-beta-lactamase from *Stenotrophomonas maltophilia* at 1.7 Å resolution. *J Mol Biol* **1998**, *284* (1), 125-36.
89. Hu, Z.; Periyannan, G.; Bennett, B.; Crowder, M. W., Role of the Zn1 and Zn2 sites in metallo-beta-lactamase L1. *J Am Chem Soc* **2008**, *130* (43), 14207-16.
90. Hu, Z.; Periyannan, G. R.; Crowder, M. W., Folding strategy to prepare Co(II)-substituted metallo-beta-lactamase L1. *Anal Biochem* **2008**, *378* (2), 177-83.
91. Miraula, M.; Brunton, C.S.; Schenk, G. and Mitic, N., Identification and Preliminary Characterization of Novel B3-Type Metallo-β-Lactamases. *American Journal of Molecular Biology*, **2013**, *3* (198-203).

References

92. Miraula, M.; Whitaker, J. J.; Schenk, G.; Mitic, N., beta-Lactam antibiotic-degrading enzymes from non-pathogenic marine organisms: a potential threat to human health. *J Biol Inorg Chem* **2015**, *20* (4), 639-51.
93. Wachino, J.; Yoshida, H.; Yamane, K.; Suzuki, S.; Matsui, M.; Yamagishi, T.; Tsutsui, A.; Konda, T.; Shibayama, K.; Arakawa, Y., SMB-1, a novel subclass B3 metallo-beta-lactamase, associated with ISCR1 and a class 1 integron, from a carbapenem-resistant *Serratia marcescens* clinical isolate. *Antimicrob Agents Chemother* **2011**, *55* (11), 5143-9.
94. Massidda, O.; Rossolini, G. M.; Satta, G., The *Aeromonas hydrophila* cphA gene: molecular heterogeneity among class B metallo-beta-lactamases. *J Bacteriol* **1991**, *173* (15), 4611-7.
95. Hernandez Valladares, M.; Kiefer, M.; Heinz, U.; Soto, R. P.; Meyer-Klaucke, W.; Nolting, H. F.; Zeppezauer, M.; Galleni, M.; Frere, J. M.; Rossolini, G. M.; Amicosante, G.; Adolph, H. W., Kinetic and spectroscopic characterization of native and metal-substituted beta-lactamase from *Aeromonas hydrophila* AE036. *FEBS Lett* **2000**, *467* (2-3), 221-5.
96. Mitic, N.; Miraula, M.; Selleck, C.; Hadler, K. S.; Uribe, E.; Pedroso, M. M.; Schenk, G., Catalytic mechanisms of metallohydrolases containing two metal ions. *Adv Protein Chem Struct Biol* **2014**, *97*, 49-81.
97. Daumann, L. J.; Schenk, G.; Ollis, D. L.; Gahan, L. R., Spectroscopic and mechanistic studies of dinuclear metallohydrolases and their biomimetic complexes. *Dalton Trans* **2014**, *43* (3), 910-28.
98. Paul-Soto, R.; Zeppezauer, M.; Adolph, H. W.; Galleni, M.; Frere, J. M.; Carfi, A.; Dideberg, O.; Wouters, J.; Hemmingsen, L.; Bauer, R., Preference of Cd(II) and Zn(II) for the two metal sites in *Bacillus cereus* beta-lactamase II: A perturbed angular correlation of gamma-rays spectroscopic study. *Biochemistry* **1999**, *38* (50), 16500-6.
99. Wommer, S.; Rival, S.; Heinz, U.; Galleni, M.; Frere, J. M.; Franceschini, N.; Amicosante, G.; Rasmussen, B.; Bauer, R.; Adolph, H. W., Substrate-activated zinc binding of metallo-beta -lactamases: physiological importance of mononuclear enzymes. *J Biol Chem* **2002**, *277* (27), 24142-7.
100. Outten, C. E.; O'Halloran, T. V., Femtomolar sensitivity of metalloregulatory proteins controlling zinc homeostasis. *Science* **2001**, *292* (5526), 2488-92.
101. Hemmingsen, L.; Damblon, C.; Antony, J.; Jensen, M.; Adolph, H. W.; Wommer, S.; Roberts, G. C.; Bauer, R., Dynamics of mononuclear cadmium beta-lactamase revealed by the combination of NMR and PAC spectroscopy. *J Am Chem Soc* **2001**, *123* (42), 10329-35.
102. Crowder, M. W.; Wang, Z.; Franklin, S. L.; Zovinka, E. P.; Benkovic, S. J., Characterization of the metal-binding sites of the beta-lactamase from *Bacteroides fragilis*. *Biochemistry* **1996**, *35* (37), 12126-32.
103. Paul-Soto, R.; Hernandez-Valladares, M.; Galleni, M.; Bauer, R.; Zeppezauer, M.; Frere, J. M.; Adolph, H. W., Mono- and binuclear Zn-beta-lactamase from *Bacteroides fragilis*: catalytic and structural roles of the zinc ions. *FEBS Lett* **1998**, *438* (1-2), 137-40.
104. Fast, W.; Wang, Z.; Benkovic, S. J., Familial mutations and zinc stoichiometry determine the rate-limiting step of nitrocefin hydrolysis by metallo-beta-lactamase from *Bacteroides fragilis*. *Biochemistry* **2001**, *40* (6), 1640-50.
105. Garau, G.; Di Guilmi, A. M.; Hall, B. G., Structure-based phylogeny of the metallo-beta-lactamases. *Antimicrob Agents Chemother* **2005**, *49* (7), 2778-84.
106. Frere, J. M.; Galleni, M.; Bush, K.; Dideberg, O., Is it necessary to change the classification of {beta}-lactamases? *J Antimicrob Chemother* **2005**, *55* (6), 1051-3.
107. Crowder, M. W.; Walsh, T. R.; Banovic, L.; Pettit, M.; Spencer, J., Overexpression, purification, and characterization of the cloned metallo-beta-lactamase L1 from *Stenotrophomonas maltophilia*. *Antimicrob Agents Chemother* **1998**, *42* (4), 921-6.

References

108. Spencer, J.; Clarke, A. R.; Walsh, T. R., Novel mechanism of hydrolysis of therapeutic beta-lactams by *Stenotrophomonas maltophilia* L1 metallo-beta-lactamase. *J Biol Chem* **2001**, *276* (36), 33638-44.
109. Moran-Barrio, J.; Gonzalez, J. M.; Lisa, M. N.; Costello, A. L.; Peraro, M. D.; Carloni, P.; Bennett, B.; Tierney, D. L.; Limansky, A. S.; Viale, A. M.; Vila, A. J., The metallo-beta-lactamase GOB is a mono-Zn(II) enzyme with a novel active site. *J Biol Chem* **2007**, *282* (25), 18286-93.
110. Rasia, R. M.; Vila, A. J., Exploring the role and the binding affinity of a second zinc equivalent in *B. cereus* metallo-beta-lactamase. *Biochemistry* **2002**, *41* (6), 1853-60.
111. Jacquin, O.; Balbeur, D.; Damblon, C.; Marchot, P.; De Pauw, E.; Roberts, G. C.; Frere, J. M.; Matagne, A., Positively cooperative binding of zinc ions to *Bacillus cereus* 569/H/9 beta-lactamase II suggests that the binuclear enzyme is the only relevant form for catalysis. *J Mol Biol* **2009**, *392* (5), 1278-91.
112. Gonzalez, J. M.; Medrano Martin, F. J.; Costello, A. L.; Tierney, D. L.; Vila, A. J., The Zn² position in metallo-beta-lactamases is critical for activity: a study on chimeric metal sites on a conserved protein scaffold. *J Mol Biol* **2007**, *373* (5), 1141-56.
113. Thomas, P. W.; Zheng, M.; Wu, S.; Guo, H.; Liu, D.; Xu, D.; Fast, W., Characterization of purified New Delhi metallo-beta-lactamase-1. *Biochemistry* **2011**, *50* (46), 10102-13.
114. Bebrone, C.; Anne, C.; Kerff, F.; Garau, G.; De Vriendt, K.; Lantin, R.; Devreese, B.; Van Beeumen, J.; Dideberg, O.; Frere, J. M.; Galleni, M., Mutational analysis of the zinc- and substrate-binding sites in the CphA metallo-beta-lactamase from *Aeromonas hydrophila*. *Biochem J* **2008**, *414* (1), 151-9.
115. Hernandez Valladares, M.; Felici, A.; Weber, G.; Adolph, H. W.; Zeppezauer, M.; Rossolini, G. M.; Amicosante, G.; Frere, J. M.; Galleni, M., Zn(II) dependence of the *Aeromonas hydrophila* AE036 metallo-beta-lactamase activity and stability. *Biochemistry* **1997**, *36* (38), 11534-41.
116. Saavedra, M. J.; Peixe, L.; Sousa, J. C.; Henriques, I.; Alves, A.; Correia, A., Sfh-I, a subclass B2 metallo-beta-lactamase from a *Serratia fonticola* environmental isolate. *Antimicrob Agents Chemother* **2003**, *47* (7), 2330-3.
117. Sharma, N. P.; Hajdin, C.; Chandrasekar, S.; Bennett, B.; Yang, K. W.; Crowder, M. W., Mechanistic studies on the mononuclear ZnII-containing metallo-beta-lactamase ImiS from *Aeromonas sobria*. *Biochemistry* **2006**, *45* (35), 10729-38.
118. King, D. T.; Worrall, L. J.; Gruninger, R.; Strynadka, N. C., New Delhi metallo-beta-lactamase: structural insights into beta-lactam recognition and inhibition. *J Am Chem Soc* **2012**, *134* (28), 11362-5.
119. Spencer, J.; Read, J.; Sessions, R. B.; Howell, S.; Blackburn, G. M.; Gamblin, S. J., Antibiotic recognition by binuclear metallo-beta-lactamases revealed by X-ray crystallography. *J Am Chem Soc* **2005**, *127* (41), 14439-44.
120. Hawk, M. J.; Breece, R. M.; Hajdin, C. E.; Bender, K. M.; Hu, Z.; Costello, A. L.; Bennett, B.; Tierney, D. L.; Crowder, M. W., Differential binding of Co(II) and Zn(II) to metallo-beta-lactamase Bla2 from *Bacillus anthracis*. *J Am Chem Soc* **2009**, *131* (30), 10753-62.
121. Fabiane, S. M.; Sohi, M. K.; Wan, T.; Payne, D. J.; Bateson, J. H.; Mitchell, T.; Sutton, B. J., Crystal structure of the zinc-dependent beta-lactamase from *Bacillus cereus* at 1.9 Å resolution: binuclear active site with features of a mononuclear enzyme. *Biochemistry* **1998**, *37* (36), 12404-11.
122. Bounaga, S.; Laws, A. P.; Galleni, M.; Page, M. I., The mechanism of catalysis and the inhibition of the *Bacillus cereus* zinc-dependent beta-lactamase. *Biochem J* **1998**, *331* (Pt 3), 703-11.

References

123. Dal Peraro, M.; Vila, A. J.; Carloni, P.; Klein, M. L., Role of zinc content on the catalytic efficiency of B1 metallo beta-lactamases. *J Am Chem Soc* **2007**, *129* (10), 2808-16.
124. Dal Peraro, M.; Llarrull, L. I.; Rothlisberger, U.; Vila, A. J.; Carloni, P., Water-assisted reaction mechanism of monozinc beta-lactamases. *J Am Chem Soc* **2004**, *126* (39), 12661-8.
125. Dal Peraro, M.; Vila, A. J.; Carloni, P., Substrate binding to mononuclear metallo-beta-lactamase from *Bacillus cereus*. *Proteins* **2004**, *54* (3), 412-23.
126. Estiu, G.; Suarez, D.; Merz, K. M., Quantum mechanical and molecular dynamics simulations of ureases and Zn beta-lactamases. *J Comput Chem* **2006**, *27* (12), 1240-62.
127. McManus-Munoz, S.; Crowder, M. W., Kinetic mechanism of metallo-beta-lactamase L1 from *Stenotrophomonas maltophilia*. *Biochemistry* **1999**, *38* (5), 1547-53.
128. Yang, H.; Aitha, M.; Hetrick, A. M.; Richmond, T. K.; Tierney, D. L.; Crowder, M. W., Mechanistic and spectroscopic studies of metallo-beta-lactamase NDM-1. *Biochemistry* **2012**, *51* (18), 3839-47.
129. C. Selleck, J. L. L., N. Mitić, D.L. Ollis, D.L. Tierney, M.M. Pedroso, G. Schenk Reaction mechanism of Adelaide Imipenemase-1 (AIM-1), a member of the B3-subgroup of metallo-β-lactamases. *submitted for publication* **2016**.
130. Cricco, J. A.; Vila, A. J., Class B beta-lactamases: the importance of being metallic. *Curr Pharm Des* **1999**, *5* (11), 915-27.
131. Walsh, T. R.; Toleman, M. A.; Poirel, L.; Nordmann, P., Metallo-beta-lactamases: the quiet before the storm? *Clin Microbiol Rev* **2005**, *18* (2), 306-25.
132. Fisher, J. F.; Meroueh, S. O.; Mobashery, S., Bacterial resistance to beta-lactam antibiotics: compelling opportunism, compelling opportunity. *Chem Rev* **2005**, *105* (2), 395-424.
133. Cornaglia, G.; Giamarellou, H.; Rossolini, G. M., Metallo-beta-lactamases: a last frontier for beta-lactams? *Lancet Infect Dis* **2011**, *11* (5), 381-93.
134. Crowder, B. F., Improved symptom management through enrollment in an outpatient congestive heart failure clinic. *Medsurg Nurs* **2006**, *15* (1), 27-35.
135. Murphy, T. A.; Catto, L. E.; Halford, S. E.; Hadfield, A. T.; Minor, W.; Walsh, T. R.; Spencer, J., Crystal structure of *Pseudomonas aeruginosa* SPM-1 provides insights into variable zinc affinity of metallo-beta-lactamases. *J Mol Biol* **2006**, *357* (3), 890-903.
136. Hernandez Villadares, M.; Galleni, M.; Frere, J. M.; Felici, A.; Perilli, M.; Franceschini, N.; Rossolini, G. M.; Oratore, A.; Amicosante, G., Overproduction and purification of the *Aeromonas hydrophila* CphA metallo-beta-lactamase expressed in *Escherichia coli*. *Microb Drug Resist* **1996**, *2* (2), 253-6.
137. Bellais, S.; Poirel, L.; Fortineau, N.; Decousser, J. W.; Nordmann, P., Biochemical-genetic characterization of the chromosomally encoded extended-spectrum class A beta-lactamase from *Rahnella aquatilis*. *Antimicrob Agents Chemother* **2001**, *45* (10), 2965-8.
138. Leiros, H. K.; Borra, P. S.; Brandsdal, B. O.; Edvardsen, K. S.; Spencer, J.; Walsh, T. R.; Samuelsen, O., Crystal structure of the mobile metallo-beta-lactamase AIM-1 from *Pseudomonas aeruginosa*: insights into antibiotic binding and the role of Gln157. *Antimicrob Agents Chemother* **2012**, *56* (8), 4341-53.
139. Galleni, M.; Lamotte-Brasseur, J.; Rossolini, G. M.; Spencer, J.; Dideberg, O.; Frere, J. M.; Metallo-beta-lactamases Working, G., Standard numbering scheme for class B beta-lactamases. *Antimicrob Agents Chemother* **2001**, *45* (3), 660-3.
140. Jacoby, G. A., Beta-lactamase nomenclature. *Antimicrob Agents Chemother* **2006**, *50* (4), 1123-9.
141. Sohn, J. H.; Kwon, K. K.; Kang, J. H.; Jung, H. B.; Kim, S. J., *Novosphingobium pentaromativorans* sp. nov., a high-molecular-mass polycyclic aromatic hydrocarbon-

References

- degrading bacterium isolated from estuarine sediment. *Int J Syst Evol Microbiol* **2004**, *54* (Pt 5), 1483-7.
142. Shieh, W. Y.; Liu, T. Y.; Lin, S. Y.; Jean, W. D.; Chen, J. S., *Simidiua agarivorans* gen. nov., sp. nov., a marine, agarolytic bacterium isolated from shallow coastal water from Keelung, Taiwan. *Int J Syst Evol Microbiol* **2008**, *58* (Pt 4), 895-900.
143. Garrity, J. D.; Paufl, J. M.; Crowder, M. W., Probing the dynamics of a mobile loop above the active site of L1, a metallo-beta-lactamase from *Stenotrophomonas maltophilia*, via site-directed mutagenesis and stopped-flow fluorescence spectroscopy. *J Biol Chem* **2004**, *279* (38), 39663-70.
144. Yang, K. W.; Crowder, M. W., Inhibition studies on the metallo-beta-lactamase L1 from *Stenotrophomonas maltophilia*. *Arch Biochem Biophys* **1999**, *368* (1), 1-6.
145. Davies, J., Inactivation of antibiotics and the dissemination of resistance genes. *Science* **1994**, *264* (5157), 375-82.
146. Maltezou, H. C., Metallo-beta-lactamases in Gram-negative bacteria: introducing the era of pan-resistance? *Int J Antimicrob Agents* **2009**, *33* (5), 405 e1-7.
147. Perez, F.; Hujer, A. M.; Hujer, K. M.; Decker, B. K.; Rather, P. N.; Bonomo, R. A., Global challenge of multidrug-resistant *Acinetobacter baumannii*. *Antimicrob Agents Chemother* **2007**, *51* (10), 3471-84.
148. Livermore, D. M.; Woodford, N., The beta-lactamase threat in Enterobacteriaceae, *Pseudomonas* and *Acinetobacter*. *Trends Microbiol* **2006**, *14* (9), 413-20.
149. Allen, H. K.; Moe, L. A.; Rodbumrer, J.; Gaarder, A.; Handelsman, J., Functional metagenomics reveals diverse beta-lactamases in a remote Alaskan soil. *ISME J* **2009**, *3* (2), 243-51.
150. IH, S., Enzyme kinetics: behavior and analysis of rapid equilibrium and steady enzyme systems. **1975**.
151. Paul-Soto, R.; Bauer, R.; Frere, J. M.; Galleni, M.; Meyer-Klaucke, W.; Nolting, H.; Rossolini, G. M.; de Seny, D.; Hernandez-Valladares, M.; Zeppezauer, M.; Adolph, H. W., Mono- and binuclear Zn²⁺-beta-lactamase. Role of the conserved cysteine in the catalytic mechanism. *J Biol Chem* **1999**, *274* (19), 13242-9.
152. Yanchak, M. P.; Taylor, R. A.; Crowder, M. W., Mutational analysis of metallo-beta-lactamase CcrA from *Bacteroides fragilis*. *Biochemistry* **2000**, *39* (37), 11330-9.
153. Dong, Y. J.; Bartlam, M.; Sun, L.; Zhou, Y. F.; Zhang, Z. P.; Zhang, C. G.; Rao, Z.; Zhang, X. E., Crystal structure of methyl parathion hydrolase from *Pseudomonas* sp. WBC-3. *J Mol Biol* **2005**, *353* (3), 655-63.
154. Lienard, B. M.; Garau, G.; Horsfall, L.; Karsisiotis, A. I.; Damblon, C.; Lassaux, P.; Papamicael, C.; Roberts, G. C.; Galleni, M.; Dideberg, O.; Frere, J. M.; Schofield, C. J., Structural basis for the broad-spectrum inhibition of metallo-beta-lactamases by thiols. *Org Biomol Chem* **2008**, *6* (13), 2282-94.
155. Heinz, U.; Bauer, R.; Wommer, S.; Meyer-Klaucke, W.; Papamichaels, C.; Bateson, J.; Adolph, H. W., Coordination geometries of metal ions in d- or l-captopril-inhibited metallo-beta-lactamases. *J Biol Chem* **2003**, *278* (23), 20659-66.
156. Schimerlik, M. I.; Cleland, W. W., pH variation of the kinetic parameters and the catalytic mechanism of malic enzyme. *Biochemistry* **1977**, *16*, 576-583.
157. Michalska, K.; Cielecka-Piontek, J.; Pajchel, G.; Tyski, S., Determination of biapenem in a medicinal product by micellar electrokinetic chromatography with sweeping in an enhanced electric field. *J Chromatogr A* **2013**, *1282*, 153-60.
158. Alekseev, V. G., Acid-base properties of penicillins and cephalosporins (a review). *Pharm Chem J* **2010**, *44*, 14-24.
159. Smith, S. J.; Casellato, A.; Hadler, K. S.; Mitic, N.; Riley, M. J.; Bortoluzzi, A. J.; Szpoganicz, B.; Schenk, G.; Neves, A.; Gahan, L. R., The reaction mechanism of the

References

- Ga(III)Zn(II) derivative of uteroferrin and corresponding biomimetics. *J Biol Inorg Chem* **2007**, *12* (8), 1207-20.
160. Hu, Z.; Spadafora, L. J.; Hajdin, C. E.; Bennett, B.; Crowder, M. W., Structure and mechanism of copper- and nickel-substituted analogues of metallo-beta-lactamase L1. *Biochemistry* **2009**, *48* (13), 2981-9.
161. Linse, S.; Helmersson, A.; Forsen, S., Calcium binding to calmodulin and its globular domains. *J Biol Chem* **1991**, *266* (13), 8050-4.
162. Permyakov, E. A.; Yarmolenko, V. V.; Kalinichenko, L. P.; Morozova, L. A.; Burstein, E. A., Calcium binding to alpha-lactalbumin: structural rearrangement and association constant evaluation by means of intrinsic protein fluorescence changes. *Biochem Biophys Res Commun* **1981**, *100* (1), 191-7.
163. Pedroso, M. M.; Larrabee, J. A.; Ely, F.; Gwee, S. E.; Mitic, N.; Ollis, D. L.; Gahan, L. R.; Schenk, G., Ca(II) Binding Regulates and Dominates the Reactivity of a Transition-Metal-Ion-Dependent Diesterase from Mycobacterium tuberculosis. *Chemistry* **2016**, *22* (3), 999-1009.
164. Clapham, D. E., Calcium signaling. *Cell* **2007**, *131* (6), 1047-58.
165. Brini, M.; Ottolini, D.; Cali, T.; Carafoli, E., Calcium in health and disease. *Met Ions Life Sci* **2013**, *13*, 81-137.
166. Bertini, I., *Biological inorganic chemistry: structure and reactivity*. . 2007.
167. Stewart, P. S.; Costerton, J. W., Antibiotic resistance of bacteria in biofilms. *Lancet* **2001**, *358* (9276), 135-8.
168. Zambelli, B.; Musiani, F.; Benini, S.; Ciurli, S., Chemistry of Ni²⁺ in urease: sensing, trafficking, and catalysis. *Acc Chem Res* **2011**, *44* (7), 520-30.
169. Schenk, G.; Mitić, N.; Graeme, R. H.; Comba, P., Purple acid phosphatase: A journey into the function and mechanism of a colorful enzyme. *Coord Chem Rev* **2013**, *257* (2), 473-482.
170. Bernhardt, P. V.; Schenk, G.; Wilson, G. J., Direct electrochemistry of porcine purple acid phosphatase (uteroferrin). *Biochemistry* **2004**, *43* (32), 10387-92.
171. Ely, F.; Hadler, K. S.; Gahan, L. R.; Guddat, L. W.; Ollis, D. L.; Schenk, G., The organophosphate-degrading enzyme from Agrobacterium radiobacter displays mechanistic flexibility for catalysis. *Biochem J* **2010**, *432* (3), 565-73.
172. Ely, F.; Hadler, K. S.; Mitic, N.; Gahan, L. R.; Ollis, D. L.; Plugis, N. M.; Russo, M. T.; Larrabee, J. A.; Schenk, G., Electronic and geometric structures of the organophosphate-degrading enzyme from Agrobacterium radiobacter (OpdA). *J Biol Inorg Chem* **2011**, *16* (5), 777-87.
173. Daumann, L. J.; McCarthy, B. Y.; Hadler, K. S.; Murray, T. P.; Gahan, L. R.; Larrabee, J. A.; Ollis, D. L.; Schenk, G., Promiscuity comes at a price: catalytic versatility vs efficiency in different metal ion derivatives of the potential bioremediator GpdQ. *Biochim Biophys Acta* **2013**, *1834* (1), 425-32.
174. Pedroso, M. M.; Ely, F.; Mitic, N.; Carpenter, M. C.; Gahan, L. R.; Wilcox, D. E.; Larrabee, J. L.; Ollis, D. L.; Schenk, G., Comparative investigation of the reaction mechanisms of the organophosphate-degrading phosphotriesterases from Agrobacterium radiobacter (OpdA) and Pseudomonas diminuta (OPH). *J Biol Inorg Chem* **2014**, *19* (8), 1263-75.
175. Badarau, A.; Damblon, C.; Page, M. I., The activity of the dinuclear cobalt-beta-lactamase from Bacillus cereus in catalysing the hydrolysis of beta-lactams. *Biochem J* **2007**, *401* (1), 197-203.
176. Ng, T. K.; Gahan, L. R.; Schenk, G.; Ollis, D. L., Altering the substrate specificity of methyl parathion hydrolase with directed evolution. *Arch Biochem Biophys* **2015**, *573*, 59-68.

References

177. Fast, W.; Tipton, P. A., The enzymes of bacterial census and censorship. *Trends Biochem Sci* **2012**, *37* (1), 7-14.
178. Roche, D. M.; Byers, J. T.; Smith, D. S.; Glansdorp, F. G.; Spring, D. R.; Welch, M., Communications blackout? Do N-acylhomoserine-lactone-degrading enzymes have any role in quorum sensing? *Microbiology* **2004**, *150* (Pt 7), 2023-8.
179. Fuqua, C.; Parsek, M. R.; Greenberg, E. P., Regulation of gene expression by cell-to-cell communication: acyl-homoserine lactone quorum sensing. *Annu Rev Genet* **2001**, *35*, 439-68.
180. Amara, N.; Krom, B. P.; Kaufmann, G. F.; Meijler, M. M., Macromolecular inhibition of quorum sensing: enzymes, antibodies, and beyond. *Chem Rev* **2011**, *111* (1), 195-208.
181. Geske, G. D.; O'Neill, J. C.; Blackwell, H. E., Expanding dialogues: from natural autoinducers to non-natural analogues that modulate quorum sensing in Gram-negative bacteria. *Chem Soc Rev* **2008**, *37* (7), 1432-47.
182. Geske, G. D.; O'Neill, J. C.; Miller, D. M.; Wezeman, R. J.; Mattmann, M. E.; Lin, Q.; Blackwell, H. E., Comparative analyses of N-acylated homoserine lactones reveal unique structural features that dictate their ability to activate or inhibit quorum sensing. *Chembiochem* **2008**, *9* (3), 389-400.
183. Duan, K.; Surette, M. G., Environmental regulation of *Pseudomonas aeruginosa* PAO1 Las and Rhl quorum-sensing systems. *J Bacteriol* **2007**, *189* (13), 4827-36.
184. Pearson, J. P.; Gray, K. M.; Passador, L.; Tucker, K. D.; Eberhard, A.; Iglewski, B. H.; Greenberg, E. P., Structure of the autoinducer required for expression of *Pseudomonas aeruginosa* virulence genes. *Proc Natl Acad Sci U S A* **1994**, *91* (1), 197-201.
185. Clamp, M.; Cuff, J.; Searle, S. M.; Barton, G. J., The Jalview Java alignment editor. *Bioinformatics* **2004**, *20* (3), 426-7.
186. Notredame, C.; Higgins, D. G.; Heringa, J., T-Coffee: A novel method for fast and accurate multiple sequence alignment. *J Mol Biol* **2000**, *302* (1), 205-17.
187. Poirot, O.; O'Toole, E.; Notredame, C., Tcoffee@igs: A web server for computing, evaluating and combining multiple sequence alignments. *Nucleic Acids Res* **2003**, *31* (13), 3503-6.
188. Waterhouse, A. M.; Procter, J. B.; Martin, D. M.; Clamp, M.; Barton, G. J., Jalview Version 2--a multiple sequence alignment editor and analysis workbench. *Bioinformatics* **2009**, *25* (9), 1189-91.
189. Gouet, P.; Robert, X.; Courcelle, E., ESPript/ENDscript: Extracting and rendering sequence and 3D information from atomic structures of proteins. *Nucleic Acids Res* **2003**, *31* (13), 3320-3.
190. Tamura, K.; Stecher, G.; Peterson, D.; Filipski, A.; Kumar, S., MEGA6: Molecular Evolutionary Genetics Analysis version 6.0. *Mol Biol Evol* **2013**, *30* (12), 2725-9.
191. Kuntal, B. K.; Aparoy, P.; Reddanna, P., EasyModeller: A graphical interface to MODELLER. *BMC Res Notes* **2010**, *3*, 226.
192. Nauton, L.; Kahn, R.; Garau, G.; Hernandez, J. F.; Dideberg, O., Structural insights into the design of inhibitors for the L1 metallo-beta-lactamase from *Stenotrophomonas maltophilia*. *J Mol Biol* **2008**, *375* (1), 257-69.
193. Liu, D.; Lepore, B. W.; Petsko, G. A.; Thomas, P. W.; Stone, E. M.; Fast, W.; Ringe, D., Three-dimensional structure of the quorum-quenching N-acyl homoserine lactone hydrolase from *Bacillus thuringiensis*. *Proc Natl Acad Sci U S A* **2005**, *102* (33), 11882-7.
194. Liu, D.; Momb, J.; Thomas, P. W.; Moulin, A.; Petsko, G. A.; Fast, W.; Ringe, D., Mechanism of the quorum-quenching lactonase (AiiA) from *Bacillus thuringiensis*. 1. Product-bound structures. *Biochemistry* **2008**, *47* (29), 7706-14.

References

195. Thomas, P. W.; Stone, E. M.; Costello, A. L.; Tierney, D. L.; Fast, W., The quorum-quenching lactonase from *Bacillus thuringiensis* is a metalloprotein. *Biochemistry* **2005**, *44* (20), 7559-69.
196. Cameron, A. D.; Ridderstrom, M.; Olin, B.; Mannervik, B., Crystal structure of human glyoxalase II and its complex with a glutathione thiolester substrate analogue. *Structure* **1999**, *7* (9), 1067-78.
197. Levin, E. J.; Kondrashov, D. A.; Wesenberg, G. E.; Phillips, G. N., Jr., Ensemble refinement of protein crystal structures: validation and application. *Structure* **2007**, *15* (9), 1040-52.
198. Maiti, R.; Van Domselaar, G. H.; Zhang, H.; Wishart, D. S., SuperPose: a simple server for sophisticated structural superposition. *Nucleic Acids Res* **2004**, *32* (Web Server issue), W590-4.
199. Pettersen, E. F.; Goddard, T. D.; Huang, C. C.; Couch, G. S.; Greenblatt, D. M.; Meng, E. C.; Ferrin, T. E., UCSF Chimera--a visualization system for exploratory research and analysis. *J Comput Chem* **2004**, *25* (13), 1605-12.
200. Morris, G. M.; Huey, R.; Lindstrom, W.; Sanner, M. F.; Belew, R. K.; Goodsell, D. S.; Olson, A. J., AutoDock4 and AutoDockTools4: Automated docking with selective receptor flexibility. *J Comput Chem* **2009**, *30* (16), 2785-91.
201. Khalifah, R. G., The carbon dioxide hydration activity of carbonic anhydrase. I. Stop-flow kinetic studies on the native human isoenzymes B and C. *J Biol Chem* **1971**, *246* (8), 2561-73.
202. Hurt, J. D.; Tu, C.; Laipis, P. J.; Silverman, D. N., Catalytic properties of murine carbonic anhydrase IV. *J Biol Chem* **1997**, *272* (21), 13512-8.
203. Schindler, J. F.; Naranjo, P. A.; Honaberger, D. A.; Chang, C. H.; Brainard, J. R.; Vanderberg, L. A.; Unkefer, C. J., Haloalkane dehalogenases: steady-state kinetics and halide inhibition. *Biochemistry* **1999**, *38* (18), 5772-8.
204. Thomas, P. W.; Fast, W., Heterologous Overexpression, Purification, and In Vitro Characterization of AHL Lactonases. In *Quorum Sensing: Methods and Protocols*, Rumbaugh, P. K., Ed. Humana Press: Totowa, NJ, 2011; pp 275-290.
205. Liu, D.; Thomas, P. W.; Momb, J.; Hoang, Q. Q.; Petsko, G. A.; Ringe, D.; Fast, W., Structure and specificity of a quorum-quenching lactonase (AiiB) from *Agrobacterium tumefaciens*. *Biochemistry* **2007**, *46* (42), 11789-99.
206. Stamp, A. L.; Owen, P.; El Omari, K.; Nichols, C. E.; Lockyer, M.; Lamb, H. K.; Charles, I. G.; Hawkins, A. R.; Stammers, D. K., Structural and functional characterization of *Salmonella enterica* serovar Typhimurium YcbL: an unusual Type II glyoxalase. *Protein Sci* **2010**, *19* (10), 1897-905.
207. Dong, Y. H.; Xu, J. L.; Li, X. Z.; Zhang, L. H., AiiA, an enzyme that inactivates the acylhomoserine lactone quorum-sensing signal and attenuates the virulence of *Erwinia carotovora*. *Proc Natl Acad Sci U S A* **2000**, *97* (7), 3526-31.
208. Wang, W. Z.; Morohoshi, T.; Someya, N.; Ikeda, T., AidC, a novel N-acylhomoserine lactonase from the potato root-associated cytophaga-flavobacteria-bacteroides (CFB) group bacterium *Chryseobacterium* sp. strain StRB126. *Appl Environ Microbiol* **2012**, *78* (22), 7985-92.
209. Tang, K.; Su, Y.; Brackman, G.; Cui, F.; Zhang, Y.; Shi, X.; Coenye, T.; Zhang, X. H., MomL, a novel marine-derived N-acyl homoserine lactonase from *Muricauda olearia*. *Appl Environ Microbiol* **2015**, *81* (2), 774-82.
210. Matthyse, A. G.; Yarnall, H.; Boles, S. B.; McMahan, S., A region of the *Agrobacterium tumefaciens* chromosome containing genes required for virulence and attachment to host cells. *Biochim Biophys Acta* **2000**, *1490* (1-2), 208-12.

References

211. Fouts, D. E.; Tyler, H. L.; DeBoy, R. T.; Daugherty, S.; Ren, Q.; Badger, J. H.; Durkin, A. S.; Huot, H.; Shrivastava, S.; Kothari, S.; Dodson, R. J.; Mohamoud, Y.; Khouri, H.; Roesch, L. F.; Krogfelt, K. A.; Struve, C.; Triplett, E. W.; Methe, B. A., Complete genome sequence of the N₂-fixing broad host range endophyte *Klebsiella pneumoniae* 342 and virulence predictions verified in mice. *PLoS Genet* **2008**, *4* (7), e1000141.
212. Park, S. Y.; Lee, S. J.; Oh, T. K.; Oh, J. W.; Koo, B. T.; Yum, D. Y.; Lee, J. K., AhlD, an N-acylhomoserine lactonase in *Arthrobacter* sp., and predicted homologues in other bacteria. *Microbiology* **2003**, *149* (Pt 6), 1541-50.
213. Kielak, A. M.; van Veen, J. A.; Kowalchuk, G. A., Comparative analysis of acidobacterial genomic fragments from terrestrial and aquatic metagenomic libraries, with emphasis on acidobacteria subdivision 6. *Appl Environ Microbiol* **2010**, *76* (20), 6769-77.
214. Zang, T. M.; Hollman, D. A.; Crawford, P. A.; Crowder, M. W.; Makaroff, C. A., Arabidopsis glyoxalase II contains a zinc/iron binuclear metal center that is essential for substrate binding and catalysis. *J Biol Chem* **2001**, *276* (7), 4788-95.
215. Boyer, M.; Bally, R.; Perrotto, S.; Chaintreuil, C.; Wisniewski-Dye, F., A quorum-quenching approach to identify quorum-sensing-regulated functions in *Azospirillum lipoferum*. *Res Microbiol* **2008**, *159* (9-10), 699-708.
216. Zarkani, A. A.; Stein, E.; Rohrich, C. R.; Schikora, M.; Evguenieva-Hackenberg, E.; Degenkolb, T.; Vilcinskis, A.; Klug, G.; Kogel, K. H.; Schikora, A., Homoserine lactones influence the reaction of plants to rhizobia. *Int J Mol Sci* **2013**, *14* (8), 17122-46.
217. Mascarenhas, R.; Thomas, P. W.; Wu, C. X.; Nocek, B. P.; Hoang, Q. Q.; Liu, D.; Fast, W., Structural and Biochemical Characterization of AidC, a Quorum-Quenching Lactonase with Atypical Selectivity. *Biochemistry* **2015**, *54* (28), 4342-53.
218. Momb, J.; Thomas, P. W.; Breece, R. M.; Tierney, D. L.; Fast, W., The quorum-quenching metallo-gamma-lactonase from *Bacillus thuringiensis* exhibits a leaving group thio effect. *Biochemistry* **2006**, *45* (44), 13385-93.
219. D'Angelo-Picard, C.; Chapelle, E.; Ratet, P.; Faure, D.; Dessaux, Y., Transgenic plants expressing the quorum quenching lactonase AttM do not significantly alter root-associated bacterial populations. *Res Microbiol* **2011**, *162* (9), 951-8.
220. Newman, T.; de Bruijn, F. J.; Green, P.; Keegstra, K.; Kende, H.; McIntosh, L.; Ohlrogge, J.; Raikhel, N.; Somerville, S.; Thomashow, M.; et al., Genes galore: a summary of methods for accessing results from large-scale partial sequencing of anonymous *Arabidopsis* cDNA clones. *Plant Physiol* **1994**, *106* (4), 1241-55.
221. Oelschlaeger, P., Outsmarting metallo-beta-lactamases by mimicking their natural evolution. *J Inorg Biochem* **2008**, *102* (12), 2043-51.
222. Ng, F. S.; Wright, D. M.; Seah, S. Y., Characterization of a phosphotriesterase-like lactonase from *Sulfolobus solfataricus* and its immobilization for disruption of quorum sensing. *Appl Environ Microbiol* **2011**, *77* (4), 1181-6.
223. Sirotkina, M.; Efremenko, E. N., Rhodococcus lactonase with organophosphate hydrolase (OPH) activity and His(6)-tagged OPH with lactonase activity: evolutionary proximity of the enzymes and new possibilities in their application. *Appl Microbiol Biotechnol* **2014**, *98* (6), 2647-56.
224. Mitic, N.; Hadler, K. S.; Gahan, L. R.; Hengge, A. C.; Schenk, G., The Divalent Metal Ion in the Active Site of Uteroferrin Modulates Substrate Binding and Catalysis. *Journal of the American Chemical Society* **2010**, *132* (20), 7049-7054.
225. Twitchett, M. B.; Schenk, G.; Aquino, M. A.; Yiu, D. T.; Lau, T. C.; Sykes, A. G., Reactivity of M(II) metal-substituted derivatives of pig purple acid phosphatase (uteroferrin) with phosphate. *Inorg Chem* **2002**, *41* (22), 5787-94.

References

226. Garrity, J. D.; Bennett, B.; Crowder, M. W., Direct evidence that the reaction intermediate of metallo-beta-lactamase L1 is metal bound. *Biochemistry* **2005**, *44* (3), 1078-87.
227. Yang, H.; Aitha, M.; Marts, A. R.; Hetrick, A.; Bennett, B.; Crowder, M. W.; Tierney, D. L., Spectroscopic and mechanistic studies of heterodimetallic forms of metallo-beta-lactamase NDM-1. *J Am Chem Soc* **2014**, *136* (20), 7273-85.
228. Carenbauer, A. L.; Garrity, J. D.; Periyannan, G.; Yates, R. B.; Crowder, M. W., Probing substrate binding to metallo-beta-lactamase L1 from *Stenotrophomonas maltophilia* by using site-directed mutagenesis. *BMC Biochem* **2002**, *3*, 4.
229. Garrity, J. D.; Carenbauer, A. L.; Herron, L. R.; Crowder, M. W., Metal binding Asp-120 in metallo-beta-lactamase L1 from *Stenotrophomonas maltophilia* plays a crucial role in catalysis. *J Biol Chem* **2004**, *279* (2), 920-7.
230. Barshop, B. A.; Wrenn, R. F.; Frieden, C., Analysis of numerical methods for computer simulation of kinetic processes: development of KINSIM--a flexible, portable system. *Anal Biochem* **1983**, *130* (1), 134-45.
231. Zimmerle, C. T.; Frieden, C., Analysis of progress curves by simulations generated by numerical integration. *Biochem J* **1989**, *258* (2), 381-7.
232. Larrabee, J. A.; Schenk, G.; Mitic, N.; Riley, M. J., Use of magnetic circular dichroism to study dinuclear metallohydrolases and the corresponding biomimetics. *Eur Biophys J* **2015**, *44* (6), 393-415.
233. Tadrowski, S.; Pedroso, M. M.; Sieber, V.; Larrabee, J. A.; Guddat, L. W.; Schenk, G., Metal Ions Play an Essential Catalytic Role in the Mechanism of Ketol-Acid Reductoisomerase. *Chemistry* **2016**, *22* (22), 7427-36.
234. Orellano, E. G.; Girardini, J. E.; Cricco, J. A.; Ceccarelli, E. A.; Vila, A. J., Spectroscopic characterization of a binuclear metal site in *Bacillus cereus* beta-lactamase II. *Biochemistry* **1998**, *37* (28), 10173-80.
235. Periyannan, G. R.; Costello, A. L.; Tierney, D. L.; Yang, K. W.; Bennett, B.; Crowder, M. W., Sequential binding of cobalt(II) to metallo-beta-lactamase CcrA. *Biochemistry* **2006**, *45* (4), 1313-20.
236. Salgado, J.; Jimenez, H. R.; Donaire, A.; Moratal, J. M., ¹H-NMR study of a cobalt-substituted blue copper protein: *Pseudomonas aeruginosa* Co(II)-azurin. *Eur J Biochem* **1995**, *231* (2), 358-69.
237. Dennison, C.; Sato, K., Paramagnetic ¹H NMR spectrum of the cobalt(II) derivative of spinach plastocyanin. *Inorg Chem* **2004**, *43* (4), 1502-10.
238. Riley, E. A.; Petros, A. K.; Smith, K. A.; Gibney, B. R.; Tierney, D. L., Frequency-switching inversion-recovery for severely hyperfine-shifted NMR: evidence of asymmetric electron relaxation in high-spin Co(II). *Inorg Chem* **2006**, *45* (25), 10016-8.
239. Thiele-bruhn, S., Pharmaceutical antibiotic compounds in soils – a review. *Journal of Plant Nutrition and Soil Science* **2003**, *166* (2), 145-167.
240. Allen, H. K.; Donato, J.; Wang, H. H.; Cloud-Hansen, K. A.; Davies, J.; Handelsman, J., Call of the wild: antibiotic resistance genes in natural environments. *Nat Rev Microbiol* **2010**, *8* (4), 251-9.
241. Dantas, G.; Sommer, M. O.; Oluwasegun, R. D.; Church, G. M., Bacteria subsisting on antibiotics. *Science* **2008**, *320* (5872), 100-3.
242. Forsberg, K. J.; Reyes, A.; Wang, B.; Selleck, E. M.; Sommer, M. O.; Dantas, G., The shared antibiotic resistome of soil bacteria and human pathogens. *Science* **2012**, *337* (6098), 1107-11.
243. Gottig, S.; Hamprecht, A. G.; Christ, S.; Kempf, V. A.; Wichelhaus, T. A., Detection of NDM-7 in Germany, a new variant of the New Delhi metallo-beta-lactamase with increased carbapenemase activity. *J Antimicrob Chemother* **2013**, *68* (8), 1737-40.

References

244. Riesenfeld, C. S.; Goodman, R. M.; Handelsman, J., Uncultured soil bacteria are a reservoir of new antibiotic resistance genes. *Environ Microbiol* **2004**, *6* (9), 981-9.
245. Clemente, J. C.; Pehrsson, E. C.; Blaser, M. J.; Sandhu, K.; Gao, Z.; Wang, B.; Magris, M.; Hidalgo, G.; Contreras, M.; Noya-Alarcon, O.; Lander, O.; McDonald, J.; Cox, M.; Walter, J.; Oh, P. L.; Ruiz, J. F.; Rodriguez, S.; Shen, N.; Song, S. J.; Metcalf, J.; Knight, R.; Dantas, G.; Dominguez-Bello, M. G., The microbiome of uncontacted Amerindians. *Sci Adv* **2015**, *1* (3).